STRUCTURE OF THE ENERGY LEVELS OF SOME LIGHT NUCLEI FROM A STUDY OF ONE- AND TWO-NUCLEON TRANSFER REACTIONS INDUCED BY 23-MeV DEUTERONS

A THESIS
Submitted for the Degree of
DOCTOR OF PHILOSOPHY
in the Faculty of Science

by
C. M. BHAT

DEPARTMENT OF PHYSICS
BANGALORE UNIVERSITY
BANGALORE-560 001
INDIA

1982

DEDICATION

To my Brother
Sri V. M. Bhat
and
To my Parents

DECLARATION

The work forming the subject matter of this thesis has been carried out by the candidate under the guidance of Dr. N. G. Puttaswamy. The nuclear reaction data used in the present study were collected by Dr. N. G. Puttaswamy at the Argonne National Laboratory cyclotron, USA, in collaboration with Dr. J. L. Yntema and Dr. H. T. Fortune. The detailed analyses of the data on $^{35,37}Cl(d,t)^{34,36}Cl$, $^{39,41}K(d,^{3}He)^{38,40}Ar$, $^{40}Ca(d,\alpha)^{38}K$ and $^{12}C(d,\alpha)^{10}B$ reactions have been undertaken by the candidate himself. The computer programme DWUCK was setup by the candidate at the computer centre of Indian Institute of Science.

The work reported in this thesis has not formed, to the best of our knowledge, the basis for the award of any degree or deploma in any institute or university.

N. G. Puttaswamy
Guide

C. M. [illegible]
Candidate

ACKNOWLEDGEMENTS

I am deeply indebted to Dr. N. G. Puttaswamy for initiating me into the field of nuclear reaction studies and for his inspiring guidance throughout the course of the present work. I am very much thankful to Dr. J. L. Yntema, Argonne National Laboratory, USA, and to Prof. H. T. Fortune, University of Pennsylvania, Philadelphia, USA, for associating themselves with this work.

Prof. K. N. Kuchela and Prof. P. Paramasivaiah have provided the much-needed encouragement during this work. I am highly grateful to them.

Dr. M. RajaRao, Dr. M. N. Anandaram, Dr. C. R. Ramaswamy and Dr. M. P. Sathyavatiamma have contributed significantly during the group discussions and seminars. My wife and colleague, Pushpalatha Bhat has generously provided her help throughout the course of this work.

I am thankful to the staff of the computer center and library of the Indian Institute of Science, Bangalore, for their cooperation.

I acknowledge with thanks the Department of Atomic Energy and the Council of Scientific and Industrial Research for their financial support.

SYNOPSIS

Nuclear reactions provide an efficient tool for the study of the structure of nuclei. The study of the nuclear reaction can throw light upon two important aspects : i) the nuclear spectroscopy and ii) the reaction mechanism. This thesis deals mainly with the studies on the spectroscopy of some light nuclei with $A \leqslant 41$ via one- and two-nucleon transfer reactions induced by 23-MeV deuterons. The experiments have been carried out at the cyclotron of Argonne National Laboratory, USA. The 60-in. scattering chamber has been used along with (dE/dX)-E counter arrangement for identifying the outgoing particles like tritons, ^{3}He-particles and α-particles. The experimental angular distributions corresponding to the observed transitions have been compared with the results of DWBA analysis performed using the code DWUCK and by including finite-range and non-locality corrections. The orbital angular momentum transfer, and the spectroscopic factors have been extracted for all the observed levels.

The ^{35,37}Cl(d,t)^{34,36}Cl reactions on enriched chlorine isotopes have been carried out at 23.35 MeV incident deuteron energy. Totally six transitions in case of ^{35}Cl(d,t)^{34}Cl and ten transitions in the case of ^{37}Cl(d,t)^{36}Cl reactions have been studied. The spectroscopic factors deduced in the present study agree well with the results of other single neutron pickup reaction

studies. The level energies in ^{34}Cl and ^{36}Cl nuclei, and the spectroscopic factors have been compared with the predictions from a full sd-shell-model calculation.

In a study of the $^{39,41}K(d,{}^{3}He)^{38,40}Ar$ reactions at 22.8 MeV, eight levels in ^{38}Ar and ten levels in ^{40}Ar have been identified. For ^{38}Ar the results compare well with the previous $(d,{}^{3}He)$ studies at $E_d = 28.9$ MeV and $E_d = 34.5$ MeV. The predictions from the full sd-shell-model and the core-excitation-model calculations have been compared with the experimental results. The experimental information on the ^{40}Ar levels have been compared with the predictions of the $d_{3/2}-f_{7/2}-p_{3/2}-$ model calculations.

In a study of the $^{40}Ca(d,\alpha)^{38}K$ reaction at 22.8 MeV, totally twenty levels in ^{38}K have been identified upto an excitation energy of 10.26 MeV. Two new levels, one at 9.88 MeV and another at 10.26 MeV have been observed. The angular distributions measured in an angular range of 11° to 165° for ten transitions have been compared with DWBA calculations performed using the spectroscopic amplitudes deduced from the full sd-shell-model calculation of Wildenthal and Chung. The present study indicates that the 7.32-MeV level has a large component of the $(s_{1/2})_p^{-1}(s_{1/2})_n^{-1}$ configuration and hence expected to have $J^{\pi} = 1^{+}$. The newly identified level at 9.88 MeV exhibits $L = 2$ angular distribution indicating $J^{\pi}=1^{+},2^{+}$ or 3^{+}.

Six levels of ^{10}B, below an excitation energy of 5.18 MeV, could be studied from an analysis of $^{12}C(d,\alpha)$ reaction data. The data have been analysed with the standard DWBA formalism by using the (1p-shell-model) two-nucleon spectroscopic amplitudes of Cohen and Kurath.

Thus a systematic study of the deuteron induced single- and two-nucleon transfer reactions discussed above have led to valuable information on the structure of ^{10}B, $^{34,36}Cl$, $^{38,40}Ar$ and ^{38}K nuclei.

CONTENTS

		Pages
SYNOPSIS		i
CHAPTER		
I	INTRODUCTION	1
	1.1. Nuclear Models	2
	1.1.1. The Nuclear Shell Model	3
	1.1.2. The Nuclear Collective Model	5
	1.2. Types of Nuclear Reactions	8
	1.3. Study of Levels in ^{10}B, $^{34,36}Cl$, $^{38,40}Ar$ and ^{38}K. and the scope of the present study.	12
II	NUCLEAR SHELL MODEL	15
	2.1. Independent Particle Motion	15
	2.2. Single Particle States	16
	2.3. Perturbation Theory for Nuclear Levels	20
	2.4. States of Mixed Configuration	23
	2.5. Effective Interactions	25
	2.6. Examples of Shell-Model Calculations	32
	2.7. Single-Nucleon Spectroscopic Factor	34
	2.8. Two-Nucleon Spectroscopic Amplitudes	37
	Table	43
	Figures	44

		Pages
III	DWBA THEORY OFOR SINGLE- AND TWO-NUCLEON TRANSFER REACTION	48
	3.1. DWBA Transition Amplitudes and Cross Sections	49
	3.1.1. Single-Nucleon Transfer Reaction	52
	3.1.2. Two-Nucleon Transfer Reaction	57
	3.2. Optical-Model Potential and Distorted Waves	65
	3.3. Non-Local Potentials	69
	3.4. Finite-Range Correction	70
	Table	73
IV	EXPERIMENTAL PROCEDURE	74
	4.1. Experimental Setup	74
	4.2. Particle Detection and Identification	77
	4.3. Targets	79
	4.4. Analysis of Pulse Height-Spectra	80
	4.4.1. Pulse Height spectrum Fitting	81
	4.4.2. Energy Calibration	83
	4.4.3. Q-Value Determination	83
	4.4.4. Differential Cross Section	84
	Table	86
	Figures	87
V	SINGLE NEUTRON PICKUP REACTION ON CHLORINE ISOTOPES	91
	5.1. Experimental Method	92
	5.2. DWBA Analysis	93

		Pages
	5.3. Results and Discussions	96
	5.3.1. Levels in ^{34}Cl	96
	5.3.2. Levels in ^{36}Cl	98
	5.4. Summary	101
	Tables	102
	Figures	105
VI	SINGLE PROTON PICKUP REACTION ON POTASSIUM ISOTOPES	114
	6.1. Experimental Method	115
	6.2. DWBA Analysis	116
	6.3. Results and Discussions	118
	6.3.1. Levels in ^{38}Ar	118
	6.3.2. Levels in ^{40}Ar	122
	6.4. Summary	124
	Tables	126
	Figures	129
VII	(d,α) REACTION ON ^{40}Ca	134
	7.1. Experimental Method	136
	7.2. Analysis	138
	7.2.1. Optical Model Parameters	138
	7.2.2. Form Factor	139
	7.2.3. DWBA Cross Sections	140
	7.3. Results and Discussion	141
	7.3.1. Even-Parity Levels	142
	7.3.2. Odd-Parity Levels	144
	7.3.3. Other Levels	145
	7.3.4. Normalization Constant	146

		Pages
	7.4. SUMMARY	147
	Tables	149
	Figures	154
VIII	(d,α) REACTION ON ^{12}C	162
	8.1. Experimental Method	162
	8.2. DWBA Analysis	163
	8.3. Discussion	164
	Tables	166
	Figures	168
IX	CONCLUSIONS	170
APPENDICES		172
	A. Coefficient of Fractional Parentage	172
	B. The Computer Code DWUCK	175
	B.1. DWBA Cross Section	175
	B.2. Finite-Range and Non-Locality Corrections	177
	C. Experimental Cross Sections for $^{40}Ca(d,\alpha)^{38}K$ Reaction at 22.8 MeV.	179
LIST OF REFERENCES		189

CHAPTER I

INTRODUCTION

One of the main objectives of studies in nuclear physics concerns the elucidation of the structure of the nuclei. To understand the nuclear structure, it is essential to have a complete idea of the forces acting between the nucleons in the nucleus. Using the presently available information on nucleon-nucleon interaction, attempts have been made to deduce the 'realistic interactions' or 'effective interations' which are then used in the nuclear-shell-model calculations. The calculated wave functions of the nuclear levels can be used to predict the detailed properties of nuclei. For example, the calculated electromagnetic transition rates can be compared with experimental values. Similarly, the predicted spectroscopic factors can be compared with the values deduced from direct reaction experiments; these studies provide a direct method to study the overlap between the initial and the final nuclear levels.

A study of direct nuclear reactions, in general, can throw light upon two important aspects, viz., (i) the rection mechanism and (ii) the nuclear spectroscopy. The exact method of approaching these two aspects, must obviously involve, solving the many-body Schrodinger equation for a nucleus. The nuclear reaction studies may involve the application of general conservation principles such as

conservation of energy, . momentum and angular momentum. The studies may also require some type of semi-empirical analysis based on a systematic study of many individual cases. The nuclear spectroscopic information that is obtained by the study of nuclear reactions include the properties of the nuclear states such as their excitation energy (E_x), angular momentum (J), parity (π), isospin (T), and the spectroscopic factors. It is through these spectroscopic factors (square of spectroscopic amplitudes) that the overlap of the wave functions of initial and final nuclear states enter into the nuclear reaction theory. These wave functions are described appropriately by the models of the nucleus.

1.1. NUCLEAR MODELS

In the study of nuclear theory, one has to cope up with two major problems. In the first place the nucleus is a many-body system; it is known that even classical three-body problem has not been exactly solved. Secondly the knowledge about the nucleon-nucleon interaction is incomplete. Even if these difficulties could be overcome, it would be necessary to look for some simplified description of the nuclei in terms of a sufficiently small number of parameters to permit ready assimilation by the human mind. At the same time, the parameters should be sufficient to give a fairly complete picture of the most important features of a particular nucleus. The accumulation of knowledge from the experimental investigations and generalisation of the

experimental facts have given rise to theoretical concepts of a purely phenomenological character. Different models of the nucleus are therefore brought in. Each model is required to closely represent atleast a chosen set of features of the nuclear system and to provide a framework for the analysis and correlation of the data. The independent-particle model (the shell model) and the collective model have been developed on the basis of different sets of assumptions pertaining to the microscopic description of the nucleus.

1.1.1. The Nuclear Shell Model

The nuclear forces become repulsive at large relative momenta (or small distances) and hence nuclear matter density is essentially A-independent. On the other hand, the attractive part of the nuclear interaction (at relatively low momenta) and the Pauli principle give rise to nearly independent-particle motion of the nucleons in the nuclear matter. From the standpoint of any one nucleon and to a first approximation, the forces exerted on it by all the nucleons in the nucleus can be represented by a potential well. This potential involves the spatial, spin and isospin coordinates of the particles. The regular appearance of the islands of isomerism near magic numbers (number of protons or neutrons being 2, 8, 20, 28, 50, 82 or 126) finds its natural explanation within the framework of the shell model. It is a particular feature of the ordering of the

levels in the shell model that sets of orbits are grouped together leading to the phenomena of shell structure and later it has been realised that the strong spin-orbit interaction reproduces the exact magic numbers (Mayer and Jensen, 1965). Experimentally it is found that the structure of the nuclei near magic numbers (for example, one particle less or one particle more than the magic number) is relatively simple as compared to the one away from the shell closure. This is expected to be due to the residual interactions which arise from the inter-nucleon interaction for the extra-core particles. In the absence of the inter-nucleon interactions in a shell, many states will be degenerate. However, the degeneracy will be lifted by the residual interaction. Further, if there is more than one nuclear configuration having the same J^{π} and T and if their energies are close to each other, then there may be finite probability for the extra nucleon to be in all such pure single-particle configurations. Thus the actual nuclear states will be states of mixed configuration. An extensive application of the nuclear shell model to nuclear spectroscopy is dealt with in a recent book by Brussard and Glaudemans (1977). The shell model is discussed in some detail in chapter II.

For magic nuclei (such as ^{16}O, ^{40}Ca) and for some nuclei near magic numbers (especially for one or two particles or holes), the low-lying level properties cannot be accounted for by the conventional shell model mentioned above. In

such cases, the core-excitation involving the configurations of the type with n-particle and m-holes (deShalit and Walecka, 1961) may be necessary. These particle-hole states are eigen states of the single-particle part of the shell-model Hamiltonian and the calculations can then be carried out within the scope of the nuclear shell model. In some cases it is found that these core-excitation-model calculations are successful in explaining properties of the nuclei (see e.g., the core-excitation model calculations for ^{38}Ar by Gray et al, 1970).

1.1.2. The Nuclear Collective Model

It has been observed that, as one goes further away from closed shell it becomes very difficult to explain the nuclear level properties within the scope of the simple shell model. The nuclear shell model especially fails to account for the large electric quadrupole moments and the electromagnetic decay properties of a number of nuclei. Interestingly enough, it is found that these nuclei show some new very simple and systematic features. Odd nuclei in this region are characterised by exceptionally large positive electric quadrupole moments and the electric quadrupole transition to the first excited state with $J^{\pi} = 2^{+}$ is strongly enhanced. Such large effects can arise only from the coordinated motion of many nucleons. The first attempt to develop a theory for explaining the large quadrupole

moments was made by Rainwater (1950). The central idea was that non-spherical equilibrium shape might be thought of as arising due to the opposing tendencies of the outer nucleons to polarize the nucleon core and of the core to resist this polarization to mentain spherical shape. This idea was extended by Bohr and Mottelson (1953). Two different approaches to the collective nature of nucleus have been considered. In the approached developed by Nilsson (1955) and commonly referred to as the Nilsson model, the particles are assumed to be moving in a deformed potential. This is essentially an extended shell-model. The Nilsson model was originally developed for axially symmetric nuclei; later it has been extended to the non-axial case by Newton (1960).

In the another approach, the nucleus is treated as a deformable drop of liquid. Accordingly nuclei are classified into two catagories viz., i) spherical and ii) permanently deformed.

<u>Phonon Excitation in Spherical Nuclei</u>: The excitation of spherical nuclei is assumed to consist of (small-amplitude) surface vibrations of the harmonic type about equlibrium spherical shape. This introduces the concept of phonon excitation.

The total Hamiltonian for surface oscillation of nuclear liquid drop, can be written as,

$$H_S = \sum_{\lambda\mu} [\frac{1}{2B_\lambda} |\pi_{\lambda\mu}|^2 + \tfrac{1}{2}C\, |\alpha_{\lambda\mu}|^2] \,. \qquad \ldots(1\text{-}1)$$

Where B_λ are inertial parameters and C_λ depend on nuclear surface tension, charge and the radius. $\pi_{\lambda\mu}$ are generalized coordinates. The energy eigenvalues for this Hamiltonian is essentially the same as that for a harmonic oscillator. For example, for $\lambda = 2$ (quadrupole oscillation), the energy eigenvalues are given by,

$$E_N = (N + \tfrac{5}{2})\, \hbar\omega, \qquad \ldots(1\text{-}2)$$

with $N = 0, 1, 2, \ldots$. Where ω is the frequency parameter given by $(C_2/B_2)^{\frac{1}{2}}$. Thus the ground state of a spherical nucleus is a state with no phonons, while the first excited state (with spin-parity 2^+) has only one phonon and is five-fold degenerate. The wave functions for these vibrational levels are simply the harmonic oscillator wave functions with $\alpha_{\lambda\mu}$ as the variables.

The nuclear properties of some odd-odd nuclei can be explained within the scope of the particle-vibration coupling model. For such cases the Hamiltonian can be written as,

$$H = H_S + H_P + H_{int} \,. \qquad \ldots(1\text{-}3)$$

Where H_S is defined in equation (1-1), H_P is the interaction energy among the extra-core particles, and

H_{int} is the interaction between the extra-core particles and the vibrating core. The details of the particle-vibration coupling model are reviewed in the recent book by Bohr and Mottelson (1975).

Rotational Levels of Deformed Nuclei: In the case of the permanently deformed even-even nuclei, the low-lying energy levels are assumed to be due to rotations. The characteristic feature of the rotational spectra is their very simple J dependence viz.,

$$E_J = \frac{\hbar^2}{2\mathcal{J}} J(J+1) - BJ^2(J+1)^2 \qquad \ldots(1\text{-}4)$$

for the ground state rotational band. Here $\mathcal{J}$ is the moment of inertia of the rotor. The second term in equation (1-4) is merely a correction factor. The wave functions for such rotational levels of nuclei are essentially the D-matrices. In some nuclei one can expect such rotational bands with the vibrational levels as band heads.

1.2. TYPES OF NUCLEAR REACTIONS

The nuclear reactions can be classified as (i) compound nuclear reaction and (ii) direct reaction. In the former, the incident particle is captured to form the so-called 'compound nucleus' (in a highly excited state) wherein the nuclear-state becomes increasingly complex. But after a certain relaxation time, a statistical equilibrium

will be reached. Then the compound nucleus spontaniously decays into all energitically possible outgoing reaction channels. The compound nuclear reactions are characterised by a) the very marked fluctuations in the excitation function, and b) the symmetric angular distribution about $\theta_{c.m.} = 90^{\circ}$. The contribution to the total reaction cross section due to the compound nuclear reaction can be evaluated by using the Hauser-Feshbach theory (Hauser and Feshbach, 1952). Since the nuclear energy-level density increases very rapidly with excitation energy, the number of channels into which the compound nucleus can decay also increases. Thus compound nuclear cross-section tends to fall off quite rapidly with increasing energy. Above 10 to 15 MeV energy incident particles (having A = 1-4), the contribution due to compound nucleus formation is small.

At higher energies of the incident particle, the interaction takes place within the time of transit of the particle in the nucleus. Although the nuclei have relatively sharp surfaces, there is a region in which a transition is made between a condition of no interaction and one in which a strong interaction occurs. In this surface region, there is an appreciable probability that a projectile can interact inelastically with, say, just one target nucleon (or some simple mode of nuclear motion such as a shape oscillation) and the residual particle escapes. These reactions are called as direct reactions. Only particles which penetrate deeper

and suffer subsequent collisions within the nucleus form a compound system. The direct reactions can therefore be thought of as 'doorways' through which the compound nucleus formation is initiated.

This picture of direct reaction leads us to their importance as sources of information on nuclear structure. Here one has a simple single-step process. The reaction amplitudes must depend on the overlap of the initial and final states; the complicated intermediate configurations of the compound nucleus do not intervene. Consequently, the direct reaction cross-section tells us directly about the relation between the two nuclear states. For example, in a neutron pickup (p,d) reaction, one learns as to how much the residual nucleus looks like the target nucleus plus a neutron hole in a shell-model orbit.(the particle-hole conjugation is discussed in detail by Bohr and Mottleson, 1969). The spectroscopic factor is a measure of this probability; such information is obviously vital for testing the predictions of the nuclear shell-model.

A good theory of direct reactions which reproduces the shape and the magnitude of the differential cross section obtained from experiments is needed. The early plane-wave theory of direct reactions (Butler, 1951) was remarkably successful as a tool for identifying orbital angular momentum transfer from measured angular distribution for light nuclei. But the predicted magnitude of cross section was larger

by an order of magnitude.

Experimental data on the heavier nuciei clearly showed that the distortion by the Coulomb field is important. In elastic scattering experiments, it has been found that when the energy of the incident particle is higher than the Coulomb barrier, the angular distribution is dominated by diffraction like pattern. It is realized that this effect is due to the finite size of the nucleus and due to the nuclear matter being partially transparent. This is effectively done by introducing a complex potential of the form $V(r) + iW(r)$, called the 'Optical-Model' (OM) potential, in the one-body Schrödinger equation. This sort of potential can explain not only the elastic scattering process but also the scattering phenomina in general (see for example, Hodgson, 1971 and 1963). From the formulation of the model it is clear that it cannot give any microscopic details of the nucleus but it gives only the gross properties of the nucleus which are responsible for the scattering.

For direct reaction studies it has been realised that the plane-wave theory is never a good approximation and therefore one must take into account the distortion due to the Coulomb field and the nuclear optical-model potential. Commonly these two put together are called as OM potential.

The distorted wave method takes into account the scattering and absorbtion of the incident and outgoing particles by assuming distorted waves instead of plane waves. The distorted waves are generated by using phenomenological OM potentials. A detailed description of the distorted--wave theory and the distorted-wave-Born-approximation (DWBA) method of direct reaction analysis, with an emphasis on single- and two-nucleon transfer reactions, is presented in chapter III.

There may be several paths by which the reactions may proceed to a given final state and the interference between these contributions become important. One has to then take into account the 'coupled reaction channels' If the transfer is still treared to first-order in the interaction, the calculation is called as coupled channel Born approximation (CCBA). In a number of cases, where DWBA fit is not satisfactory, the CCBA has been able to reproduce the experimental cross section .

1.3. STUDY OF LEVELS IN ^{10}B, $^{34,36}Cl$, $^{38,40}Ar$, AND ^{38}K AND THE SCOPE OF THE PRESENT STUDY

During the last two decades there has been a great deal of interest in the study of the structure of 1p-, sd- and fp-shell nuclei both experimentally and theoritically (in particular from shell model point of view). The direct one- and two-nucleon transfer reactions provide valuable

information on the properties of the low-lying levels of the residual nuclei and thus enable us to varify the model wave functions. Another feature of these transfer reactions arises from the particular type of reaction used in studying the nuclei. A state in the residual nucleus can be excited differently in different types of reactions. The cross section further depends on the energy of the projectile and the Q-value of the reaction. If there is good angular momentum matching, the angular distribution will be strongly structured and will be distinctly dependent on the orbital angular momentum transfer of the particles or the cluster of particles. For reactions with a large negative (or positive) Q-value, the angular momentum carried by the incident and the outgoing particles may be very much different, leading to an angular momentum mismatch for that transition. Hence the transition amplitude and the cross section are very much reduced.

In view of these advantages of one- and two-nucleon transfer reactions, a study of the structure of $^{34,36}Cl$ via $^{35,37}Cl(d,t)$ reactions, of $^{38,40}Ar$ via $^{39,41}K(d,{}^{3}He)$ reactions, of ^{38}K via $^{40}Ca(d,\alpha)$ reaction, and of ^{10}B via $^{12}C(d,\alpha)$ reaction at $E_d \cong 23$ MeV has been made in this thesis. Though the single-nucleon pickup spectroscopic strengths for the various levels in $^{34,36}Cl$ and ^{38}Ar are available in literature from other similar single-nucleon transfer reactions (see e.g., collections by Endt and Van der

Leun, 1978; Endt, 1977), the study on ^{40}Ar levels via $^{41}K(d,^{3}He)$ reaction has been made for the first time here. In the case of our study of the ^{38}K via the (d,α) reaction some new levels have been identified. DWBA calculations have been performed for both one- and two-nucleon transfer reactions. The results have been compared with the previous experimental studies and with the shell-model predictions for these nuclei. A discussion of the structure of the nuclei is presented in the appropriate chapters.

CHAPTER II

THE NUCLEAR SHELL MODEL

A brief introduction to the nuclear shell model was given in section 1.1. Prominent features of the shell model and some details which are essential in the elucidation of nuclear structure via nuclear reaction studies are outlined here. Excellent books on the development of the shell model and its detailed application to nuclear spectroscopy are available (Brussaard and Glaudemans, 1977; deShalit and Feshbach, 1974; Bohr and Mottelson, 1969; deShalit and Talmi, 1963).

2.1 INDEPENDENT-PARTICLE MOTION

The basic assumption of the nuclear shell model is that, to a first approximation, each nucleon moves independently in a potential which represents the average interaction with the other nucleons in the nucleus. The Hamiltonian for a nucleus containing A nucleons consists of two terms viz., the kinetic energy term T(i) and the two-particle interaction term W(i,j). Then the Schrödinger equation reads as,

$$H\Psi(1,2,..,A) = [\sum_{i=1}^{A} T(i) + \sum_{j>i=1}^{A} W(i;j)]\ \Psi(1,2,..,A)$$

$$= E\ \Psi(1,2,..,A) \qquad ...(2\text{-}1)$$

where $\Psi(1,2,..,A)$ is the totally antisymmetric wave function of the nucleus. In principle one can introduce any single-particle potential U(r) that leads to a complete set of proper single-particle eigen functions $\phi_a(r)$ and write the Hamiltonian H in the equation (2-1) as,

$$H = \sum_{i=1}^{A}[T(i) + U(i)] + [\sum_{j>i=1}^{A} W(i,j) - \sum_{i=1}^{A} U(i)]$$

$$= H^{(o)} + H^{(1)}. \qquad ...(2-2)$$

The $H^{(o)}$ term defines the independent particle motion and $H^{(1)}$ represents the 'residual interaction' reflecting the fact that the particles do not move completely independently. If the residual interaction is negligible, the true functions $\Psi(1,2,..,A)$ can be represented by an independent-particle Slater determinant. But, in general, these residual interactions cannot be neglected.

2.2 SINGLE-PARTICLE STATES

In the previous section, it is assumed that the interaction between the ith particle and the remaining (A-1) particles in the nucleus can be approximated by the potential U(r). The short range of the nucleon-nucleon force suggests that U(r) should approximately resemble the nuclear density distribution. Numerical results of Hartree-Fock calculations indicate that the harmonic-oscillator (HO) potential,

$$U(r) = -\tfrac{1}{2} M\omega^2 r^2 , \qquad \ldots(2\text{-}3)$$

is a good approximation to the self-consistent potential. Here M denotes the mass of the nucleon and ω the angular frequency. The eigen function of the particle in the HO potential is characterised by three quantum numbers viz., the principal quantum number (n), orbital quantum number (l) and the quantum number corresponding to the projection of orbital angular momentum (m_l), and has the form

$$\psi_{nlm_l}(r) = R_{nl}(r)\, Y_{lm_l}(\Theta,\varphi) . \qquad \ldots(2\text{-}4)$$

$R_{nl}(r)$, the radial wave function essentially consists of confluent hypergeometric series and $Y_{lm_l}(\Theta,\varphi)$ is the spherical harmonic. The energy eigen value corresponding to the eigen state $\psi_{nlm_l}(r)$ is given by

$$E_n = (N + 3/2)\, \hbar\omega \qquad \ldots(2\text{-}5)$$

where

$$N = 2(n - 1) + l \qquad \ldots(2\text{-}6)$$

and $n = 1,2,\ldots,$ $l = 0,1,2,\ldots,$etc. A schematic diagram of the allowed single-particle energies is shown in Fig. 2-1(a). In Fig. 2-1(b) are shown the energy eigen values obtained by using a realistic Woods-Saxon (WS) potential defined by,

$$U(r) = -U_o\, [1 + \exp(\overline{r - R}/a)]^{-1} . \qquad \ldots(2\text{-}7)$$

Here U_o is the depth of the potential and $R = r_o A^{1/3}$ is the radius of the potential. The value of the radius parameter r_o is ~ 1.2 fm and the diffuseness parameter a is ~ 0.7 fm. WS potential requires the use of numerical methods for solving the Schrödinger equation. A comparison of these two types of potentials (Brussaard and Glaudemans, 1977; Bohr and Mottelson, 1969) reveals that the shapes of the two potentials are similar for bound particles. Therefore, almost all shell-model calculations are made using the HO potential (which can be solved exactly). It can however be noticed that the number of particles at shell-closure for either of these potentials agrees only for the magic numbers 2, 8 and 20 even though the levels from WS potential are less degenerate. The higher magic numbers viz., 28, 50, 82, 126 are not reproduced. However, the addition of a one-body spin-orbit interaction of the form $U_{\ell s} = -2\alpha(\vec{\ell}.\vec{s})$ to the central potential does generate the observed shell closing. The effect of spin-orbit interaction on the central (HO and WS) potentials is shown in Fig. 2-1(c). $N_j = 2j + 1$ is the number of identical particles that can occupy each state.

The theoretical justification for the spin-orbit potential is not completely satisfactory. Using the basic nucleon-nucleon potential, the effective spin-orbit interaction has been shown (Harnyok, 1975) to be of the form,

$$U_{\ell s}(r) = k \frac{1}{r} \frac{d\rho(r)}{dr} \vec{\ell}.\vec{s} \qquad \ldots(2\text{-}8)$$

where k is a constant and $\rho(r)$ is the nuclear density distribution. If the nuclear interaction has zero-range, $\rho(r)$ would be identical with the potential shape. This spin-orbit coupling splits each level into a doublet and the sign of k is such as to lower the level with $j = \ell + \frac{1}{2}$ relative to the one with $j = \ell - \frac{1}{2}$.

Thus a nucleon moving in a single-particle potential

$$U'(r) = U(r) + U_{\ell s}(r) + V_C(r) \qquad \ldots(2\text{-}9)$$

is characterised by the radial quantum number n, the orbital quantum number ℓ, the total quantum number j $(=\ell \pm \frac{1}{2})$ and the projection quantum number $m = m_j$. $V_C(r)$ in equation (2-9) is the Coulomb potential of a uniform charge distribution. The single-particle wave function $\phi_{n\ell jm}(\vec{r})$ takes the form,

$$\begin{aligned} \phi_{n\ell jm}(\vec{r}) &= |n\ell jm\rangle \\ &= R_{n\ell}(r) \sum \langle \ell\, m-m_s\, \tfrac{1}{2} m_s | j\, m\rangle\, Y_\ell^{m-m_s}(\theta,\varphi)\, \chi_{\frac{1}{2}}^{m_s} \end{aligned} \qquad \ldots(2\text{-}10)$$

where $\chi_{\frac{1}{2}}^{m_s}$ is the spinor.

The introduction of the spin-orbit interaction into the shell model of the nucleus could not only reproduce the

magic numbers (indicated by rectangles in Fig. 2-1) but also predict a large number of observed phenomena on odd-nuclei (Mayer and Jensen 1955). The interpretation of the nuclear levels is particularly simple for low-lying configurations consisting of a single nucleon (or a hole) in an otherwise filled shell of neutrons and protons (Bohr and Mottelson 1969).

2.3. PERTURBATION THEORY FOR NUCLEAR LEVELS

In order to calculate the various properties of nuclear ground-states and excited states, one must have available the wave functions of these state. The wave functions can be obtained by solving the many body Schrödinger equation (2-1). It has been shown (see equation 2-2) that the total Hamiltonian can be written as sum of two terms : first term containing independent particle motion $H^{(o)}$ and second term $H^{(1)}$ containing the residual interaction. One usually employes either the harmonic oscillator potentials or the Woods-Saxon potentials for the single-particle central potential $U(r)$. The basis of the single-particle states $\phi_a(r)$ is determined by the single-particle Schrödinger equation

$$T\phi_a(\vec{r}) + U\phi_a(\vec{r}) = e_a\phi_a(\vec{r}). \qquad \ldots(2\text{-}11)$$

Here e_a represents the single-particle energy with 'a' labelling the single-particle state $|nljm\rangle$. Any product of $\Phi_a^{(o)} = \phi_a(\vec{r}(1)) \ldots \phi_{a_A}(\vec{r}(A))$ satisfies the equation

$$H^{(o)}\Phi_a^{(o)} = E_a^{(o)}\Phi_a^{(o)} \qquad \ldots(2\text{-}12)$$

where $H^{(o)}$ is the unperturbed Hamiltonian. The unperturbed energy is

$$E_a^{(o)} = \sum_{i=1}^{A} e_{a_i}. \qquad \ldots(2\text{-}13)$$

The wave function $^{(o)}_{a}$ of equation (2-12) is not totally antisymmetric. For the description of the nuclear states, however, the wave function should be totally antisymmetric. Therefore a Slater determinant (which is only an antisymmetric wave function for A-particles) is not enough and a more complicated linear combination of the functions $\Phi_a(\vec{r}(1),\ldots,\vec{r}(A))$ is required to satisfy the above conditions. Let such a wave function be denoted by $\Phi_\Gamma(\vec{r}(1),\ldots,\vec{r}(A))$, where Γ indicates all quantum numbers including total spin J and isospin T. The true wave function Φ_Γ and the energy E_Γ being the solution of the equation (2-1), can now be found when the residual interaction given by $H^{(1)}$ is treated as a perturbation. By first ordered perturbation theory (Brussaard and Glaudemans, 1977) it is evident that

$$E_T = \langle \Phi_\Gamma^{(o)} | H^{(o)} + H^{(1)} | \Phi_\Gamma^{(o)} \rangle$$

$$= \sum_i e_{a_i} + \langle \Phi_\Gamma^{(o)} | H^{(1)} | \Phi_\Gamma^{(o)} \rangle. \qquad \ldots(2\text{-}14)$$

This shows that for the calculation of first order change

in energy needs zeroth order wave functions. It can be shown that, when there are n-particles in shell ρ and m particles in another shell λ (where ρ and λ are two shells outside a core), the binding energy is given by the expression

$$E_\Gamma^b(\text{core} + \rho^n + \lambda^m) = E_C + E^b(\text{core}) + ne_\rho + me_\lambda + E_\Gamma^{(1)}(\rho^n, \lambda^m), \qquad \ldots(2\text{-}15)$$

where E_C is the Coulomb energy and

$$E^b(\text{core}) = \langle \Phi_{oo}(\text{core}) \mid H_{\text{core}} \mid \Phi_{oo}(\text{core}) \rangle \qquad \ldots(2\text{-}16)$$

is the binding energy of the particles in the core. Further e_ρ and e_λ in equation (2-15) are single particle energies and $E_\Gamma^{(1)}(\rho^n, \lambda^m)$ has the form

$$E_\Gamma^{(1)}(\rho^n, \lambda^m) = \langle \rho^n \lambda^m \mid \sum_{j>i=1}^{n+m} V(i,j) \mid \rho^n \lambda^m \rangle_\Gamma$$

$$= \sum_{\Gamma'} c_{\Gamma'} E_{\Gamma'}^{(1)}(\rho\lambda) \qquad \ldots(2\text{-}17)$$

where the two-body matrix elements are defined by

$$E_{\Gamma'}^{(1)}(\rho\lambda) = \langle \rho\lambda \mid V(1,2) \mid \rho\lambda \rangle_{\Gamma'} \qquad \ldots(2\text{-}18)$$

with

$$V(1,2) = [\sum_{j=3}^{A} W(1,j) - U(1)] + [\sum_{j=3}^{A} W(2,j) - U(2)]$$

$$+ W(1,2). \qquad \ldots(2\text{-}19)$$

The coefficients $c_{\Gamma'}$ are purely geometrical in nature. It is to be noted that the above expression is meaningful only when it is assumed that the state $|\rho^n \lambda^m\rangle_\Gamma$ is described uniquely by one unperturbed wave function.

2.4. STATES OF MIXED CONFIGURATION

It is evident from the equation (2-14) that energy of the pure state $\Phi_\Gamma^{(o)}$ is given by $E = E^{(o)} + E^{(1)}$. The contribution to $E^{(o)}$ comes from the Hamiltonian $H^{(o)}$ which describes the independent particle motion. $E^{(1)}$ is derived from residual interations $H^{(1)}$. Suppose there are g-states $(\Phi_\Gamma^{(o)})_i$ with $i = 1,2,\ldots,g$ (having the same J and T) and with energies $E_i = E_i^{(o)} + E_i^{(1)}$ being very close. Then one cannot neglect that, due to the residual interaction, the nucleons may scatter from one state to the other. Thus the actual state must be given by an admixture of these states. Then the many-particle wave function takes the form,

$$\Psi_p = \sum_{i=1}^{g} a_{i_p} \Phi_i^{(o)}, \qquad p = 1,2,\ldots,g. \qquad \ldots(2\text{-}20)$$

The label T denoting J and T is supressed. This feature to form a linear combination of different basis states which describes a particular state (true state) is referred to as 'configuration mixing'.

The normalisation condition on $_p$ is given by

$$\sum_{i=1}^{g} a_{i_p}^2 = 1, \quad \text{with } p = 1,2,\ldots,g. \qquad \ldots(2\text{-}21)$$

The square of a_{i_p} may be interpreted as the probability that the nucleus is in the state described by $_i^{(o)}$. The many-particle energy eigen-values are obtained by solving

$$H \,|\, \Psi_p \rangle = E_p \,|\, \Psi_p \rangle \qquad \ldots(2\text{-}22)$$

The energy matrix element is constructed from the matrix element H_{ji} defined by

$$H_{ji} = \langle \phi_j^{(o)} \,|\, H \,|\, \phi_i^{(o)} \rangle$$

$$= E_i^{(o)} \delta_{ji} + \langle \phi_j^{(o)} \,|\, H^{(1)} \,|\, \phi_i^{(o)} \rangle \ldots(2\text{-}23)$$

The unperturbed Hamiltonian $H^{(o)}$, leading to the single-particle energies, only contributes to the diagonal matrix element as indicated above.

The diagonalisation of the matrix H_{ji} leads to the required eigenvalues (energies) and eigenvectors

(mixed configuration wave function) of the Hamiltonian.

It is difficult to say 'apriori' as to how many configurations $\phi_i^{(o)}$ should be taken into account. Often, there are many states $\phi_i^{(o)}$ with energy E_i lying rather close together. The dimension of the configuration space increases very rapidly with the number of (sub) shells that one wishes to take into account explicitly (Brussaard and Glaudemans, 1977). Therefore some 'ad hoc' truncation procedure must be employed.

2.5. THE EFFECTIVE INTERACTION

One can setup a system of basis wave functions and subsequently determine the energies and wave functions as mentioned in the section 2-4. Diagonalization in a complete configuration space involves matrices of infinite size. In order to make computation feasible one has to truncate the configuration space. Therefore in a model calculation one has to work with approximate wave functions and consequently the residual interaction should be replaced by an " effective (residual) interaction".

The matrix element of a given interaction between the many-particle states can be expressed in terms of two-body matrix elements according to the equation (2-17). If the particles are identical i.e., either protons or neutrons, the Pauli exclusion principle requires that a

many-nucleon wave function be antisymmetric in all coordinates. In the isospin formalism the generalized Pauli exclusion principle requires that the wave function should reverse its sign upon odd permutation of all coordinates (i.e., space, spin and isospin) of any two nucleons.

Let $\psi_\Gamma(\rho_a \rho_b)$ represent an antisymmetric wave function of a two-body system with one particle in orbit ρ_a and another orbit ρ_b coupled to total spin J and isospin T. If the two particles are in the same orbit, the generalized Pauli exclusion principle allows only those combinations of J and T which satisfy J + T = odd; on the other hand if the particles are in different orbitals, two-particle wave function can always bw antisymmetrized for any combination of J and T. The expectation value of the effective two-body interaction is given according to the equation (2-17) by,

$$E_\Gamma^{(1)}(\rho_a \rho_b) = \langle \rho_a \rho_b | V(1,2) | \rho_a \rho_b \rangle_\Gamma \quad \ldots(2\text{-}24)$$

The value of the matrix element depends on the effective interaction V(1,2), the single-particle wave functions $|\rho_a\rangle$ and $|\rho_b\rangle$, and the total spin and isospin of the two-particle system.

Essentially three different methods have been suggested to evaluate the effective interaction:

a) Empirical Approach

Here one assumes that a nucleus can be described by an inert core and many active nucleons. The level scheme is determined by equation (2-15). Then one expresses the many-particle matrix element of the residual interaction in terms of the two-body matrix elements which are treated as parameters. These parameters can then be determined from a comparison with experimental data in several nuclei. (This method makes sense only if one assumes that the two-body matrix elements of the effective interaction do not change in the mass region considered). The optimum values of the two-body matrix elements can be obtained from a least-squares fit to the experimental data.

The number of parameters will increase very fast with the dimension of the truncated configuation space.

A limitation of this method is that the calculated energies are insensitive to the sign of some of the off-diagonal matrix elements. Due to the sign ambiguities, however, the wave functions thus obtained may be only moderately good for a calculation of the phase-dependent properties such as the cross-section for a reaction involving the transfer of two nucleons.

b) Realistic Interaction

The nuclear potentials derived from a description of

free nucleon-nucleon scattering are referred to as realistic interactions. With a parametrised form of the nucleon-nucleon interaction, one can fix the parameters so as to reproduce i) the phase shifts observed in free nucleon-nucleon scattering experiments and, ii) some properties of the deuteron such as its binding energy. The parametrisation can be such that only the lower partial waves viz., S-, P- and D-waves are taken into account or such that the phase shifts of all partial waves are described.

Unfortunately, direct use of the realistic interaction in the shell-model calculation leads to a poor agreement between theoretical predictions and experimentally measured quantities. This is expected because, for a model calculation in truncated model space, one needs effective operators. In principle, for a given configuration space, the effective interaction can be constructed with the help of the perturbation theory. But this is very much complicated because of the problem of convergence of the perturbation expansions. In spite of these difficulties, methods have been developed to deduce effective interactions from the realistic interactions. One of such widely used effective interactions has been obtained by Kuo and Brown (1966) using the Hamada-Johnston nucleon-nucleon interaction potential. This has the form,

$$V = V_c + S_{12}V_T + \vec{l}\cdot\vec{s}\, V_{LS} + L_{12}V_{LL} \qquad \ldots(2\text{-}25)$$

where c, T, LS and LL denote respectively central, tensor, spin-orbit and quadratic spin-orbit terms; the symbols V_c, V_T, etc., include the radial dependence.

A detailed discussion of the realistic effective interactions used in the shell-model calculations is given in the review article by Kuo (1974) and in the book by Brussaard and Glaudemans (1977).

c) Schematic Interactions

To correlate many observed nuclear properties some simple schematic two-body interactions have been used in truncated model-space. Some of these are discussed below.

Exchange Potential: The nucleon-nucleon scattering experiments have revealed that the nucleon-nucleon interaction has a certain exchange character i.e., the interaction depends on spin and isospin of nucleons and the parity of the states involved. The interaction in its simplest form can be written as,

$$V_{eff}(r) = - f(r) \left[W + BP^{\sigma} - HP^{\tau} - MP^{\sigma}P^{\tau}\right]. \qquad \ldots(2\text{-}26)$$

Here W, B, H and M are the coefficients corresponding to various exchange characters (e.g., W: Wigner-space exchange, B: Bartlett-spin exchange, H: Heisenberg-space and isospin exchange and M: Majorana spin and isospin exchange).

The radial function f(r) is essentially a function of the inter-nucleon distance and has the form of either an exponential- or a Gaussian- or a Yukawa potential. The parameters are determined by fitting various experimental results. W, B, H and M are treated as parameters.

Surface Delta Interaction: One of the simplest forms of the effective interaction used in the shell-model calculations is the surface delta interaction (SDI). For the SDI some very crude assumptions are made about the nature of the effective interaction (Arviu and Moszkowski, 1966). The assumptions are that a) the interactions takes place only at the nuclear surface, b) the two-body force is a delta force, and c) the probability of finding a particle at the nuclear surface is independent of the shell-model orbit in which the particle moves. None of these assumptions can be justified exactly. The support for this interaction is its success in reproducing a lot of experimental data. Taking the first two assumptions one can write down an explicit expression for the SDI between two particles 1 and 2 as,

$$V^{SDI}(1,2) = -4\pi A_{T'}\delta(\vec{r}(1)-\vec{r}(2))\ \delta(r(1)-R_o). \qquad \ldots(2\text{-}27)$$

Where $\vec{r}(1)$ and $\vec{r}(2)$ are the position vectors of the interacting particles, R_o is the nuclear radius, and $A_{T'}$ is the strength parameter.

<u>Modified Surface Delta Interaction</u>: In order to overcome some systematic descripances between the experimental and the SDI predictions of the level energies and the spacing of $T = 0$ and $T = 1$ centroids of energy levels, and ad hoc addition of two J-independent terms have been made. These terms can be looked upon as a linear combination of the Heisenberg and Wigner terms. Then the modified surface delta interaction (MSDI) potential between particles 1 and 2 is given by (Brussaard and Glaudemans, 1977),

$$V^{MSDI}(1,2) = V^{SDI}(1,2) + B'(\tau(1)\cdot\tau(2)) + C'. \qquad \ldots(2\text{-}28)$$

B' and C' are parameters which are constants in coordinate space. Therefore they contribute only to the diagonal two-body matrix elements. The expectation value of isospin dependent term in the above equation is $2T(T+1) - 3$. Therefore the contribution due to the additional term is given by

$$\langle B'(\tau(1).\tau(2)) + C'\rangle = \begin{cases} -3B + C & \text{for } T = 0 \\ B + C & \text{for } T = 1 \end{cases}, \qquad \ldots(2\text{-}29)$$

where B and C denote the product of B' and C' with the radial integral. The values of all these parameters are de determined from fits to the experimental data in various mass regions.

A comparison of the various types of two-body matrix elements of effective interactions discussed above is shown in Figs 2-2(a) and 2-2(b). The Fig. 2-2(a) compares the emperically deduced matrix elements with those obtained from the MSDI. The emperical matrix elements were obtained from a fit to 35 experimental energies in A = 8 - 16 nuclei (Cohen and Kurath, 1965) and assuming the particles to be moving only in $1p_{3/2}$ and $1p_{1/2}$ shells. In Fig. 2-2b, the two-body matrix elements in fp-shell calculated from MSDI are compared with those obtained by Kuo and Brown (1966) using the realistic Hamada-Johnston interaction. In both the cases the agreement with MSDI is strikingly good.

2.6: EXAMPLES OF SHELL-MODEL CALCULATIONS

Many shell-model calculations are available in litrature following the methods described section 2.5. The first calculation in $1p_{3/2}$-$1p_{1/2}$ model-space (Cohen and Kurath, 1965) assumed an emperical approach, to get the matrix elements of effective interaction. A comparison of experimental (Ajzenberg-Selove, 1974) and predicted energy levels for ^{10}B is made in Fig. 2-3. Good agreement is obtained for the positive-parity levels below 6-MeV excitation. The experimentally observed negative-parity levels however cannot be explained within the scope of this model space. In 1964, Glaudemans <u>et al</u> have performed

a shell-model calculation treating ^{28}Si and ^{40}Ca as closed cores and permitting all configurations in the $2s_{1/2}$-$1d_{3/2}$ orbits. The matrix elements of the effective interaction have been treated as parameters. Recently, shell-model calculations have been made in the complete sd-shell model space by Wildenthal et al (1971) using the Kuo-Brown interaction and also the MSDI, and more recently by Wildenthal and Chung (private communication) and Wildenthal (1981) using the "Chang-Wildenthal particle Hamiltonian" for A = 17-24 nuclei and using the "Chung-Wildenthal hole Hamiltonian" for A = 32-39. A comparison of i) the experimental levels ii) the predictions by the Chung-Wildenthal hole Hamiltonian and iii) the predictions by Glaudemans et al (1964) in the more restricted $2s_{1/2}$-$1d_{3/2}$ model space for ^{38}K is shown in Fig. 2-4. Very recently a model calculation in the $2s_{1/2}$-$1d_{3/2}$-$1f_{7/2}$-$2p_{3/2}$ space has been performed by Hasper (1979) to explain the level properties for nuclei with A = 36-39. The properties of the low-lying levels of the Ar isotopes with A = 39-42, have been predicted by a shell-model calculation in the $(1d_{3/2})_p^{-2}\ (1f_{7/2}\ 2p_{3/2})_n^n$ space by Gloeckner et al (1973); here the matrix elements of the residual two-body interactions have been determined by the emperical approach. Several shell-model calculations in the fp-shell region are also available (McGrory and Raman, 1979). A comprehensive review of shell-model calculations for nuclei with $50 \leqslant A \leqslant 150$ is given in the book on structure of

medium mass nuclei by Anagnostatos et al (1979).

Using shell-model wave functions one can evaluate various measurable quantities like level energies, spectroscopic factors and electromagnetic transition probabilities. In view of the emphasis in this thesis on a study of nuclear structure via single- and two-nucleon transfer reactions, the evaluation of spectroscopic factors deserve special attention and have therefore been dealt with in the next two sections.

2.7. SINGLE-NUCLEON SPECTROSCOPIC FACTOR

Consider a single-nucleon pickup reaction of the type

$$A + a \longrightarrow B + b$$

with $A = B + x$ and $b = a + x$ where x is either proton or neutron. The cross section for the reaction of this type can be written as the product of two terms (Satchler 1964). The first part contains spectroscopic information and the second part contains details of the reaction mechanisms. (The details of the reaction mechanism will be discussed in the chapter III.). The spectroscopic information is contained in the spectroscopic factor (S-factor). The single-nucleon S-factor for pickup of a nucleon from the shell ρ containing n-active particles is given by (Macfarlane and French 1960),

$$S(\rho) = n[I(\rho)]^2 . \qquad \ldots(2\text{-}30)$$

$I(\rho)$ is essentially an overlap integral. For active particles in one orbit ρ, we have

$I(\rho) =$ 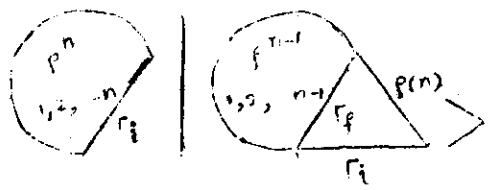

$$= \langle \rho^n \Gamma_i \| \rho^{n-1} \Gamma_f \rangle . \qquad \ldots(2\text{-}31)$$

The right hand side of the above equation contains the coefficient of fractional parentage (c.f.p.) outlined in the Appendix-A. For active nucleons in two orbits and with the pickup from orbit λ, we may write

$\Phi_i =$ 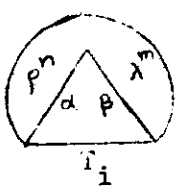 , $\Phi_f =$ 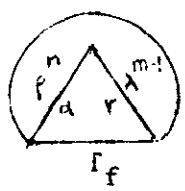

and

$$I(\rho) = \sqrt{(m/(m+n))}\, \langle \lambda^m \beta \| \lambda^{m-1} \gamma \rangle\, U(\alpha\gamma\Gamma_i\lambda\,;\Gamma_f\beta)\,\delta_{\alpha\alpha'} . \qquad \ldots(2\text{-}32)$$

For pickup from orbit ρ, and with

$\Phi_i =$ 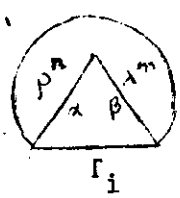 $\Phi_f =$ 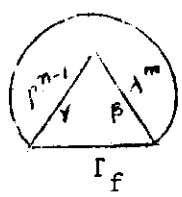

the overlap integral is given by,

$$I(\rho) = (-1)^{\Gamma_i+\Gamma_f+\alpha+\gamma+m} \sqrt{(n/(m+n))} \langle \rho^n \alpha | \rho^{n-1} \gamma \rangle$$

$$\times\ U(\beta\gamma\Gamma_i\rho\ ;\ \Gamma_f\alpha)\delta_{\beta\beta'}. \qquad \ldots(2\text{-}33)$$

On similar lines the S-factors for pickup reactions of particles from states described by a configuration with three active orbits can be written down (Macfarlane and French, 1960).

The S-factors for single-nucleon pickup from $2s_{1/2}$-$1d_{3/2}$ shells has been calculated by Glaudemans et al (1964). Wildenthal et al (1971) have calculated the S-factors for sd-shell nuclei. A comparison between theory and experimental information about the S-factors can provide an essential test of the wave functions.

When, for a given ℓ-value transfer, two j-values are allowed (because $j = \ell \pm \frac{1}{2}$), one determines theoretically the S-factors corresponding to each of them. In most cases, however, only the sum of the two S-factors can be compared with the experimental data. When polarised beam and/or the target are used, one can experimentally distinguish the two spectroscopic factors for $j = \ell \pm \frac{1}{2}$ by measuring the vector analysing power.

Using the properties of the c.f.p. (discussed in Appendix-A), the expression for the sum rules (Macfarlane and French, 1960) can be obtained for transfer reactions. It takes the form,

$$\sum_{T_f} S^{p.u.}(\rho) = n \qquad \ldots(2\text{-}34)$$

where the summation over T_f includes spin and isospin, as well as other labels, for example, seniority and reduced isospin. The number n gives the number of particles in the initial state $^{n}\,T_i$.

It can also be shown that the particles in the other active shells are not affected. These sum rules will be very useful in putting an upper limit on the experimentally measured S-factors. The sum rules for single-nucleon pickup and stripping reactions are listed in table 2-1 (Macfarlane and Schiffer, 1974; Puttaswamy, 1973).

2.8. TWO-NUCLEON SPECTROSCOPIC AMPLITUDES

In this section a discussion of the importance of shell-model calculations in direct two-nucleon transfer reaction of the type,

$$A + a \longrightarrow B + b,$$

with $A = B + 2$ and $b = a + 2$ has been made. It will be shown (in Chapter III) that, unlike in the case of single-nucleon transfer reaction, the nuclear structure part cannot be separated from the kinematics part in the reaction cross section (Glendenning, 1963, 1965, 1978). Here, each term containing the kinematical and mechanism parts will be

weighted by spectroscopic amplitudes defined by an overlap of initial and final states of the reaction. These amplitudes are given by ,

$$S^{\frac{1}{2}}(\rho\lambda;\Gamma) = \sqrt{\tfrac{1}{2}n(n-1)}\int(\quad)$$

$$= \sqrt{\tfrac{1}{2}n(n-1)}\langle$$

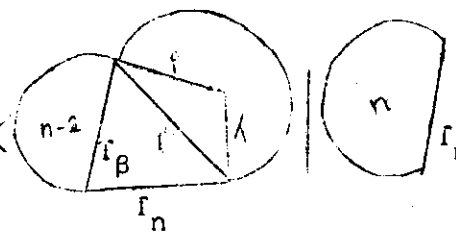

$$\Big|\, \Gamma_n \rangle, \qquad \ldots(2\text{-}35)$$

where β refers to $[n_1\ l_1 j_1][n_2\ l_2 j_2]$ and other quantum numbers of the transferred pair of particles. The bra function for n-2 particles represents a configuration of (n-2) nucleons distributed over one or more single-particle orbits. This group is coupled to the transferred anti-symmetric two-particles group $(\rho\lambda)_\Gamma$ to a total spin and isospin Γ_n. Similarly, the ket function for n particles represents the configuration of n particles distributed over one or more single-particle orbits.

The angular momentum and isospin considerations in equation (2-35) gives some special selection rules for two-nucleon transfer reactions on even-even target nuclei (details of this aspect are discussed in section 3.1.2.)

Now let us consider a nucleus which can be regarded as consisting of a core with the remaining particles moving

in three active orbits ρ_1, ρ_2 and ρ_3, and having occupation number n_1, n_2 and n_3 respectively. Then by the notation used in Macfarlane and French (1960), one can write the wave function for the initial state as (Towner and Hardy 1969),

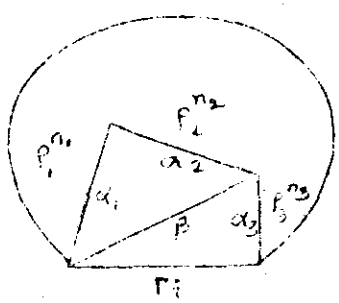

If the two nucleons are picked up from the outermost shell ρ_3 then the wave function $_f$ can be written as,

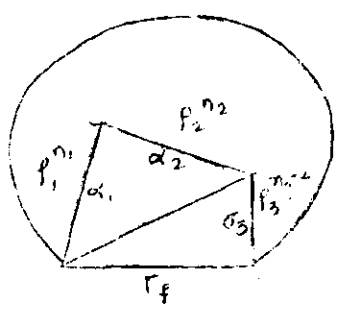

The overlap of initial and final states then takes the form,

$$\mathcal{J}_{if}(\rho_3^2\ ;\ \Gamma) \;=\; \binom{n_3}{1}^{\frac{1}{2}} \binom{n_1+n_2+n_3}{2}^{\frac{1}{2}}$$

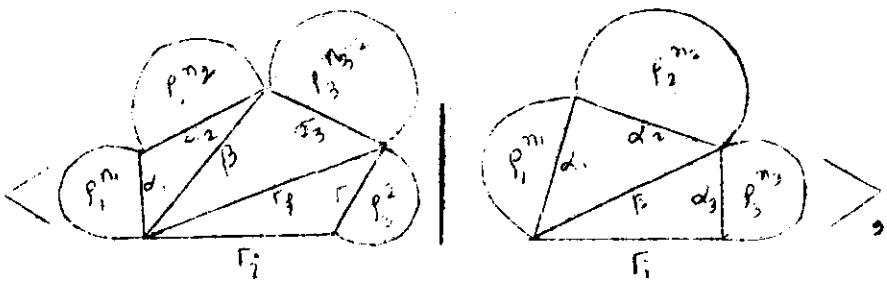

...(2-36)

where the antisymmetrised wave function in the matrix element has been written as a product of wave functions in which the three shells are separately antisymmetrised. Now expanding the ket in terms of the double parentage coefficient (d.p.c., for example see Appendix-A), we get,

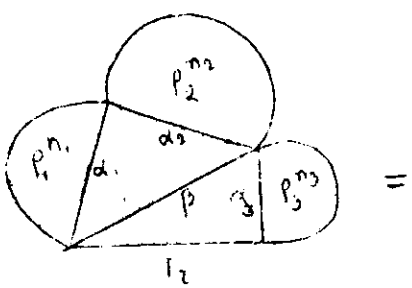

$$= \sum_{y_3'\sigma_3'\Gamma'\Gamma_f'} \langle \rho_3^{n_3}(x_3\alpha_3) \| \rho_3^{n_3-2}(y_3'\sigma_3')\ \rho_3^2(\Gamma') \rangle$$

$$\times\ U(\beta\sigma_3'\Gamma_i\Gamma'\ ;\ \Gamma_f'\alpha_3)$$

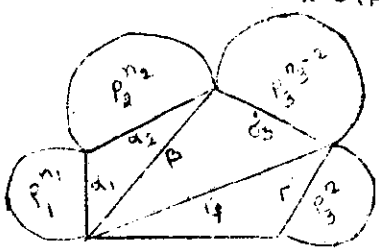

...(2-37)

Substituting (2-37) in (2-36) the spectroscopic amplitude takes the form,

$$S^{\frac{1}{2}}_{if}(\rho_3^2;\Gamma) = \binom{n_3}{2}^{\frac{1}{2}} \langle \rho_3^{n_3}(x_3\alpha_3)| \rho_3^{n_3-2}(y_3\sigma_3)\rho_3^2(\Gamma)\rangle$$

$$\times U(\beta\sigma_3\Gamma_i\Gamma\ ;\Gamma_f\alpha_3). \qquad \ldots(2\text{-}38)$$

Similarly for the cases wherein

i) both particles are picked up from the ρ_2-shell,

ii) both particles are picked up from the ρ_1-shell,

iii) one from the ρ_2 and another from the ρ_3-shell,

iv) one from the ρ_1 and the other from ρ_3-shell, and

v) one from the ρ_1 and the other from ρ_2-shell

are involved, have been discussed in detail by Towner and Hardy (1969) (see also Brussaard and Glaudemans, 1977, Puttaswamy, 1979). Similar expressions hold good for stripping reactions.

These expressions can be generalized for a realistic case wherein mixed configurations are involved. The wave functions for initial and final nuclear states can be written as per equation (2-20) as,

$$\Psi^{J_iT_i} = \sum_p a_p\Phi_p \qquad \text{and} \qquad \Psi^{J_fT_f} = \sum_q b_q\Phi_q$$

where $_p$ and $_q$ are the basic sets (described in section 2.4) and the expansion coefficients can be determined as mentioned earlier. Then the spectroscopic amplitudes is

given by,

$$S^{\frac{1}{2}}(\gamma,JT) = \sum_{p,q} a_p b_q S^{\frac{1}{2}}_{pq}(\gamma,JT) \qquad \ldots(2\text{-}39)$$

Where $S^{\frac{1}{2}}_{pq}$ is spectroscopic amplitude for pure shell-model configuration and is similar to equation (2-38). (This essentially contains d.p.c., normalized Racah coefficients and the Wigner 9-j symbols).

A number of shell-model calculations on two-nucleon spectroscopic amplitudes are available in litrature. See for example, Cohen and Kurath (1970), Wildenthal and Chung (unpublished) and very recently by Glaudemans et al (quoted in Nann et al, 1981).

It can be seen from equation (2-39) that the two-nucleon spectroscopic amplitudes are very sensitive to the sign and the values of the coefficients a_p and b_q, which are determined by shell-model calculations. Also a consistent procedure should be adopted in determining $S^{\frac{1}{2}}(\gamma,F)$. The two-nucleon transfer reactions thus can be used as an efficient tool to verify the shell-model predictions provided the mechanism of the reaction is fairly well understood.

The S-factors and the two-nucleon spectroscopic amplitudes deduced from the shell-model calculations have been used to interpret and to elucidate the nuclear structure of many nuclei in the later chapters.

Table 2-1. Sum Rules in Single-Nucleon-Transfer Reactions

STRIPPING :

$$(\text{Neutron holes})_j = \sum gS_+$$

$$(\text{Proton holes})_j = \frac{2T}{2T+1}\sum gS_- + \frac{1}{2T+1}\sum gS_+$$

$$(\text{All holes})_j = \sum \frac{2T_f+1}{2T+1}\, gS$$

PICKUP :

$$(\text{Protons})_j = \frac{2T+1}{2T+2}\sum S_+$$

$$(\text{Neutrons})_j = \sum S_- + \frac{1}{2T+2}\sum S_+$$

$$(\text{Nucleons})_j = \sum S$$

Notation :

J, T are spin and isospin of the target respectively, J_f, T_f are the spin and isospin of the final nuclear level. S_+, S_- refers to the values of S-factor for $T_f = T\pm\frac{1}{2}$ respectively and $g = (2J_f+1)/(2J+1)$.

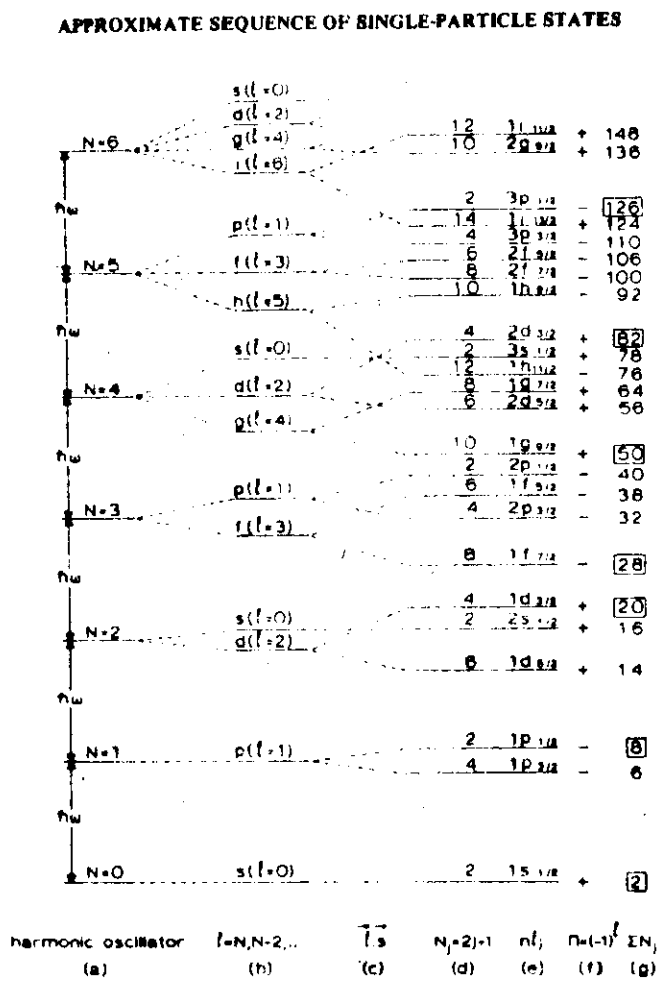

Fig. 2.1. Single-particle energy-level diagram for HO and WS potentials, and the effect of spin-orbit potential.

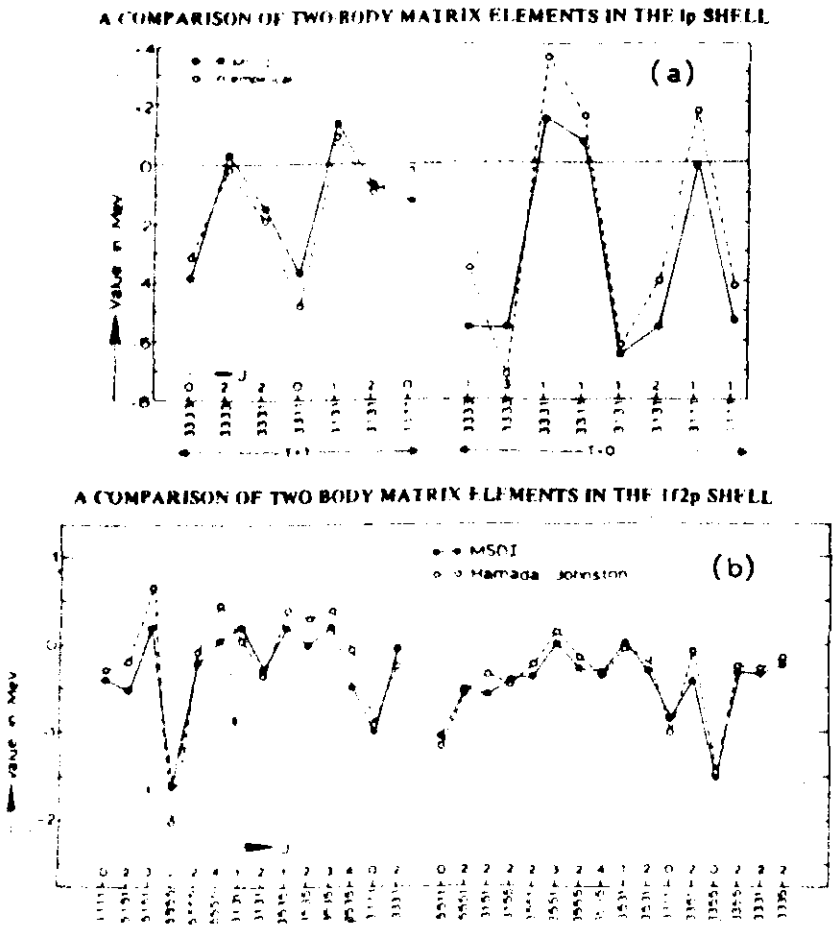

Fig. 2.2. Comparison of values of two-body matrix elements. (a) For 1p-shell configuration space MSDI (with A_1= 2.64 MeV, A_0= 1.15 MeV, B= 1.40 MeV and C= -0.19 MeV) is compared with those obtained empirically (Cohen and Kurath, 1965). (b) For 1f2p shell configuration space the MSDI calculation (A_1=0.6 MeV, B=0.2 MeV and C=0) are compared with matrix elements obtained from a realistic Hamada-Johnston potential (Lowson et al 1966). The n j values are specified by e.g., 3 for $p_{3/2}$, 1 for $p_{1/2}$; 3331 denotes $\langle 33|V|31\rangle$.

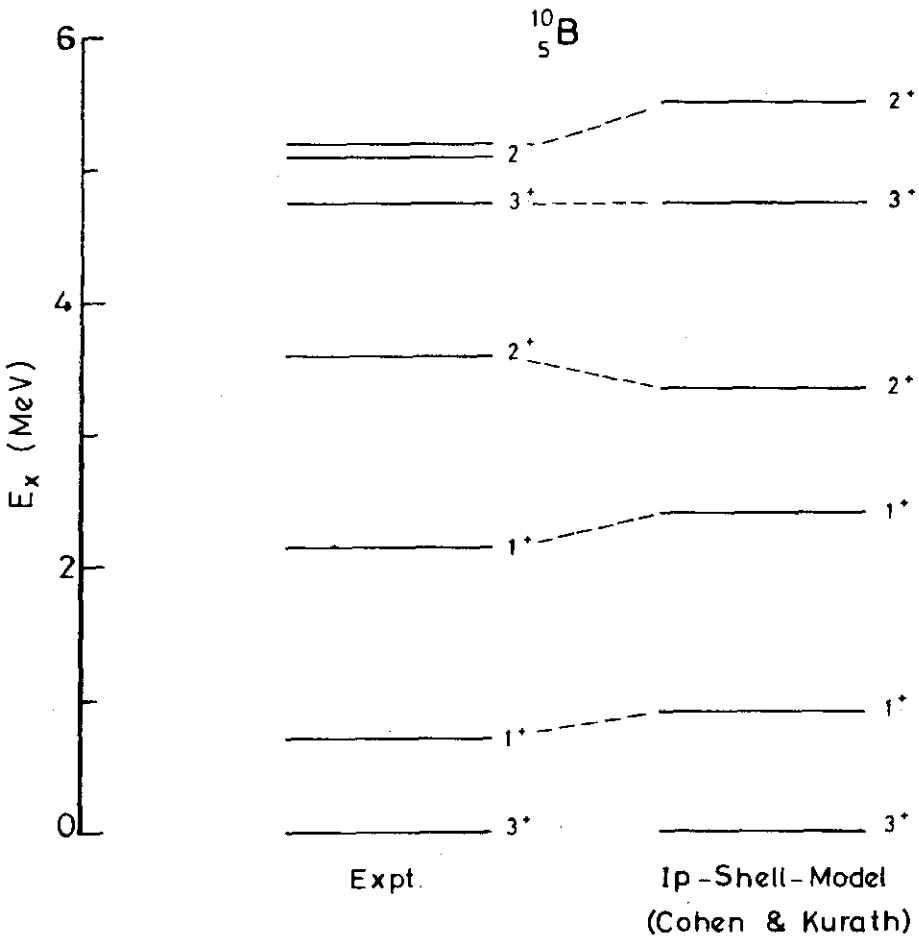

Fig. 2.3. Comparison of the experimental and the predicted level energies for ^{10}B.

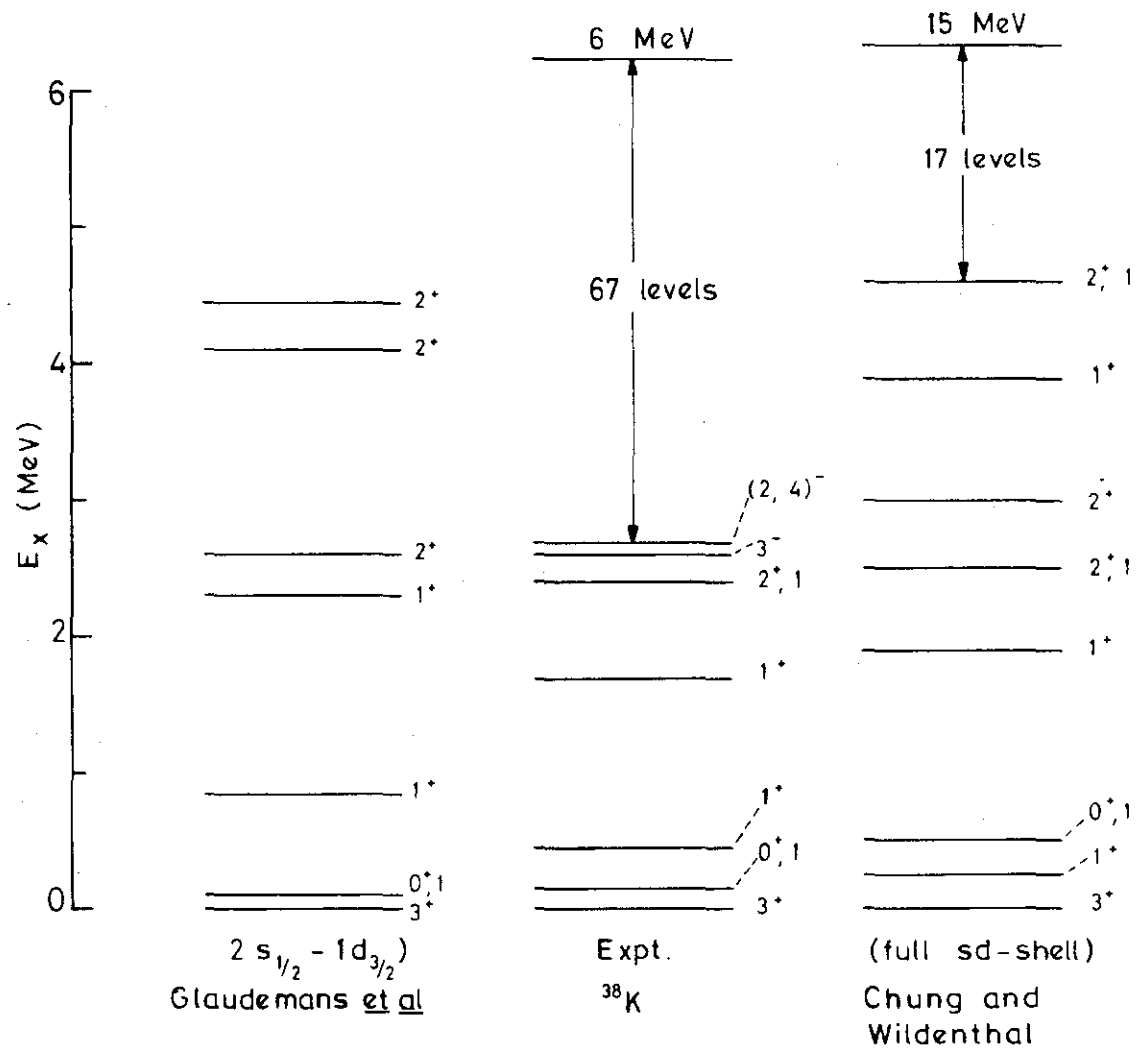

Fig. 2.4. Comparison of the energy levels of ^{38}K from various shell-model calculations with the experimental spectrum. The isospin quantum number is indicated only for the T=1 levels.

CHAPTER III

DWBA THEORY FOR SINGLE- AND TWO-NUCLEON TRANSFER REACTION

The importance of nuclear models in the nuclear structure studies has been considered in the previous chapter. In order to understand as to how the level properties of the nucleus can be deduced by the direct reaction studies, a quantitative description of the direct-reaction theory is given here.

Direct reactions assume that a transition from the incident channel to the reaction channel takes place in one step. The formalism successfully used is the distorted wave Born approximation (DWBA). In the DWBA theory of nuclear reaction it is assumed that a perturbation gives rise to non-elastic processes. This additional interaction affects some simple internal degrees of freedom of one of the two nuclei involved in the collision. Most widely used type of internal degree of freedom is that, one nucleus is regarded as consisting of two nuclides held together in a bound state by their mutual attraction. The other nucleus is then allowed to interact directly with one of these two to produce an inelastic scattering or a rearrangement collision. This interaction is regarded as a perturbation added to the optical-model potential which acts between the centre of mass of the two interacting nuclei. The detailed quantum mechanical theory of DWBA formalism for

single- and two-nucleon transfer reactions and their applications in the analysis of various reactions is available in several references published in recent years (Glendenning, 1978; Hodgson, 1971; Austern, 1970; Jackson, 1970; Towner and Hardy, 1969; Tobocman, 1961).

3.1. DWBA TRANSITION AMPLITUDES AND CROSS SECTIONS

A direct nuclear réaction can be represented as,

$$a + A \longrightarrow B + b ,$$

where a and A represent the projectile and the target nuclei respectively and, B and b the residual nucleus and the out-going light particle respectively. The channels a + A and b + B are called as entrance and exit channels respectively. The direct reactions are normally devided into stripping and pickup reactions. In a stripping reaction the projectile is stripped off x nucleons so that the target nucleus A has x nucleons add to it thus forming the residual nucleus B (=A + x). In a pickup reaction the x nucleons are pickedup by the projectile from the target causing the transition $B \rightarrow A$.

The transition amplitude for a direct reaction is derived from basic quantum mechanical considerations (see for example, Glendenning, 1978 and 1963). This has the form,

$$\mathcal{J}_{\beta\alpha} = \langle \chi_\beta^{(-)} \Phi_\beta \mid V_\beta - U_\beta \mid \Psi_\alpha^{(+)} \rangle \qquad \ldots(3\text{-}1)$$

Where $\Psi_\alpha^{(+)}$ is the exact wave function for the entrance channel α. Φ_β is a function of the internal coordinates of the particles involved in the exit channel β. The function $\chi_\beta^{(-)}$ describes the relative motion of the pairs b and B. V_β is the interaction between two nuclei in the channel β and the U_β is the corresponding optical potential. The exact expression for $\mathcal{J}_{\beta\alpha}$ given in equation (3-1) can not be solved because it involves the exact scattering solution to the many-body problem . Physically useful results are obtained by developing approximate methods for the computation of Ψ. . In Born approximation one assumes that the function can be replaced by the product of Φ_α and $\chi_\alpha^{(+)}(\vec{k}_\alpha, \vec{r}_\alpha)$, where the Φ_α is the function of the internal coordinates and χ_α describes the relative motion of the particles a and A. Thus the equation takes the form,

$$\mathcal{J}_{\beta\alpha}^{DW} = \langle \chi_\beta^{(-)} \Phi_\beta \mid V_\beta - U_\beta \mid \chi_\alpha^{(+)} \Phi_\alpha \rangle \qquad \ldots(3\text{-}2)$$

The distorted waves χ_β and χ_α are essentially obtained from solvable optical-model problem in the channels α and β. Thus the DWBA theory assumes that the final channel β is reached directly from the entrance channel α.

The above form of the DWBA amplitude is referred to as "post" form of the exact transition amplitude. A similar amplitude may be derived from the "prior" form of the exact amplitude. This differes from equation (3-2) only in that $(V_\beta - U_\beta)$ is replaced by $(V_\alpha - U_\alpha)$. However it can be shown that the two forms of DW amplitudes are equal on the energy shell (Austern, 1970). Therefore one is free to use any form of the DW transition amplitude.

The explicit form for Φ_α and Φ_β are

$$\Phi_\alpha = \Phi_{J_A}^{M_A}(\vec{A})\ \phi_a(r)\ X_{s_a}^{m_a}$$
$$\Phi_\beta = \Phi_{J_B}^{M_B}(\vec{A},\vec{r}_x)\phi_b(r)\ X_{s_b}^{m_b} \qquad \ldots(3\text{-}3)$$

Here $\vec{A}$ refers to the nucleon coordinates. X denotes the spin wave function. ϕ indicates the radial wave function. J refers to the angular momentum and M is the corresponding projection quantum number.

The interaction potential $V_\beta - U_\beta$ can be written as,

$$V_\beta - U_\beta = V_{b,B} - U_{b,B}$$
$$= V_{b,x} + V_{b,A} - U_{b,B}\ . \qquad \ldots(3\text{-}4)$$

It is customarily argued that $V_{b,A} - U_{b,B} \approx 0$. Then the equation (3-2) becomes

$$\mathcal{T}_{\beta\alpha} = J \int \chi_{\beta}^{(-)*}(\vec{k}_{\beta},\vec{r}_{\beta}) \langle \Phi_B \phi_b | V_{b,x} | \phi_a \Phi_A \rangle \chi_{\alpha}^{(+)}(\vec{k}_{\alpha},\vec{r}_{\alpha}) d\vec{r}_{\alpha} \qquad \ldots(3\text{-}5)$$

where $\vec{r}_{\alpha} = \vec{r}_a - \vec{r}_A$ and $\vec{r}_{\beta} = \vec{r}_b - \vec{r}_B$ are the relative coordinates. J refers to the Jacobian of transformation of coordinates.

In this thesis, mainly two types of reactions have been considered, viz., single-nucleon (x is either proton or neutron) and two-nucleon (e.g., x is a n-p pair) transfer reaction. Depending on the type of the reaction, the situation slightly differs. In any case the wave function of the residual nucleus can be expanded in terms of the eigen states of the target nucleus i.e., an antisymmetrised (A+x)-nucleon wave function for the residual nucleus is expanded in terms of the states for the first A nucleons in the target (see Appendix A).

In the next two sub-sections the single- and two-nucleon transfer reactions are separately discussed.

3.1.1. Single-Nucleon Transfer Reactions

The application of the general results to particular cases often involves additional assumptions. Therefore, the DW formalism is developed here with reference to a particular example of a stripping reaction viz., (d,p) reaction and then it is outlined as to how this is modified

for (d,t) and (d,^{3}He) reactions.

The angular momentum conservation for single-nucleon transfer reaction suggests that,

$$\vec{j} = \vec{J}_A - \vec{J}_B, \quad \vec{s} = \vec{s}_d - \vec{s}_p, \quad \vec{\ell} = \vec{j} - \vec{s} \qquad \ldots(3\text{-}6)$$

and in addition, the parities are connected by

$$\pi_B = \pi_A(-1)^{\ell} \qquad \ldots(3\text{-}7)$$

where $\vec{j}$, $\vec{s}$, and $\vec{\ell}$ are the total angular momentum, spin and orbital angular momentum of the transferred particle. π refers to the parity of nuclear state. Considering the fractional parentage expansion of the residual nuclear wave function, we may write,

$$\Phi^{M_B}_{J_B}(\vec{A},\vec{r}_n) = \sum_{A'\ell j} \beta_{\ell j}(B,A') \mathcal{A}[\Phi_{J_{A'}}(\vec{A})\ \phi_{n\ell j}(\vec{r}_n)]^{M_B}_{J_B} \qquad \ldots(3\text{-}8)$$

where $\mathcal{A}$ is an antisymmetrisation operator. The β's are generalized coefficients of fractional parentage and their values depend on the detailed structure of nuclear wave functions. The square bracket denotes the vector coupling. The $\phi_{n\ell j}$ denotes a spin-orbit function for a shell-model state (see e.g., equation (2-7)). The square of the amplitudes $\beta_{\ell j}$ are called spectroscopic factor $S_{\ell j}$. Substituting these results into equation (3-5) the DW

transition amplitude takes the form,

$$\mathcal{J}_{pd}(J_A M_A \mu_d \rightarrow J_B M_B \mu_p) = \sum_{lj} \langle J_A M_A j m_j | J_B M_B \rangle \langle \tfrac{1}{2}\mu_p \tfrac{1}{2}\mu_n | 1\mu_d \rangle \langle l m \tfrac{1}{2}\mu_n | j m_j \rangle \sqrt{(2l+1)}\; B_l^{m_l}\; S_{lj}^{\frac{1}{2}} \qquad \ldots(3\text{-}9)$$

where

$$B_l^{m_l}(\vec{k}_p, \vec{k}_d) = i^{-l}(2l+1)^{-\frac{1}{2}} \int \chi_p^{(-)*}(\vec{k}_p, \vec{r}_p)\; \phi_{nl}^{m_l *}(r_n) V_{pn}(r)\; \chi_d^{(+)}(\vec{k}_d, \vec{r}_d)\; \phi_d(r)\, d\vec{r}_n d\vec{r}_p \; . \qquad \ldots(3\text{-}10)$$

Then the cross section for the case where unpolarized beam and targets are involved, is obtained by summing over all magnetic quantum numbers, and it takes the form,

$$\frac{d\sigma}{d\Omega} = \frac{1}{2} \frac{m_d m_p}{(2\pi\hbar^2)^2} \frac{k_p}{k_d} \frac{2J_B+1}{2J_A+1} \sum_{jl} S_{lj} \left| B_l^{m_l} \right|^2 \qquad \ldots(3\text{-}11)$$

Where m_d and m_p are reduced masses. This expression exhibits a division into two factors viz., a factor S_{lj} called the spectroscopic factor which depends only on properties of the nuclear levels wherein the transition has taken place, and a factor $|B|^2$ which contains all of kinematical dependence through the wave function of the relative motion and their overlap with each other. In addition it contains the wave function of the neutron.

To calculate the cross section (3-11), it remains to evaluate $B_l^{m_l}$: A direct evaluation is more difficult since a six-fold integration is involved. However in many cases the zero-range approximation is employed to simplyfy the evaluation. In this approximation

$$D(\vec{r}) = V_{pn}(\vec{r})\ \phi_d(r) = D_o\delta(r). \qquad \ldots(3\text{-}12)$$

There are several wavs of estimating the values of D_o. With the zero-range approximation the coordinates are,

$$\vec{r}_d \longrightarrow \vec{r}_n \quad \text{and} \quad \vec{r}_p \longrightarrow \frac{A}{A+1}\vec{r}_n\ , \qquad \ldots(3\text{-}13)$$

so that B becomes,

$$B_l^{m_l} = (i)^{-l}\ (2l+1)^{-\frac{1}{2}}D_o \int \chi_p^{(-)*}(\vec{k}_p, \frac{A}{A+1}\vec{r})\ \phi_l^{m_l}((\vec{r})$$
$$\chi_d^{(+)}(\vec{k}_d, \vec{r})\, d\vec{r}. \qquad \ldots(3\text{-}14)$$

The formalism can be extended to the other single-nucleon stripping reactions induced by tritons, ^{3}He or α-particles. Then the $B_l^{m_l}$ will be modified due to the wave function of the incident and exit particles, which will be independent of the transition involved. The reaction cross section (3-11) will differ by a normalization constant N'.

The expression for the pickup reactions can be obtained by using the principle of detailed balance. For calculational convenince the equation (3-11) with zero-range approximation will be factorized into a reduced

cross section $\sigma_{\ell sj}$ and a factor $S_{\ell j}$ as,

$$\frac{d\sigma}{d\Omega} = N \sum_{\ell j} S_{\ell j} \sigma_{\ell sj} \, . \qquad \ldots(3\text{-}15)$$

where N depends on the overlap of the wave function of the light particles. Hence the value of N is different for different types of reactions and can be obtained either empirically or theoretically (Hodgson 1971). Recently, available values for (d,t) and (d,^{3}He) reactions have been listed in a table B-1 in Appendix B.

So far, the isospin of the interacting particles have not been taken into account. In the isospin formalism, equation (3-15) includes an extra factor $C^2 = \langle T_A M - m \tfrac{1}{2} m | T_B M \rangle^2$ where $T_A = \frac{1}{2}(N-Z)$, $M_A = T_A$, $m = \frac{1}{2}$ and T_B is the isospin of the residual nuclear state. The values of C^2 are listed in table 3-1. Thus the expression that is to be compared with the experimental differential cross section is,

$$\frac{d\sigma}{d\Omega} = N \sum_{\ell j} C^2 S(\ell j) \; \sigma^{DW}_{\ell sj}(\Theta) \qquad \ldots(3\text{-}16)$$

The $\sigma_{\ell sj}(\Theta)$ will be calculated by using standard DWBA codes (discussed further in Appendix B). The quantity $C^2S(\ell j)$ is called as the spectroscopic strength.

The central aim of the single-nucleon transfer reactions is to determine the spectroscopic factor $C^2S(\ell j)$ and thereby measure the overlap between the initial state

and the final state plus one nucleon (or one hole).

In practice, the spectroscopic strength $C^2S(\ell j)$ for a transition is determined by comparing the experimentally measured $d\sigma/d\Omega$ with the theoretically determined $\sigma_{\ell j}(\Theta)_{DW}$. They naturally tend to be quite sensitive to the choice of the radial wave function in the single-particle form factor. A 10 % change in the radius of the single-particle potential may change the spectroscopic factor by a factor of two, without changing the shape of the angular distribution appreciably (Macfarlane and Schiffer 1974). Therefore the best procedure is to use a cosistent average set of parameters which have been tested against a number of nuclei in the same vicinity including some closed shell nuclei where the same (ℓj) orbit is involved. The spectroscopic factors can also be tested against the sum rules given in table 2-1 (Chapter II), which puts the upper limits to the measured spectroscopic strengths. An uncertainty of 20 % should be regarded as implicit in all spectroscopic factors, and this uncertainty is still larger for weaker transitions (Macfarlane and Schiffer 1974)

3.1.2. Two-Nucleon Transfer Reactions

Basically the DWBA theory of two-nucleon transfer reactions is very similar to that for the single-nucleon transfer reactions. The formalism is more involved because of the difficulty in describing the group of transferred

particles. The angular momentum coupling is much more complicated. In particular, this has an additional selectivity that depends upon the degree to which the transferred nucleons are correlated in the nucleus. Such correlations can be imposed by the angular momentum coupling as well as by the inter-nucleon forces.

Here the DWBA formalism of two-nucleon transfer reaction with reference to (α,d) reaction is developed. The DWBA transition amplitude for (α,d) reaction takes the form (Glendenning 1963)

$$\mathcal{J} = w \int \chi_d^{(-)*}(\vec{k}_d,\vec{R}'_d) \langle \Phi_B(A+x)\phi_d(\vec{r}_d)X_1^{\mu_d}(\vec{\sigma}_d) \left| V \right| \Phi_A(A) \phi_\alpha(\vec{r}_\alpha)X_0^0(\vec{\sigma}_x,\vec{\sigma}_d)\rangle \chi_\alpha^{(+)}(\vec{k}_\alpha,\vec{R}_\alpha)\, d\vec{r}_d d\vec{r}_1 d\vec{r}_2 d\vec{A} \qquad \ldots(3\text{-}17)$$

x refers to the stripped particle and d refers to the outgoing particle. $\vec{r}_\alpha$ stands for the internal coordinate of α-particle and the center-of-mass coordinate of the outgoing deuteron is given by,

$$\vec{R}'_d = \vec{R}_d - \frac{m_d}{M_B}\vec{R}_x$$

For the wave function of the nucleus B an expansion analogous to equation (3-8) is introduced viz.,

$$\Phi_{J_B}^{M_B}(A+x) = \sum_{F\gamma LSJ} \beta_{F\gamma LSJ} \sum_{M_{A'}M_J} \langle J_A, M_A, JM_J | J_B M_B \rangle \Phi_{J_{A'}}^{M_{A'}}(\vec{A}) \; \phi_{\gamma LSJ}^{M_J}(\vec{r}_x, \vec{R}_x, \vec{\sigma}_x) \qquad \ldots(3\text{-}18)$$

where

$$\Phi_{\gamma LSJ}^{M_J} = i^L \sum_{M_L M_S} \langle LM_L SM_S | JM_J \rangle \, \chi_S^{M_S}(\vec{\sigma}_x) \; \phi_{\gamma L}^{M_L}(\vec{r}_x, \vec{R}_x). \qquad \ldots(3\text{-}19)$$

Here S refers to the spin of the transferred pair of particles and γ refers to the quantum numbers $(n_p l_p j_p, n_n l_n j_n)$ for stripped particles p and n. L and S refer to the orbital angular momentum quantum number and spin of the p-n pair, respectively.

For α-particles, the space wave function corresponds to the relative s-state of motion among all the particles and hence is symmetric. The spin wave function must therefore be antisymmetric with respect to the interchange of the protons or neutrons. That is,

$$\chi_0^0(\vec{\sigma}_x, \vec{\sigma}_d) = \tfrac{1}{2} \sum_{S'M_{S'}} (-)^{S'+M_{S'}} \chi_{S'}^{-M_{S'}}(\vec{\sigma}_x) \; \chi_{S'}^{M_{S'}}(\vec{\sigma}_d) \qquad \ldots(3\text{-}20)$$

where S' is summed over 0 and 1. Using the orthogonality properties of the wave functions, the final expression for the DW transition amplitude becomes,

$$\mathcal{J} = \tfrac{1}{2}(-)^{1+\mu_d}\, fC \sum_{\gamma L 1} \beta_{\gamma L 1 J} \langle J_A M_A J M_J | J_B M_B \rangle$$

$$\sum_{M_L} \langle L M_L 1 - \mu_d | J M_J \rangle \quad \sqrt{2L+1}\; B_{\gamma L}^{M_L} \qquad \ldots(3\text{-}21)$$

where fC is a statistical factor with

$$f = \tfrac{1}{2}\left(\frac{a!}{(a-2)!}\,\frac{(A+2)!}{A!}\right)^{\frac{1}{2}}$$

and $\qquad \ldots(3\text{-}22)$

$$C = \langle T_A M_{T_A} T M_T | T_B M_{T_B} \rangle$$

The value of C is unity for (α,d) reaction because only $T = 0$ states are excited. The spin overlap in equation (3-17) requires that $S = 1$, i.e., only the triplet part of the wave function for the stripped nucleons can be excited. The $B_{\gamma L}^{M_L}$ is given by,

$$B_{\gamma L}^{M_L}(\vec{k}_\alpha,\vec{k}_d) = i^L (2L+1)^{-\frac{1}{2}} \int [\chi_d^{(-)}(\vec{k}_d,\vec{R}_d)\phi_d(\vec{r}_d)\phi_{\gamma L}^{M_L}(\vec{r}_x,\vec{R}_x)]^*$$

$$V_{x,d}[\chi_\alpha^{(+)}(\vec{k}_\alpha,\vec{R}_\alpha)\phi_\alpha(\vec{r}_\alpha)]\, d\vec{r}_x d\vec{R}_x d\vec{R}_d d\vec{r}_d \,. \qquad \ldots(3\text{-}23)$$

Then the cross section is given by,

$$\frac{d\sigma}{d\Omega} = \frac{1}{4}\,\frac{m_\alpha m_d}{(2\pi\hbar^2)^2}\,\frac{k_d}{k_\alpha}\,\frac{2J_B+1}{2J_A+1}(fC)^2 \sum_{LJM}\left|\sum_\gamma \beta_{\gamma L 1 J}\; B_{\gamma L}^{M}\right|^2 . \qquad \ldots(3\text{-}24)$$

From the equation (3-24) it can be noticed that the different L, J and M contribute incoherently. But the sum on γ

introduces a coherent effect thus increasing the sensitivity of the differential cross section to the sign of the spectroscopic amplitudes. Thus the two-nucleon transfer reactions can be used as an efficient tool to check the shell-model wave functions.

The cross section for the (d,α) reaction can be obtained by using principle of detailed balance and can be written as,

$$\left(\frac{d\sigma}{d\Omega}\right)_{(d,\alpha)} = \frac{11}{12} \frac{m_d m_\alpha}{(2\pi\hbar^2)^2} \frac{k_\alpha}{k_d} f^2 \sum_{LJM} \left| \sum_{\gamma} \beta_{\gamma L 1 J} B^M_{\gamma L} \right|^2 . \qquad \ldots(3\text{-}25)$$

Assuming zero-range interaction between the incoming particle and the center-of-mass position of the transferred nucleons, the above equation for the cross section takes the form,

$$\left(\frac{d\sigma}{d\Omega}\right)_{expt} = N \sum_J \frac{1}{2J+1} \sigma_{DWUCK}(\Theta) . \qquad \ldots(3\text{-}26)$$

Here N is the normalization constant which depends on the overlap of the deuteron and α-particle wave functions and on the strength of the interaction potential. Therefore N should be independent of the specific transition studied. It is customary to write N interms of D_0^2 (Towner and Hardy, 1969; Baer et al, 1973). D_0^2 can be estimated by knowing the wave function of the light particles and the strength of the interaction causing the transition (for

example see Amusa, 1975). The $\sigma_{DWUCK}(\Theta)$ is the reduced cross section and it has the form,

$$\sigma_{DWUCK} = \frac{1}{(2\pi\hbar^2)^2} \frac{A\alpha}{(A+\alpha)^2} (A+x)(\alpha-x)$$

$$\sum_{ML} \frac{1}{2L+1} \left| \int d^3R \; \chi_d^{(-)*} F_{JL1O}(R) Y_L^M(R) \chi_\alpha \right|^2 \qquad \ldots(3\text{-}27a)$$

where

$$F_{JL1O}(R) = \sum_\gamma S_{AB}^{\frac{1}{2}}(\gamma, JO) f_{L\gamma}(R) \qquad \ldots(3\text{-}27b)$$

with two-nucleon spectroscopic amplitudes given by,

$$S_{AB}^{\frac{1}{2}}(\gamma, JO) = \sqrt{\tfrac{1}{2}n(n-1)}\,\beta_{\gamma L1J}$$

where n is the number of the active particles. The $f_{L\gamma}(R)$ is essentially a two-nucleon form factor for pure configuration $(n_p \ell_p j_p, n_n \ell_n j_n)$ and the radial wave function for the center-of-mass motion of the pair in the configuration γ coupled to L. R is the center-of-mass coordinate of the pair relative to the residual nucleus.

Three different methods have been suggested in literature for the evaluation of $f_{L\gamma}(R)$ (Hodgson, 1971). The methods which are widely used are outlined below,

1. In the first method (Glendenning, 1963, 1965, 1978) the single-particle wave function for bound particles is obtained as a solution of the Schrödinger equation

in a harmonic oscillator potential. The two-particle wave function can be transferred to relative and center-of-mass coordinates of the pair. Explicit expression for the expansion coefficents and their values are tabulated by Glendenning (1975).

In direct two-nucleon transfer reactions the surface region of the nucleus is of interest. Therefore the tail region of the projected wave function $f_{L\gamma}(R)$ taken in this way has to be improved. A way of improving this is suggested by Glendenning (1965), wherein the tail of $f_{L\gamma}(R)$ is equated to a Hankel function $i^L h_L^{(1)}(ikR)$ where $k^2=(4m/h^2)\varepsilon_B$, 2m is the reduced mass of the pair in A and $-\varepsilon_B$ is their effective binding energy to the core B.

2. In the second method the two-nucleon wave function for the transferred particles is taken to be the product of the single-particle Woods-Saxon wave function with different radial dependence. These are expanded in terms of harmonic-oscillator wave functions (upto 10 terms) and separated into radial and center-of-mass components by Moshinsky transformation. A more direct method which contains only the zero angular momentum part of the wave function has been developed by Bayman and Kallio (1967). Kunz (1969) has adopted this method in the computer code DWUCK (see Appendix B).

The method of Bayman and Kallio (1967) uses single-particle wave functions of realistic potential (viz., Woods-Saxons shape) whose parameters are adjusted to reproduce the binding energy of individual particle (generally taken to be one half of the two-particle separation energy). This way of selecting single-particle wave functions may lead to an ambiguity. Recently a systematic study of the dependence of the DWBA cross section on the single-particle separation energy has been made by using different options for the single-particle separation energy for (d,α) reaction on 1p-shell nuclei (Van der Woude and de Meijer, 1976). It is found that the variation for the different options is not much. This method of evaluating the $f_{L\gamma}(R)$ is widely used in literature even though it is limited to the relative angular momentum zero part of the wave function of the two particles.

In the present analysis of the (d,α) reaction data on ^{40}Ca and ^{12}C, the Bayman and Kallio method of form factor derivation has been used.

The conservation of angular momentum used in writing down the equation (3-25) gives some selection rules peculiar to the (d,α) reaction on even-even target nuclei. Generally,

$$\vec{J} = \vec{J}_B - \vec{J}_A = \vec{j}_n + \vec{j}_p = \vec{L} + \vec{S}$$

where $\vec{L} = \vec{\ell}_n + \vec{\ell}_p$, $j_i = \ell_i \pm \frac{1}{2}$, and $\vec{T} = \vec{T}_B - \vec{T}_A = 0$. Since the nucleons in the deuteron and the α-particle are assumed to be in a relative S-state of motion, additional selectional rules will arise, viz.,

$$S + T = 1, \quad S = 1, \quad \text{and} \quad \pi_B \pi_A = (-1)^L = (-1)^{\ell_n + \ell_p},$$

where π_i is the parity of the particle i. For zero-spin target nuclei the selection rules can be summarised as follows:-

1. when two nucleons are transferred from different shells, the total angular momentum transferred is given by

   $J = L, \quad S = 1, \quad T = 0$, if J is even, and
   $J = L \pm 1, \quad S = 1, \quad T = 0$, if J is odd,

2. if the transferred nucleons have the same $(n\ell j)$ quantum numbers, J + T must be odd and $(j)^2_{even}$ pickup is forbidden.

The selection rule-2 will not allow a 0^+ level to be excited in the (d,α) reaction.

3.2. OPTICAL-MODEL POTENTIAL AND DISTORTED WAVES

It is mentioned in the earlier section that the wave functions χ_α and χ_β are essentially the eigen functions of the 'optical-model potentials' (OMP) U_α and U_β respectively.

An elaborate discussion of the OMP for composite particles can be found in Hodgson (1971) and Perey and Perey (1976). The phenomenological OMP for scattering below 300 MeV is written as (see Daehnick et al 1980)

$$U(r) = V_C(r) - V_R f(x) - i[W_S f(x_S) - 4W_D \frac{d}{dx} f(x_D)]$$
$$+ \left(\frac{\hbar}{m_\pi c}\right)^2 2V_{LS}\, \vec{S}\cdot\vec{l}\, \frac{1}{r}\frac{d}{dr} f(x_{LS}) \qquad \ldots(3\text{-}28)$$

where $V_C(r)$ is the Coulomb potential of a spherical uniform charge distribution and

$f(x) = (1 + e^x)^{-1}$ with $x = (r-R)/a$, $R = r_o A^{1/3}$, and $(\hbar/m_\pi c)^2 = 2.00\ fm^2$.

The operator $\vec{S}$ is defined in terms of the spin operator $\vec{\sigma}$ as follows,

$\vec{S} = (\hbar/2)\vec{\sigma}$, for nucleons, ^3He and t,
$= \hbar\vec{\sigma}$, for deuterons, and
$= 0$, for α-particles.

V_R, W_S, W_D and V_{LS} are respectively the real, volume absorption, surface absorption and spin-orbit depths. For spinless particles naturally the spin-orbit term vanishes. For targets with non-zero spin J, the possibility of the spin-spin interaction arises ; at present, there is no evidence that such an interaction is required to fit the data and hence it is not normally included in optical-model calculations (Jackson 1970).

The various parameters of the OMP $U_{a,A}$ or $U_{b,B}$ are obtained by fitting elastic scattering angular distribution data of 'a' on A or 'b' on B (Perey and Perey 1976). It is expected that the potentials vary in a systematic and regular fashion from nucleus to nucleus.

To be completely consistent with the DWBA theory one would need OMP for entrance and exit channels which are determined by the elastic scattering at those energies and on the same nuclei. Further, in the exit channel the energy of the outgoing particle is a function of the Q-value of the reaction leading to each specific level. It is impossible to perform elastic scattering experiments on the excited states (and the ground states of many residual nuclei reached by the (d,t), (d,^{3}He) and (d,α) reactions are unstable). Some concession must therefore be given for the selection of OMP parameters for the outgoing particles.

In some cases the elastic scattering exhibits anomalous behaviour (e.g., in the case of α-scattering on ^{28}Si, ^{39}K and ^{40}Ca). Here reliable set of OMP parameters may not belong to any average set. Then the potential parameters may have to be chosen to optimise the fit to the reaction data (Hodgson 1971).

To evaluate the DWBA transition amplitude, the partial wave expansion of (for example) $\chi_{a,A}$ is used in the form,

$$\chi_{a,A}(\vec{k}_a,\vec{r}_a) = \frac{4\pi}{k_a r_a} \sum_{L_a M_a} Y_{L_a}^{M_a}(\hat{r}_a) Y_{L_a}^{M_a}(\hat{k}_a) i^{L_a} \chi_{L_a}^{(a)}(k_a r_a), \qquad \ldots(3\text{-}29)$$

where each partial distorted wave χ_{L_a} is a solution of a radial Schrödinger equation with central potential $U_{a,A}(r)$ viz.,

$$\left[\frac{d^2}{dr^2} + k^2 - \frac{2\eta k}{r} - \frac{2\mu U_{a,A}(r)}{h^2} - \frac{L(L+1)}{r^2}\right] \chi_L^i(kr) = 0 . \qquad \ldots(3\text{-}30)$$

The center of mass system kinetic energy is $\frac{\hbar^2 k^2}{2\mu}$, where μ is the reduced mass of the pair and η is the Coulomb energy parameter. Dependeng on the energy of the incident particle the number of terms in the partial wave expansion will have to be chosen.

In practice a unique set of parameter values for $U_{a,A}$ (or $U_{b,B}$) cannot be found; it is normally possible to get a family of OMP parameters which fit elastic scattering angular distribution equally well (see for example Perey and Perey, 1976). This ambiguity in OMP parameter sets causes difficulties in DWBA analysis of reaction data because the DWBA transition amplitude depends on the wave function in the region of the nucleus. It is often possible to select a set of parameters which gives a good fit to the experimental angular distributions.

In the case of two-nucleon transfer reactions

such as the (d,α) reaction the DWBA cross section is a coherent sum over various two-nucleon configurations, unlike in the case of single-nucleon transfer reactions. A given set of OMP parameters will have to be tried in combination with the two-nucleon spectroscopic amplitudes predicted by a shell-model calculation.

3.3. NON-LOCAL POTENTIALS

The OMPs dealt with in the previous sections are usually taken to have a simple local form. By 'local' it is meant that at the point '$\vec{r}$' the particle feels the potential at that point. In reality the situation is more complicated because the incident particle can excite the nucleus. Therefore the true state vector describing a system must have many components and these are coupled to each other by virtue of mutual interactions. The fundamental theory shows that the complicated problem involving many channels can be reduced to sa simpler one containing only elastic channel by suitably modifying interaction between the interacting particles. This implies that the OMP should be non-local (Austern, 1970). Thus $U(r)\chi(r)$ in the Schrödinger equation must be replaced by,

$$\int U(\vec{r},\vec{r}\,')\ \chi(\vec{r}\,')\ d\vec{r}\,',$$

where $U(\vec{r},\vec{r}\,')$ is the non-local potential. Perey and Buck (196) have given a separable form for the non-local potential as,

$$U(r,r') = U_o(\tfrac{1}{2}|\vec{r}-\vec{r}'|)\, H(|\vec{r}-\vec{r}'|), \qquad \ldots(3\text{-}31)$$

where H is the non-locality function characterised by a range parameter β. The potential $U(\vec{r},\vec{r}')$ tends to a local potential as the range $\beta \longrightarrow 0$. It has been found that the equivalent local potential obtained in this manner is consistently weaker than $U_o(r)$, and that these two potentials bear a simple relation to each other. It is also found that within the range U_o the magnitude of the local eigen function is consistently larger than that of $\chi(\vec{r})$. This effect has bcommonly been called as the Perey effect. In numerical applications H is taken to be a Gaussian. Then the non-local wave function is related to the local function by,

$$\chi_{NL}(r) = [1 + (\mu\beta^2/h^2)U_L(r)]^{-\frac{1}{2}}\, \chi_L(r), \qquad \ldots(3\text{-}32)$$

where theμ is the reduced mass. (The values of β for various particles have been listed in a table B-2).

3.4. FINITE-RANGE CORRECTION

In the previous sections viz., 3.1.1. and 3.1.2. the zero-range approximation has vbeen described. This approximation is fairly good in many cases because the direct reaction transition amplitude is proportional to the interaction $V(r_{b,x})$. But $V(r_{b,x})$ is short ranged. It is pointed that, for rearrangement collision, the zero-range

approximation cannot be adequate. But an exact finite range calculation involves more computation and therefore takes more computer time. The limitation of the zero-range approximation and an elaborate treatement for finite-range calculation is discussed by Austern (1970). However an approximate procedure which gives fairly good results is to use the local-energy approximation. Buttle and Goldfarb (1964), and Perey and Saxon (1964) have obtained a corfection factor for the zero-range approximation. The potential $V(r_{b,x})$ is assumed to have Gaussian dependence rather than the previously assumed δ-function.

The finite-range integration is based on an expansion about the zero-range limit. This expansion utilizes what is called as the 'local WKB approximation' or 'local energy approximation' (LEA). The result is to modify the form factor by a multiplicative factor,

$$W(r) = [1 + A(r)]^{-1} \qquad \ldots(3\text{-}33a)$$

or

$$W(r) = \exp[-A(r)] \qquad \ldots(3\text{-}33b)$$

with

$$A(r) = \frac{2}{\hbar^2} \frac{m_x m_a}{m_b} R^2 [U_b(r) - U_x(r) - U_a(r) - S_x] \qquad \ldots(3\text{-}34)$$

where S_x is the separation energy of x from B. R is the finite-range parameter. The first form is commonly called as the Hulthen form and is used in single-nucleon transfer

reactions. The second form is used in the case of multi-nucleon transfer reactions (Park et al, 1971; DelVecchio and Daehnick, 1972). Because these are based on the zero-range limit, the approximate procedure is most applicable for reactions in which finite-range effects are not too severe.

An application of DWBA theory developed in this chapter, is given in chapters V - VIII. The first two chapters viz., V and VI use single-nucleon transfer reaction option and the last two deal with the two-nucleon transfer reactions (induced by 23-MeV deuterons).

Table 3-1. Expressions for C^{2*}

	Stripping		Pick-up	
	Proton	Neutron	Proton	Neutron
$T_f = T_i - \frac{1}{2}$	$\frac{T_i + T_{iz}}{2T_i + 1}$	$\frac{T_i - T_{iz}}{2T_i + 1}$	$\frac{T_f - T_{fz} + 1}{2T_f + 1}$	$\frac{T_f + T_{fz} + 1}{2T_f + 1}$
$T_f = T_i + \frac{1}{2}$	$\frac{T_i - T_{iz} + 1}{2T_i + 1}$	$\frac{T_i + T_{iz} + 1}{2T_i + 1}$	$\frac{T_f + T_{fz}}{2T_f + 1}$	$\frac{T_f - T_{fz}}{2T_f + 1}$

* T_i and T_f denote the isospin of the initial and final state, respectively. with $t_z(\text{neutron}) = \frac{1}{2}$.

CHAPTER IV

EXPERIMENTAL PROCEDURE

The experimental setup used in the study of single- and two-nucleon transfer reactions and the procedure for data analysis are briefly described in this chapter.

4.1. EXPERIMENTAL SETUP

The experiments have been carriedout with the Argonne National Laboratory 60-in. cyclotron. It can accelerate α-particles to 43.2 MeV, ^{3}He to 33 MeV, deuterons to about 22 MeV and protons to 10.8 MeV. In the present experiment, 22.8-, 23.25- and 23.35-MeV deuteron beams have been used. The energies are accurate to $\pm$50 keV.

The beam transfort system near the cyclotron is shown in Fig. 4.1. The cyclotron can produce external beams at the shutter in excess of 0.1 mA. The beam is switched into any one of the experimental tunnels using switching magnets. The external deflected beam is focused into the tunnel by means of quadrupole magnets. Two sets of deflection magnets which can steer the beam in both the horizantal and verticle planes are provided.

The normal energy spread of the cyclotron beam is about 1% of the particle energy. For experiments in which the beam resolution is very important, two 120° analyzing magnets shown in Fig. 4.2. are provided. The analyzing

magnets provide an energy resolution of 0.1% or less. The analyzing magnets may be operated in the dispersive mode (at the cost of beam intensity). Another switching magnet directs the analyzed beam to any one of the three stations in the target room. The beam intensity available is about 200-300 nA at the target chamber.

All the reaction experiments have been carried out using the 60-in. scattering chamber built by Yntema and Ostrander (1962). A cross sectional view of the scattering chamber is shown in Fig. 4.3. The scattering chamber consists of eight segements viz.,

1. the scattering table and spindle housing,
2. the collimator and collimator adjustments,
3. the vacuum chamber and vacuum system,
4. supporting framework,
5. the Faraday cup assembly,
6. the detector arms,
7. the detector units, and
8. the target holder.

The scattering chamber is evacuated by mechanical pumps to its normal vacuum of about 5×10^{-3} Torr (mm Hg). The diffusion pump provided on the scattering chamber is then turned on. After the vacuum reaches about 8×10^{-6} Torr, the chamber is connected directly to the vacuum system of the cyclotron.

The detector arms are moveable about the axis of the chamber and are readily set at any given angle with respect to the beam direction. The scattering chamber permits operations over an angular range from 4° to 176° with an accuracy of $\pm 0.05^{o}$. The detectors can be moved along the detector arms whose length is 75 cms. The distance 'r' is of the detector from the scattering center can be measured to an accuracy better than 0.5 mm. In the present experiment 'r' is of the order of 20 cm in all the cases. The scattering chamber is designed so that eight different targets can be fixed on the target holder at any one time.

The accuracy of the measured diffential cross section is determined by the accuracy with which of the following quantities are determined:-

1. solid angle subtended by the detecting aperture, (The error is usually less than 0.2%),
2. the angle of scattering, read directly (which is accurate to $\pm 0.1^{o}$),
3. the target angle (which is usually known to an accuracy of $\pm 0.05^{o}$), and
4. the accuracy of the current integration (which is good to 1% and with some care it can be measured to $\pm$ 0.5%).

The transmitted beam is collected in a Faraday cup (I) placed at about 75 cm from the scattering chamber so that it does not produce an excessive background counting

rate in the detectors.

4.2. PARTICLE DETECTION AND IDENTIFICATION

The particle-detection unit carries the detectors and the defining aperture that determines the angle of scattering and the subtended solid angle. The types of nuclear radiation detectors used in the nuclear reaction experiments have been discussed by various authors in literature (see e.g., Cerny, 1974).

In the present experiments the ΔE-E particle detectors are used. Both ΔE and E detectors (with window diameter $\sim$0.35 cm) are surface barrier silicon diodes. The thickness of the ΔE detector is selected to be in the range of 76 μ to 500 μ, and for the E detector it is in the range 1000 μ to 2000 μ depending upon the type and the energy of the particle to be detected. Normally a detector bias of the order of 50-100 volts for the ΔE detector and 150-300 volts for the E detector is applied. Each particle leaves some energy in ΔE detector, The identification of the type of the particle can be accomplished by using the ΔE and E signals and performing a calculation based on the range-energy relation for the charged particles. If E is the energy deposited in the E detector, and ΔE is the energy lost in the ΔE detector, then

$$\frac{T}{\Lambda} = (E + \Delta E)^B - E^B \qquad \ldots(4\text{-}1)$$

where T is the thickness of the ΔE detector, B is a

constant ($\sim$1.73 but changes for low-energy particles) and A depends on the type of the particle. By calculating the value of $(E + \Delta E)^B - E^B$ for each particle stopping in the detector telescope,aa signal is generated whose amplitude is dependent only on the type of the particle and not on its energy. This calculation may be carried out in a particle identifier (PI). A block diagram showing the electronics used in the present experiment for particle detection is given in Fig. 4.4. The output of the PI is fed to a single channel analyzer which is adjusted to select the particle required.

Energy signals, produced by summing the E and E signals and suitably delayed, are fed to a linear gate and then to a multichannel analyzer, which gives the pulse-height spectrum. (A typical spectrum is shown in Fig. 5.1.).

The laboratory cross section for the transition to any level can be readily calculated from the yield Y (i.e., the number of counts under the peak) using the relation

$$\left(\frac{d\sigma}{d\Omega}\right)_{lab} = \frac{(Y/\Delta\Omega)}{IN_t} . \qquad \ldots(4\text{-}2)$$

Where $\Delta\Omega$ is the solid angle substended by the detector at the target, N_t is the number of target nuclei per cm^2 and I is the number of incident particles.

4.3. TARGETS

The target material used in the transfer reaction experiments have been obtained from Oak-Ridge National Laboratory, Tennessee, USA. These materials are evaporated onto thin carbon films. The target materials are listed in table 4-1. A rough idea of the target thickness will be available from the weight of the target material used in the evaporation process. The correct thickness of the target in the nuclear reaction experiments can be determined by the following methods:-

1. The target thickness can be obtained by comparing the lab cross section (found using equation (4-2)) for low-energy elastic scattering, with the predictions from the Rutherford scattering formula,(Marion and Young, 1961),

$$\left(\frac{d\sigma}{d\Omega}\right)_{lab} = 1.296\left(\frac{Z_1 Z_2}{E}\right)^2 \left[\operatorname{cosec}^4(\theta/2) - \frac{2M}{A}\right] \qquad \ldots(4\text{-}3)$$

where Z_1 and Z_2 are the atomic numbers of the interacting particles and E is the lab kinetic energy of the incident particle. θ is the lab angle of the scattered particle. M and A are the masses of the incidents and target nuclei respectively. (Eventhough this method is most accurate it may not be always possible to apply

this method essentially because the Rutherford scattering experiments have to be done using a different low-energy accelerator.).

2. In the second method the angular distribution for elastic scattering is measured at the energy at which the reaction data is collected. These cross section are then compared with the optical-model predictions to extract the thickness of the target.

In the present series of experiments, the target thickness have been determined in all cases, only by the second method mentioned above by using the optical-model parameters of Daehnick et al (1980). The target thickness of the various targets are tabulated in table 4-1. The error in the target thickness is estimated to be about 25/ in all these cases. These target thicknesses are used to obtain the absolute reaction cross sections.

4.4. ANALYSIS OF THE PULSE HEIGHT SPECTRA

A pulse height spectrum obtained at a given angle in a direct reaction experiment consists of a number of peaks corresponding to various levels of the residual nucleus (see e.g., Fig. 5.1.). The analysis of the spectrum involves mainly four steps viz.,

1. fitting each peak in a pulse height spectrum to a standard line shape to facilitate evaluation of the centroid and the area under the peak,

2. energy calibration of the spectrum,
3. the evaluation of the Q-values for various transitions and hence determination of the excitation energy of the levels in the residual nucleus, and
4. the reaction cross section for transitions to various levels.

These analyses have been done by using computer programs.

4.4.1. Pulse Height Spectrum Fitting

To fit peaks in the pulse-height spectrum, the computer program MALIK (Grard, 1965) has been used. The shapes of peak is assumed to be a Gaussian with a polynomial back ground i.e., the function used to fit the peaks is of the for ,

$$f(a,b,\sigma,c) = \sum_{i=1}^{n} a_i \exp[-\tfrac{1}{2}\left(\frac{x-b_i}{\sigma_i}\right)^2] + \sum_{j=1}^{k} c_j x^{j-1}. \qquad \ldots(4\text{-}4)$$

Where a_i, b_i and σ_i are intensity, centroid and (FWHM/1.117)-value of the ith peak in the spectrum respectively. c_j's are constants determining the background.

In the present analysis the maximum values for n and k were 6 and 3 respectively. For a pulse-height spectrum where more than 6 peaks are involved, the spectrum is fitted in parts.

The program MALIK determines the appropriate values

of the parameters a, b, σ and c for which the likelyhood function L defined by,

$$L = \prod_{i=1}^{N} [f(a,b,\sigma,c,x_i) / \int f(a,b,\sigma,c,x)dx] \quad ...(4-5)$$

has the maximum value. The function f is the assumed probability function and x is the channel number. The programme handles $F = \ln L$ instead of the function L itself.

The programme starts with the initial values of the parameters a, b, σ and c. For each of them a step of appropriate size is assigned by the users. The experimental data with errors are given as input along with the initial values of the parameters. The best fit parameters a, b, σ and c, determined by this programme have been used to calculate

1. the excitation energies of the levels using the peak centroids, and
2. the differential cross section using the peak area below the peak, which is given by,

$$A_i = \sqrt{2\pi}\, a_i \sigma_i \ , \text{ (for the } i^{th} \text{ peak)}$$

The programme also gives the error on the parameters which directly helps in estimating the errors on the excitation energy and the differential cross section.

4.4.2. Energy Calibration

The peak centroids are determined either by the method described in the section 4.4.1. or by using the expression,

$$\bar{b} = {}_{i}(x_i n_i) / \; n_i \qquad \ldots(4\text{-}6)$$

where n_i is the number of counts in channel i. The energy of the outgoing particles E_b corresponding to a peak in the pulse-height spectrum of the reaction A(a,b)B is given by .

$$E_b = \alpha + \beta\bar{b}$$
$$\text{or } E_b = \alpha + \beta\bar{b} + \gamma\bar{b}^2 \qquad \ldots(4\text{-}7)$$

with a very small value of γ.

Initially the values of E_b (in MeV) for various known peaks in the pulse-height spectrum are determined from kinematics by using the Q-values and masses of the interacting particles (Marion and Young 1961). Then the calibration constants α, β (or α, β and γ) are determined by a least square fit.

4.4.3. Q-Value Determination

From the knowledge of the energy calibration, the values of E_b for various peaks in the pulse-height spectrum are determined. The E_b is related to the Q-value of the

reaction A(a,b)B by,

$$Q = \left(\frac{M_b+M_B}{M_B}\right) E_b - \left(\frac{M_B-M_a}{M_B}\right) E_a - 2\frac{\sqrt{M_a E_a M_b E_b}}{M_B} \cos\Theta, \qquad \ldots(4\text{-}8)$$

where the E_a is the incident particle energy in the lab system. Θ is the lab angle of the outgoing particle, and M's represent the masses.

The final r.m.s. Q-value is determined for a particular transition by determining the average from spectra at a number of angles. The excitation energies of the states in the residual nucleus are then determined relative to the ground state Q-value as,

$$E_x = \left|Q - Q_{g.s.}\right| \qquad \ldots(4\text{-}9)$$

4.4.4. <u>Differential Cross Section</u>

The differential cross section at an angle Θ in the centre-of-mass (c.m.) system is defined by,

$$\sigma(\Theta) = \left(\frac{d\sigma}{d\Omega}\right)_{c.m.} = R_{sa}\left(\frac{d\sigma}{d\Omega}\right)_{lab}. \qquad \ldots(4\text{-}10)$$

Where R_{sa} is the solid angle ratio that converts the calculated cross section from the lab system to , given by the expression (4-2), to that in the c.m. system. The accuracy of $\sigma(\Theta)$ is determined mainly by the accuracy in the evaluation of the target thickness (N_t) and to some

extent by the statistical errors on the yield Y.

The total cross section is defined by,

$$\sigma = 2\pi \int_0^{\pi} \sigma(\theta) \sin \theta \, d\theta \qquad \ldots(4\text{-}11)$$

and can be calculated numerically using the expression,

$$\sigma = 2\pi \sum_{i=1}^{M} \sigma(\theta_i) \sin \theta_i \, \Delta\theta_i \qquad \ldots(4\text{-}12)$$

Where $\Delta\theta_i$ is the angular step and M is the number of intervals.

A detailed analysis of the reaction data of some deuteron induced single- and two-nucleon pickup reactions a and the investigation of nuclear structure of the levels of the residual nuclei viz., $^{34,36}Cl$, $^{38,40}Ar$, ^{38}K and ^{10}B are described in the following chapters.

Table 4-1. Target materials and thicknesses

Target required	Compound used	Enrichment of the target material	Target thickness ($\mu g/cm^2$)
^{35}Cl	$PbCl_2$	100%	47
^{37}Cl	$PbCl_2$	85%	63
^{39}K	KI	93.08%*	130
^{41}K	KI	95%	160
^{40}Ca	Ca	96.97%	60
^{12}C	C	98.90%*	62

* Natural abundance

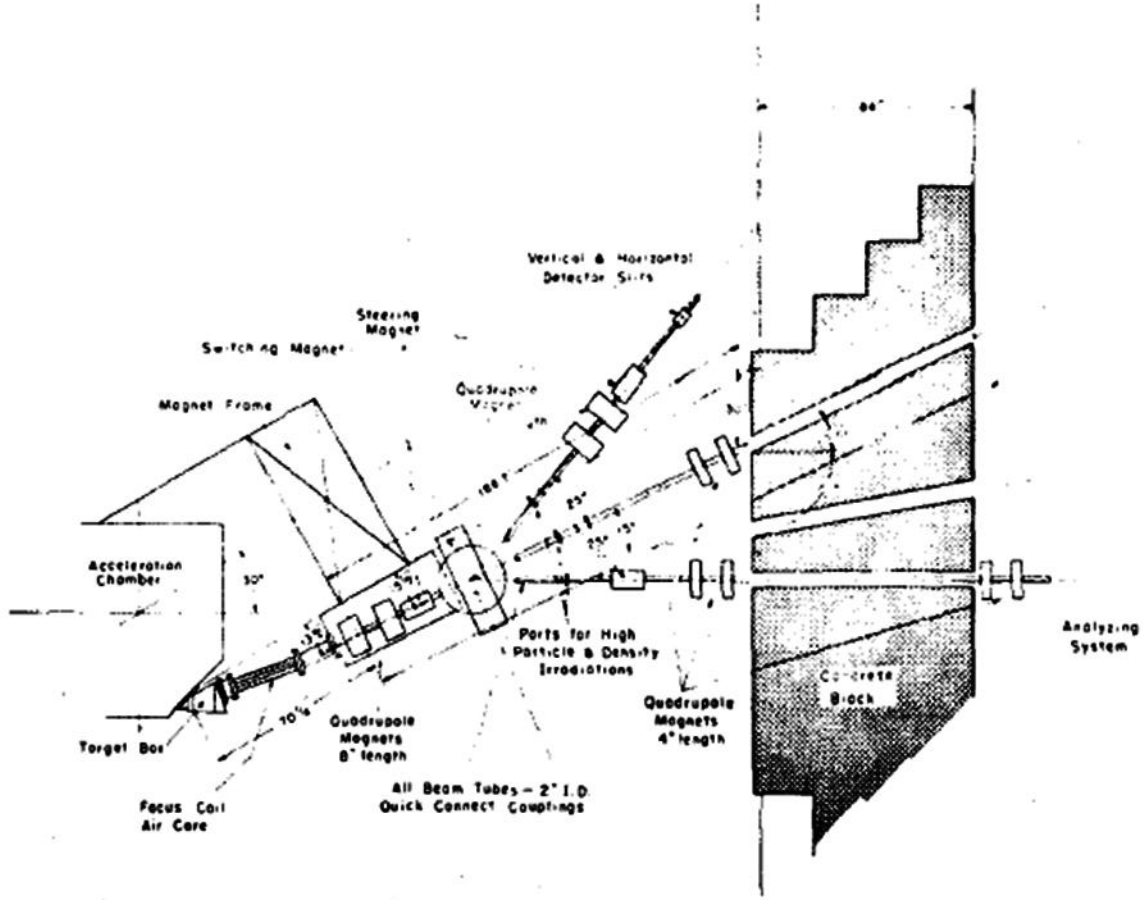

Fig. 4.1. Floor plan of the cyclotron showing the acceleration chamber, beam transfort system for low-resolution experiments and the first switching magnet.

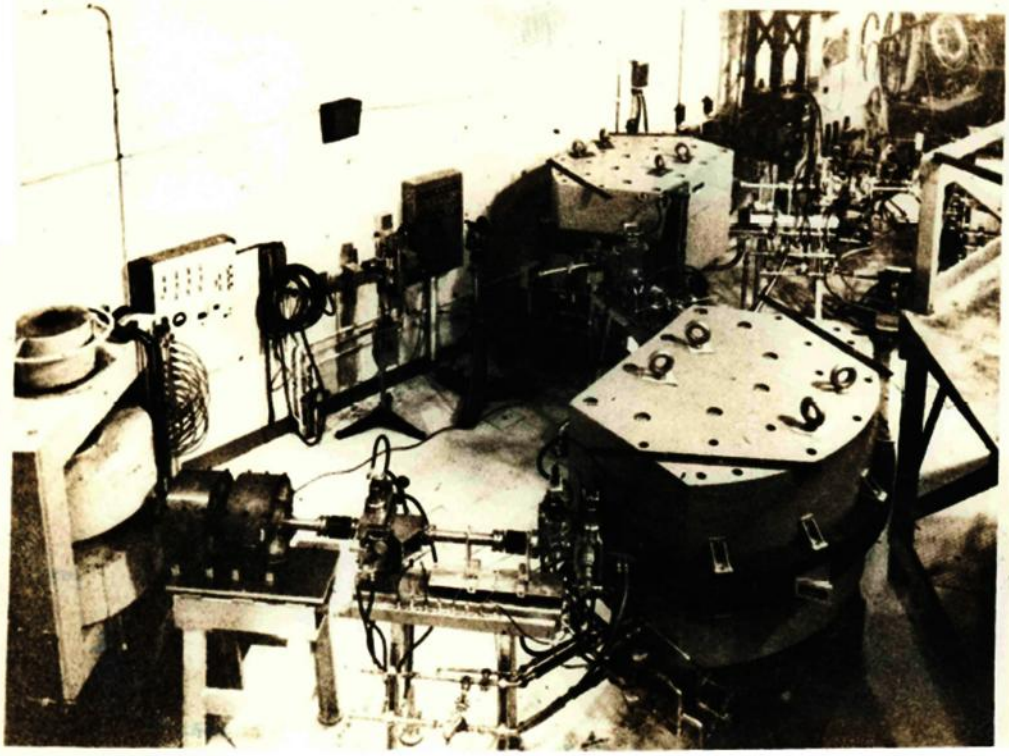

Fig. 4.2 The two 120° analysing magnets at the 60-in cyclotron. The switching magnets on the far left side directs the analysed beam to any one of the three stations in the target room.

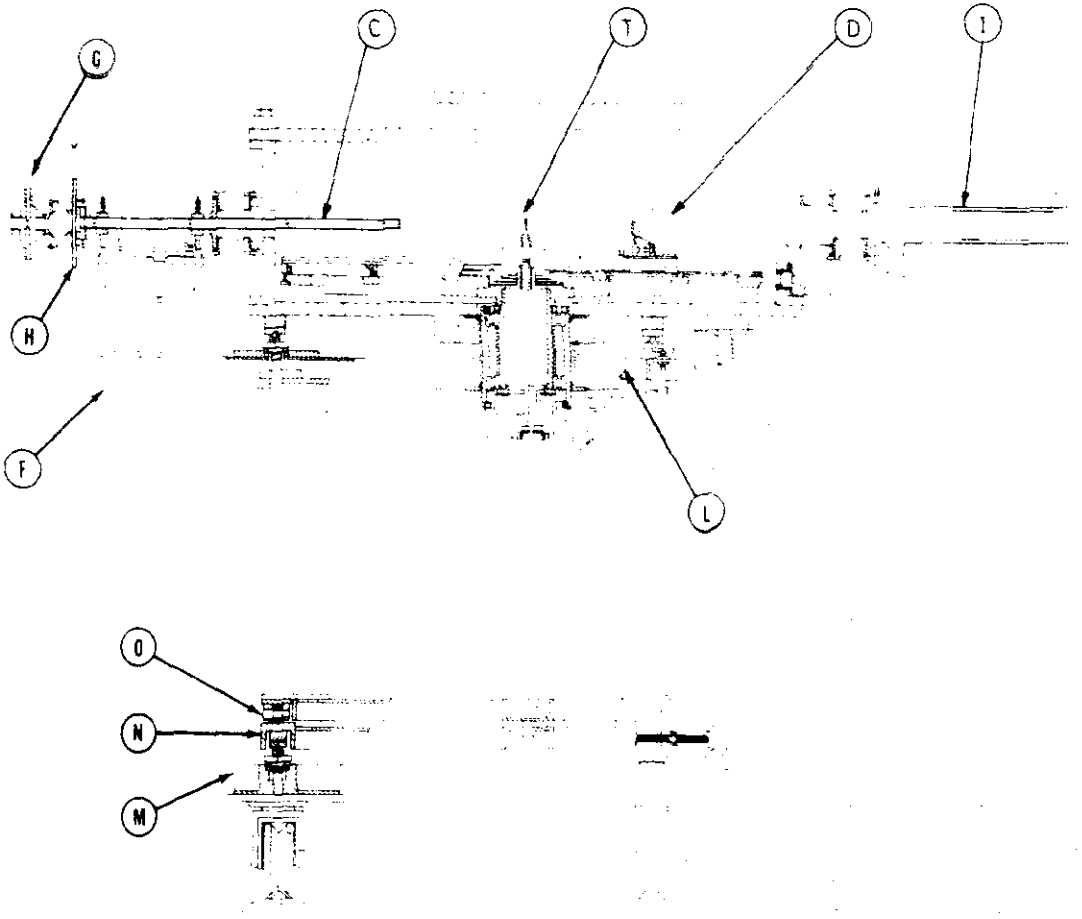

Fig. 4.3. Cross-sectional view of the 60-in. scattering. G - alignment clamps, H - foil changer, C - collimator tube, F - supporting frame, T - target, D - detector, I - current integrator (Faraday cup), L - legs, and O, N, M - triangular frames.

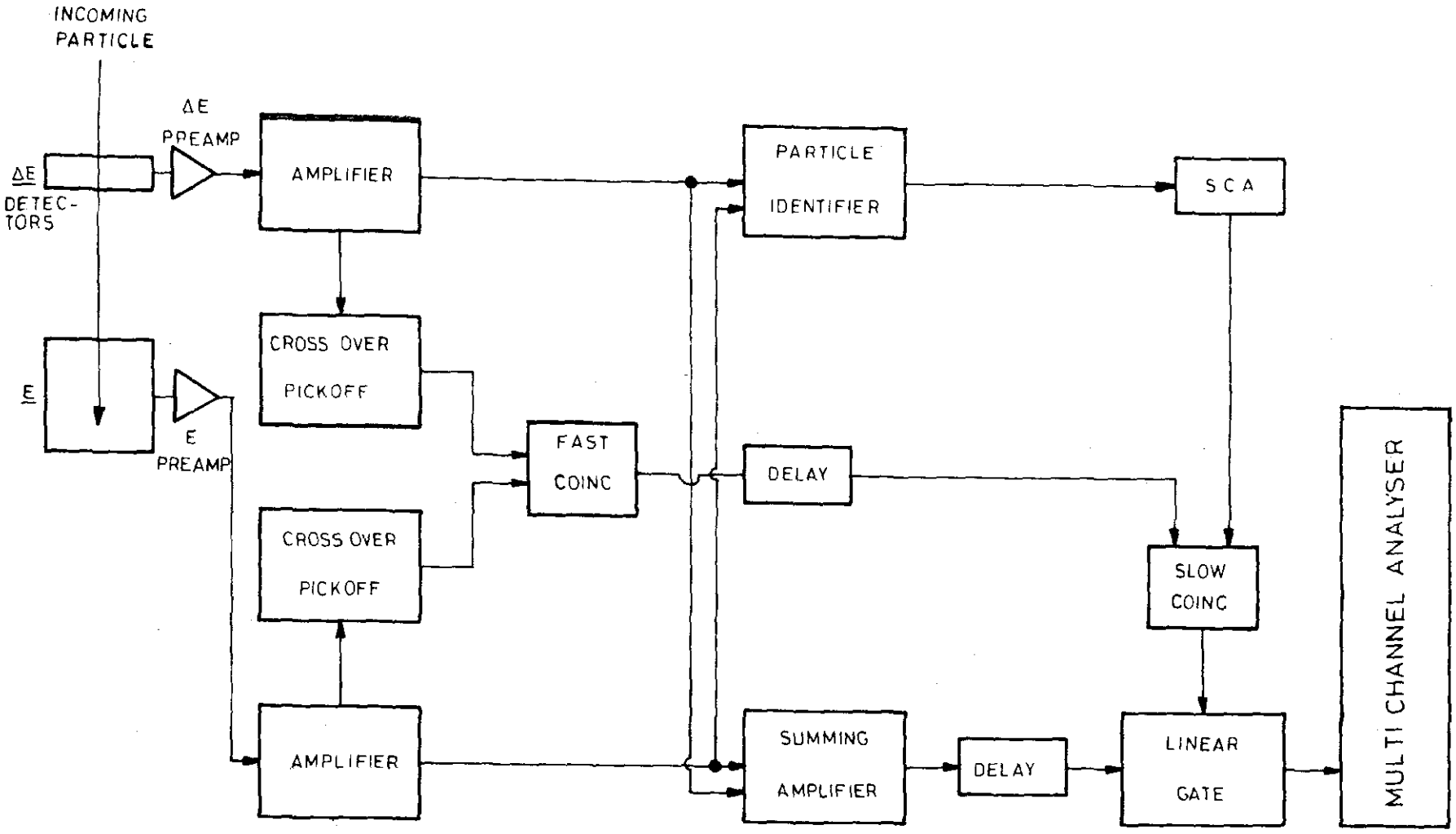

Fig. 4.4. Block diagram of the electronics setup used in the transfer reaction experiments.

CHAPTER V

SINGLE NEUTRON PICKUP REACTION ON THE CHLORINE ISOTOPES*

This chapter deals with a study of the levels in ^{34}Cl and ^{36}Cl via the (d,t) reaction on chlorine isotopes. A study of the structure of doubly odd nuclei in the sd-shell region is of considerable importance from both the theoretical and experimental points of view. In the simplest model description, the low-lying positive parity states of ^{34}Cl can be understood to result from the coupling of one proton and one neutron in $1d_{3/2}$ shell while those in ^{36}Cl results from the coupling of one proton and one neutron hole in the same shell. Calculations in the complete $1d_{5/2}$-$2s_{1/2}$-$1d_{3/2}$ shell-model space by Wildenthal et al (1971; Wildenthal and Chung, private communication) predict spectroscopic factors for pickup reactions leading to final states in ^{34}Cl and ^{36}Cl and a comparison can then be made with the values deduced experimentally.

The low-lying states of ^{34}Cl and ^{36}Cl have been studied previously by (p,d), ($^{3}He,\alpha$), (d,p) and (^{3}He,d) reactions (Endt and Van der Leun, 1978). The $^{37}Cl(\vec{d},t)^{36}Cl$ reaction has been studied recently by Berg and Quin(1976). This work constitutes the first study of $^{35}Cl(d,t)^{34}Cl$ reaction.

5.1. EXPERIMENTAL METHOD

The details of the experimental arrangement have been described in chapter IV.

The $^{35,37}Cl(d,t)$ reactions have been carried out with the 23.35-MeV deuteron beam. The spectra have been recorded at eight angles in an angular range from 10° to 40°. Typical pulse height spectra for the $^{35}Cl(d,t)^{34}Cl$ and the $^{37}Cl(d,t)^{36}Cl$ reactions are shown in Figs, 5.1a and 5.1b respectively. The spectra are analysed and differential cross sections have been deduced by the method described in sect. 4.4. The energy resolution obtained with the counter telescope is about 140 keV FWHM.

The targets are prepared by evaporating lead chloride enriched in ^{35}Cl and ^{37}Cl onto thin carbon films. The target thickness in each case is determined by comparing the experimental elastic scattering angular distribution of deuterons around the maximum at 53° (i.e., between 47° to 66°) with that obtained by using optical-model parameters (listed in table 5-1.). Target thicknesses of 47 $\mu g/cm^2$ for ^{35}Cl and 63 $\mu g/cm^2$ for ^{37}Cl have been obtained; the ^{37}Cl target thickness is corrected for the fact that its enrichment is about 85%. The estimated error in the target thickness is expected to be about 25%.

A consistent energy calibration of the spectra is obtained using the ground state (Q = -4.054 MeV), 0.788-

and 1.165-MeV levels of ^{36}Cl in the case of $^{37}Cl(d,t)$ reaction (Endt and Van der Leun 1978); for $^{35}Cl(d,t)$ reaction, the calibration is made using the 0.0-, 0.159-, 1.825- and 2.365-MeV states in ^{47}Ti (Halbert 1977) populated in the $^{48}Ti(d,t)$ reaction run under similar conditions. The Q-value of the ground-state transition in $^{35}Cl(d,t)$ reaction is -6.390 MeV (Endt and Van der Leun 1978). In most of the spectra the ground state and the first excited state (0.15 MeV) in ^{34}Cl are not well resolved. The centroids of these levels are determined by the curve fitting routine and the Q-values for all the levels are determined relative to the transition to the 0.15-MeV (Q = -6.536 MeV) level in ^{34}Cl. The excitation energies obtained are indicated in Fig. 5.1, and the estimated accuracy is $\pm$ 30 keV. A few spectra for the $^{35}Cl(d,t)$ reaction have also been taken at E_d= 23.35 MeV (at Θ_{lab}= 14°, 16°, 18° and 21°) and, in the region of overlap, the cross sections agreed, to within errors, with the corresponding values for E_d = 23.35 MeV.

5.2. DWBA ANALYSIS

The DWBA analysis has been carried out using the computer code DWUCK (see Appendix B). The OM-parameters used in the present calculations are listed in table 5-1. The deuteron OM-parameters are taken from Daehnick et al (1980) and the triton parameters are from Becheetti and Greenlees (1971). The real (V_R) and imaginary (W_S) well

depths of the triton parameters given in table 5-1 are only for the ground-state transition. These parameters are energy and mass dependent and therefore, for the other transitions, they are varied according to,

$$\left.\begin{aligned} V_R &= 165.0 - 0.17\ E - 6.4\ \eta \\ W_S &= 46.0 - 0.33\ E - 110\ \eta \end{aligned}\right\}, \qquad \ldots(5\text{-}1)$$

where $\eta = (N-Z)/A$ and E is the triton laboratory energy. An alternative set of OM-parameters for triton from Hardekopf et al (1980) has also been tried and in this case the predicted angular distributions do not differ significintly and the spectroscopic strengths agree to within 5%. Further the σ_{DW} is found to be not very sensitive to the change in the spin-orbit term V_{LS} and increasing V_{LS} to twice its value for the exit channel resulted in a change in σ_{DW} by less than 5%. The DWBA analysis for all the transitions have been carried out using the global combinations given in table 5-1.

The sensitivity of the DWBA cross section, σ_{DW}, to finite range and non-locality corrections within the local energy approximation has also been studied. This study has been made for the transition to the ground state of ^{36}Cl. The DWBA curves obtained with (a) zero-range with local potential (ZRL), (b) finite-range with local potential (FRL), (c) finite-range with non-local potentials for incoming ang outgoing particles (FRNL1) and

(d) finite-range and non-local potentials for incoming, for outgoing and for bound particles (FRNL), are compared in Fig. 5.2. The shapes of the angular distributions are very much similar in all these cases. A comparative study of the DWBA curves of the type (a), (c), and exact FRNL1 has been made by Suehiro et al (1979) in their study of the $^{54}Fe(p,d)$ reaction at E_p = 40 MeV. They have also found that the shapes of the angular distribution curves with FRNL1 and exact FRNL1 are very similar. In the present case the values of σ_{DW} are fuund to change as follows:

$$\sigma_{DW}^{FRNL1} \approx \sigma_{DW}^{FRL} \approx 1.37\ \sigma_{DW}^{ZRL}$$

and

$$\sigma_{DW}^{FRNL} \approx 1.27\ \sigma_{DW}^{FRNL1} \qquad \ldots(5\text{-}2)$$

For all the other transitions DWBA analyses of the type FRNL1 are made using a FR correction of 0.845 fm and the NL corrections β_{NL} listed in table 5-1.

The pickup spectroscopic strengths are calculated using the expression (3-16). A normalization constant N = 3.33 (Bassel 1966) has been used. (A different value of N = 2.664 has been suggested by Ioannides et al (1981) for the (d,t) reactions; this value of N has been obtained by assuming the Phillips wave function for the three-nucleon system and enhances the spectroscopic strengths by a factor of 1.25. Thus using N = 2.664 with σ_{DW}^{FRNL} would give spectroscopic strengths almost the same as those obtained by Bassel's value of N.)

The chlorine isotopes lie in the latter part of the sd-shell-model space. Therefore most of the low-lying states can be excited by zero and two units of orbital angular momenta. The single-particle wave functions of these states contain considerable amount of 1d- as well as 2s-shell components. When both $\ell = 0$ and $\ell = 2$ are possible, the relative admixtures for the possible ℓ-values are determined by minimising the quantity,

$$\chi^2 = \frac{1}{M}\sum_{i=1}^{M} \frac{(A\sigma_0(\Theta) + B\sigma_2(\Theta) - \sigma_{expt}(\Theta))_i^2}{(\Delta\sigma_{expt})^2}$$

where σ_0 and σ_2 are DW-cross sections for $\ell = 0$ and $\ell = 2$ transfer respectively. M is the number of data points. The values of A and B then give the appropriate spectroscopic strengths.

5.3. RESULTS AND DISCUSSIONS

5.3.1. Levels in ^{34}Cl

The angular distributions measured for the transitions to the states of ^{34}Cl are shown in Figs. 5.3 and 5.4 together with the DWBA fits and ℓ values transferred. The experimental results for ^{34}Cl are summarised in table 5-2 together with the values evaluated by Endt (1977) from other experiments and the results of recent sd-shell-model calculations by Wildenthal and Chung (private communication).

In the simplest shell-model description, the low-lying even-parity states of ^{34}Cl can result from the coupling of one proton and one neutron in the $1d_{3/2}$ shell. According to the jj-coupling model for odd-odd nuclei, (Brennan and Bernstein, 1960), a $J^{\pi} = 0^{+}$ or 3^{+} could be expected for the ground state of ^{34}Cl. The Nordheim number N $(=j_p+\ell_p+\frac{1}{2}+j_n+\ell_n+\frac{1}{2})$ is 8; hence the lowest state is expected to be 3^{+} $(=j_p+(-1)^N j_n)$ (de Shalit and Walecka, 1961). But ^{34}Cl is the one exception among nuclei with $A \leqslant 40$, in that the ground state is found to be 0^{+} and the first excited state is 3^{+} (Endt and Van der Leun, 1978). Therefore, from angular momentum selection rules, only $\ell = 2$ transfer is expected for the ground state and for the 0.15-MeV states in the ^{34}Cl. This is in agreement with the results obtained from this study. The transitions to other levels contain both $\ell = 2$ and $\ell = 0$ components.

There is good agreement between the experimental spectroscopic strengths and the values predicted by Wildenthal and Chung (private communication) for levels in ^{34}Cl. However this model calculation predicts the 1^{+},0 state to be at a lower energy than the 3^{+},0 state (see Fig. 5.5) in contradiction to the experimental results. By extending the shell-model space and adding a tensor force to the modified surface δ-interaction, Evers and Stocker (1970) get the correct ordering of the levels. A vibrational unified model calculation which includes anharmonic and

quasiparticle effects has also been made by Singh et al (1972). In this model, ^{32}S is taken as the core and the quasi particles are coupled to the anharmonic phonon states. This describes both T = 0 and T = 1 levels; the calculated level energies are compared with the experimental spectrum and the results of the sd-shell-model calculation in Fig. 5.5. This model gives the correct ordering of the levels. No detailed information regarding the single neutron pickup spectroscopic strengths is available from this calculation.

5.4.2. Levels in ^{36}Cl

The measured angular distributions of tritons for transitions to ten levels in ^{36}Cl are displayed in Figs. 5.6 and 5.7 (along with their DWBA fits). The spectroscopic strengths measured for the levels have been listed in table 5-3. The previous experimental results of Rice et al (1975), of Berg and Quin (1976), the values evaluated by Endt (1977) from other experiments and the sd-shell-model predictions of Wildenthal and Chung (private communication) are also tabulated for comparison.

The ground state and the 0.79-, 2.86- and 4.30-MeV levels exhibit dominant ℓ = 2 transfer. For all these transitions DWBA calculations have been made assuming a $1d_{3/2}$ neutron pickup. The ground state spin-parity is correctly predicted to be 2^+ i.e., $J = j_1+j_2-1$, by the

simple jj-coupling model of Brennan and Bernstein (1960). The angular momentum selection rules allow both $\ell = 0$ and $\ell = 2$ transfer, since the spin-parity of the ground-state of ^{37}Cl is $3/2^+$ (Endt and Van der Leun, 1978). Recent tensor analysing power measurements on the ground-state and the 0.79-MeV transition in $^{37}Cl(\vec{d},t)$ reaction (Berg and Quin, 1976), show characteristic $1d_{3/2}$-neutron pickup. The higher levels, with $\ell = 2$ pickup, on the other hand are likely to have contribution due to excitation from deeper sub-shells like $1d_{5/2}$. In the present study only the ℓ-values could be assigned without any ambiguity. A comparison with the sd-shell model calculation (Wildenthal and Chung, private communication) suggests that the 2.86-MeV level is probably the second 2^+ state in ^{36}Cl. The 4.30-MeV state is known to arbe the analog of the ground state of ^{36}S (Endt and Van der Leun, 1978).

All other states exhibit $\ell = 0 + 2$ transfer and hence $J^\pi = 1^+$ or 2^+. The DWBA analyses have been made assuming $2s_{1/2}$ and $1d_{3/2}$ neutron pickup. The vector analysing power measurements (Berg and Quin, 1976) strongly support this assumption for the 1.16-MeV transition. In the case of the 1.60-MeV and 1.96-MeV transitions, however, the C^2S values obtained here differ from those obtained in previous studies (Rice et al, 1975; Endt, 1977) These differences can arise due to,

1. the procedure adopted to estimate the admixture of two ℓ-transfers,
2. the fact that the soectroscopic strength depends sensitively on the exact shapes assumed for DWBA curves which in turn depends on the OM parameters for the entrance and exit channels, hthe bound-particle parameters, and the various corrections applied.

The levels for $E_x \leq 3.5$ MeV in ^{36}Cl are well reproduced in both types of shell-model calculations viz., sd—shell model (Wildenthal and Chung, private communication) and sdfp-shell-model (Hasper, 1979). The level scheme obtained by these two calculations have been compared with the experimental spectrum in Fig. 5.8. The later calculation predicts some negative parity levels below 3 MeV (not indicated in the Fig. 5.8.). Perhaps these can be identified with the level scheme obtained in a high resolution study by Rice et al (1975) via the (p,d) reaction. These levels are however weak and are not resolved in the present (d,t) experiment. The sdfp-shell-model calculation predicts that the ground state of ^{36}Cl has about 66% of the d^{-4} contribution, while the second 2^+ level at $E_x \sim 2.03$ MeV is predicted to be $s^{-1}d^{-3}$ with a small amount of $s^{-1}d^{-5}f^2$. The third 2^+ state is predicted to be a typical intruder from fp-shell.

5.4. SUMMARY

The values of neutron pickup spectroscopic strengths extracted from the present experiments are generally in good agreement with the previous reports. The experimental and sd-shell-model neutron pickup spectroscopic strengths (Wildenthal and Chung, private communication) for ^{34}Cl and ^{36}Cl have been shown in Fig. 5.9.

The spin of the ground state of ^{34}Cl is predicted well by sd-shell-model calculation. But the sequence of first and second excited levels viz., the 3_1^+ and 1_1^+ levels are reversed; the spectroscopic strengths, however, agree well with the experimental results. The summed spectroscopic strength $\sum C^2S(1d_{3/2};T=0)$ is 1.82 and is close to the theoretically predicted value of 1.47. Both theory and experiments indicate that only about 25% of the $\ell = 0$ strengths is exhausted below 2-MeV excitation in ^{34}Cl.

In the case of ^{36}Cl, the level below an excitation of 2.68 MeV is fairly well reproduced by sd-shell-model calculation (Wildenthal and Chung, private communication) and also by sdfp-model calculation. (Harper 1979). The former of the model-calculations, reproduces the spectroscopic strengths for the ^{36}Cl levels fairly well. The summed strength $\sum C^2S(1d_{3/2};T=1)$ is 4.21 while a value of 3.24 is predicted theoretically.

Table 5-1. Optical-model parameters used in the DWBA analysis of the (d,t) reaction on $^{35,37}Cl$

	V_R (MeV)	r_0 (fm)	a_0 (fm)	W_S (MeV)	W_D[a] (MeV)	r_I (fm)	a_I (fm)	V_{LS} (MeV)	r_{LS} (fm)	a_{LS} (fm)	r_c (fm)	β_{NL} (fm)
$^{35}Cl+d$ [b]	87.0	1.17	0.749	0.7	12.1	1.325	0.744	6.7	1.07	0.66	1.3	0.54
$^{34}Cl+t$ [c]	162.2	1.2	0.72	40.5	—	1.4	0.84	2.5	1.2	0.72	1.3	0.20
$^{37}Cl+d$ [b]	86.9	1.17	0.749	0.7	12.1	1.325	0.723	6.7	1.07	0.66	1.3	0.54
$^{36}Cl+t$ [c]	161.4	1.2	0.72	33.6	—	1.4	0.84	2.5	1.2	0.72	1.3	0.20
n	~55 [d]	1.2	0.65					$\lambda=25$			1.25	—

[a] A value of $4W_D$ is used in DWUCK.

[b] A value of $2V_{LS}$ is used in DWUCK.

[c] A value of $4V_{LS}$ is used in DWUCK.

[d] The bound neutron well-depth is adjusted to give a proper separation energy for neutron.

Table 5-2. Neutron pickup spectroscopic strengths for the levels in ^{34}Cl [a].

E_x[b] (MeV)	$J^\pi; T$[b]	l	$100C^2S$[c]	$100C^2S$[d]	Theory[e] E_x(MeV)	$J^\pi; T$	$100C^2S$
0.0	$0^+;1$	2	; 41;	; 43 ± 7;	0.0	$0_1^+;1$	; 30;
0.146	$3^+;0$	2	; 118;	; 140 ± 30;	0.448	$3_1^+;0$	; 109; 2
0.461	$1^+;0$	0, 2	11; 21;	9 ± 3; 27 ± 5;	0.324	$1_1^+;0$	9; 28; 7
0.666	$1^+;0$	0, 2	6; 22;	9 ± 6; 31 ± 8;	1.069	$1_2^+;0$	13; 4; 0
1.230	$2^+;0$	0, 2	23; 9;	36 ± 14; 7 ± 2;	1.416	$2_1^+;0$	32; 0; 6
1.887	$2^+;0$	0, 2	4; 12;	11 ± 5; 14 ± 4;	2.108	$2_2^+;0$	1; 6; 3
	$\Sigma C^2S(2s_{1/2}; T=0)=0.44$						0.55
	$\Sigma C^2S(1d_{3/2}; T=0)=1.82$						1.47
	$\Sigma C^2S(1d_{3/2}; T=1)=0.41$						0.30

[a] In the columns labelled $100C^2S$, the spectroscopic strengths are given in the notation $100C^2S(s_{1/2})$; $100C^2S(d_{3/2})$; $100C^2S(d_{5/2})$.
[b] Endt and Van der Leun (1978). Energies measured in the present experiment are indicated in figure 1(*a*).
[c] Present work.
[d] Endt (1977). For a complete listing of spectroscopic strengths from all the previous experiments, see Endt and Van der Leun (1978).
[e] Wildenthal *et al* (1971); also Wildenthal and Chung (private communication).

Table 5-3. Neutron pickup spectroscopic strengths for the levels in ^{36}Cl [a].

E_x [b] (MeV)	$J^\pi; T$ [b]	l	$100C^2S$ [c]	$100C^2S$ [d]	$100C^2S$ [e]	$100C^2S$ [f]	Theory [g] E_x(MeV)	$J^\pi; T$	$100C^2S$
0.0	$2^+; 1$	2	; 90;	; 110;	; 121;	; 95 ± 17;	0.0	$2_1^+; 1$	2; 101; 2
0.788	$3^+; 1$	2	; 130;	; 166;	; 141;	; 150 ± 20;	0.928	$3_1^+; 1$	; 159;
1.165	$1^+; 1$	0, 2	1; 28;	5; 36;	5; 36;	9 ± 3; 34 ± 5;	1.101	$1_1^+; 1$	3; 25; 3
1.601	$1^+; 1$	0, 2	8; 28;	16; 11;	19; 8; 17; ; 11	20 ± 3; 15 ± 8;	1.640	$1_2^+; 1$	27; ;
1.959	$2^+; 1$	0, 2	10; 43;	23; 24;	20; 25; 20; ; 20	38 ± 8; 21 ± 5;	1.767	$2_2^+; 1$	30; 1; 23
2.492	$2^+; 1$	0, 2	13; 25;	17; 19;			2.397	$2_3^+; 1$	13; 2; 3
2.675	$1^+; 1$	0, 2	6; 28;	7; 31;		6 ± 2; 32 ± 4;	2.793	$1_3^+; 1$	2; 34; 3
2.864	$(2, 3)^+; 1$	2	; 42;	; 45;			2.424	$3_2^+; 1$	; 1; 70
3.469	$(1, 2)^+; 1$	0, 2	2; 7;	5; 7;			3.361	$1_4^+; 1$	9; 1;
4.300	$0^+; 2$	2	; 14;	; 29;			4.340	$0^+; 2$	; 23;
	$\Sigma C^2S(2s_{1/2}; T=1) = 0.40$								0.85
	$\Sigma C^2S(1d_{3/2}; T=1) = 4.21$								3.24
	$\Sigma C^2S(1d_{3/2}; T=2) = 0.14$								0.23

[a] In the columns labelled $100C^2S$, the spectroscopic strengths are given in the notation $100C^2S(s_{1/2})$; $100C^2S(d_{3/2})$; $100C^2S(d_{5/2})$.

[b] Endt and Van der Leun (1978). Energies measured in the present experiment are indicated in figure 1(*b*).

[c] Present work.

[d] Rice *et al* (1975). The spectroscopic factors have been normalised to yield $C^2S = 1.10$ for the ground-state transition.

[e] Berg and Quin (1976).

[f] Endt (1977). For a complete listing of spectroscopic strengths from previous experiments, see Endt and Van der Leun (1978).

[g] Wildenthal *et al* (1971); also Wildenthal and Chung (private communication).

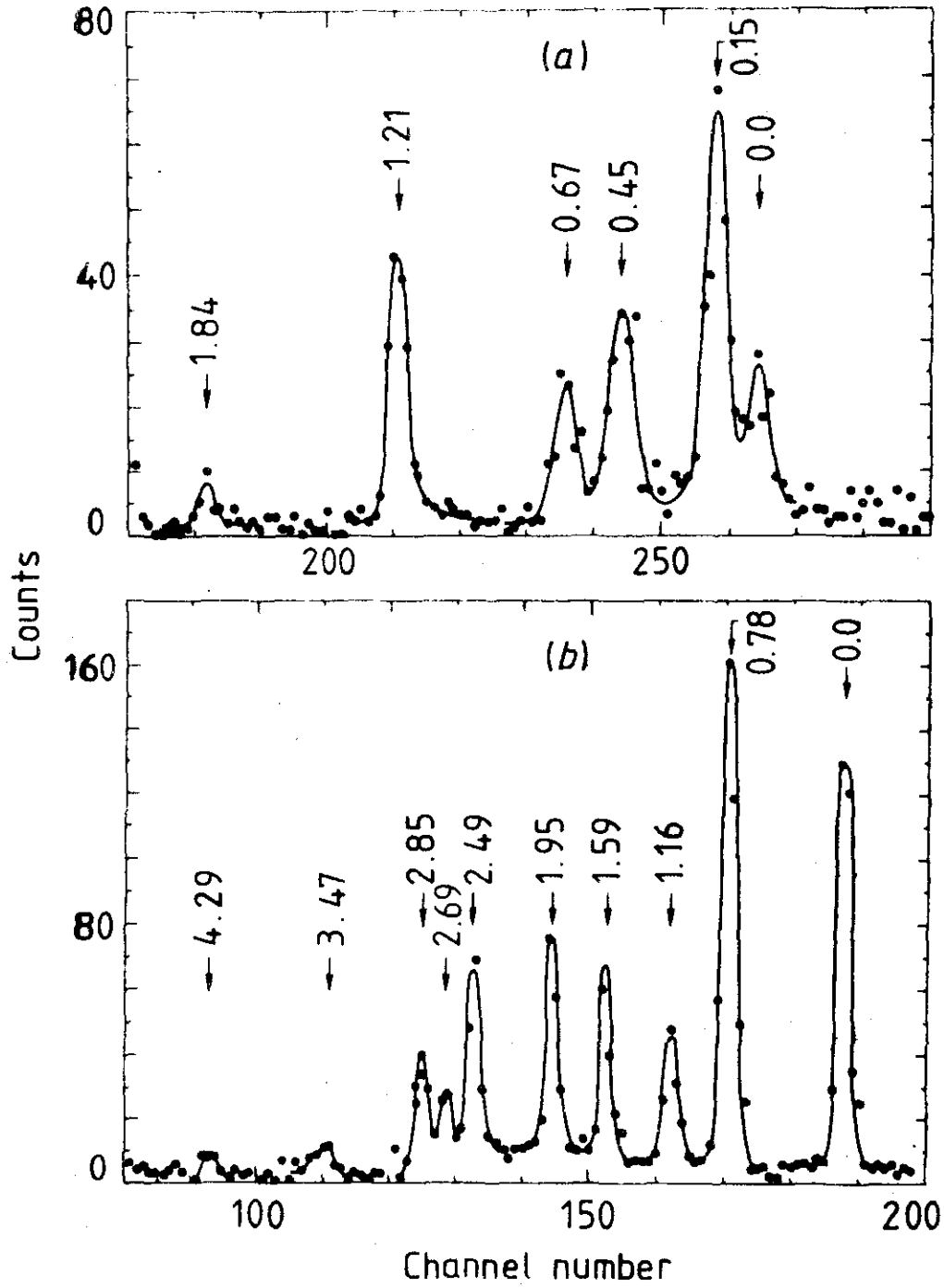

Fig. 5.1. Spectrum of tritons from the (d,t) reaction on chlorine isotopes at 23.35 MeV. (a) The spectrum from the $^{35}Cl(d,t)^{34}Cl$ reaction at $\theta_{lab} = 21^{o}$. (b) The spectrum from the $^{37}Cl(d,t)^{36}Cl$ reaction at $\theta_{lab} = 18^{o}$. The excitation energies (in MeV) determined from this experiment are indicated above the peaks.

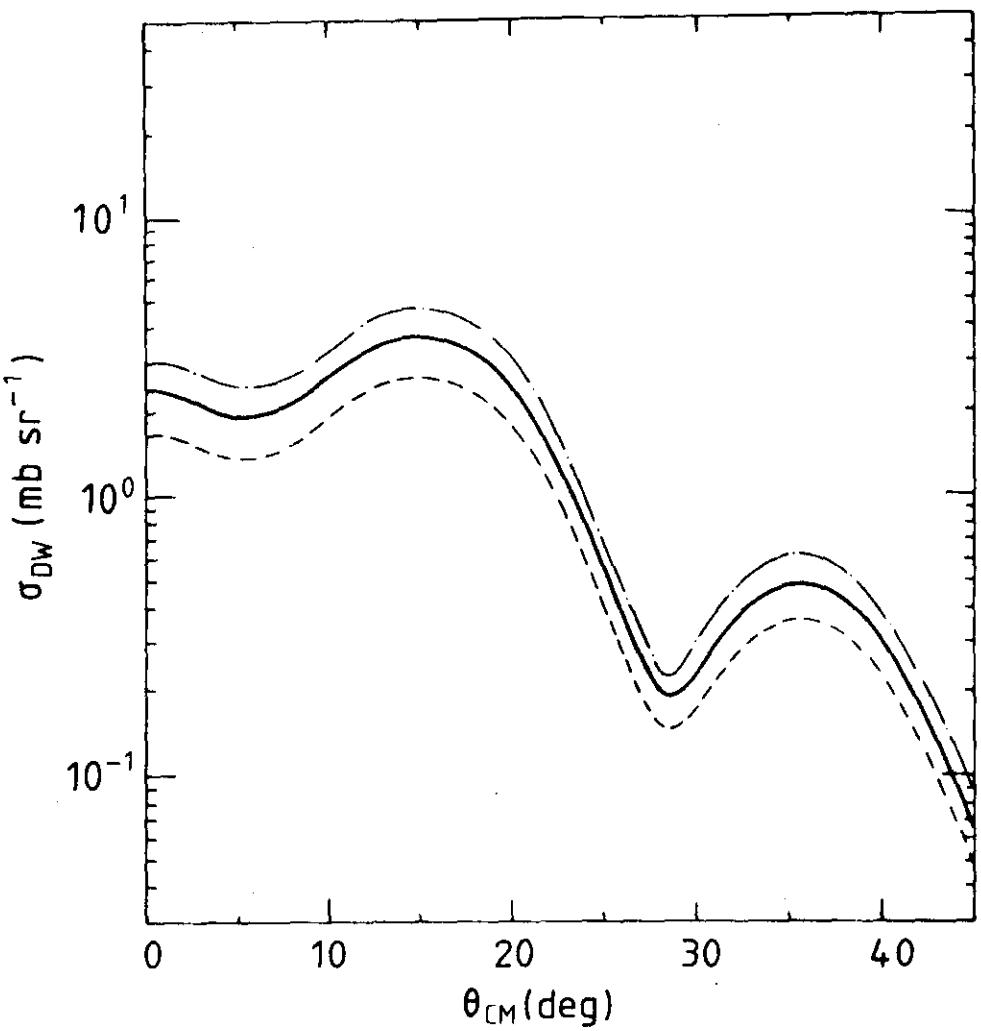

Fig. 5.2. Comparison of the DWBA curves with $\ell = 2$ (and $j=3/2$) for the ground state transition in the $^{37}Cl(d,t)^{36}Cl$ reaction at 23.35 MeV. The FRNL calculation has been made using the nonlocality correction β =0.85fm for the neutron bound state. ——— · ———, FRNL; ————, FRNL1 or FRL; -------, ZRL.

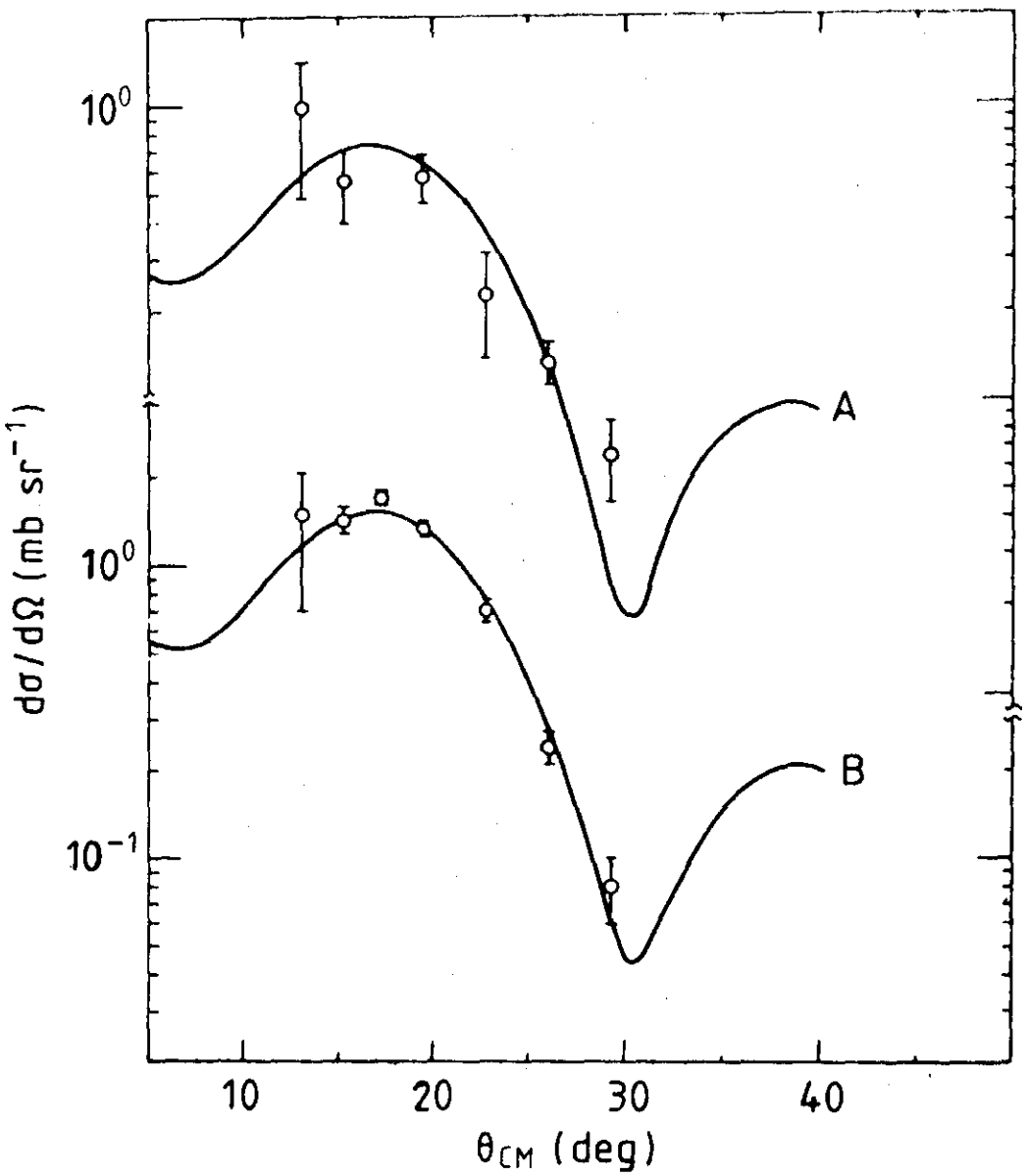

Fig. 5.3. Angular distributions for states with $\ell = 2$ transfer in the $^{35}Cl(d,t)^{34}Cl$ reaction at E_d=23.35 MeV; the full curves are the DWBA predictions. A, 0.0 MeV; B, 0.[illegible] MeV.

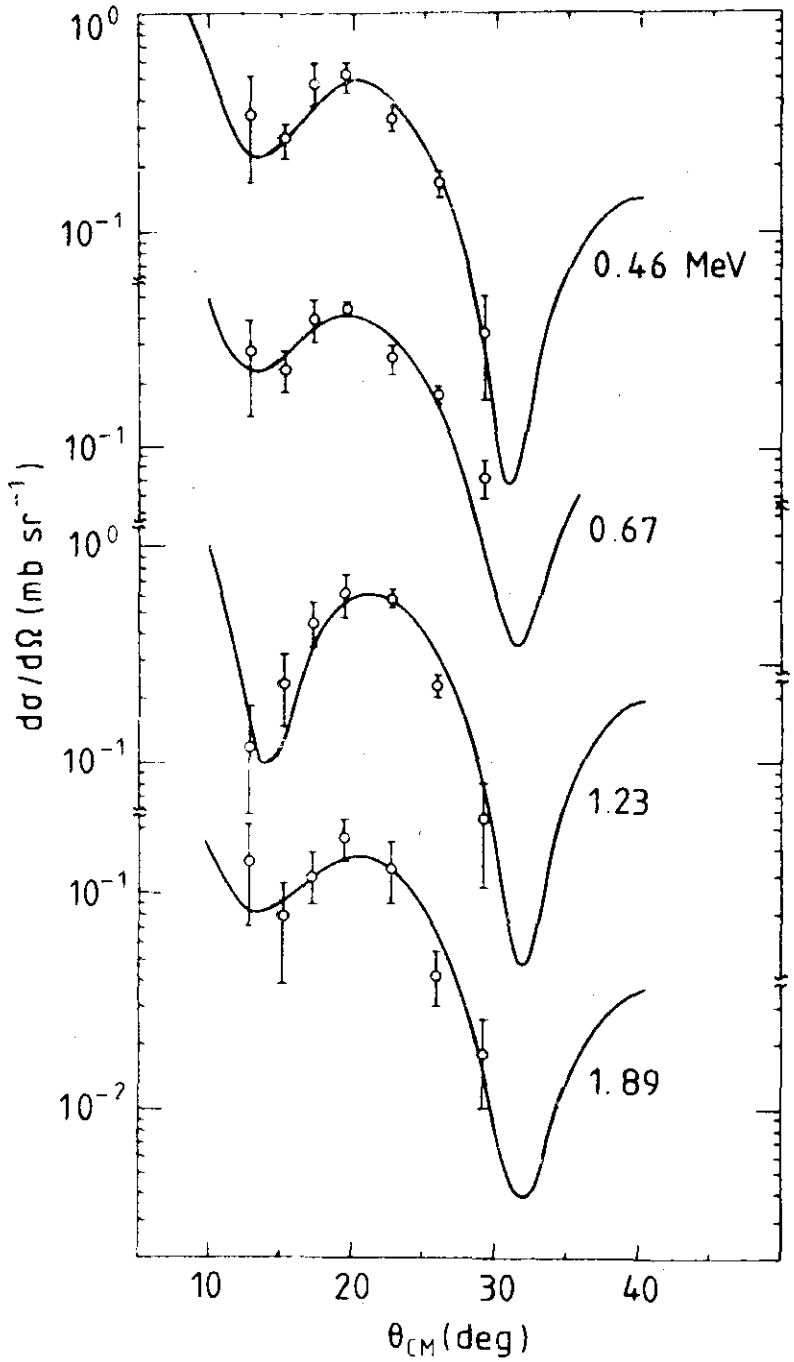

Fig. 5.4 Angular distributions for states in ^{34}Cl having $\ell = 0+2$ transfer; the full curves are linear combinations of the DWBA predictions for $\ell = 0$ and $\ell = 2$ as described in the text.

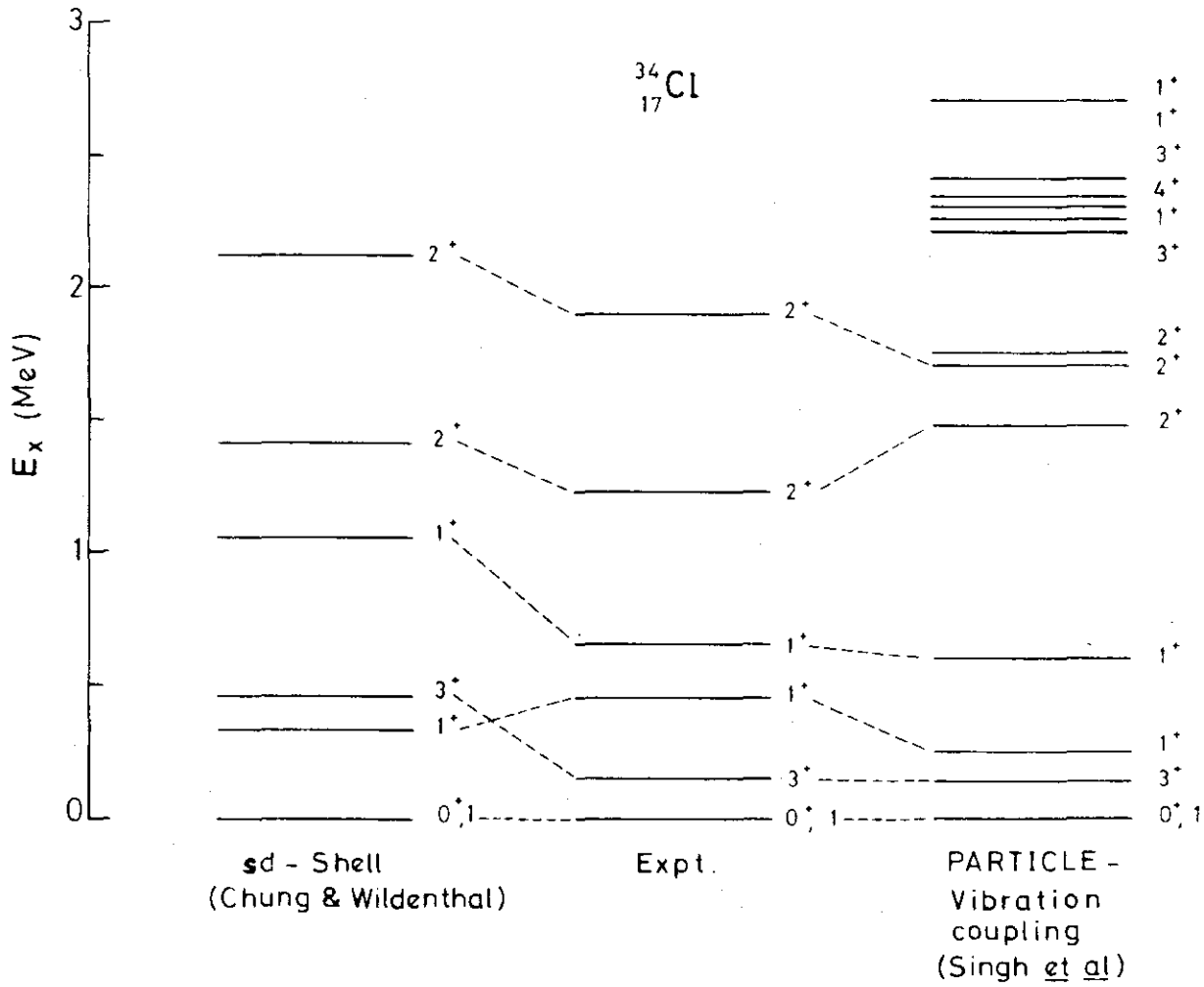

Fig. 5.5. Comparison of theoretical and experimental level scheme for ^{34}Cl.

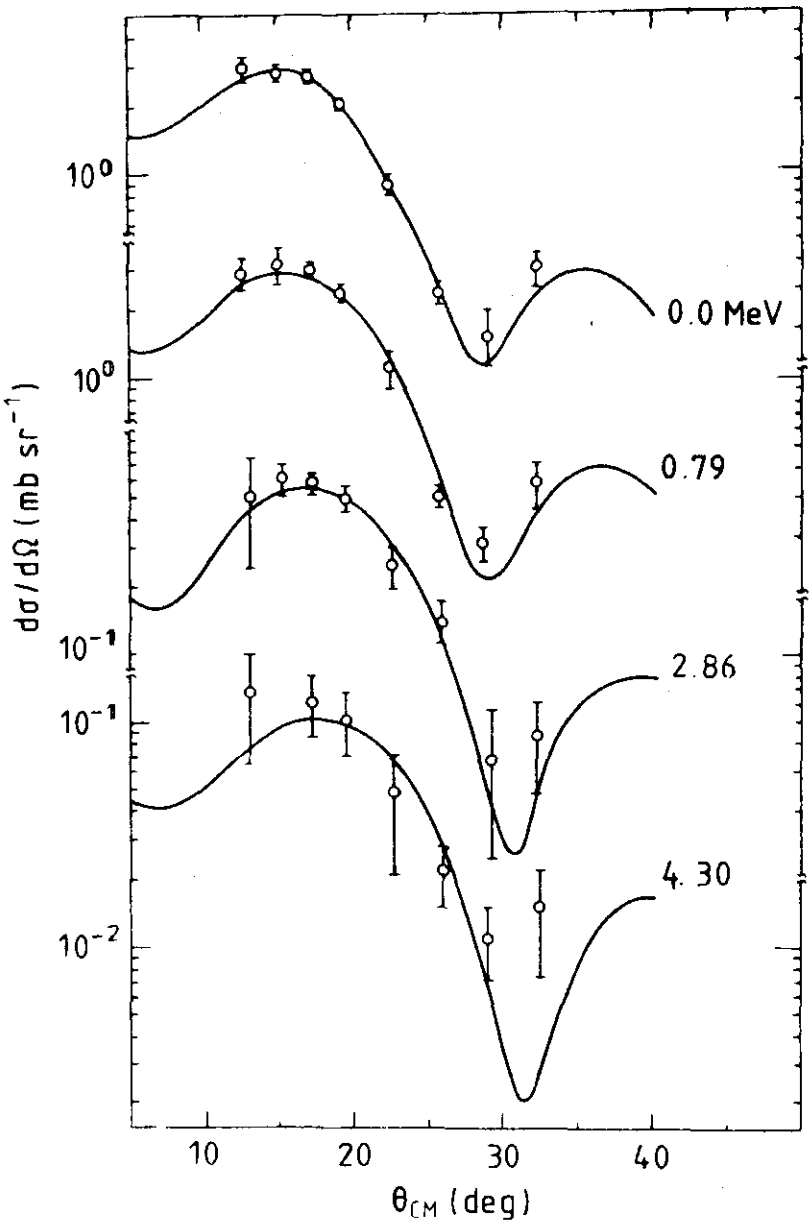

Fig. 5.6 Angular distributions for states populated in the $^{37}Cl(d,t)^{36}Cl$ reaction with $L = 2$; the full curves are the DWBA predictions.

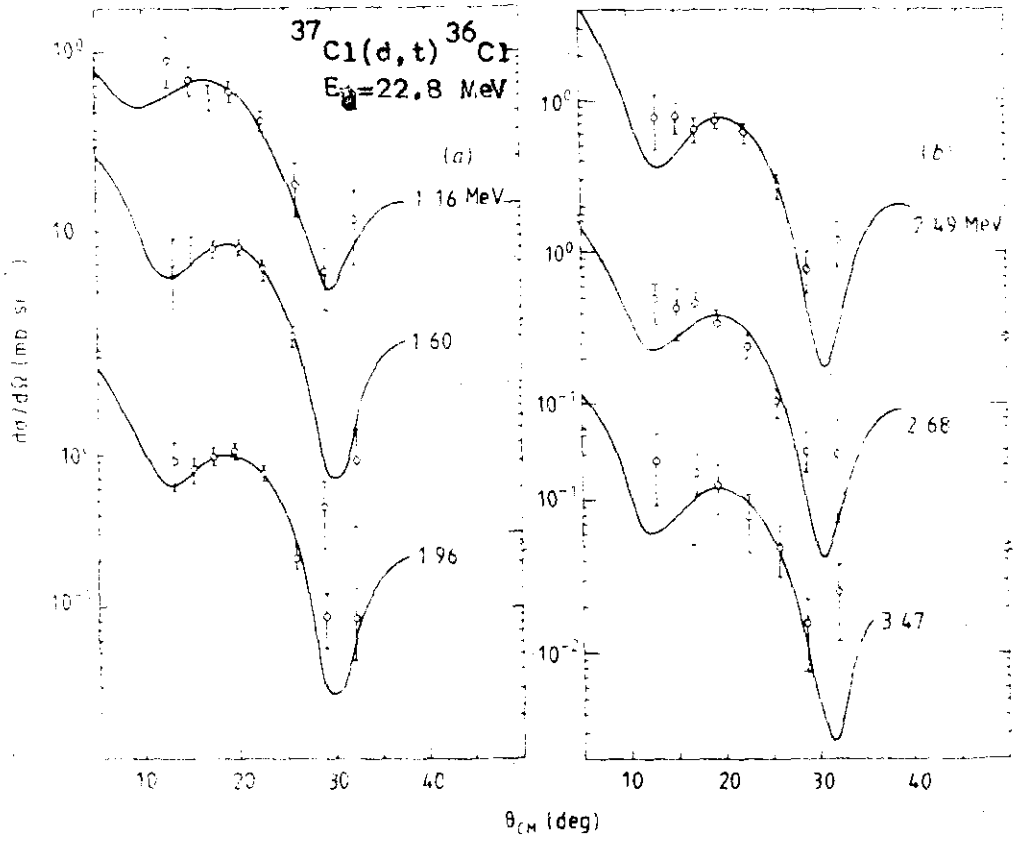

Fig. 5.7 Angular distributions for the states in ^{36}Cl having $l = 0+2$ transfer; the full curves are linear combinations of DWBA predictions for $l = 0$ and $l = 2$ as described in the text.

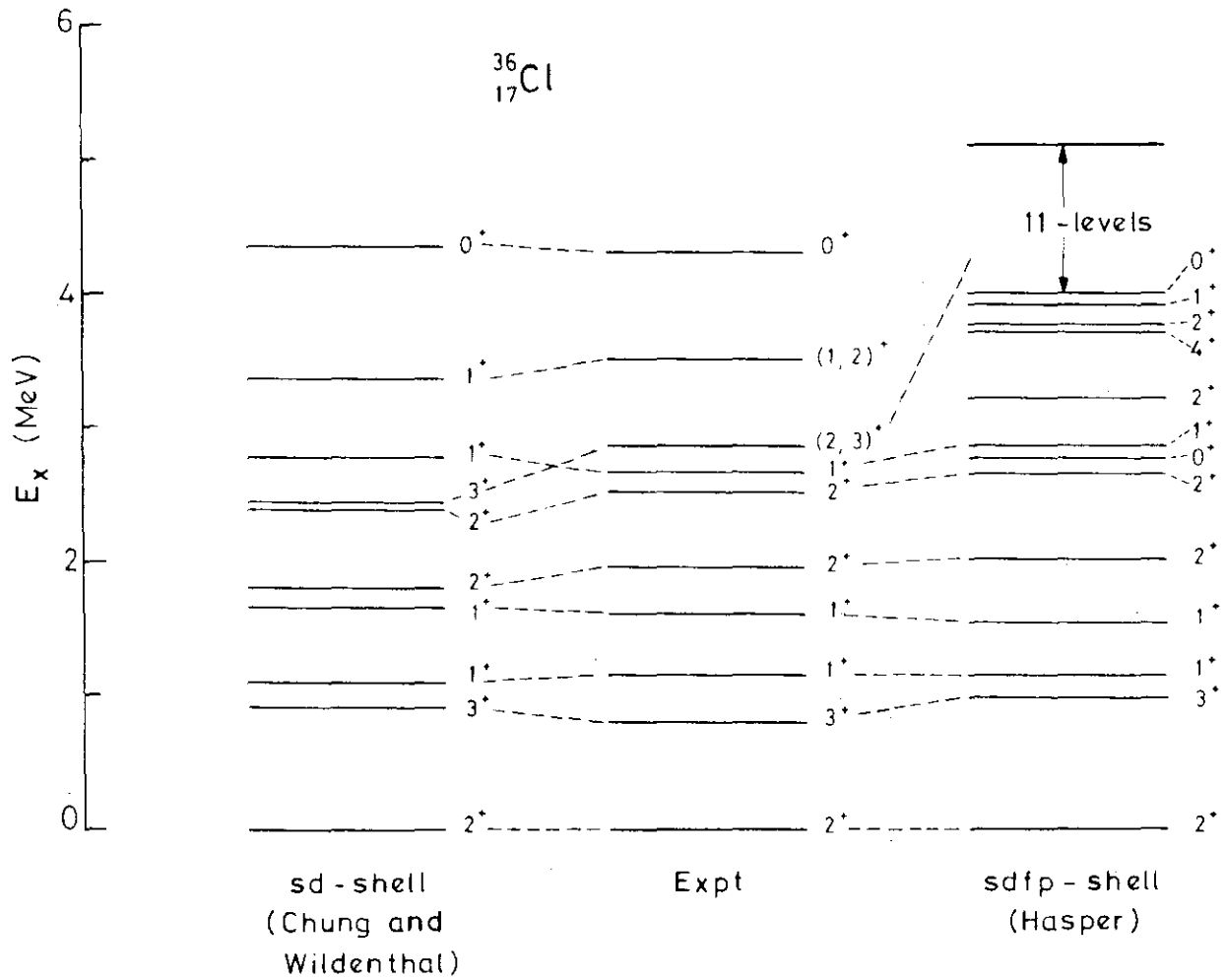

Fig. .8. Comparison of theoretical and experimental level scheme for ^{36}Cl

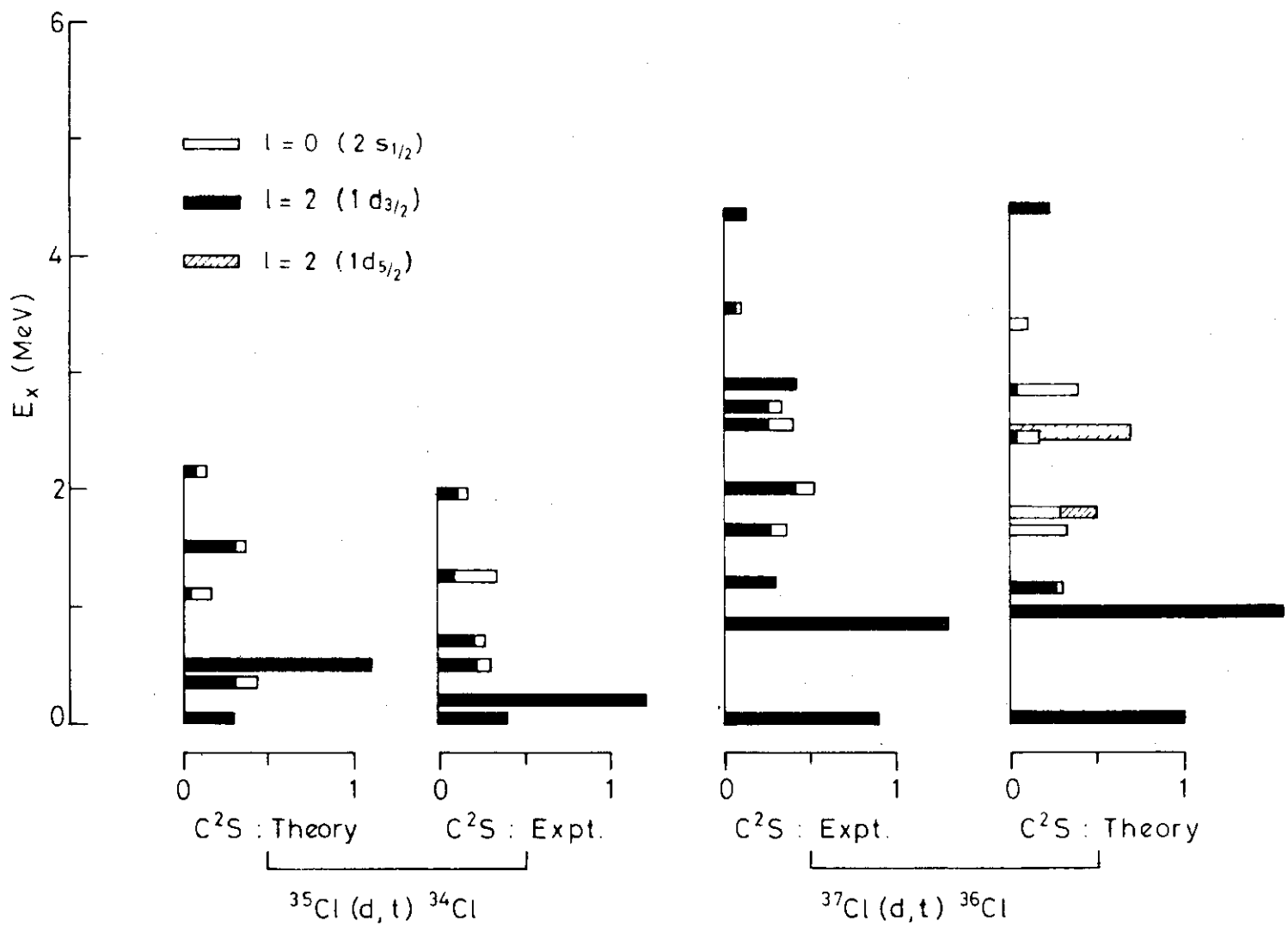

Fig. 5.9. Comparison of sd-shell-model and experimental spectroscopic strengths for the transitions to the levels in ^{34}Cl and ^{36}Cl.

CHAPTER VI

SINGLE PROTON PICKUP REACTION ON THE POTASSIUM ISOTOPES

From the simplest shell-model point of view the low-lying positive-parity levels of ^{38}Ar can be characterised by two proton holes in $1d_{3/2}$-shell. Calculations involving the complete sd-shell-model space by Wildenthal et al (1971) and, Wildenthal and Chung (private communication) and core-excitation model by Gray et al (1970) predict the proton pickup spectroscopic factors for the levels in ^{38}Ar. The $^{39}K(d,{}^{3}He)^{38}Ar$ reaction has been studied earlier by Gray et al (1970) at E_d = 28.9 MeV and by Wildenthal and Newman (1968) at E_d = 34.5 MeV. For ^{40}Ar the situation is more complicated because of the presence of two extra neutrons in the $1f_{7/2}$ shell. Gloeckner et al (1973) have performed a shell-model calculation in the $(1d_{3/2})^{-2}_{p}(1f_{7/2}, 2p_{3/2})^{2}_{n}$ - model space and have predicted the spectroscopic factors.

In this chapter a detailed analysis of the $^{39,41}K(d,{}^{3}He)$ reactions at E_d = 22.8 MeV is presented and the proton pickup spectroscopic factors for the levels in ^{38}Ar and ^{40}Ar are reported; the results on ^{40}Ar are presented here for the first time.

6.1. EXPERIMENTAL METHOD

The details of the experimental setup used in $^{39,41}K(d,{}^{3}He)$ reaction experiments have been described in chapter IV.

The targets have been prepared by evaporating onto thin carbon films, natural potassium iodide in the case of ^{39}K target and potassium iodide enriched (to 95%) in ^{41}K in the case of ^{41}K target. The target thickness is estimated by comparing the experimental angular distributions of elastically scattered deuterons in the angular range of 45° to 65° with the optical-model predictions (using the deuteron optical-model parameters listed in table 6-1). Target thicknesses of 130 $\mu g/cm^2$ for ^{39}K and 160 $\mu g/cm^2$ for ^{41}K have been obtained. The estimated error on the target thickness is expected to be 25% .

The spectra of ^{3}He-particles have been recorded in an angular range $10^{\circ} \leqslant \theta_{lab} \leqslant 40^{\circ}$ using counter telescopes. The energy resolution (FWHM) obtained is about 140 keV. Typical excitation spectra taken at 21° have been shown in Fig. 6.1. The energy calibration of the spectra from the $^{39}K(d,{}^{3}He)$ reaction has been made by using the ground state (Q = -0.880 MeV), 2.167- and 4.564-MeV (Endt and Van der Leun, 1978) levels of ^{38}Ar. For the $^{41}K(d,{}^{3}He)$ reaction the energy calibration has been made using the ground state (Q = -0.878 MeV), 2.127-, 3.303- and 4.114-MeV levels of

^{34}S (Endt and Van der Leun, 1978; Puttaswamy and Yntema, 1969) which are populated in the $^{35}Cl(d,^{3}He)$ reaction run under similar conditions. The excitation energies determined in the present study have been indicated in Fig. 6.1 and the estimated accuracy is $\pm$ 30 keV for $E_x \leqslant 6$ MeV. The excitation energies for ^{38}Ar are compared with the theoretical calculations (to be discussed latter) in Fig. 6.2.

The peak areas are obtained mostly by adding the counts under each peak and subtracting a reasonable background. Whenever overlapping peaks are observed, the peak centroids and the area for each peak is determined by fitting the peaks to Gaussians using MALIK and the differential cross section have been determined (for details see sec. 4.4).

6.2. DWBA ANALYSIS

The DWBA analysis has been made using the code DWUCK (see Appendix B) to extract spectroscopic information for the levels in the residual nuclei. The deuteron optical-model parameters of Daehnick _et al_ (1980) and the ^{3}He-particle parameters of Becchetti and Greenlees (1971) have been used in all DWBA calculations. The optical-model parameters have been listed in table 6-1. The real (V_R) and imaginary (W_S) well depths of ^{3}He-parameters given in table 6-1 are only for the ground state transition. The energy and A-dependence of V_R and W_S for ^{3}He-particle is given by,

$$\left.\begin{aligned} V_R &= 151.9 - 0.17\ E + 150\ \eta \\ W_S &= 41.7 - 0.33\ E + 44\ \eta \end{aligned}\right\}. \qquad \ldots(6\text{-}1)$$

Where $\eta = (N-Z)/A$ and E is the energy of ^{3}He-particle in the lab system. The proper energy dependence of the optical-model parameters is taken for the other transitions. Some alternative sets of optipal-model parameters for deuterons from the collections of Perey and Perey (1976) and the mass-dependent ^{3}He-parameters of Trost et al (1980) have also been tried in combination with the parameters given in table 6-1 for a few transitions. The spectroscopic strengths determined with these different sets of parameters are found to lie within about 20% . The DWBA calculations in all these cases employed corrections for finite-range and non-locality in the local energy approximation. A finite-range correction parameter of 0.77 fm has been used. The non-locality corrections have been used only for the deuteron and the ^{3}He channels and the values of the parameters have been listed in table 6-1. For all transitions the DWBA analyses of the type FRNL1 has been made (see sec. 5.2.).

The proton pickup spectroscopic strength have been evaluated by using the expression (3-16). The (d,^{3}He) reaction normalization constant N = 2.95 (Bassel, 1966) has been used in all the cases. (If one uses N = 2.363, given by Ioannides et al (1981) the C^2S values would be increased by a factor 1.2. However, σ_{DW} would increase

by a factor 1.25 if a non-locality correction $\beta = 0.85$ fm is also included in the proton bound state. Thus if one uses $N = 2.363$ and σ_{DW} with non-locality corrections for bound protons, one would get nearly the same values for C^2S as those quoted in tables 6-2 and 6-3.)

The angular distribution of ^3He particles for low-lying proton-hole states in ^{38}Ar and ^{40}Ar excited in the $(d,^3He)$ reaction have characteristic $\ell = 0$ or 2, or admixtures of $\ell = 0$ and 2 shapes. When both ℓ-values are possible, the relative $\ell = 0$ and 2 strengths have been adjusted manually so as to get good visual fits.

6.3. RESULTS AND DISCUSSIONS

6.3.1. Levels in ^{38}Ar

The angular distributions for the transitions to the levels in ^{38}Ar with their DWBA fits are shown in Fig. 6.3. The experimental results deduced from $^{39}K(d,^3He)$ reaction have been summarised in table 6-2. The previous experimental results (Gray *et al*, 1970; Wildenthal and Newman, 1968) along with two different model calculations (Wildenthal and Chung, private communication; Gray *et al*, 1970) have also been tabulated for comparison.

In the present study of $^{39}K(d,^3He)$ reaction, the ground-state (0^+) and the 2.17-MeV (2^+) transitions exhibit characteristic $\ell = 2$ transfer. The ground state of ^{38}Ar

can be populated only by $\ell = 2$ ($j = 3/2$) pickup whereas the 2.17-MeV level can show an admixture of $\ell = 0$ and 2. In a previous study on the $^{39}K(d,{}^{3}He)$ reaction at $E_d = 28.9$ MeV (Gray et al, 1970), the forward angle cross section measurements ($\theta_{lab} > 2.5^{o}$) indicated the presence of a small admixture of $\ell = 0$ ($C^2S(2s_{1/2}) \sim 0.05$).

Four levels, viz., the 3.94-, 4.56-, 5.16- and 5.55-MeV are populated with an appreciable $\ell = 0$ strength. Only the 3.94-MeV level shows clear evidence of $\ell = 0$ and 2 mixing. The 4.56-, 5.16- and 5.56-MeV levels have been excited dominantly by $\ell = 0$ transfer even though the angular momentum selection rule permits both $\ell = 0$ and 2. The 6.24-MeV level excited inweakly in the present experiment is expected to have $\ell = 3$ and $C^2S \leq 0.08$ from Gray et al (1970). For the transition to the 7.13-MeV level in ^{38}Ar, a proton pickup from the $1d_{5/2}$ shell is assumed.

It can be seen that there is, in general, good agreement between the spectroscopic strengths deduced from the present experiment as compared to the previous experimental results (Gray et al, 1970; Wildenthal and Newman, 1968). Small differences in the values of the spectroscopic strengths deduced by various studies may be expected to arise from the differences in the optical-model parameters and in the bound-state parameters.

About seven weak levels, which are suspected to have the $\ell = 3$ character had been observed by the earlier

$^{39}K(d,{}^{3}He)$ study of Gray et al (1970). They are most likely to be due to the pickup from particle-hole admixtures of the type $(f_{7/2})^2(sd)^{-3}$ in the ground state of ^{39}K. The 0^+ state at 3.377 MeV, which is probably of a core excited nature, has not been excited with detectable strength.

The sum rule limit for $1d_{3/2}$ pickup is exhausted by the three levels below 4-MeV excitation. Therefore a $1d_{5/2}$ pickup is assumed for the 7.13-MeV transition. The summed spectroscopic strengths indicated in table 6-2 are in good agreement with each other. The value of $\sum C^2S(2s_{1/2}) = 2.37$ is slightly higher than the values of 2.0 and may be due to the fact that the experimental spectroscopic strengths have been deduced by normalising at the second maximum of the DWBA curves.

A shell-model basis space of only $2s_{1/2}$ and $1d_{3/2}$ orbits provides two levels in ^{38}Ar with $(1d_{3/2})^{-2}_{0^+,2^+}$ to be excited by $\ell = 2$ transfer and two levels with $(1d^{-1}_{3/2}, 2s^{-1}_{1/2})_{1^+,2^+}$ to be excited by $\ell = 0$ transfer. A comparison of experimental and theoretical C^2S-values reveals that the ground state and 2.17 MeV states are indeed multiplets of the $(1d_{3/2})^{-2}$ configuration. However, the $\ell = 0$ strength seems to be distributed over four levels below 6-MeV instead of only two levels. Various alternatives for the extra $\ell = 0$ levels have been proposed by Wildenthal and Newman (1968). It has been strongly felt that these extra $\ell = 0$ levels might be due to excitation of an even number of

(core) particles from the $1f_{7/2}$ shell; they are strongly mixed with the regular $(2s_{1/2}^{-1}, 1d_{3/2}^{-1})$ states. The sum of the fragmented $\ell = 0$ strength is indeed equal to 2.

Core-Excitation Calculation for ^{38}Ar

A quantitative calculation has been made by Gray et al (1970) using a model where two particles from the sd shell are allowed to be excited to the $1f_{7/2}$ shell. Accordingly three core excited states in ^{38}Ar have been defined as

$$[(f_{7/2})^2_{0^+,1}, (d_{3/2})^{-4}_{0^+,0}]_{0^+,1},$$

$$[(f_{7/2})^2_{2^+,1}, (d_{3/2})^{-4}_{0^+,0}]_{2^+,1}, \text{ and}$$

$$0.78[(f_{7/2})^2_{0^+,1}, (d_{3/2}, \text{ seniority}= 2)^{-4}_{2^+,0}]_{2^+,1}$$
$$-0.62[(f_{7/2})^2_{0^+,1}, [(d_{3/2})^{-3}_{3/2^+,1/2}(s_{1/2})^{-1}]_{2^+,0}]_{2^+,0}.$$

The matrix elements for the particle-hole interaction energy have been calculated by assuming a Yukawa-type potential. The calculated excitation energies have been compared in Fig. 6.2. with the experimental spectrum. The C^2S values derived by the core-excitation model of Gray et al (1970) are also compared with the results of present study in the table 6-2. It can be seen that the fragmentation of the $\ell = 0$ strength is quite well reproduced by this model. In particular the 3.94-MeV level is largly of the 2p-4h nature. The C^2S values for the 2_2^+ and 2_3^+ levels

agree with those for the 3.94- and 4.56-MeV levels. The level at 5.55 MeV remains as the best candidate for the two-hole 1_1^+ level.

sdfp-Model Calculation

Very recently a shell-model calculation in the $2s_{1/2}$-$1d_{3/2}$-$1f_{7/2}$-$2p_{3/2}$- model space (Hasper,1979) has been performed. The spectrum at low excitation energies are well reproduced. The level scheme obtained by this calculation is displayed in Fig. 6.2. It is interesting to note that the excitation spectrum for positive-parity levels matches well with the spectrum of the core-excitation model of Gray ey al (1970). Unfortunately, the proton pickup spectroscopic factors for the calculation of Hasper (1979) are not available and it would be interesting to compar these experimental values with the results of this calculation.

6.3.2. Levels in ^{40}Ar

The angular distributions for the transitions to the levels in ^{40}Ar observed in the $^{41}K(d,{}^3He)$ reaction are shown in Fig. 6.4. The ℓ -values and the spectroscopic strengths have been listed in table 6-3. The results of $(1d_{3/2})^{-2}_p(1f_{7/2},2p_{3/2})^2_n$ -model calculation of Gloeckner et al (1973) for sets A and B are also listed for comparison. (Set A: the 0.7-MeV level of ^{37}S is assumed to have pure $p_{3/2}$ configuration. Set B: the 1.4-MeV level of ^{37}S is assumed to have pure $p_{3/2}$ configutation.)

The ground-state (0^+), the 1.46-MeV (2^+) and 3.52-MeV levels are populated dominantly by $\ell = 2$ transfer. The predicted (Gloeckner et al, 1973) $1d_{3/2}$-proton pickup strength for the ground-state and for the 1.46-MeV level are in agreement with the measured values. The levels at 2.52 MeV (2^+) and 3.21 MeV(2^+) exhibit an admixture of $\ell = 0$ and 2. However the model prediction of $C^2S(1d_{3/2})$-value (Gloeckner et al, 1973) for the 2.52-MeV level is much larger than the experimental value by an order of magnitude. For the higher excited levels, the predicted C^2S values are very small. The 4.36- and the 5.17-MeV levels have been populated dominantly by $\ell = 0$ transfer and hence the assigenment 1^+ or 2^+ is suggested for both these levels. The levels at 4.53, 5.82 and 6.23 MeV are weakly excited in the present experiment and hence the angular distributions for these levels could not be extracted.

In order to explain the splitting of the $\ell = 0$ strength among the 3.20-, 4.36- and 5.17-MeV levels, it is suggested that a core-excitation model (similar to that of Gray et al ^{38}Ar) can perhaps be attempted. It looks promising that the properties of the levels of ^{40}Ar can be explained by a model calculation in the sdfp-model space. Because of the complications involved, such calculations have not so far been attempted.

6.4. SUMMARY

The experimental and the theoretical spectroscopic strengths for the positive-parity levels in ^{38}Ar and ^{40}Ar are summarised in Fig. 6.5.

In the case of ^{38}Ar, there is good agreement for the $1d_{3/2}$ pickup between the experimental values and the pridictions from the full sd-shell-model calculation for the first two levels. However, the strength for the $2s_{1/2}$ pickup is not correctly predicted. This deficiency is overcome in the core-excitation model (Gray et al, 1970). Infact the recent shell-model calculation by Hasper (1979) in $2s_{1/2}$-$1d_{3/2}$-$1f_{7/2}$-$2p_{3/2}$ space predicts more 0^+ and 2^+ levels around an excitation energy of 4 MeV as compared to those from the full sd-shell-model calculation and hence shows that the spectrum of core-excited states (obtained by promoting pairs of particles to $1f_{7/2}$ orbit) as assumed by Gray et al (1970) is essentially correct. The experimental summed spectroscopic strengths for $\sum C^2S(1d_{3/2})$ and $\sum C^2S(2s_{1/2})$ are respectively 3.02 and 2.37 and compare favourably with the values 2.94 and 1.99 from the full sd-shell-model calculation, and the values 2.86 and 1.90 from the core-excitation-model calculation. The proton pickup spectroscopic strengths are not available from the sdfp-shell-model calculation of Hasper (1979).

In the case of ^{40}Ar the level properties of only the first two levels are very well explained by the $(1d_{3/2})_p^{-2}$ $(1f_{7/2},2p_{3/2})_n^{2}$- model calculation of Gloeckner et al (1973). Experimentally the $\sum C^2S(1d_{3/2})$ is 2.10 while theoretically a value of about 2.70 is predicted. It is noted that the splitting of the $1d_{3/2}$ strength is not accounted for by the model calculations of Gloeckner et al (1973). Further, inclusion of the $2s_{1/2}$ excitations would be necessary to account for the $\ell = 0$ pickup strength. The sum-rule values for the spectroscopic strengths indicate that substantial strengths lie at higher excitation energies in ^{40}Ar. Hence, a shell-model calculation in the space used by Hasper (1979) is desirable for the nuclei ^{40}Ar and ^{41}K.

Table 6-1 Optical-model parameters used in the DWBA analysis of the $(d,{}^3He)$ reaction on potassium isotopes.

	V_R (MeV)	r_o (fm)	a_o (fm)	W_S (MeV)	$4W_D$ (MeV)	r_I (fm)	a_I (fm)	V_{LS} (MeV)	r_{LS} (fm)	a_{LS} (fm)	r_C (fm))	β_{NL} (fm)
$^{39}K + d$	87.5	1.17	0.748	0.6	48.4	1.325	0.727	13.4	1.07	0.66	1.3	0.54
$^{38}Ar + {}^3He$	150.8	1.20	0.720	36.9	-	1.40	0.880	10.0	1.2	0.72	1.3	0.2
$^{41}K + d$	87.4	1.17	0.745	0.6	48.4	1.325	0.757	13.4	1.07	0.66	1.3	0.54
$^{40}Ar + {}^3He$	153.3	1.20	0.720	39.3	-	1.40	0.880	10.0	1.2	0.72	1.3	0.2
p^a		1.2	0.65					$\lambda=25$			1.25	

[a] The bound proton well-depth is adjusted to give a binding energy of (5.494 - Q) MeV.

Table 6-2. Proton pickup spectroscopic strengths for the levels in ^{38}Ar [a].

E_x [b] (MeV)	J^π [b]	Present Study				Theory			
		ℓ	$100C^2S$	$100C^2S$ [c]	$100C^2S$ [d]	E_x [e] (MeV)	J^π [e]	$100C^2S$ [e]	$100C^2S$ [c]
0.0	0^+	2	; 44;	; 53;	; 49;	0.0	0^+	; 45;	; 39;
2.167	2^+	2	;241;	5;250;	;250;	2.025	2^+	;246;	9;200;
3.937	2^+	0,2	26; 17;	16; 17;	26; 13;	4.145	2^+	117; ;	22; 32;
4.564	2^+	0	81; ;	49; ;	52; ;	8.604	2^+	; ; 120	80; 9;
5.157	2^+	0	37; ;	23; ;	33; ;	10.760	2^+	7; 3; 4	4; 6;
5.552	$(1,2)^+$	0	93; ;	63; ;	78; ;	5.078	1^+	75; ;	75; ;
7.130	$(1-4)^+$	2	; ; 50	; ; 40	; ; 44	7.786	4^+	; ; 221	; ;220
$\sum C^2S(2s_{1/2})$		=	2.37	1.56	2.00			1.99	1.90
$\sum C^2S(1d_{3/2})$		=	3.02	3.20	3.12			2.94	2.86
$\sum C^2S(1d_{5/2})$		=	0.50	0.40	0.44			3.45	2.20

[a] For notations see the foot note of table 5-2.

[b] Taken from the Endt and Van der Leun (1978). Energies measured in the present experiment are indicated in Fig. 6.1(a)

[c] Gray et al (1970). [d] Wildenthal and Newman (1968); the values of C^2S are normalized to give $\sum C^2S(2s_{1/2}) = 2.00$.

[e] Wildenthal and Chung (private communication).

Table 6-3. Proton pickup spectroscopic strengths for the levels in ^{40}Ar [a]

E_x [b] (MeV)	J^π [b]	Present Study ℓ	Present Study $100C^2S$	Theory [c] J^π	Set A E_x (MeV)	Set A $100C^2S$	Set B E_x (MeV)	Set B $100C^2S$
0.0	0^+	2	; 43;	0^+	0.0	; 50;	0.0	; 50;
1.461	2^+	2	; 72;	2^+	1.44	; 71;	1.42	; 69;
2.524	2^+	0,2	2; 11;	2^+	2.91	;142;	2.89	;149;
3.208	2^+	0,2	28; 18;	2^+	3.68	; 9;	3.65	; 6;
3.511	$(1,2^+)$	2	; 66;	2^+	4.53	; ;	4.37	; ;
4.358	$(1,2^+)$	0	39; ;	2^+	5.53	; ;	5.36	; ;
5.166	$(1,2)^+$	0	35; ;	2^+	5.79	; ;	5.54	; ;
$\sum C^2S(2s_{1/2})$	=		1.04			-		-
$\sum C^2S(1d_{3/2})$	=		2.10			2.72		2.74

[a] For notations see the foot note of table 5-2.

[b] Taken from Endt and Van der Leun (1978),

[c] Gloeckner et al (1973). For the details see text.

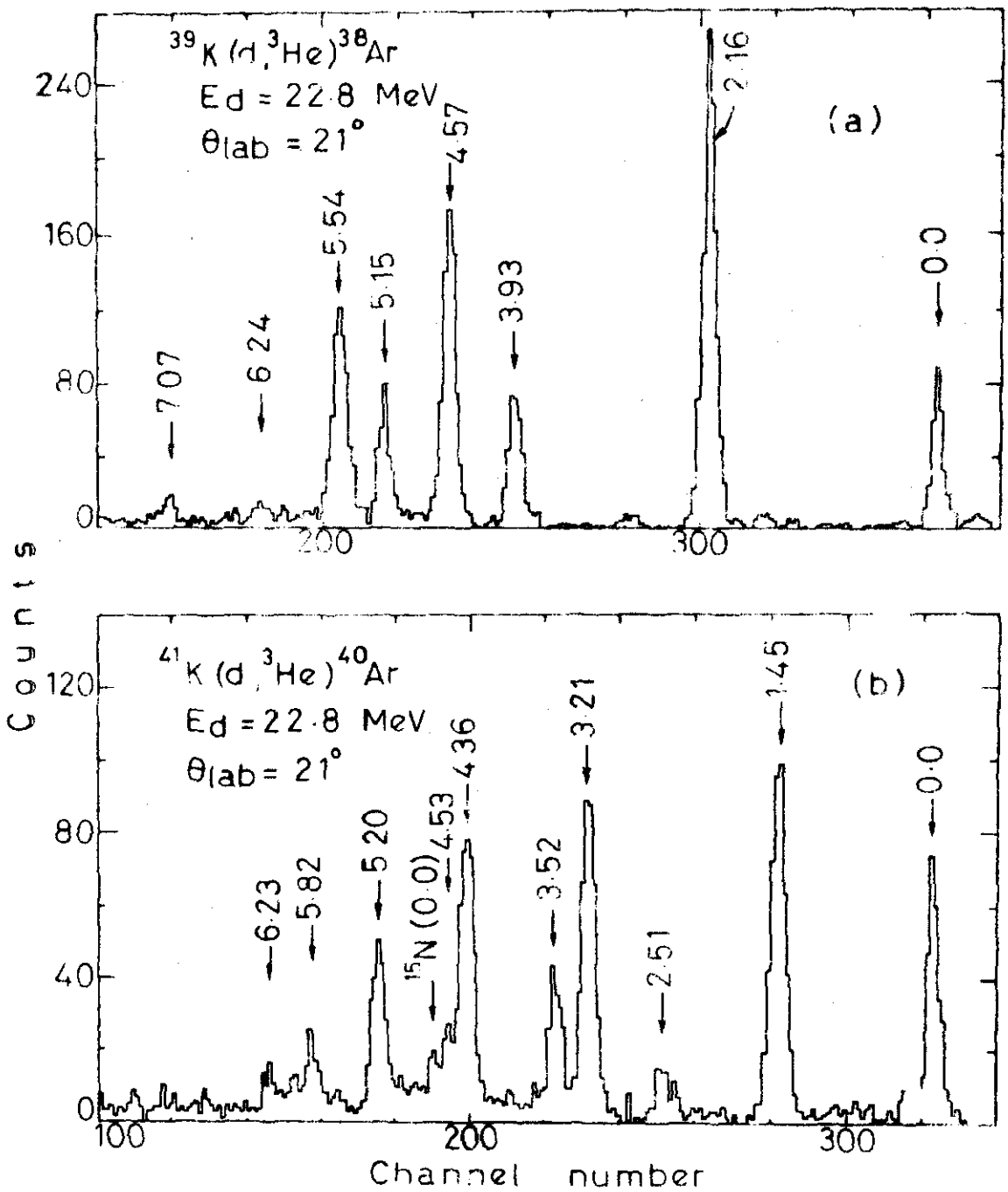

Fig. 6.1. Spectrum of ^{3}He from (d, ^{3}He) reaction on potassium isotopes at 22.8 MeV. (a) ^{39}K(d,^{3}He)^{38}Ar reaction spectrum at θ_{lab} = 21°. (b) ^{41}K(d, ^{3}He) ^{40}Ar reaction at θ_{lab} = 21°. The excitation energies (in MeV) determined in the present experiment are indicated above the peaks.

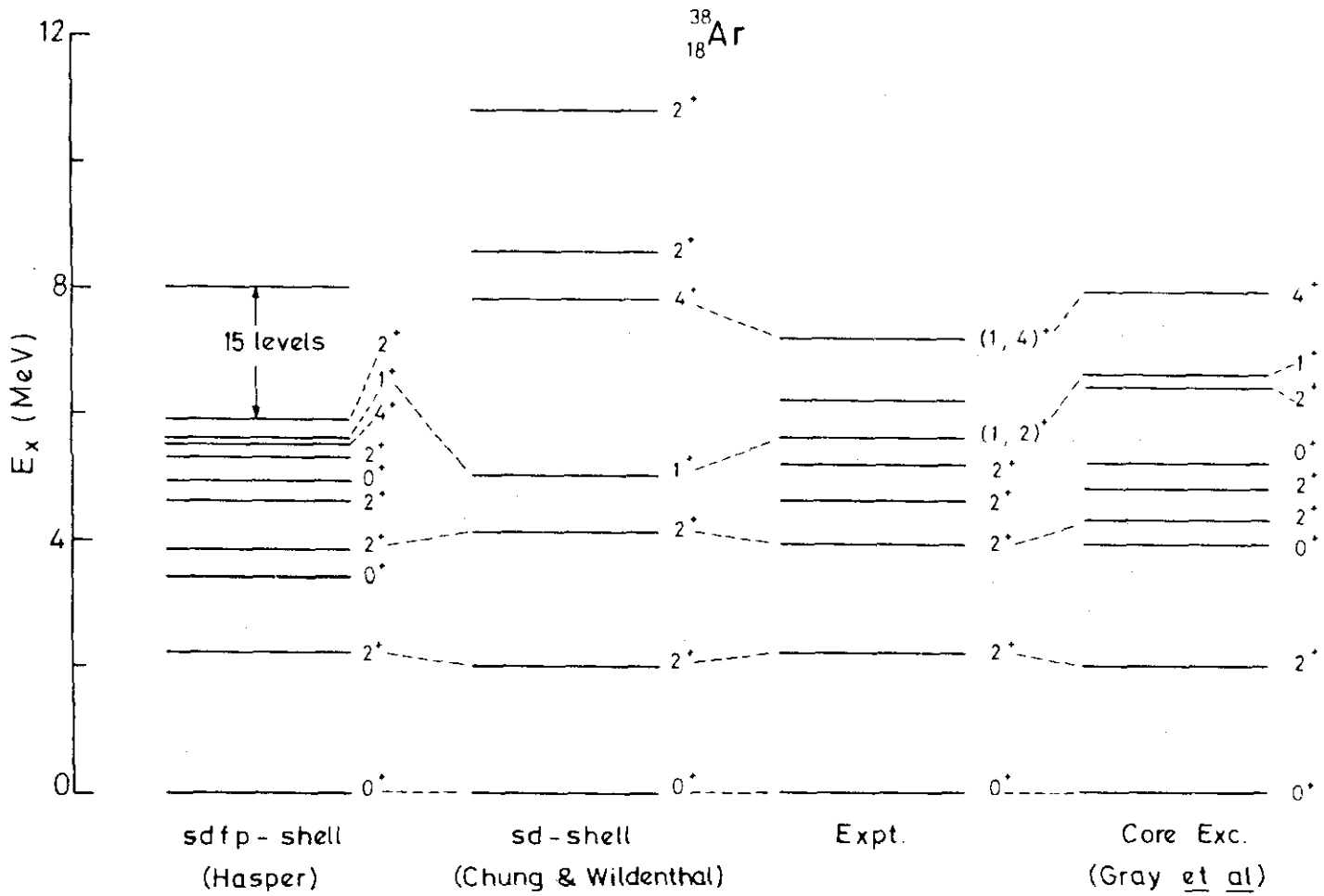

Fig. 6.2 Comparison of the theoretical and expetimental level scheme for ^{38}Ar.

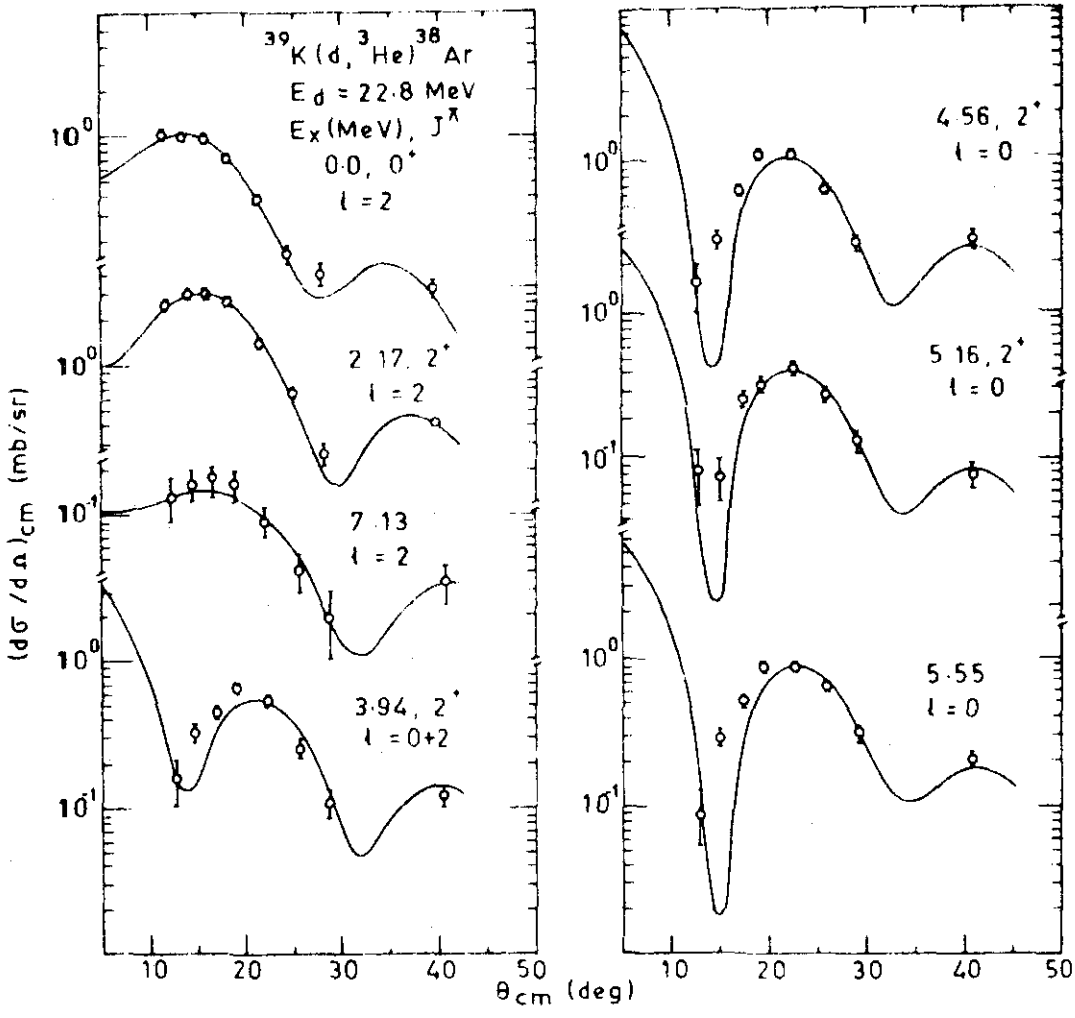

Fig. 6.3 Angular distribution for the levels in ^{38}Ar populated in the ^{39}K(d,^{3}He)^{38}Ar reaction. The curves are the results of DWBA fits.

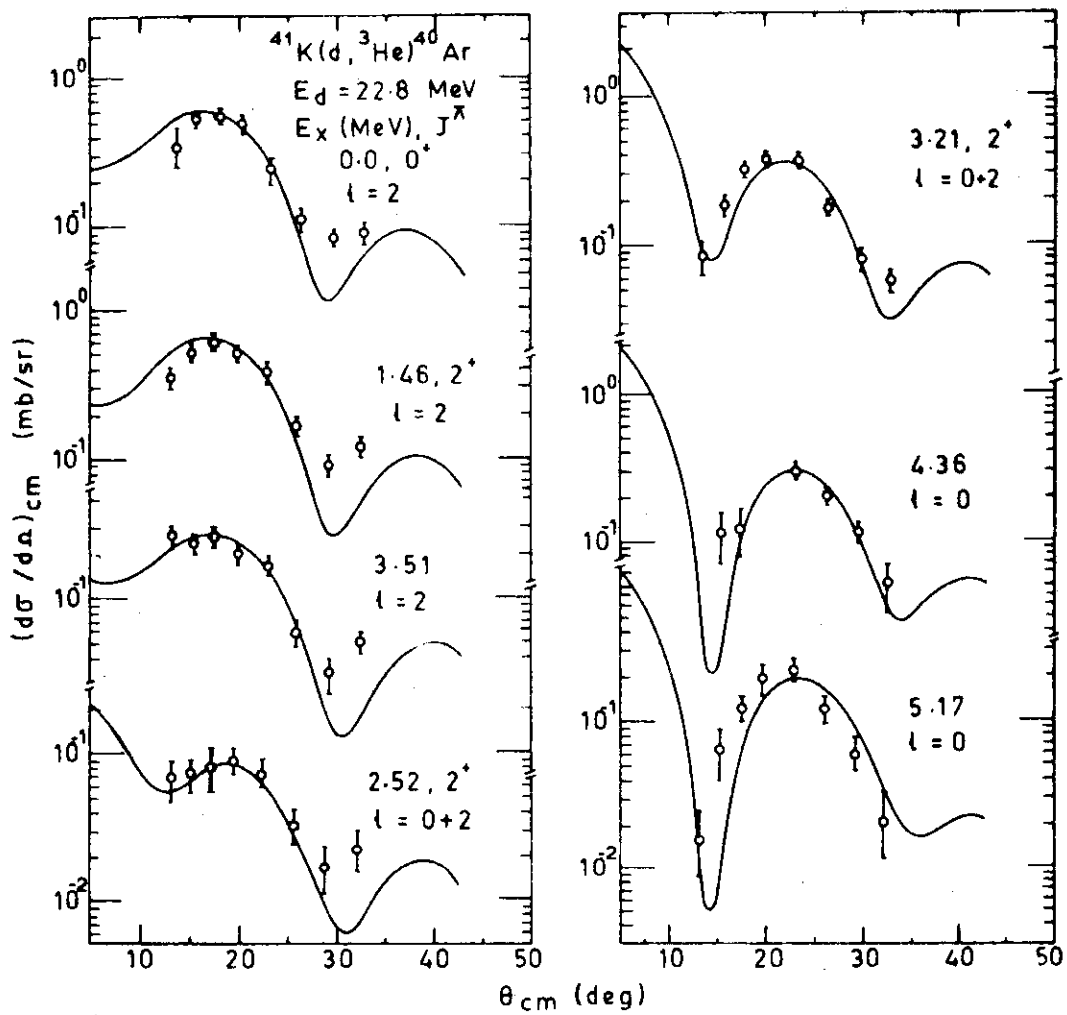

Fig. 6.4 Angular distribution for the levels in Ar populated in the $^{41}K(d,{}^3He)^{40}Ar$ reaction. The curves are the results of DWBA fits.

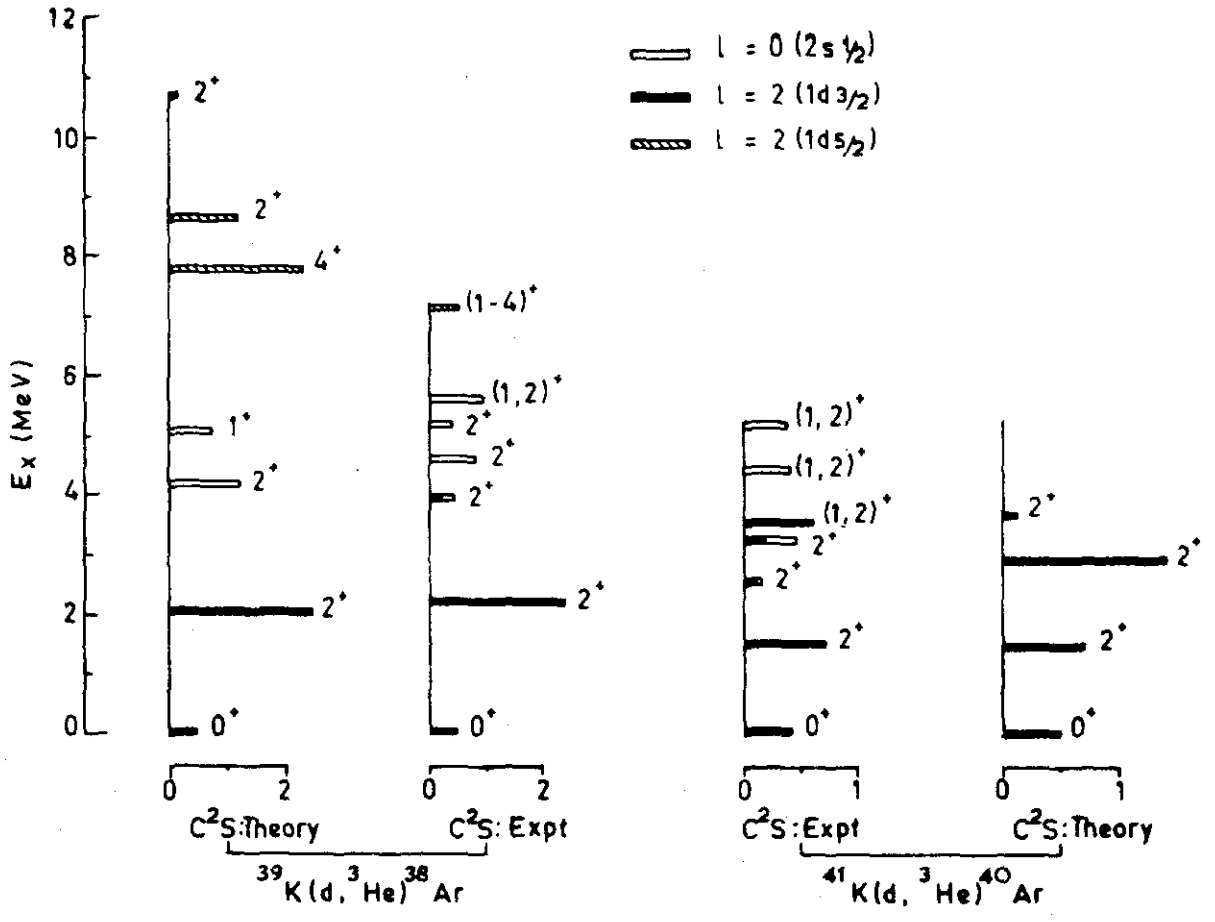

Fig. 6.5 Comparison of shell-model and experimental spectroscopic strengths for the transitions to the levels in ^{38}Ar and ^{40}Ar.

CHAPTER VII

(d,α) REACTION ON ^{40}Ca

In recent years, two-nucleon transfer reactions have been studied extensively to extract information about nuclear structure. Hoot et al (1973), and Van der Woude and de Meijer (1976) have studied the 1p-shell nuclei via the (p,^{3}He) and (d,α) reactions respectively; the spectroscopic amplitudes derived from the shell-model wave functions of Cohen and Kurath (1970) have been used by them. A study of (p,t) and (p,^{3}He) reactions on some sd-shell nuclei has been undertaken by various investigators (King et al, 1976; Nann and Wildenthal, 1975; 1978, 1979; Fortune et al, 1978; Abou-Zeid et al, 1979) and the sd-shell-model wave functions of Wildenthal and Chung (private communications) have been used. However, studies on the (d,α) reactions have been rather limited. DelVecchio and Daehnick (1972) have investigated (d,α) reactions on several nuclei ranging from ^{48}Ti to ^{208}Pb with particular emphasis on the seneitivity of DWBA cross sections towards i) the choice of OM parameters and ii) the use of ' FR correction. In view of these developments particular attention has been given towards a detailed study of the $^{40}Ca(d,\alpha)^{38}K$ reaction.

In a simple shell-model picture, the low-lying positive-parity levels of ^{38}K are expected to have dominant $(1d^{-1}_{3/2})_p(1d^{-1}_{3/2})_p$ configuration. The pickup reactions

such as (d,α) and (p,^{3}He) reactions on ^{40}Ca, are expected to populate levels with such configurations and ought to give direct information on proton-neutron hole states in ^{38}K. Higher levels are necessarily excited by pickup of nucleons from deeper subshells. Spectroscopic amplitudes derived from a full sd-shell-model calculations (Wildenthal and Chung, private communication can be used in a DWBA prediction of the cross section and the results can then be compared with experiments. Excitation of some odd-parity levels of ^{38}K can also be expected because the ground state of ^{40}Ca is known to contain fp-shell admixtures (Endt and Van der Leun, 1978; Gerace and Green, 1967).

The levels of ^{38}K have been studied previously by single- as well as multi-nucleon transfer reactions (Endt and Van der Leun, 1978). Abou-Zeid et al (1979) and Sen and Meijer (1979) have studied the low-lying levels via the (p,^{3}He) reaction at E_p = 42.5 MeV and 30 MeV respectively. Frascaria et al (1974) have investigated the ^{40}Ca(d,α) reaction at E_d = 80 MeV with emphasis on excitation of $(1f_{7/2}^{-1})_p(1f_{7/2}^{-1})_n$, $J^\pi = 7^+$ configuration in ^{38}K. Recently, a study of the dependence of the vector analysing power on the orbital angular momentum L and on the total angular momentum J transferred in the reaction has been made for the ground state and for the 0.46-MeV level of ^{38}K via the ^{40}Ca($\vec{d}$,α) reaction at E_d = 16.5 MeV (Ludwig et al, 1978) and the data have been analysed

by assuming a proton-neutron cluster pickup. A study of the levels at 0.0, 0.46 and 1.69 MeV has been made by Merzet et al (private communication) at E_d = 23 MeV with a view to understand the mechanism of $(\vec{d},\alpha)$ reactions. No levels beyond an excitation energy of 7.35 MeV have been reported in any of the above experiments. Further, none of the earlier $^{40}Ca(d,\alpha)^{38}K$ reaction data have been analysed with a microscopic DWBA prescription using shell-model spectroscopic amplitudes. Other $^{40}Ca(d,\alpha)$ reaction studies have been performed at very low incident energies (Endt and Van der Leun, 1978).

In the present investigation of $^{40}Ca(d,\alpha)^{38}K$ reaction at E_d = 22.8, MeV, the levels upto an excitation energy of 10.26 MeV in ^{38}K have been studied. The angular distributions have been measured over a wide angular range. DWBA analysis has been performed for ten out of twenty transitions observed; orbital angular momentum L transferred and J^{π} values are deduced.

7.1. EXPERIMENTAL METHOD

The experimental setup used in the study of $^{40}Ca(d,\alpha)$ reaction is essentially the sameas described in chapter IV.

The experiment has been carried out with a 22.8-MeV beam. ^{40}Ca target has been prepared by evaporating the enriched isotope onto a thin carbon film. The target

has always been kept in vacuum in order to aviod oxidation. The outgoing α-particles have been simultaniously detected using a set of four dE/dX-E counter telescopes which are separated by 7.5° from each other. An energy resolution (FWHM) of about 135 keV has been obtained. The spectra have been recorded at forty four angles in an angular range from 11° to 165°.

The target thickness has been determined to be 60 $\mu g/cm^2$ by comparing the experimental deuteron elastic scattering cross section around the maximum at 55° (i.e., between 48° to 68° in lab system) with that obtained by using optical-model potential parameters for deuterons listed in table 7-1. The estimated error in the target thickness is expected to be about 25% .

The α-particle spectra are analysed with a peak-fitting computer code MALIK (see sec. 4.4.1). A typical α-particle spectrum at a laboratory angle 45° is shown in Fig. 7.1. A consistent energy calibration has been obtained using the levels of ^{38}K at 0.0 (Q = 4.666 MeV), 0.459, 1.698, 3.431 and 3.978 MeV (Endt and Van der Leun, 1978), and the levels of ^{10}B at 0.0 (Q = -1.341 MeV), 0.718 and 2.155 MeV (Ajzenberg-Selove and Lauritsen, 1974). The excitation energies of the ^{38}K levels determined in the present experiment are indicated in Fig. 7.1. and are also listed in table 7-2. The accuracy of the excitation energies is expected to ± 30 keV for the levels below

4 MeV excitation and about ± 50 keV for levels above 4 MeV.

The differential cross sections for the various transitions have been measured as discussed in sec. 4.4.4. and the values for the ten transitions (which have well srructured angular distributions) have been listed in Appendix C (see also Figs. 7.4 to 7.7). The error in the differential cross section is due to the statistical error and due to the background subtraction. The integrated cross sections, given by the relation (4.12), have also been obtained for many transitions and are listed in table 7-1.

7.2. ANALYSIS

7.2.1. Optical-Model Parameters

Previous studies on (d,α) reactions (Frascaria *et al*, 1977; Frascaria *et al*, 1974; Paul *et al*, 1977) had indicated that the shapes of the DWBA angular distribution is not very sensitive to the choice of the deuteron optical-model parameters while it is quite sensitive to the choice of α-particle parameters. Therefore, the DWBA angular distributions calculated using different sets of α-particle optical-model parameters have been compared with the experimental angular distributions for the 0.0-MeV (3^+) and the 3.43-MeV (2^+) transitions. The 3.43-MeV level can be excited by pure L = 2 transfer.

The deuteron optical-model parameters are taken from the global fits (potential set L))of Daehnick et al (1980). For α-particles, two different sets from the compilation of Perey and Perey (1976) have been tried. The optical-model parameters sets are listed in table 7-1. The set α_1 is the average parameter set used by Bock et al (1967) to fit elastic scattering of 19.47-MeV α-particles on nuclei near ^{40}Ca. The set α_2 is derived from an analysis of elastic scattering of 27-MeV α-particles on ^{39}K. The fits corresponding to these α-particle optical-model parameters are shown in Fig. 7.2. (The shell-model spectroscopic amplitudes for the DWBA calculations are taken from table 7-3.). The set d-α_1 seems to give better fits and hence the DWBA analysis for all other transitions have been performed using this set.

7.2.2. Form Factors

The two-nucleon form factors have been calculated from a microscopic model using the method of Bayman and Kallio (1967). The single-particle wave functions of the transferred proton and neutron have been generated using the Woods-Saxon shape with the values of r_o = 1.18 fm and a_o= 0.68 fm for the radius and for the diffuseness parameters respectively. These bound-state parameters have been derived from an extrapolation of the parameters obtained in a proton elastic scattering experiment (Nadasen et al

1981). For comparison, the set r_o = 1.25 fm and a_o = 0.65 fm commonly used for the calculation of form factors has also been tried (see Fig. 7.3.). The nucleon separation energy has been taken to be $\frac{1}{2}S_d$, where S_d is the deuteron separation energy of the level under consideration; a relative s-state has been assumed for the transferred pair of nucleons.

Mixed configurations in the sd-shell-model space (Wildenthal and Chung, private communication) have been used in the evaluation of the form factors for most of the levels. The two-nucleon spectroscopic amplitudes used in the analyses are listed in table 7-3. For negative parity-levels pure two-particle configurations from sdf-shell-model space have been tried.

7.2.3. DWBA Cross Sections

The sensitivity of the DWBA cross section $\sigma_{DW}(\Theta)$ to the finite-range and non-locality corrections within the local energy approximation has been studied. It is found that the shape of the angular distribution curves with and without the FRNL corrections are very much similar. The ratio $\sigma_{DW}^{FRNL}/\sigma_{DW}^{ZRL}$ lies in the range 1 to 5 at the forward angles ($\Theta_{c.m.} \leqslant 60^o$) and it is about unity elsewhere. The $\sigma_{DW}(\Theta)$, however, is very sensitive to the changes in the bound-state parameters. A comparison of σ_{DW} for the g.s. transition with different bound-state parameters, viz.,

r_o = 1.18 fm and a_o = 0.68 fm, and r_o = 1.25 fm and a_o = 0.65 fm has been shown in Fig. 7.3; the shape of the angular distribution is very similar in both the cases. The DWBA analyses for all the transitions have been made using the bound-state parameter set r_o = 1.18 fm and a_o = 0.68 fm, a finite-range correction of 0.4 fm, and non-locality corrections given in table 7-2.

The contributions from different L-transfers for a given transition is determined by the shell-model two-nucleon spectroscopic amplitudes. These contributions have been added together incoherently and the summed curves have been represented by solid lines in Fig. 7.5 and Fig. 7.6. Each of them has been independently normalized with the experimental angular distribution according to the equation (3-26),

$$\left(\frac{d\sigma}{d\Omega}\right)_{expt} = \frac{N}{2J+1}\left(\frac{d\sigma}{d\Omega}\right)_{DWUCK}$$

These values of N are listed in table 7-3. For negative parity levels the values of N are listed in table 7-4.

7.3. RESULTS AND DISCUSSION

The excitation energies of the levels in ^{38}K deduced from the present experiment are compared in table 7-2 with those adopted by Endt and Van der Leun (1978), and with the results of earlier $^{40}Ca(d,\alpha)$ reaction (Frascaria et al, 1974).

A one to one correspondence of our results with the various levels of ^{38}K could be made only for levels upto an excitation energy of 4 MeV, since the excitation energy level density in ^{38}K is large above 4 MeV. These results compare well with those obtained by Frascaria et al (1974) excetp for the 5.28-MeV level ($J^{\pi} = 7^{+}$), which is weakly excited in the present experiment.

The excitation energies of positive-parity levels of ^{38}K deduced here are shown in Fig. 7.4. along with the theoretical predictions of $1d_{5/2}$-$2s_{1/2}$-$1d_{3/2}$-shell-model (Wildenthal and Chung, private communication) and $2s_{1/2}$-$1d_{3/2}$-$1f_{7/2}$-$2p_{3/2}$-shell-model (Hasper, 1979) calculations.

7.3.1. Even-Parity Levels

The angular distributions to eight even-parity transitions studied in the present $^{40}Ca(d,\alpha)^{38}K$ reaction are shown in Figs. 7.5 and 7.6. The DWBA curves calculated using the spectroscopic amplitudes of Wildenthal and Chung (private communication) are also shown in the figures. The ground state and the 3.66-MeV level show dominant L = 4 and 2 transfer respectively. Previous studies by Frascaria et al (1974) and VAP measurements in the $(\vec{d},\alpha)$ experiment (Ludwig et al, 1978) had strongly suggested the ground state angular distribution to be L = 4. The level at 3.43 MeV is found to show characteristic L = 2

shape; a pure $L = J = 2$ is expected on the basis of the selection rules for this level.

The newly identified level at 9.88 MeV has been excited with a total cross section of 3.16 mb, which is three times that for the ground state transition (see e.g., table 7-2). The DWBA calculation has been made initially with all possible pure two-nucleon configurations in the sdf-shell-model space. This suggested an unambiguous $L = 2$ shape for the experimental angular distribution for the 9.88-MeV level. Hence a $J^{\pi} = 1^{+}$, 2^{+}, or 3^{+} is expected for the 9.88-MeV level. A DWBA calculation has been performed with mixed configurations corresponding to the theoretically predicted 3^{+}_{3} level at 9.06 MeV and the the spectroscopic amplitudes listed in table 7-3. The predicted shape fits the experimental data quite well (see Fig. 7.5) and hence the 9.88-MeV level is most likely to have the assignment 3^{+}, $T = 0$.

The levels at 0.45-, 1.71- and 4.00 MeV are known to $J^{\pi} = 1^{+}$ (Endt and Van der Leun, 1978). Therefore an $L = 0 + 2$ transfer is expected.. The experimental angular distributions and the curves calculated by using sd-shell-model wave functions (Wildenthal and Chung, private communication) are shown in Fig. 7.6. The shape of the experimental angular distributions for all these transitions indicate distinct L transfer. The partial contributions due to $L = 0$ and 2 in the case of 0.45-

and 4.00-MeV levels are indicated in Fig. 7.6 along with their incoherent sums. It can be seen that the 0.45-MeV level has largely L = 2 shape which supports the VAP measurements by Ludwig et al (1978). The 1.71-MeV and 4.00-MeV levels show dominant L = 0 shapes.

In the 80-MeV study of $^{40}Ca(d,\alpha)$ reaction by Frascaria et al (1974), a level at 7.35-MeV excitation has been observed; no spectroscopic information was however deduced. In the present study, the level at 7.32 MeV has been excited very strongly. The integrated cross section for the transitionto this level is about five times that for the ground state transition (see table 7-2). DWBA calculation has been made initially with all possible pure two-nucleon configurations in the sdf-shell-model space; the DWBA angular distributions obtained by assuming $(2s_{1/2})_p(2s_{1/2})_n$ pickup, and $J^\pi = 1^+$, and L = 0 have been found to fit the experimental angular distribution fairly well. Calculation have therefore been made assuming the two-nucleon spectroscopic amplitudes (see table 7-3) for a predicted level at 5.75 MeV (1_4^+). The results of DWBA analyses are shown in Fig. 7.6. The 7.32-MeV level is therefore most likely to have a value $J^\pi = 1^+$.

7.3.2. Odd-Parity Levels

Two levels in ^{38}K, one at 2.64 MeV and another at 2.85 MeV are weakly excited in the present (d,α) experiment.

From a study of the $^{39}K(d,t)$ reaction, Fortune et al (1969) have found that the 2.64-MeV level has $\ell = 1$ angular distribution while a high resolution study of $^{39}K(p,d)$ reaction by Wildenthal et al (1974), suggests an $\ell = 3$ pickup for the same level. However the parity of the level is determined to be negative and the value $J^{\pi} = (2,4)^{-}$ is adopted for this level by Endt and Van der Leun (1978).

In the present experiment angular distribution patterns for the 2.64-MeV and 2.85-MeV transitions (as shown in Fig. 7.7) are almost similar. A good DWBA fit is obtained with $L = 1 + 3$ and $J^{\pi} = 2^{-}$ transfer for both the transitions. The assumed two-nucleon configurations for these levels are given in the table 7-4. According to the sdfp-shell-model calculation (Hasper, 1979) the lowest odd-parity level, having significant fp-shell configuration is at 2.52 MeV excitation and has $J^{\pi} = 4^{-}$. We expect that the 2.64- MeV level is probably a 2^{-} state. Our spin assignment for the 2.85-MeV level, however is $J^{\pi} = 2^{-}$, in agreement with previous studies (Endt and Van der Leun, 1978).

7.3.3. Other Levels

The experimental angular distributions for a few other weak levels in ^{38}K are displayed in Fig. 7.8 and they do not exhibit distinctive patterns. Therefore, not

much spectroscopic information could be obtained for them. There is clear indication for the presence of a level in ^{38}K at 10.26-MeV excitation energy. The present data however, do not enable us to extract angular distribution for this level.

7.3.4. Normalization Constant

The normalization constant N for the (d,α) reaction, is defined by equation (3-26), essentially consists of the overlap integral for the light particles involved in the the reaction. Therefore the value of N is expected to be the same for all transitions. An empherical value of N = 3700 for the (d,α) reaction has been suggested by Van der Woude and de Meijer (1976). The values of N obtained for the various levels in ^{38}K from the present analysis of $^{40}Ca(d,\alpha)$ reaction at E_d = 22.8 MeV have been listed in tables 7-3 and 7-4. The variation in the normalization constant for the levels below 4.00-MeV excitation is rather small. The variations in the values of the normalization constant could perhaps be further reduced with improvements in the shell-model calculations. The sd-shell-model calculation (Wildenthal and Chung, private communication) assumes that ^{40}Ca is a good closed shell nucleus Several experiments have established (Endt and Van der Leun, 1978) that a small amount of 2p-2h and 4p-4h admixtures have to be included in the ground

state of ^{40}Ca nucleus. Therefore it is strongly felt that an elaborate sdfp-shell-model calculation of two-nucleon spectroscopic amplitudes for the levels in ^{38}K is highly necessary. Unfortunately the two-nucleon spectroscopic amplitudes for the levels in ^{38}K are not available from the sdfp-shell-model calculation of Hasper (1979).

The relative values of N obtained from the present (d,α) experiment are compared with the values deduced from the earlier $(p,{}^{3}He)$ experiments of Abou-Zeid et al (1979), and Sens and de Meijer (1979), in table 7-5. The agreement may be considered satisfactory.

7.4. SUMMARY

The excitation energies of the various levels in ^{38}K obtained in the present study are in good agreement with the previous results.

Inspite of the ambiguities in the detailed DWBA predictions for the (d,α) reaction significant spectroscopic information on ^{38}K has been obtained via the $^{40}Ca(d,\alpha)$ reaction. The shapes of the angular distribution for positive-parity levels below 9.88-MeV excitation are rather well predicted by DWBA calculations performed using the two-nucleon spectroscopic amplitudes from the full sd-shell-model calculation (Wildenthal and Chung private communication). Tentative J^{π} assignments made

here are consistent with the previous assignments.

Our analysis indicates that the 7.32-MeV level has a large $(2s_{1/2}^{-1})_p(2s_{1/2}^{-1})_n$ component and hence has $J^\pi = 1^+$. Two new levels, one at 9.88 MeV and another at 10.26 MeV have been identified. The 9.88-MeV level exhibits characteristic L = 2 transfer and probably corresponds to the predicted 3_3^+,T = 0 level at 9.06 MeV

The energies in ^{38}K deduced from a recent shell-model calculation (Hasper, 1979) in the $2s_{1/2}$-$1d_{3/2}$-$1f_{7/2}$-$2p_{3/2}$- model space compare well with that obtained in the present work upto an excitation energy of 3.5 MeV. The calculation however, does not predict any 1^+, 2^+, or 3^+ levels above 4 MeV excitation. Since the spectroscopic amplitudes are not available from this sdfp-calculation, it has not been possible to compare our experimental angular distributions with the theoretical predictions.

Table 7-1. Optical-model potential parameters used in the analysis of $^{40}Ca(d,\alpha)^{38}K$ reaction at 22.8 MeV.

Channel	V_R (MeV)	r_o (fm)	a_o (fm)	W_S (MeV)	$4W_D$ (MeV)	r_I (fm)	a_I (fm)	$2V_{LS}$ (MeV)	r_{LS} (fm)	a_{LS} (fm)	r_C (fm)	β_{NL} (fm)
d	87.7	1.17	0.748	0.7	48.4	1.325	0.729	13.4	1.07	0.66	1.3	0.54
α_1	183.7	1.4	0.564	26.6		1.4	0.564				1.4	0.2
α_2	215.8	1.111	0.785	22.6		1.111	0.785				1.34	0.2
n [a]		1.18	0.68					$\lambda = 25$			1.25	0.85

[a] The proton and neutron Woods-Saxon well-depths are adjusted to reproduce the proper separation energy. Another set with r_o = 1.25 fm and a_o = 0.65 has also been tried for the ground-state transition (see Fig. 7.3).

Table 7-2. Comparison of the excitation energies of the levels in ^{38}K.

Adopted Energy Levels[a]		$^{40}Ca(d,\alpha)^{38}K$			
		Present work		Frascaria *et al*[b]	
E_x (MeV)	J^π	E_x[c] (MeV)	σ_{Int} (mb)	E_x (MeV)	L
0.0	3^+	0.0	0.99	0.0	4
0.459	1^+	0.45	1.46	0.45	
1.698	1^+	1.71	0.74	1.70	0,2
2.649	$(2,4)^-$	2.64	0.14	2.63	
2.870	2^-	2.85	0.26	2.85	
3.431	2^+	3.43	1.06	3.42	
3.668	3^+	3.66	0.37	3.60	
3.857	1^+	3.85			
3.978	1^+	4.00	0.52	3.97	
		4.23		4.28	
		4.38			
		5.38		5.28	6
		5.80			
		6.06			
		6.42		6.35	
		6.72		6.60	
		7.00		6.90	
		7.32	5.51	7.35	
		9.88	3.16		
		10.26			

[a] Endt and Van der Leun (1978). [b] E_x values are taken from Fig. 4 of Frascaria *et al* (1974). [c] The errors in E_x are estimated to be ± 30 keV for the levels below 4-MeV and about ± 50 keV for higher levels.

Table 7-3. Two-nucleon spectroscopic amplitudes for the $^{40}Ca(d,\alpha)^{38}K$ reaction and the results of DWBA analysis [a].

E_x (MeV)	L	J^{π} [b]	Two-nucleon spectroscopic amplitudes [b] (D5,D5)	(D5,S1)	(D5,D3)	(S1,S1)	(S1,D3)	(D3,D3)	$N \times 10^{-4} \times 2J_f + 1$
0.0	2,4	3_1^+	-0.0073	0.0159	-0.2147			0.9765	2.08
0.45	0,2	1_1^+	0.0655		-0.5382	0.2751	-0.7126	0.3501	1.04
1.71	0,2	1_2^+	-0.2020		0.4238	-0.1928	0.0102	0.8616	1.13
3.43	2	2_1^+		0.2784	0.4425		0.8524		0.80
3.66	2,4	3_2^+	-0.2674	-0.6645	0.6797			0.1582	0.29
4.00	0,2	1_3^+	-0.1073		0.4208	-0.4880	-0.6799	-0.3333	0.54
7.32	0,2	1_4^+	0.1111		-0.5463	-0.8054	0.1672	0.1126	14.06
9.88	2,4	3_3^+	0.0822	-0.7298	-0.6694			-0.1351	14.57

[a] The DWBA angular distributions for these transitions are shown in Figs. 7.5 and 7.6.

[b] Wildenthal and Chung (private communication)

Table 7-4. Two-nucleon configurations assumed for odd-parity levels in ^{38}K, and the results of the DWBA analysis[a].

E_x (MeV)	L	Assumed J^{π}	Two-nucleon (configurations[b]	$N \times 10^{-4} \times 2J_f+1$
2.64	1,3	2^-	(D3,F7)	2.20
2.85	1,3	2^-	(D3,F7)	5.07

[a] The resulting DWBA angular distributions are shown in Fig. 7.7. [b] The notation (D3,F7) implies $(1d_{3/2}^{-1})_p(1f_{7/2}^{-1})_n$ configuration. The L = 1 and L = 3 contributions have been added in coherently.

Table 7-5. The relative values of normalization constants [a] derived from the various two-nucleon transfer reactions on the levels in ^{38}K.

E_x (MeV)	Present study	From $(p,{}^3He)$ studies	
	$N_{g.s.} \times \frac{2J_f+1}{2J_{g.s.}+1}$	$N_{g.s.}$ [b]	$N_{g.s.}$ [c] $\times \frac{2J_f+1}{2J_{g.s.}+1}$
0.0	1.00	1.00	1.00
0.45	0.50	6.99	0.80
1.71	0.54	2.01	2.00
3.43	0.38		
3.66	0.14		
4.00	0.26		
7.32	6.76		
9.88	7.00		

[a] The normalization constants are given relative to the ground state.

[b] From the $(p,{}^3He)$ study by Abou-Zeid et al (1979); the Wildenthal and Chung wave functions have been used for the analysis.

[c] Sens and de Meijer (1979); they use the two-nucleon spectroscopic amplitudes of Zuker (Strasbourg)

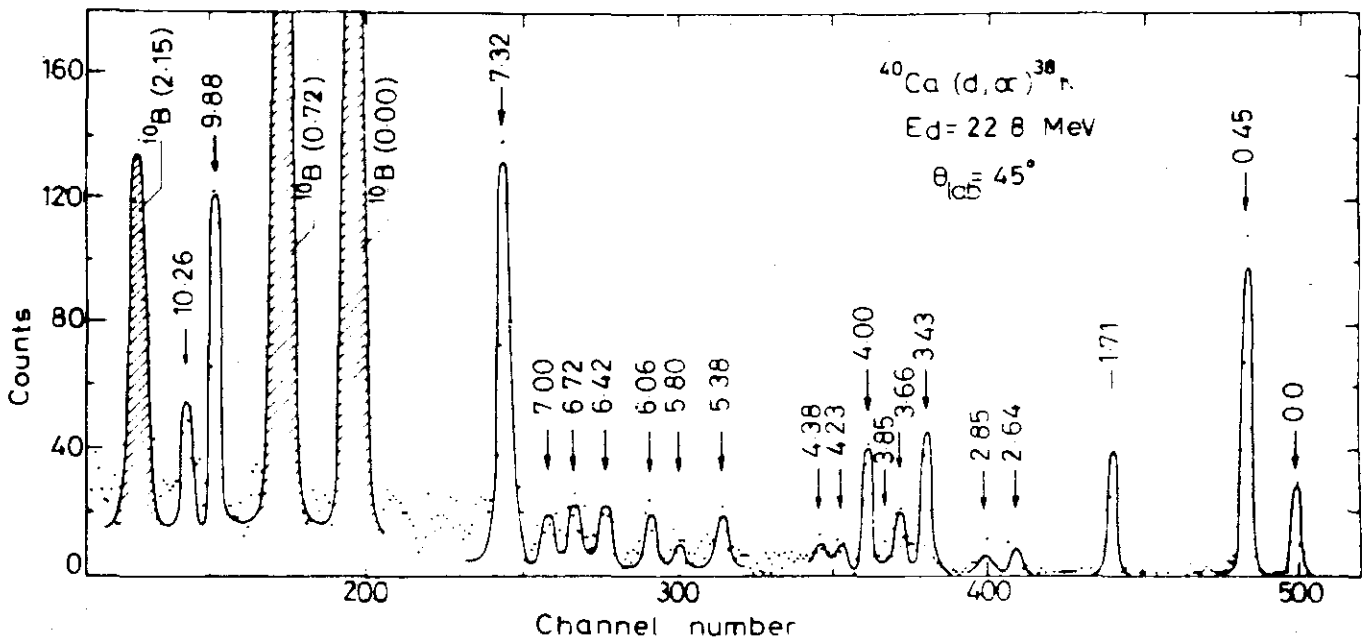

Fig. 7.1. Spectrum of α-particles. The excitation energies (in MeV) shown on the peaks have been deternined from the present experiment. The transition from the $^{12}C(d,\alpha)^{10}B$ reaction are shown by hatched peaks.

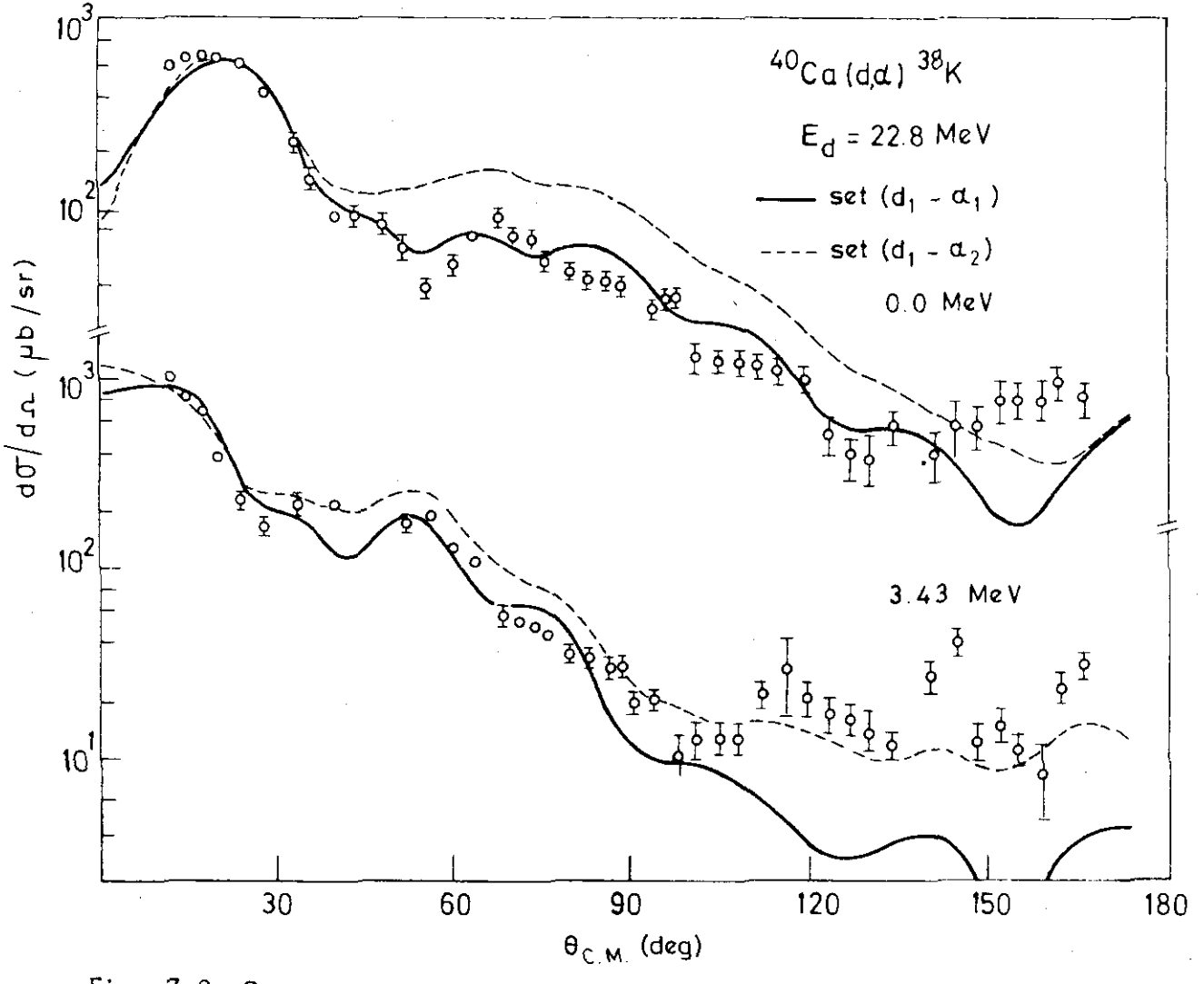

Fig. 7.2 Comparison of the experimental angular distributions with the DWBA curves obtained using different sets of OM parameters listed in table 7-1.

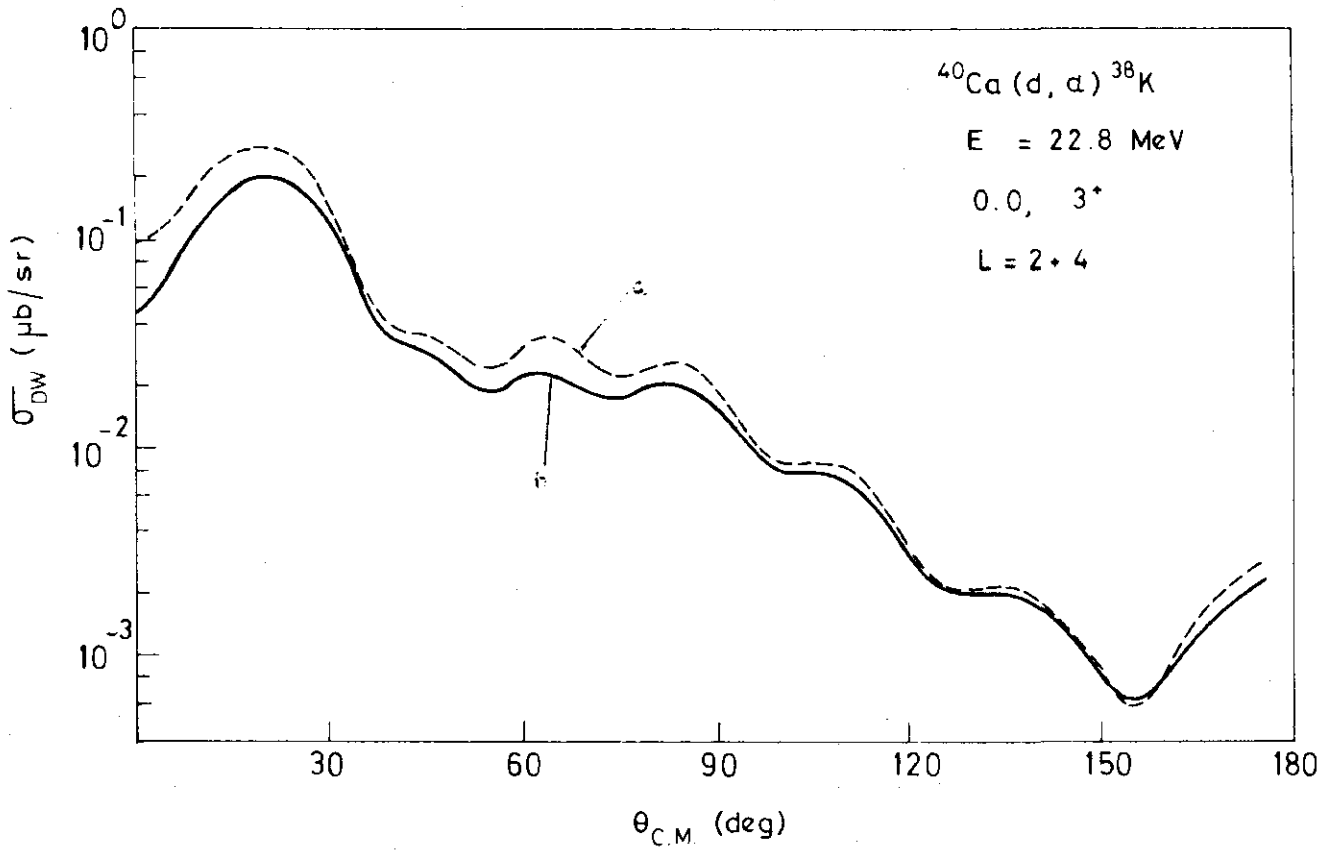

Fig. 7.3 Comparison of the DWBA curves with different bound state parameters.
Curve a : r_o = 1.25 fm, a_o = 0.65 fm
Curve b : r_o = 1.18 fm, a_o = 0.68 fm.

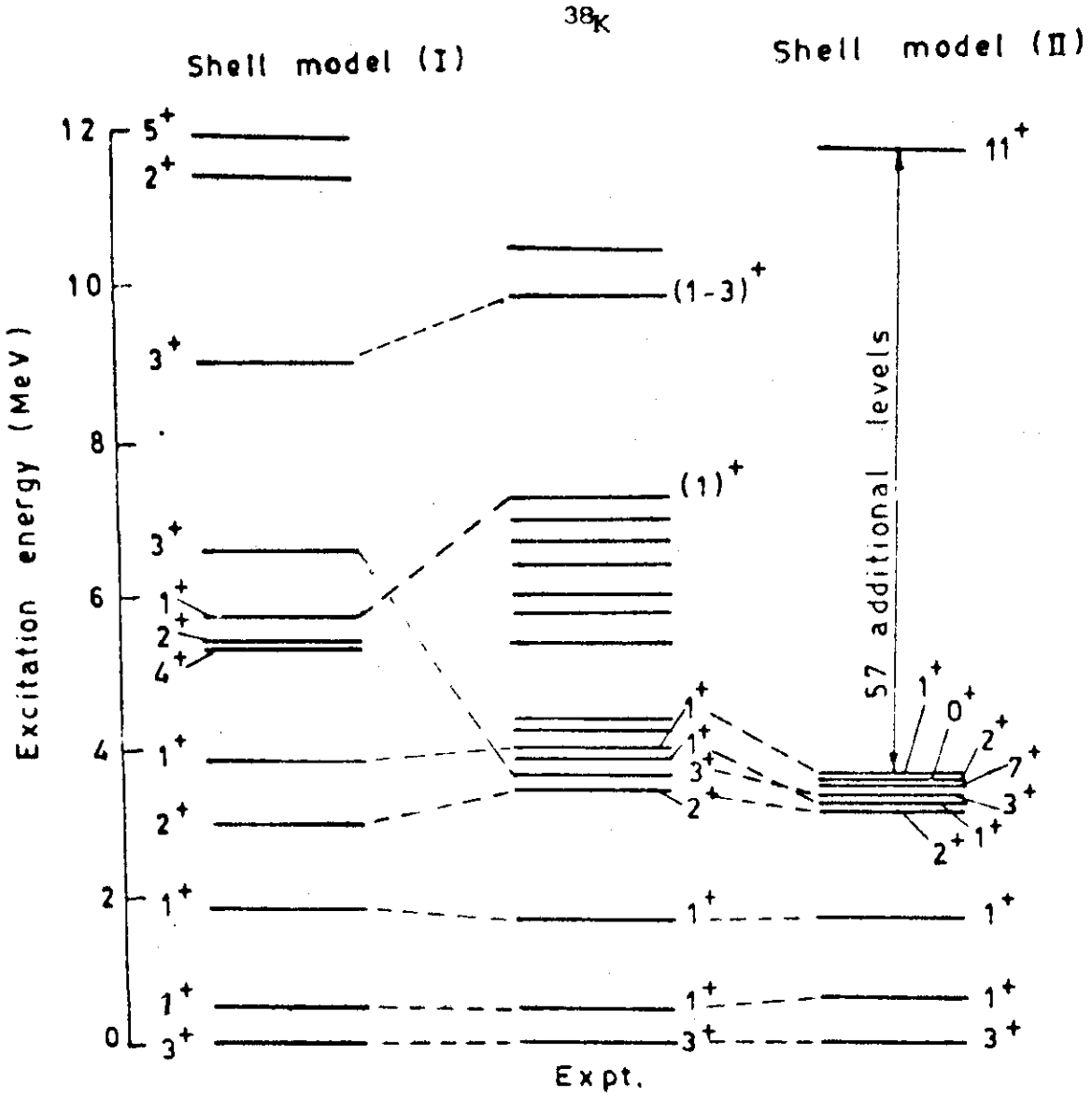

Fig. 7.4 Comparison of the experimental and theoretical level scheme for ^{38}K. Shell-model I : sd-shell-model Shell model II : sdfp-shell-model.

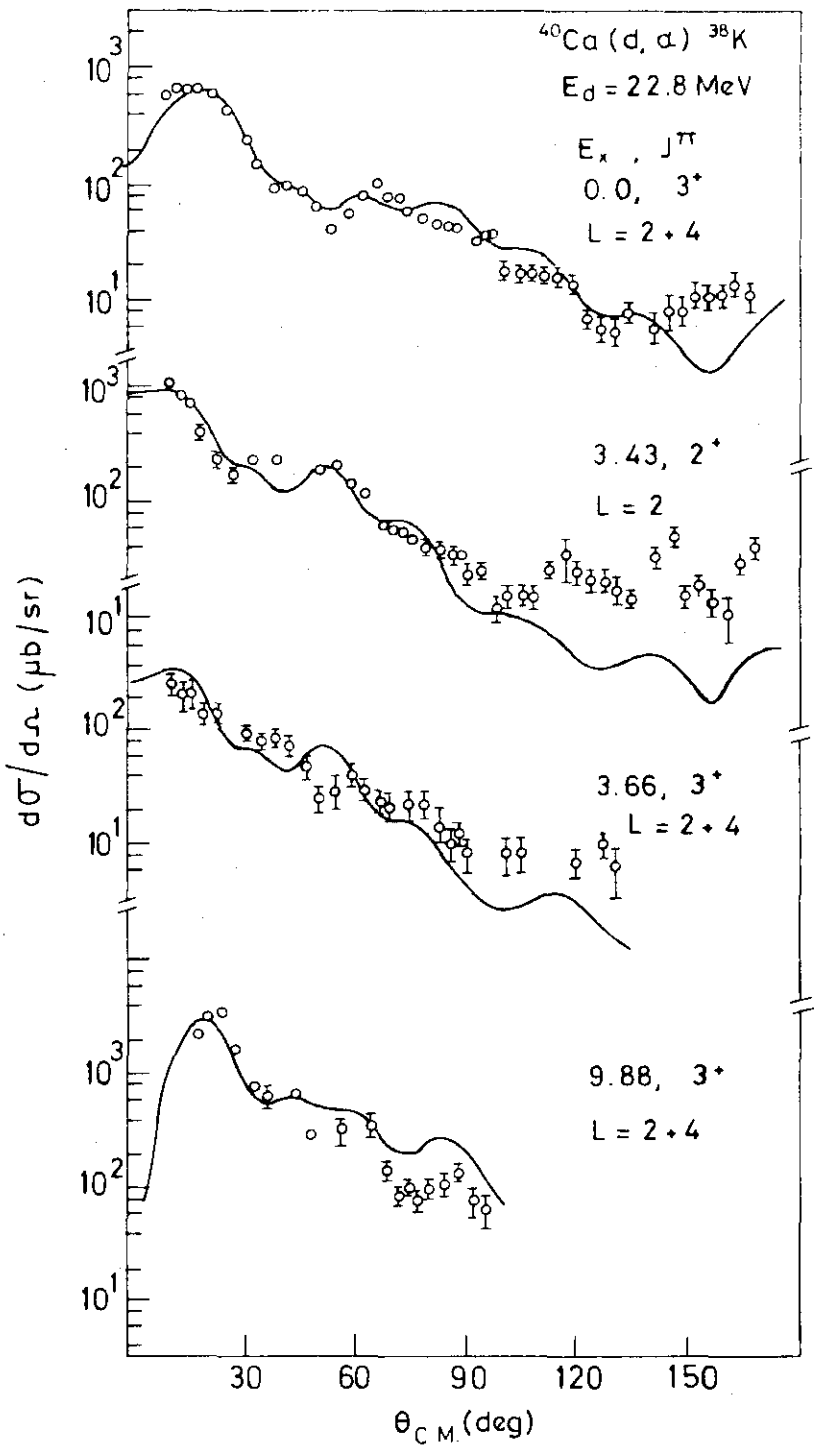

Fig. 7.5 Angular distribution for the levels in ^{38}K
The curves are results of DWBA analyses.

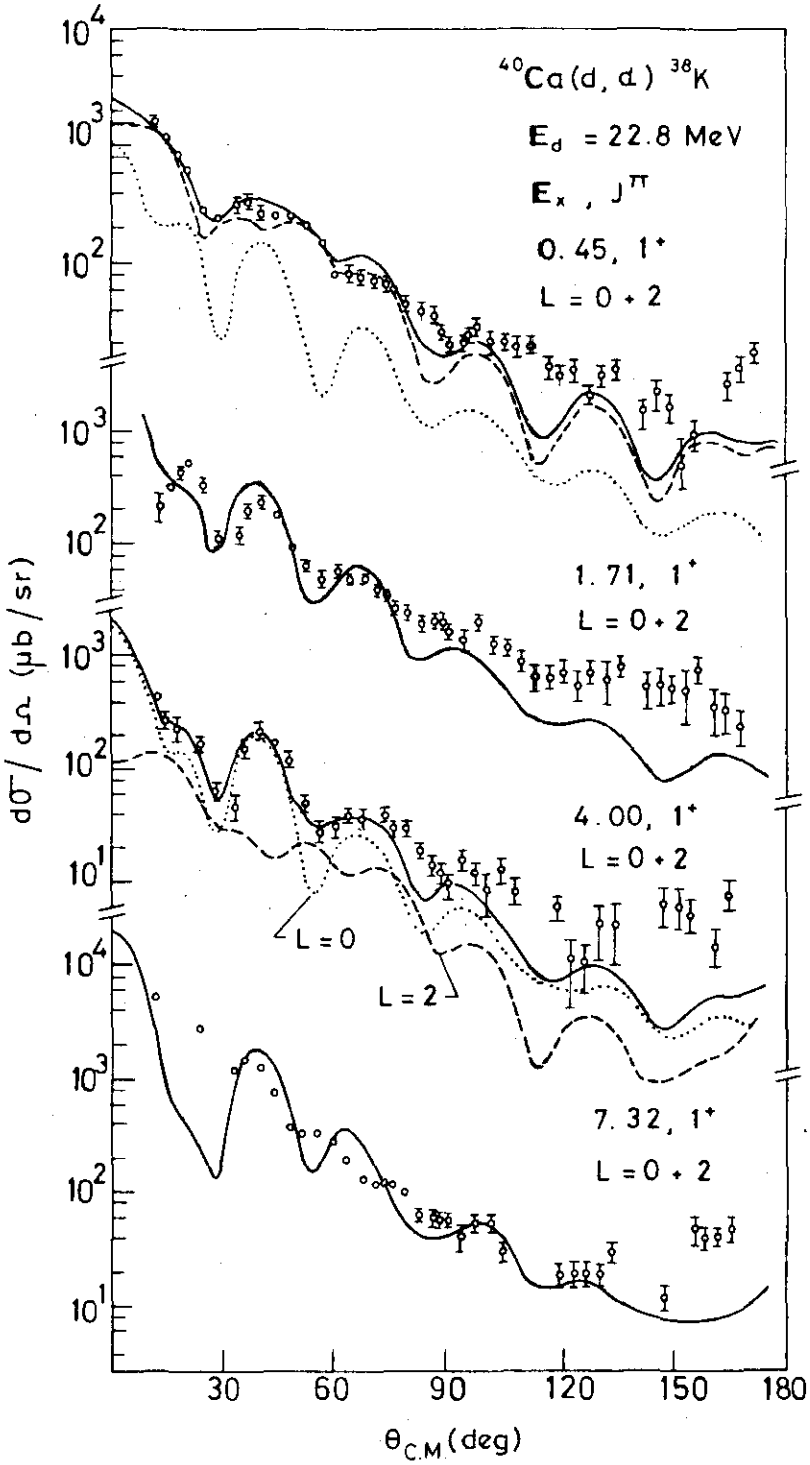

Fig. 7.6 Angular distributions for the 1^+ levels in ^{38}K. Curves are DWBA fits for L = 0+2 transfer.

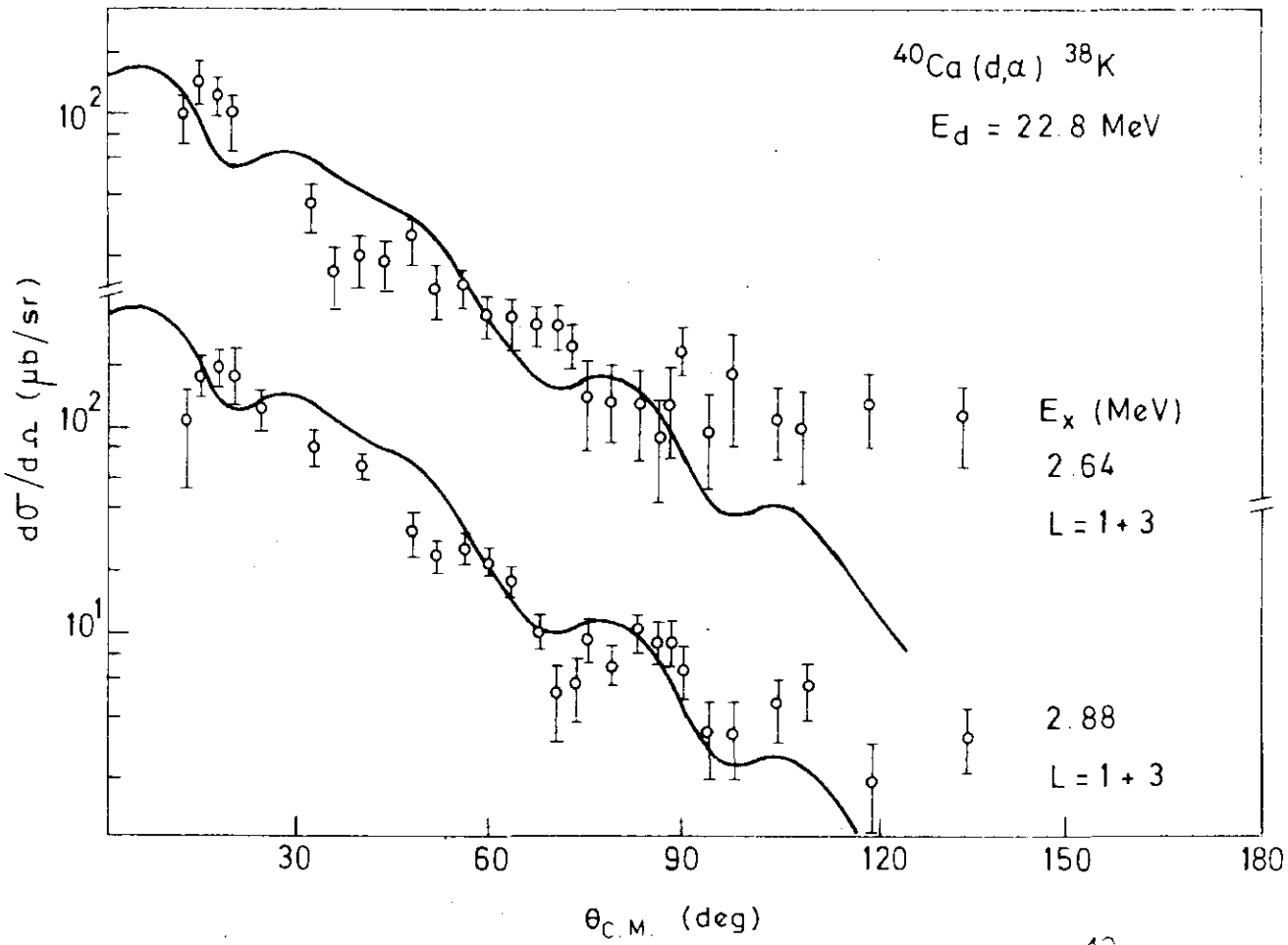

Fig. 7.7 Angular distributions for odd-parity levels excited in ^{40}Ca(d,α) reaction at 22.8 MeV. The curves are the results of DWBA analysis using the configurations indicated in table 7-4.

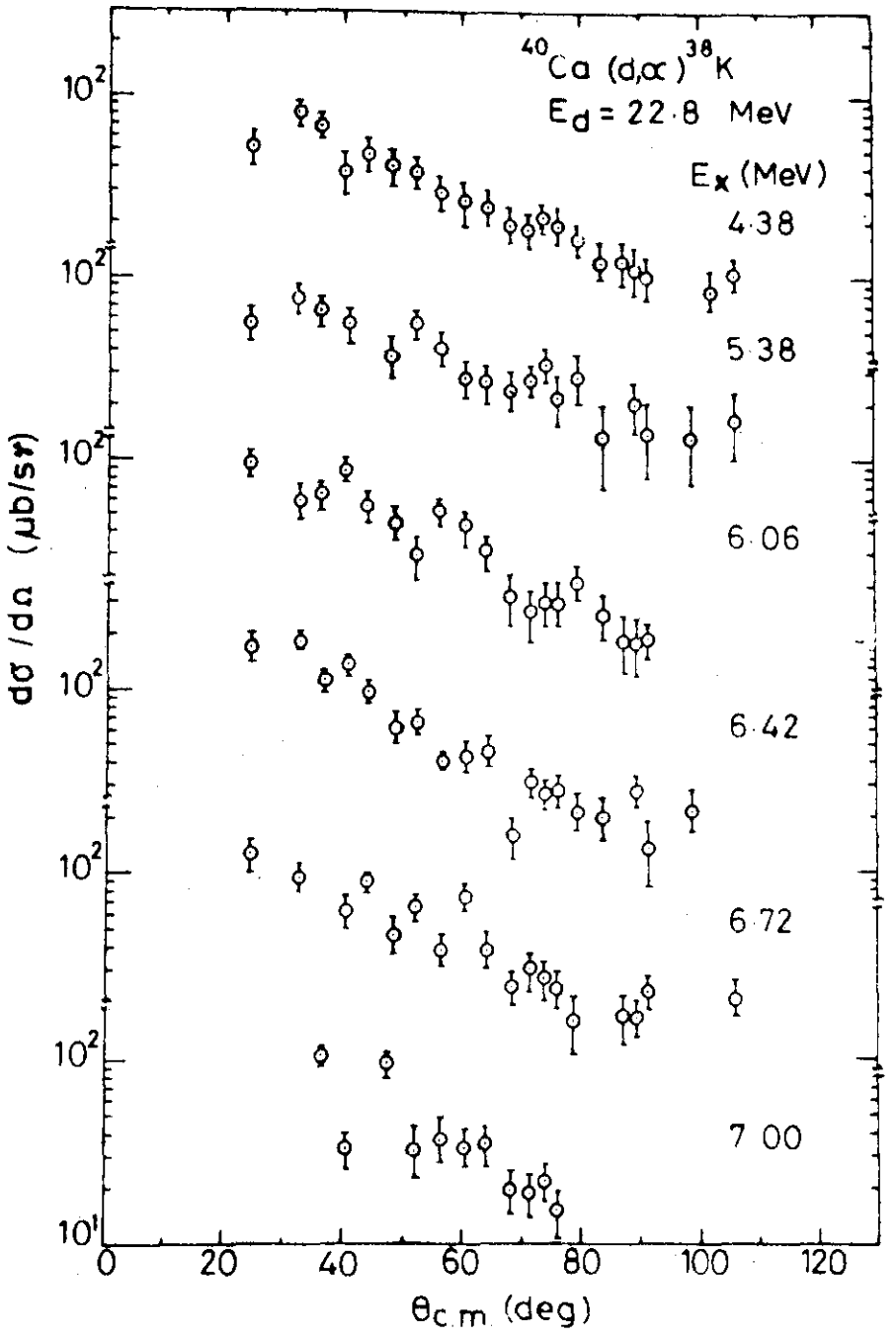

Fig. 7.8 Angular distributions for which a definite L assignment could not be made.

CHAPTER VIII

(d,α) REACTION ON ^{12}C

During the study of the $^{40}Ca(d,\alpha)^{38}K$ reaction, carbon had been used as the backing material for the ^{40}Ca target. Six peaks corresponding to the low-lying levels of ^{10}B appeared in the energy spectrum of α-particles and the analysis of these levels is presented in this chapter. A microscopic DWBA analysis for the transitions to the low-lying levels of ^{10}B have been carried out by using the spectroscopic amplitudes deduced from the 1p-shell-model calculations of Cohen and Kurath (1970).

8.1. EXPERIMENTAL METHOD

The experimental method used for a study of $^{12}C(d,\alpha)^{10}B$ reaction at E_d = 22.8 MeV is same as the that described in sec. 7.1 for the case of the $^{40}Ca(d,\alpha)$ reaction. The pulse-height spectrum of α-particles (essentially corresponding to the lower energy part of the Fig. 7.1.) is shown in Fig. 8.1. The excitation energies measured here are indicated in the figure. (see also table 8-2). The estimated error in each case is about ± 50 keV. The energy resolution (FWHM) is found to be about 275 keV. The measured angular distributions for all the transitions have been shown in the Fig. 8.2.

8.2. DWBA ANALYSIS

The angular distribution of α-particles corresponding to the various levels in ^{10}B excited in $^{12}C(d,\alpha)$ reaction have been analysed using DWBA prescription and the two-nucleon-transfer option in the code DWUCK. (The procedure for the analysis is similar to that discussed in sec. 7.2.) The optical model (OM) parameters are listed in table 8-1. The globel deuteron parameter set of Daehnick et al (1980) are denoted by set d_1. The α-particle OM parameter set α_1 has been taken from the compilation by Perey and Perey (1976). Initially the angular distributions for the ground state (3^+) and 3.59 MeV (2^+) have been fitted by DWBA calculations. Both these transitions are expected to exhibit pure L = 2 transfer. The solid curves in Fig. 8.2 are the result of DWBA calculations with FRNL and sets d_1-α_1 . The calculations have been made by using the 1p-shell two-nucleon spectro scopic amplitudes of Cohen and Kurath (1970). The curves in the Fig. 8.2 have been independently normalized to the experimental angular distributions.

In an attempt to improve fits to the angular distributions DWBA calculations have also been made with other OM parameters available in litrature; these are also listed in table 8-1. The results of the DWBA calculations with FRNL corrections, by using the set d_2-α_1 (shown by dotted curve) and by using the set d_3-α_3 (shown by

dashed curve) are shown in Fig. 8.2. The shape of the DWBA curve for the set d_2-α_1 is very much similar to that obtained for set d_1-α_1. However simultanious fit to both the experimental angular distributions could not be obtained for any combination of the deuteron and α-particle OM parameter sets listed in table 8-1. The DWBA analysis has also been performed for all other levels with the set d_1-α_1 and the fits at are shown in the Fig. 8.2. The values of the normalization constants obtained from the present experiments have been listed in table 8-2.

8.3. DISCUSSIONS

The excitation energies deduced for the various levels from the present experimental data are in good agreement with the previous values (Ajzenburg-Selove, 1974; Van der Woude and de Meijer, 1976).

The 0.0-MeV and 4.77-MeV levels atare known to be 3^+ and are expected to have pure $(1p_{3/2})_p(1p_{3/2})_n$ configuration; these states can only be populated by L = 2 transfer. The states at 0.72 MeV, 2.16 MeV and 5.18 MeV are all 1^+ and are expected to have a mixture of all two-nucleon configurations in the 1p-shell space; these states can be populated by both L = 0 and 2 transfers.

It has been found that in the case of 1p-shell

nuclei (generally light nuclei), there are obvious difficulties in selecting OM parameters (Van der Woude and de Meijer, 1976). It is suspected that at E_d = 30 MeV compound nucleus and /or multstep processes could be still important (Janecke et al, 1971). Additional difficulties have been noticed by Yang (1969) while explaining the angular distributions at E_d = 21.2 MeV; one may have to take into account 'heavy particle stripping' in addition to direct pickup of two-nucleons. But Yang finds that the forward part of the angular distributions could be well accounted for by considering only a direct two-nucleon pickup process. Even at 40 MeV, Van der Woude and de Meijer (1976) could not succeed in fitting the angular distributions using the OM parameters derived from the elastic scattering data. They adopted the prescription given by DelVecchio and Daehnick (1972) and have used lower cut-off radius $R_{min} = 1.75 \times A^{1/3}$ to get reasonably good fits.

The relative values of the reaction normalization constant N listed in table 8-2, indicate that the values of N obtained in the present experiment are in reasonable agreement with the values obtained by Van der Woude and de Meijer (1976).

Table 8-1 Optical-model parameters used in the DWBA analysis of $^{12}C(d,\alpha)^{10}B$ reaction.[Y]

Channel	V_R (MeV)	r_o (fm)	a_o (fm)	W_S (MeV)	$4W_D$ (MeV)	r_I (fm)	a_I (fm)	$2V_{LS}$ (MeV)	r_{LS} (fm)	a_{LS} (fm)	r_C (fm)	β_{NR} (fm)
d_1	84.9	1.17	0.748	0.65	48.6	1.325	0.676	13.3	1.07	0.66	1.3	0.54
d_2	109.0	0.9	0.85		32.5	1.659	0.68	16.0	1.1	0.45	1.3	0.54
d_3	100.0	1.4	0.6	25.0		1.74	0.85				1.3	0.54
α_1	212.1	1.375	0.52	4.83		1.699	0.563				1.34	0.2
α_2	195.0	1.6	0.52	20.0		1.44	0.635				1.3	0.2
n[a]		1.25	0.65					$\lambda = 25$			1.25	0.85

[Y] A finite range correction of 0.4 fm is used in the DWBA analysis

[a] The proton and neutron Woods-Saxon well-depths are adjusted to reproduce the propre separarion energy.

Table 8-2 The results of $^{12}C(d,\alpha)^{10}B$ reaction and the comparison with the DWBA analysis.

E_x [a] (MeV)	J^π [a]	E_x [b] (MeV)	E_x [c] (MeV)	L^c	Spectroscopic amplitudes [d] (P3,P3)	(P3,P1)	(P1,P1)	$N/N_{g.s.}$ Present [c]	Previous [b]
0.0	3^+	0.0	0.0	2,4	-1.814			1.0	1.0
0.718	1^+	0.72	0.72	0,2	-0.660	1.136	0.047	0.85	1.0
2.155	1^+	2.15	2.16	0,2	-1.041	-0.153	0.521	0.99	0.33
3.590	2^+	3.59	3.59	2		-1.035		1.72	0.17
4.773	3^+	4.77	4.77	2,4	1.055			2.68	0.33
5.180	1^+		5.18	0,2	0.283	0.161	0.412	44.24	

[a] Ajzenberg-Selove (1974).

[b] Van der Woude and de Meijer (1976); $N_{g.s.} = 6660$

[c] Present study; $N_{g.s.} = 226$

[d] The two-nucleon spectroscopic amplitudes have been taken from Cohen and Kurath (1970).

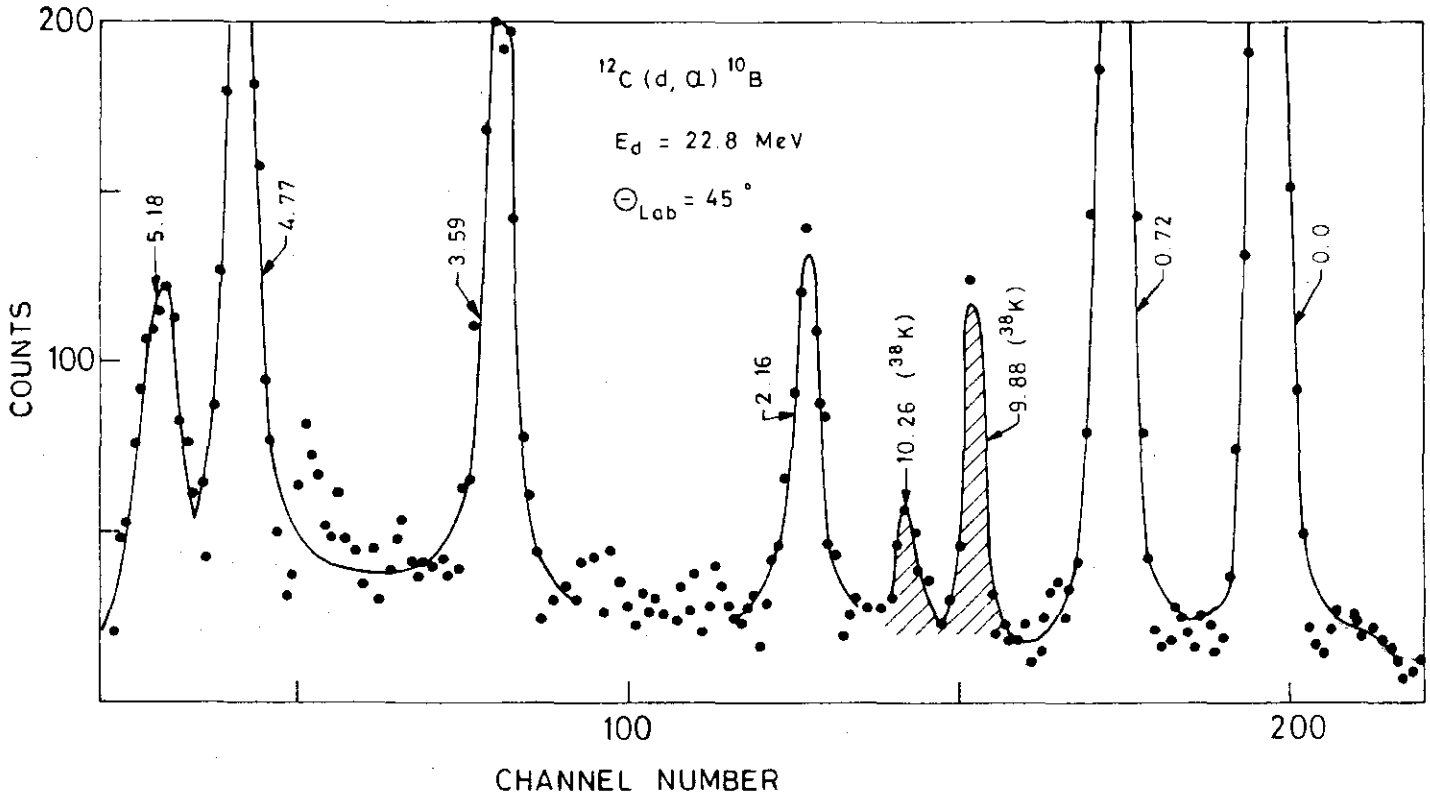

Fig. 8.1. Spectrum of α-particle from $^{12}C(d,\alpha)^{10}B$ reaction at 45°. The excitation energies determined from the present experiment are indicated above the peaks. The hatched peaks are due to $^{40}Ca(d,\alpha)^{38}K$ reaction.

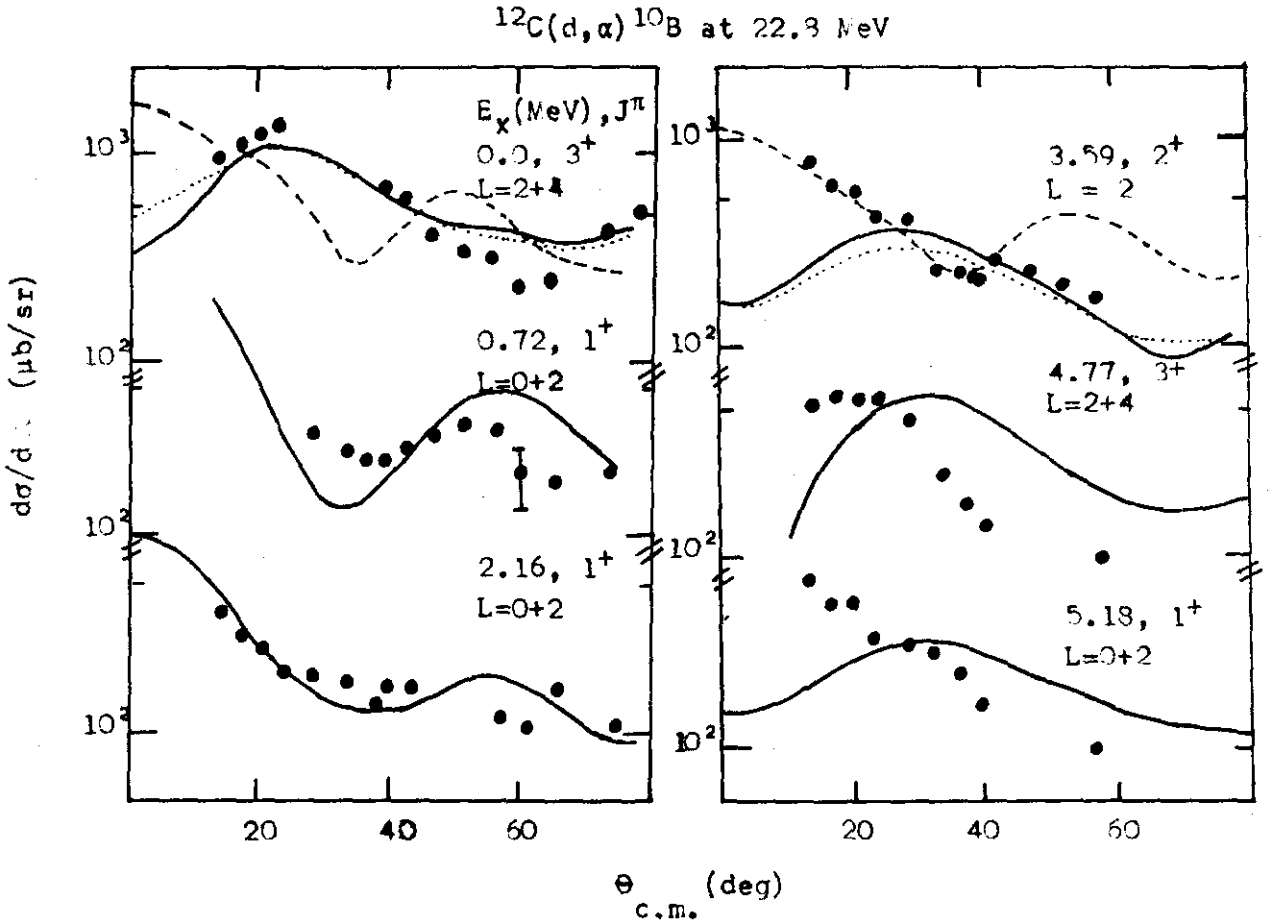

Fig. 8.2 Angular distribution for the levels in ^{10}B populated in the $^{12}C(d,\alpha)^{10}B$ reaction. The solid lines are the results of DWBA calculation with set d_1-α_1, the dotted lines are for set d_2-α_1, the dashed lines are for set d_3-α_2.

CHAPTER IX

CONCLUSIONS

The $^{35,37}Cl(d,t)$, the $^{39,41}K(d,^{3}He)$, the $^{40}Ca(d,\alpha)$ and the $^{12}C(d,\alpha)$ reactions have been studied at a deuteron incident energy of 23 MeV and the nuclear structure of $^{34,36}Cl$, $^{38,40}Ar$, ^{38}K and ^{10}B have been elucidated.

The absolute values of the experimental pickup strengths C^2S for the low-lying levels in $^{34,36}Cl$ have been fairly well reproduced by sd-shell-model calculation. The sd-shell model calculation does not predict the proper level sequence of the first two excited levels in ^{34}Cl.

In the case of ^{38}Ar the sd-shell model calculation does not explain the splitting of the $2s_{1/2}$ spectroscopic strength The inclusion of the $1f_{7/2}$ shell into the sd-shell space is very much needed. From the $^{41}K(d,^{3}He)$ reaction the experimental proton pickup strengths C^2S for seven levels below 5.166 MeV excitation in ^{40}Ar have been deduced. The present study indicate that the spin-parity of the 3.511- and the 4.358-MeV levels in ^{40}Ar as 1^+ or 2^+. Only 70% of the $1d_{3/2}$- proton pickup strength is observed below 5-MeV excitation in ^{40}Ar. The sum rule for the C^2S values indicates that a substantial amount of the $\ell = 0$ and 2 strengths lie at higher excitation energies. The experimental values

of C^2S are compared with the shell-model calculation in the $d_{3/2}$-$f_{7/2}$-$p_{3/2}$- model space.

Twenty levels in ^{38}K upto an excitation energy of 10.26 MeV have been identified in a study of the $^{40}Ca(d,\alpha)$ reaction. Microscopic DWBA analysis has been performed for eight transitions using two-nucleon spectroscopic amplitudes derived from a full sd-shell-model calculation. The strongly excited level at 7.32 MeV is found to have dominant $(2s_{1/2}^{-1})_p(2s_{1/2}^{-1})_n$ configuration and indicates a $J^\pi = 1^+$ assignment. The newly identified level at 9.88 MeV exhibits characteristic $L = 2$ shape and hence the spin-parity is restricted to 1^+, 2^+, or 3^+. The relative values of normalization constants obtained in the present experiment are reasonably constant.

All the one- and two-nucleon transfer reaction studies made on sd-shell and near sd-shell nuclei in this thesis suggest that the calculations in the complete sdfp-model space are highly desirable.

APPENDIX A

COEFFICIENT OF FRACTIONAL PARENTAGE

In principle it is possible to construct n-particle wave functions by successive coupling of the single particle angular momenta. In constructing such a wave function one might face the problem that the wave function with different intermediate sums of angular momenta, which are orthogonal to each other, may lose orthogonality after antisymmetrisation. Such complication arise if there are several equivalent particles. The coefficients of fractional parentage (c.f.p.) are essentially transformation coefficients which appear in the process of expressing antisymmetric wave function of n particles in terms of one particle coupled to an antisymmetric wave function of n-1 particles.

For convenience, the notation due to French (1960) has been followed. Let an n-particle function with all particles in orbit ρ be given by

$\bar{\Phi}_{\Gamma}(1,2,..,n) =$ 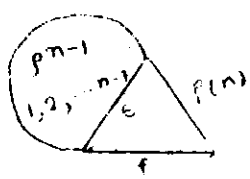 ...(A-1)

The diagram on the R.H.S. of equation (A-1) implies that the function is antisymmetrized in the first n-1 particles but not necessairly with respect to the last particle. The group of n-1 particles are coupled to J_{ε}, T_{ε} and x_{ε}

with x_ε denoting all further quantum numbers needed to specify $|\rho^{n-1}\rangle_\varepsilon$ uniquely. Then the totally antisymmetric function Φ_Γ^{as} can be written as a linear combination of the functions given in equation (A-1) (see for example Macfarlane and French, 1960 and Brussaard and Glaudemans 1977) and is written as,

$$\Phi_\Gamma^{as}(1,2,\ldots,n) = \sum_\varepsilon \langle \rho^n \Gamma \} \rho^{n-1}\varepsilon \rangle$$ 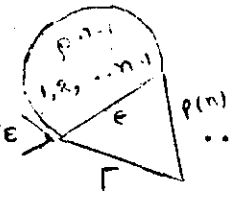 $\ldots$(A-2)

the (r al) expansion coefficients are called as coefficients of fractional parantage (c.f.p.). The quantity $\langle \rho^n \Gamma \ \rho^{n-1}\varepsilon \rangle^2$ gives the probability that when a single particle is removed from the antisymmetric state $|\rho^n\rangle$ (coupled to Γ), the remaining n-1 particles are in an antisymmetric state $|\rho^{n-1}\rangle$(coupled to ε). The application of c.f.p. is discussed in section 2.7.

Instead of expressing the interaction energy of a n-particle system in terms of that between n-1 particles and $n \rightarrow n-1$ c.f.p., it is sometimes useful to express the n-particle interaction directly in two-particle energies (deShalit and Talmi, 1963). The wave function for n-particle system in the following form is required:

$= \sum_{\eta,\delta} \langle \rho^n \Gamma \} \rho^{n-2}\eta(\rho^2\delta) \rangle$ 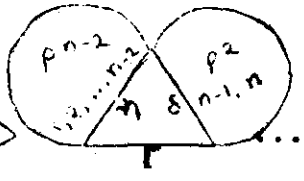 $\ldots$(A-3)

The expansion coefficients are called as double perantage coefficients (d.p.c.). They have the form,

$$\langle \rho^{n}\Gamma | \} \rho^{n-2}\eta(\rho^{2}\delta)\rangle = \sum_{\varepsilon} \langle \rho^{n}\Gamma | \} \rho^{n-1}\varepsilon\rangle \times \langle \rho^{n-1}\varepsilon | \} \rho^{n-1}\eta\rangle \; U(\eta\rho F\rho;\; \varepsilon\delta) \qquad \ldots(A-4)$$

where $U(\eta\rho\Gamma\rho\,;\varepsilon\delta)$ is the normalized Racah coefficient These d.p.c. are useful in the analysis of two-nucleon transfer reactions and are used in section 2.8.

APPENDIX B

THE CODE DWUCK

The computer programme DWUCK (Kunz, 1969) calculates the differential cross section for scattering from a general form of the distorted wave Born approximation (DWBA). The incoming and outgoing wave may be having spin $\leqslant 1$. The particle transfer reaction can be treated with a local energy approximation for finite-range and non-locality effects.

B.1. DWBA CROSS SECTION

The code DWUCK calculates the transition amplitude for the reaction A(a,b)B given by the equation (3-5). The radial part of the distorted wave is obtained by solving the Schrödinger equation (3-30). The distorted wave $\chi_{m',m}(\vec{k},\vec{r})$ is related to the partial waves by the relation (3-29) and the transition amplitude for a stripping reaction is

$$\mathcal{J} = \frac{\sqrt{4\pi}}{k_a k_b} \frac{C^2}{AB} \sum_{\ell sj} \sqrt{2\ell+1}\; B_{\ell sj} \langle J_A M_A j M_B - M_A | J_B M_B \rangle \times \mathcal{S}_{\ell sj}^{m\, m_a m_b} \qquad \ldots(B-1)$$

Where $B_{\ell sj}$ essentially depends on the spectroscopic amplitudes and $\mathcal{S}_{\ell sj}^{m\, m_a m_b}$ depends on the radial form of the distorted wave, radial form factors of the transferred particle and the various vector coupling coefficients

(the explicit forms are given in the DWUCK manual). The radial form factor for the bound particles are obtained by assuming the Woods-Saxon potential for the bound particle. The well depths have been adjusted to reproduce the separation energy of the nucleons. The explicit form of the differential cross section used by the code DWUCK is

$$\sigma^{\ell sj}_{DWUCK} = \frac{1}{4\pi}\frac{1}{E_a E_b}\frac{k_b}{k_a}\frac{C^2}{AB}\frac{1.0 \times 10^4}{2s_a+1}[2\ell+1]$$

$$\times \sum_{m\, m_a m_b} \left| S^{m\, m_a m_b}_{\ell sj} \right|^2 \qquad \ldots(B-2)$$

which is in units of fm^2/sr. The expression for a pickup reaction is obtained by using the principle of detailed balance.

The relation between experimental and DWBA cross section for the single-nucleon pickup reaction becomes,

$$\left(\frac{d\sigma}{d\Omega}\right)_{expt} = N \sum_{\ell j} \frac{C^2 S(\ell j)}{2j+1} \sigma^{\ell j}_{DWUCK} \qquad \ldots(B-3)$$

j is the angular momentum of the picked up particle. The values of the normalization N depends on the assumed wave function for the light particles involved in the reaction. The values of N for (d,t) and (d,^{3}He) reactions are given in table B-1.

For the two-nucleon transfer reaction the method

of computation of σ_{DW} is essentially the same as that for single-nucleon transfer reaction except for the evaluation of two-particle wave function. In particular for the (d,α) reaction the single particle separation energy is taken to be half the deuteron cluste sep ration energy (a few other methods of evaluating the single particle separation energies are discussed by Van der Woude and de Meijer,1976). The two-nucleon form factor for a particular configuration is obtained by the method of Bayman and Kallio (1967). Each such two-nucleon form factor is weighted by the shell-model spectroscopic amplitudes for the two-nucleons (if available, or else it is assumed to be unity) to get the total two-nucleon form factor.

B.2. FINITE-RANGE AND NON-LOCALITY CORRECTIONS

Provision is made in the code DWUCK to apply the nonlocality and finite-range corrections as discussed in sections 3.3 and 3.4. The nonlocality correction β_{NL} are listed in table B-2. The finite-range correction parameters for (d,t), (d,^{3}He) and (d,α) reactions are also listed in table B-2.

Table B-1. The normalization constants for (d,t) and (d,^{3}He) reactions.

Reaction	Values of N	
	Bassel (1966)[a]	Ioannides *et al* (1981)[b]
(d,t)	3.33	2.632
(d,^{3}He)	2.95	2.363

[a] Bassel's normalization constants uses Irvine-Gunn type of wave-function for the three-nucleon system and relative s-state of for the d, t and ^{3}He.

[b] This uses Phillips wave-function for the three-nucleon system and includes the d-state effects for the deuteron.

Table B-2. Typical values of the non-locality correction parameters β_{NL} and the finite-range correction parameters R.

Non-locality Corrections		Finite-range Corrections	
channel	β_{NL}(fm)	Reaction	R(fm)
p	0.85	(d,t)	0.845
n	0.85	(d,^{3}He)	0.770
d	0.54	(d,α)	0.4
t	0.2		
^{3}He	0.2		
α	0.2		

APPENDIX C

EXPERIMENTAL CROSS SECTIONS FOR $^{40}Ca(d,\alpha)^{38}K$ REACTION AT 22.8 MeV

($\sigma(\Theta)$ in mb/sr and $\Delta\sigma$ in mb/sr)

E_x = 0.0 MeV (3^+,0)

$\Theta_{c.m.}$	$\sigma(\Theta)$	$\Delta\sigma$	$\Theta_{c.m.}$	$\sigma(\Theta)$	$\Delta\sigma$
11.99	0.564	0.085	14.65	0.617	0.034
17.31	0.624	0.084	19.97	0.634	0.051
23.95	0.579	0.020	27.93	0.411	0.019
33.22	0.230	0.020	35.86	0.145	0.013
39.81	0.090	0.009	43.75	0.094	0.009
47.94	0.083	0.009	51.60	0.061	0.007
55.70	0.039	0.004	59.92	0.051	0.004
63.54	0.075	0.006	67.67	0.092	0.006
70.75	0.075	0.005	73.31	0.071	0.005
75.35	0.055	0.004	79.92	0.047	0.005
82.98	0.043	0.005	86.51	0.042	0.004
88.53	0.040	0.004	90.54	0.024	0.003
94.04	0.030	0.003	96.04	0.034	0.004
98.03	0.035	0.004	101.57	0.017	0.003
105.46	0.016	0.002	108.91	0.016	0.002
112.34	0.015	0.002	116.25	0.015	0.003
119.65	0.013	0.002	123.53	0.007	0.002
126.90	0.005	0.001	130.75	0.005	0.002
134.10	0.007	0.001	141.25	0.005	0.002
145.04	0.007	0.002	148.36	0.007	0.002
152.13	0.010	0.003	155.42	0.010	0.002
159.19	0.010	0.003	162.47	0.015	0.002
166.22	0.010	0.002			

E_x = 0.45 MeV (1^+,0)

$\theta_{c.m.}$	$\sigma(\theta)$	$\Delta\sigma$	$\theta_{c.m.}$	$\sigma(\theta)$	$\Delta\sigma$
12.00	1.669	0.150	14.66	1.199	0.050
17.32	0.841	0.040	19.98	0.600	0.050
23.96	0.280	0.024	27.94	0.240	0.015
33.23	0.310	0.050	35.87	0.330	0.050
39.83	0.270	0.026	43.77	0.250	0.016
47.97	0.250	0.016	51.60	0.206	0.012
55.79	0.146	0.008	59.95	0.076	0.005
63.57	0.080	0.006	67.69	0.072	0.004
70.78	0.068	0.004	73.34	0.061	0.005
75.32	0.059	0.005	78.95	0.042	0.005
83.00	0.038	0.004	86.55	0.034	0.004
88.56	0.026	0.003	90.57	0.019	0.003
94.08	0.020	0.003	96.07	0.023	0.003
98.07	0.027	0.003	101.54	0.027	0.003
105.50	0.020	0.002	108.94	0.018	0.002
112.37	0.018	0.002	116.28	0.012	0.002
119.68	0.011	0.002	123.55	0.011	0.002
126.93	0.095	0.002	130.77	0.014	0.003
134.12	0.012	0.002	141.25	0.005	0.002
145.04	0.007	0.002	148.37	0.005	0.002
152.15	0.002	0.001	155.44	0.004	0.002
159.19	0.012	0.003	162.47	0.012	0.002
166.22	0.016	0.003			

E_x = 1.71 MeV (1^+,0)

$\theta_{c.m.}$	$\sigma(\theta)$	$\Delta\sigma$	$\theta_{c.m.}$	$\sigma(\theta)$	$\Delta\sigma$
12.01	0.216	0.065	14.68	0.327	0.027
17.35	0.429	0.036	20.01	0.506	0.048
23.99	0.334	0.016	27.98	0.114	0.010
33.28	0.112	0.017	35.93	0.194	0.010
39.83	0.222	0.012	43.83	0.172	0.010
48.03	0.094	0.007	51.70	0.063	0.005
55.87	0.048	0.005	60.03	0.056	0.004
63.65	0.046	0.004	67.78	0.048	0.004
70.86	0.039	0.004	73.43	0.034	0.004
75.47	0.026	0.004	79.04	0.024	0.003
83.10	0.019	0.003	86.64	0.021	0.003
88.65	0.020	0.003	90.66	0.017	0.003
94.17	0.015	0.002	98.16	0.020	0.003
101.63	0.017	0.005	105.59	0.012	0.002
109.03	0.009	0.002	112.46	0.006	0.002
116.37	0.006	0.002	119.77	0.007	0.001
123.64	0.006	0.002	127.00	0.009	0.004
130.85	0.008	0.004	134.20	0.008	0.002
141.33	0.005	0.002	145.12	0.006	0.002
148.43	0.005	0.002	152.19	0.005	0.002
159.23	0.005	0.002	162.51	0.003	0.001
166.25	0.002	0.001			

E_x = 2.64 MeV (2^-,0)

$\Theta_{c.m.}$	$\sigma(\Theta)$	$\Delta\sigma$	$\Theta_{c.m.}$	$\sigma(\Theta)$	$\Delta\sigma$
12.03	0.097	0.018	14.70	0.141	0.027
17.37	0.124	0.024	20.02	0.100	0.017
24.08	0.077	0.016	32.26	0.036	0.009
35.97	0.016	0.005	39.90	0.020	0.004
43.88	0.018	0.005	48.09	0.024	0.005
51.75	0.014	0.003	55.93	0.014	0.003
60.09	0.010	0.002	63.72	0.009	0.002
67.85	0.009	0.002	70.93	0.009	0.002
73.49	0.007	0.002	75.54	0.004	0.002
79.11	0.004	0.002	83.18	0.004	0.002
86.71	0.003	0.001	88.73	0.004	0.002
90.74	0.007	0.002	94.25	0.003	0.001
98.16	0.005	0.003	105.66	0.003	0.001
109.10	0.003	0.001	119.80	0.004	0.001
134.20	0.003	0.001			

E_x = 2.88 MeV (2^-,0)

$\theta_{c.m.}$	$\sigma(\theta)$	$\Delta\sigma$	$\theta_{c.m.}$	$\sigma(\theta)$	$\Delta\sigma$
12.03	0.105	0.054	14.70	0.175	0.027
17.37	0.194	0.036	20.04	0.177	0.068
24.04	0.127	0.017	32.27	0.078	0.017
39.94	0.041	0.007	43.90	0.017	0.006
48.10	0.031	0.007	51.77	0.024	0.005
55.95	0.026	0.004	60.11	0.023	0.003
63.74	0.018	0.003	67.87	0.010	0.002
70.95	0.005	0.002	73.52	0.006	0.002
75.56	0.010	0.010	79.13	0.007	0.002
83.20	0.010	0.002	86.73	0.009	0.002
88.75	0.009	0.002	90.76	0.007	0.002
94.27	0.003	0.002	98.25	0.003	0.002
105.68	0.005	0.002	109.12	0.005	0.002
119.52	0.002	0.001	134.25	0.003	0.001

E_x = 3.43 MeV (2^+,0)

$\theta_{c.m.}$	$\sigma(\theta)$	$\Delta\sigma$	$\theta_{c.m.}$	$\sigma(\theta)$	$\Delta\sigma$
12.04	1.057	0.063	14.72	0.834	0.048
17.39	0.687	0.024	20.06	0.397	0.043
24.06	0.231	0.024	28.05	0.169	0.015
33.36	0.218	0.024	39.97	0.219	0.014
51.81	0.174	0.012	55.99	0.187	0.010
60.15	0.129	0.008	63.78	0.109	0.008
67.91	0.057	0.005	71.00	0.051	0.005
73.57	0.049	0.004	75.61	0.044	0.005
79.18	0.036	0.004	83.25	0.034	0.004
86.78	0.031	0.005	88.80	0.031	0.004
90.91	0.020	0.003	94.32	0.022	0.003
98.31	0.010	0.003	101.78	0.013	0.002
105.73	0.013	0.002	108.17	0.013	0.002
112.60	0.023	0.003	123.76	0.018	0.003
134.31	0.012	0.002	141.43	0.027	0.003
145.21	0.040	0.004	148.51	0.013	0.002
152.27	0.015	0.003	155.54	0.011	0.003
159.29	0.009	0.003	162.56	0.023	0.003
166.28	0.032	0.005			

E_x = 3.66 MeV (3^+,0)

$\theta_{c.m.}$	$\sigma(\theta)$	$\Delta\sigma$	$\theta_{c.m.}$	$\sigma(\theta)$	$\Delta\sigma$
12.05	0.267	0.054	14.72	0.213	0.061
17.39	0.220	0.069	20.06	0.140	0.030
24.06	0.140	0.009	32.30	0.097	0.010
36.02	0.078	0.010	39.99	0.083	0.010
43.94	0.073	0.010	48.15	0.046	0.009
51.82	0.026	0.006	56.00	0.029	0.010
60.17	0.039	0.006	63.80	0.029	0.005
67.93	0.024	0.005	70.02	0.021	0.005
73.59	0.024	0.005	75.63	0.022	0.005
79.20	0.022	0.005	83.27	0.014	0.003
86.81	0.011	0.003	88.82	0.012	0.003
90.83	0.008	0.003	94.33	0.012	0.003
98.33	0.007	0.003	101.80	0.008	0.003
105.75	0.008	0.002	119.91	0.007	0.002
127.15	0.010	0.002	130.98	0.006	0.002

E_x = 4.00 MeV (1^+,0)

$\theta_{c.m.}$	$\sigma(\theta)$	$\Delta\sigma$	$\theta_{c.m.}$	$\sigma(\theta)$	$\Delta\sigma$
12.05	0.310	0.026	14.73	0.252	0.027
17.40	0.215	0.044	24.07	0.162	0.021
28.07	0.061	0.010	33.39	0.044	0.017
36.04	0.141	0.010	40.00	0.197	0.013
43.96	0.155	0.013	48.17	0.110	0.011
51.84	0.049	0.007	56.03	0.027	0.009
60.19	0.031	0.004	63.82	0.038	0.004
67.96	0.036	0.004	73.61	0.040	0.004
75.66	0.029	0.003	79.23	0.030	0.004
83.29	0.019	0.003	86.83	0.014	0.003
88.85	0.012	0.003	90.86	0.009	0.003
94.37	0.014	0.002	98.35	0.012	0.003
101.83	0.009	0.003	105.78	0.013	0.002
109.22	0.008	0.002	119.94	0.006	0.002
123.81	0.002	0.001	127.17	0.002	0.009
131.00	0.004	0.002	134.34	0.004	0.002
148.54	0.007	0.002	152.29	0.006	0.002
155.57	0.005	0.002	162.57	0.003	0.001
166.30	0.008	0.002			

E_x = 7.32 MeV (1^+,0)

$\theta_{c.m.}$	$\sigma(\theta)$	$\Delta\sigma$	$\theta_{c.m.}$	$\sigma(\theta)$	$\Delta\sigma$
12.12	5.230	0.260	24.21	2.960	0.080
33.56	1.190	0.040	36.23	1.480	0.030
40.21	1.280	0.040	44.19	0.750	0.030
48.42	0.370	0.025	52.10	0.340	0.014
56.30	0.340	0.013	60.48	0.270	0.010
64.12	0.190	0.010	68.26	0.130	0.010
71.36	0.120	0.010	73.93	0.120	0.010
75.98	0.120	0.008	79.56	0.094	0.007
83.63	0.061	0.006	87.17	0.059	0.007
89.19	0.056	0.006	91.20	0.056	0.005
94.71	0.041	0.011	98.70	0.053	0.006
102.17	0.053	0.006	106.12	0.031	0.004
120.25	0.019	0.004	124.10	0.019	0.004
127.56	0.019	0.004	131.27	0.019	0.004
134.60	0.029	0.004	148.72	0.012	0.003
155.72	0.046	0.011	159.40	0.040	0.008
162.82	0.038	0.005	166.38	0.046	0.008

E_x = 9.88 MeV (2^+,0)

$\theta_{c.m.}$	$\sigma(\theta)$	$\Delta\sigma$	$\theta_{c.m.}$	$\sigma(\theta)$	$\Delta\sigma$
17.59	2.085	0.081	20.29	2.970	0.114
24.34	3.244	0.057	28.37	1.524	0.040
33.74	0.740	0.037	36.42	0.637	0.136
44.42	0.640	0.031	48.66	0.287	0.024
56.57	0.320	0.085	64.42	0.336	0.057
68.57	0.134	0.013	71.68	0.081	0.011
74.26	0.095	0.007	76.31	0.077	0.004
79.89	0.094	0.016	83.97	0.107	0.022
87.52	0.131	0.012	91.55	0.077	0.023
95.06	0.063	0.020			

LIST OF REFERENCES

Abou-Zeid, O., Roesch, L. Ph., and Falk, W. R. (1979), Phys. Rev. C20, 1198.

Ajzenberg-Selove, F. and Lauritsen, T., (1974), Nucl. Phys. A227, 1.

Amusa, A., (1975), Nucl. Phys. A255, 419.

Anagnostatos, G. S., et al, (1979), (ed), 'Structure of Medium Heavy Nuclei 1979', Proceedings of the Sixth European Phys. Soc. Nucl. Div. Conf., (Grecee).

Arviu, R. and Moszkowski, S. A., (1966), Phys. Rev. 145, 830.

Austern, N., (1970), Direct Nuclear Reaction Theories, John and Wiley.

Baer, H. W., (1973), Ann. Phys. (N. Y) 76, 437.

Bassel, R. H., (1966), Phys. Rev. 149, 791.

Bayman, B. F. and Kallio, A., (1967), Phys. Rev. 156, 1121.

Becchetti Jr, R. D. and Greenlees, G. W., (1971), Polarization Phenomina in Nuclear Reactions, ed. H. H. Barschali and W. Haeberli, the University of Wisconsin Press, Madison Wis., P. 628.

Berg, G. P. A. and Quin, P. A. (1976), Nucl. Phys. A274, 141.

Bock, R., David, P., Duhm, H. H., Hefele, H., Lynen, U., and Stock, R., (1967), Nucl. Phys. A92, 539.

Bohr, A. and Mottelson, B. R., (1969), Nuclear Strucutre, Benjamin, Vol. I.

Bohr, A. and Mottelson, B. R., (1975), Nuclear Structure, Benjamin, Vol. II.

Bohr, A. and Mottelson, B. R., (1953), K. Danske Vidensk Selsk, Mat.-Fys, Medd. 27, No.16.

Brennan, M H. and Bernstein, A. M., (1960), Phys. Rev. 120, 927.

Brussard, P. J. and Glaudemans, P. W. M., (1977), Shell-model Applications in Nuclear Spectroscopy, North Halland Pub. Co.

Butler, S. T., (1951), Proc. Roy. Soc. (London) A208, 559.
Buttle, P. J. A., and Goldfarb, L. J. B., (1964), Proc. Phys. Soc. 83, 701.
Cerny, J., (1974) (ed), 'Nuclear Spectroscopy and Reaction Academic Press.
Cohen, S. and Kurath, D., (1965), Nucl. Phys. 73, 1.
Cohen, S. and Kurath, D., (1970), Nucl. Phys. A141, 45.
Daehnick, W. W., Childs, J. D., and Vrcelj, Z., (1980), Phys. Rev. C21, 2253.
deShalit, A. and Feshbach, H., (1974), Theoretical Nuclear Physics, John Wiley, Vol. I.
deShalit, A. and Talmi, I., (1963), Nuclear Shell Theory, Academic Press.
deShalit, A. and Walecka, J. D., (1961), Nucl. Phys. 22, 184.
DelVecchio, R. M., and Daehnick, W. W., (1972), Phys. Rev. C6, 2095.
Endt, P. M., (1977), Atomic Data and Nucl. Data Tables, 19, 52.
Endt, P. M. and Van der Leun C., (1978), Nucl. Phys. A310, 1.
Evers, D. and Stocker, W., (1970), Phys. Lett. 33B, 559.
Frascaria, N., Didelez, J. P., Chant, N. S., and Chang, C. C., (1977), Phys. Rev. C16, 603.
Frascaria, N., Didelez, J. P., Garron, J. P., Gerlic, E., and Roynette, J. C., (1974), Phys. Rev. C10, 1422.
French, J. B., (1960), Nuclear Spectroscopy Part B, ed. F. Ajzenberg Selove, P. 890.
Fortune, H. T., Puttaswamy, N. G., and Yntema, J. L., (1969), Phys. Rev. 185, 1546.
Fortune, H. T., Medsker, L. R., Nann, H., and Wildenthal, B. H., (1978), Nucl. Phys. A301, 441
Gerace, N. J. and Green, A. M., (1967), Nucl. Phys. A93, 110.
Glaudemanns, P. W. M., Wiechers, G., and Brussaard, P. J., (1964), Nucl. Phys. 55, 529 and 548.
Glendenning, N. K., (1963), Ann. Rev. Nucl. Sci. 13, 191, (1965), Phys. Rev. 137, B102; (1975), Atomic Data and Nucl. Data Tables 17, 1; (1975), Nuclear Spectroscopy, Part D, ed. J. Cerney, Academic Press; (1978), Lectures on Microscopic Theory of Nuclear Direct Reactions, (TIFR), Bombay, India.

Gloeckner, D. H., Lawson, R. D., and Serduke, F. J. D., (1973), Phys. Rev. C7, 1913.

Grard, F., (1965), Nucl. Instrum. Meth. 34, 242.

Gray, W. S., Ellis, P. L., Wei, T., Polichar, R. M., and Janecke, J., (1970), Nucl. Phys. A140, 494.

Halbert, M. L., (1977), Nucl. Data Sheets 22, 59.

Hardekopf, R. F., Haglund Jr. R. F., Ohlesen, G. G., Thompson, W. J., and Veeser, L. R., (1980), Phys. Rev. C21, 906.

Harnyak, W. F., (1975), Nuclear Structure, Academic Press.

Hasper, H., (1979) Phys. Rev. C19, 1482.

Hauser, W. and Feshbach, H., (1952), Phys. Rev. 87, 336.

Hodgson, P. E., (1963), The Optical Model of Elastic Scattering, Oxford Univ. Press.

Hodgson, P. E., (1971), Nuclear Reactions and Nuclear structure, Oxford Univ. Press.

Hoot, C. G., Olsen, D. K., Brown, R. E., Maxwell, J. R., and Scott, A., (1973), Nucl. Phys. A203, 339

Ioannides, A. A., Nagarajan, M. A., and Shyam, R., (1981), Nucl. Phys. A263, 150.

Jackson, D. F., (1970), 'Nuclear Reaction' Metheun and Co. Ltd.

King, C. H., Shahabuddin, M. A. M., and Wildenthal, B. H., (1976) Nucl. Phys. A270, 399.

Kuo, T. T. S. and Brown, G. L., (1966), Nucl. Phys. A114, 241.

Kuo, T. T. S., (1974), Ann. Rev. of Nucl. Sci. 24, 101.

Kunz, P. D., (1969), DWUCK, University of Colorado,

Lewis, M. S. and Daehnick, W. W., (1970), Phys. Rev. C1, 1577.

Ludwig, E. J., Clegg, T. B., Jacobs, W. W., and Tonsfeldt, S. A., (1978), Phys. Rev. Lett. 40, 441.

Macfarlane, M. H. and French, J. B., (1960), Rev. Mod. Phys. 32, 567.

Macfarlane, M. H. and Schiffer, J. P., (1974), Nuclear Spectroscopy and Reactions, Part B, (ed. J.Cerny), Aca. Press.

Marion, J. B., and Young, F. C., (1961), Nuclear Reaction Analysis, North-Holland.

Mayer, M. G. and Jensen, J. H. D., (1965), Elementary Theory of Nuclear Shell Structure, John Wiley.

McGrory, J. B. and Raman, S., (1979), Phys. Rev. C20, 830.

Merz, F., Clement, H., Frick, R., Graw, G., Seichero, N., and Schiemenz, P., (private communication).

Nadesan, A., Schwandt, P., Singh, P. P., Jacobs, W. W., Bacher, A. D., Debevec, P. T., Kaitchuck, M. D., and Meck, J. T., (1981), Phys. Rev. C23, 1023.

Nann, H., Bacher, A. D., Jacobs, W. W, Jones, W. P., and Stephenson, E. J., (1981), Phys. Rev. C24, 1984.

Nann, H. and Wildenthal, B. H., (1979), Phys. Rev. C19, 2146; (1978), Phys. Rev. C17, 916; (1976), Phys. Rev., C13, 1009.

Newton, T. D., (1960), Can. J. Phys. 38, 700.

Nilsson, S. G., (1955), Kgl. Danske. Videnskab. Selskab, Mat.-Fys. Medd. 29, No. 16.

Park, Y. S., Jones, H. D., and Bainum, D. E., (1971), Phys. Rev. C4, 778.

Paul, M., Marinov, A., Burde, J., Drory, Ch., Lichtentstadt, J., Mordechi, S., and Navon, E., (1977), Nucl. Phys. A289, 94.

Perey, C. M. and Perey, F. G., (1976), Atomic Data and Nucl. Data Tables 17, 1.

Perey, F. G. and Buck, B., (1963), Nucl. Phys. 32, 353.

Petty, D. T., Ikossi, P. G., Kuehner, J. A., and Szucs, J., (1976), Phys. Rev. C14, 908.

Puttaswamy, N. G., (1979), 'Proceedings of the Workshop on heavy ion Reactions', B.A.R.C. 368.

Puttaswamy, N. G., (1973), Nucl. Phys., and Solid State Phys. (India) 16A, 87.

Puttaswamy, N. G. and Yntema, J. L.,((1969), Phys. Rev. 177, 1624.

Rainwater, J., (1950), Phys. Rev. 79, 432.

Rice, J. A., Wildenthal, B. H., and Preedom, B. M., (1975), Nucl. Phys. A239, 189.

Satchler, G. R., (1964), Nucl. Phys. 55, 1

Sens, J. C. and de Meijer, R. J., (1979), KVI Report, 15.

Singh, B. P., Castel, B., Johostone, I. P., and Stewart, K. W. C., (1972), Phys. Rev. C5, 1613.

Suehiro, T., Finck, J. E., and Nolen, J. A., (1979), Nucl. Phys. A313, 141.

Tobocman, W., (1961), Theory of Direct Nuclear Reactions, Oxford Univ. Press.

Towner, I. S. and Hardy, J. C., (1969), Adv. in Phys. 18, 401.

Trost, H. -J.,SSchwarz, A., Feindt, U., Heimlich, F. H., Heinzel, S., Hintze, J., Körber, F., Lekebusch, R., Lezoch, P., Möck, G., Paul, W., Roick, E., Wolff, M., Worzeck, J., and Strohbusch, U., (1980), Nucl. Phys. A337, 377.

Van Gastern, J. J. M., Sikora, B., and Van der Steld, A., (1974), Nucl. Phys. A231, 411.

Van der Woude, A. and de Meijer, J., (1976), Nucl. Phys. A258, 199.

Wildenthal, B. H., Rice, J. A., and Preedom, B. M., (1974) Phys. Rev. C10, 2184.

Wildenthal, B. H., Halbert, E. C., McGrory, J. B., and and Kuo, T. T. S., 6(1971), Phys. Rev. C4, 1266.

Wildenthal, B. H., and Chung, W. (private communication).

Wildenthal, B. H. and Newmann, E. (1968), Nucl. Phys. A118, 347.

Wildenthal, B. H. (1981), Oxford Lectures.

Wilkinson, D. H., (1969), Isospin in Nuclear Phssics, ed. Wilkinson, D. H., North Holland.

Yntema, J. L., and Ostrander, H. W., (1962), Nucl. Instrm. Meth. 16, 69.

Yang, T., (1969), Thesis, University of Michigan, 70-14, 689.

LIST OF PUBLICATIONS

1. 'The Quadrupole coupling constant of $^3P_1$ and $^1P_1$ levels of Mg^{25}, Zn^{67} and Kr^{83} and, ^3D and ^1D levels of Zn^{67}' by B. R. Pushpalatha and C. M. Bhat, Ind. J. Phys. 53B, 80 (1979).★

2. 'Life times of single-particle states near ^{48}Ca' by C. M. Bhat and N. G. Puttaswamy, Ind. J. of Pure and Appl. Phys. 18, 728 (1980).★

3. '(d,^{3}He) reaction on potassium isotopes at 22.8 MeV' by C. M. Bhat, M. Raja Rao, N. G. Puttaswamy and J. L. Yntema, Nucl. Phys. and Solid State Phys. (India) 23B, 199 (1980).

4. (d,t) reaction on chlorine isotopes at 23 MeV' by C. M. Bhat, N. G. Puttaswamy and J. L. Yntema, J. Phys. G (London) 7, 1529 (1981).★♥

5. 'A study of 7.32-MeV and 9.88-MeV levels of ^{38}K' by C. M. Bhat, N. G. Puttaswamy, H. T. Fortune, J. L. Yntema, Nucl. Phys. and Solid State Phys. (India) 24B, 21 (1981).

6. Study of the $^{39,41}K(d,^3He)^{38,40}Ar$ Reactions at 22.8 MeV, C.M. Bhat, M Raja Rao, N. G. Puttaswamy, and J.L. and Yentema (published in Nucl. Phys. A).★♥
7. Study of the $^{40}Ca(d, \alpha)$ reaction at 22.8 MeV, C.M.Bhat et al., Nucl. Phys. And Solid State Phys. 25B (1982).
8. Levels in 38K from $^{40}Ca(d, \alpha)$ reaction at 22.8 MeV, C. M. Bhat et.al., Phys. Rev. C 28 (1983) p 141-149.★♥

★ Refereed Journal Research Publications, ♥ The research reported in the thesis-see the attachments

J. Phys. G: Nucl. Phys. 7 (1981) 1529–1538. Printed in Great Britain

The (d, t) reaction on chlorine isotopes at 23 MeV

C M Bhat†, N G Puttaswamy† and J L Yntema‡

† Department of Physics, Bangalore University, Bangalore 560001, India
‡ Physics Division, Argonne National Laboratory, Argonne, Illinois 60439, USA

Received 12 May 1981

Abstract. The ^{35,37}Cl(d, t) reactions at $E_d = 23.35$ MeV have been employed to study the properties of the low-lying positive-parity states in ^{34}Cl and ^{36}Cl. A DWBA analysis of angular distributions has been performed and the spectroscopic strengths have been deduced. The results are compared with the previous experimental values and the recent shell-model calculations.

NUCLEAR REACTIONS ^{35,37}Cl(d, t), $E_d = 23.35$ MeV; measured $\sigma(E_t, \theta_t)$. ^{34,36}Cl; deduced levels; DWBA analysis, C^2S.

1. Introduction

A study of the structure of doubly odd nuclei in the sd-shell region is of considerable importance from both the theoretical and experimental points of view. In the simplest model description, the low-lying positive-parity states of ^{34}Cl can be understood to result from the coupling of one proton and one neutron in the $1d_{3/2}$ shell while those in ^{36}Cl result from the coupling of one proton and one neutron hole in the same shell. Calculations in the complete $1d_{5/2}$–$2s_{1/2}$–$1d_{3/2}$ shell-model space by Wildenthal *et al* (1971; also Wildenthal and Chung, private communication) predict spectroscopic factors for pick-up reactions leading to final states in ^{34}Cl and ^{36}Cl and a comparison can then be made with the values deduced experimentally.

The low-lying states of ^{34}Cl and ^{36}Cl have been studied previously by (p, d), (^{3}He, α), (d, p) and (^{3}He, d) reactions (Endt and Van der Leun 1978). The ^{37}Cl($\bar{d}$, t)^{36}Cl reaction has been studied recently by Berg and Quin (1976). There are so far no reports on the ^{35}Cl(d, t) reaction. In this paper we report on a study of the positive-parity states in ^{34}Cl and ^{36}Cl excited via the ^{35,37}Cl(d, t) reactions at $E_d = 23.35$ MeV. A preliminary analysis of our ^{37}Cl(d, t) reaction has been reported elsewhere (Puttaswamy and Yntema 1967, Puttaswamy 1973).

2. Experimental procedure

The reactions have been carried out with the 23.35 MeV deuteron beam from the Argonne National Laboratory Cyclotron. The 60 in scattering chamber has been used together with a (dE/dX)–E counter arrangement to detect tritons. The details of the experimental set-up and procedure have been discussed by Fortune *et al* (1969). The energy resolution obtained with the counter telescope is about 140 keV FWHM.

 © 1981 The Institute of Physics

Table 1. Optical-model parameters used for the DWBA analysis[a].

	V_R (MeV)	r_0 (fm)	a_0 (fm)	W_S (MeV)	W_D^b (MeV)	r_I (fm)	a_I (fm)	V_{LS} (MeV)	r_{LS} (fm)	a_{LS} (fm)	r_c (fm)	β_{NL} (fm)
$^{35}Cl + d^c$	87.0	1.17	0.749	0.7	12.1	1.325	0.744	6.7	1.07	0.66	1.3	0.54
$^{34}Cl + t^d$	162.2	1.2	0.72	40.5	—	1.4	0.84	2.5	1.2	0.72	1.3	0.20
$^{37}Cl + d^c$	86.9	1.17	0.749	0.7	12.1	1.325	0.723	6.7	1.07	0.66	1.3	0.54
$^{36}Cl + t^d$	161.4	1.2	0.72	33.6	—	1.4	0.84	2.5	1.2	0.72	1.3	0.20
n	$\sim 55^e$	1.2	0.65					$\lambda = 25$			1.25	—

[a] The notation used here is the same as in Daehnick *et al* (1980).
[b] A value of $4W_D$ is used in DWUCK.
[c] Daehnick *et al* (1980); the potential set L has been used. A value of $2V_{LS}$ is used in DWUCK.
[d] Becchetti and Greenlees (1971). The values of V_R and W_S are given for the ground-state transition and are varied according to the expressions $V_R = 165.0 + 0.17E - 6.4\xi$ and $W_S = 46.0 - 0.33E - 110\xi$, where $\xi = (N-Z)/A$ and E is the triton laboratory energy. A value of $4V_{LS}$ is used in DWUCK.
[e] Well depth adjusted to give the pick-up neutron a binding energy of $6.257 - Q(d, t)$ MeV.

The targets are prepared by evaporating lead chloride enriched in ^{35}Cl and ^{37}Cl onto thin carbon films. The target thickness in each case is determined by comparing the experimental elastic scattering angular distribution of deuterons around the maximum at 53° with that obtained by using optical-model parameters (listed in table 1). Target thicknesses of 47 μg cm^{-2} for ^{35}Cl and 63 μg cm^{-2} for ^{37}Cl have been obtained; the ^{37}Cl target thickness is corrected for the fact that its enrichment is about 85%. The estimated error in the target thickness is expected to be about 25%.

The spectra are analysed with a peak-fitting computer program MALIK (Grard 1965). Typical triton spectra for both reactions are shown in figure 1. A consistent energy calibration is obtained using the ground, first and second excited states of ^{36}Cl in the case of the ^{37}Cl(d, t) reaction (Endt and Van der Leun 1978); for the ^{35}Cl(d, t) reaction, the calibration is made using the 0.0, 0.159, 1.825 and 2.365 MeV states in ^{47}Ti (Halbert 1977) populated in the ^{48}Ti(d, t) reaction run under similar conditions. The excitation energies obtained are indicated in figure 1, and the estimated accuracy is ± 30 keV. A few spectra for the ^{35}Cl(d, t) reaction have also been taken at $E_d = 23.25$ MeV and, in the region of overlap, the cross sections agreed, to within errors, with the corresponding values for $E_d = 23.35$ MeV.

3. DWBA analysis

Spectroscopic information on the levels of the residual nuclei is obtained by making a DWBA analysis using the code DWUCK (Kunz 1969). The deuteron optical-model

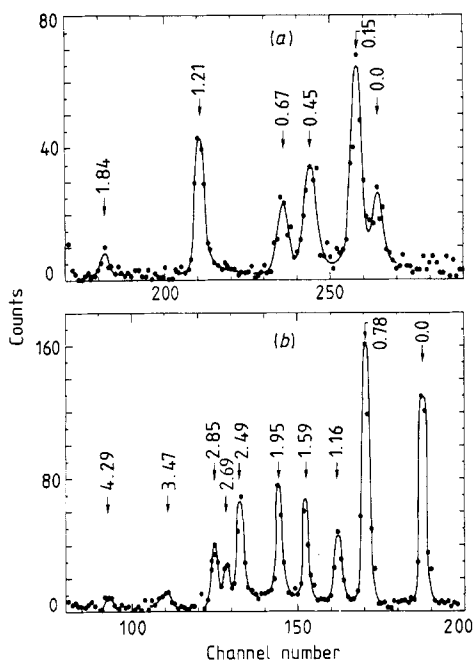

Figure 1. Spectrum of tritons from the (d, t) reaction on chlorine isotopes at 23.35 MeV. (*a*) The spectrum from the ^{35}Cl(d, t)^{34}Cl reaction at $\theta_{lab} = 21°$. (*b*) The spectrum from the ^{37}Cl(d, t)^{36}Cl reaction at $\theta_{lab} = 18°$. The excitation energies (in MeV) determined from this experiment are indicated above the peaks.

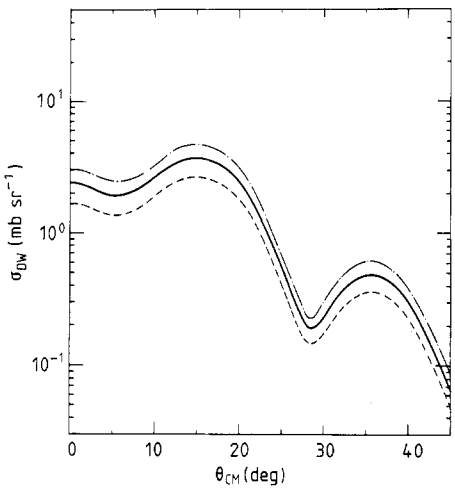

Figure 2. Comparison of the DWBA curves with $l=2$ (and $j=\frac{3}{2}$) for the GS transition in the ^{37}Cl(d, t)^{36}Cl reaction at 23.35 MeV. The FRNL calculation has been made using the nonlocality correction $\beta_n=0.85$ for the neutron bound state. ——— · ———, FRNL; ————, FRNL1 or FRL; – – – –, ZRL.

parameters of Daehnick *et al* (1980) and the triton optical-model parameters of Becchetti and Greenlees (1971) are used in all DWBA calculations. The optical-model parameters are listed in table 1, and the notation used here is the one given by Daehnick *et al* (1980). An alternative parameter set has also been tried for tritons (Hardekopf *et al* 1980), and in this case the predicted angular distributions do not differ significantly and the spectroscopic factors agree to within 5%.

The sensitivity of the DWBA cross section, $\sigma_{DW}(\theta)$, to finite-range (FR) and nonlocality (NL) corrections within the local energy approximation has also been studied. This study has been made for the transition to the ground state of ^{36}Cl. The DWBA curves shown in figure 2 have been obtained with (*a*) zero-range and local potentials (ZRL), (*b*) finite-range and local potentials (FRL), (*c*) finite-range and nonlocal potentials for incoming and outgoing particles only (FRNL1) and (*d*) finite-range and nonlocal potentials for incoming, outgoing and bound particles (FRNL). The shapes of the angular distributions are very similar in all cases, but the values of σ_{DW} change as follows: $\sigma_{DW}^{FRNL1} \sim \sigma_{DW}^{FRL} \sim 1.37\ \sigma_{DW}^{ZRL}$ and $\sigma_{DW}^{FRNL} \sim 1.27\ \sigma_{DW}^{FRNL1}$. For all the other transitions DWBA analyses of the type FRNL1 are made using a FR correction of 0.845 fm and the NL corrections β_{NL} listed in table 1.

The pick-up spectroscopic strength (C^2S_{lj}) is calculated using the expression

$$\sigma_{expt}(\theta)=N\sum_{l,j} C^2S_{lj}\sigma_{DW}^{lj}(\theta)$$

where l and j are the orbital and total angular momenta transferred in the reaction. $\sigma_{expt}(\theta)$ is the experimental differential cross section at the angle θ, S_{lj} is the spectroscopic factor and C^2 is the isospin Clebsch–Gordan coefficient. A normalisation constant $N=3.33$ (Bassel 1966) has been used†.

† It may be noted that the C^2S values quoted in tables 2 and 3 would reduce by a factor 1.27 if a nonlocality correction for the neutron bound state is also included. However, recent calculations by Ionnides *et al* (1980) indicate a value of $D_0=-163.22$ MeV fm$^{3/2}$ for the (d, t) reaction and hence $N=2.664$; the use of this value of N would enhance the spectroscopic factor by 1.25. Thus if one uses $N=2.664$ together with σ_{DW}^{FRNL} one would get almost the same values of C^2S as those quoted in tables 2 and 3.

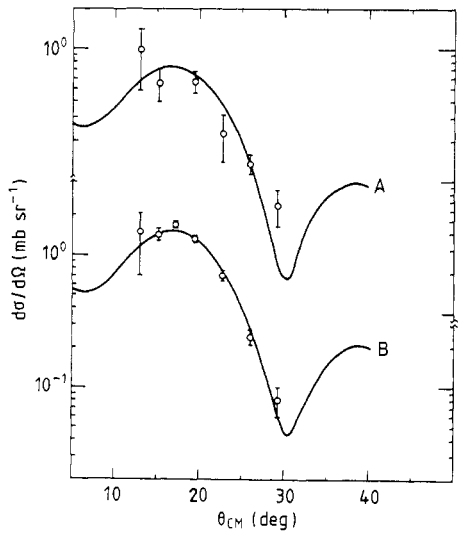

Figure 3. Angular distributions for states with $l=2$ transfer in the $^{35}Cl(d, t)^{34}Cl$ reaction at $E_d = 23.35$ MeV; the full curves are the DWBA predictions. A, 0 MeV; B, 0.15 MeV.

Most of the low-lying states in ^{34}Cl and ^{36}Cl which are excited in the (d, t) reaction are characterised by $l=0$ or $l=2$ or both. When both l values are possible, the relative

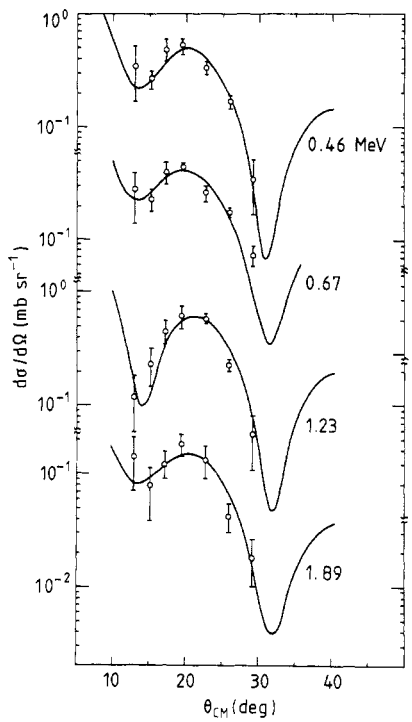

Figure 4. Angular distributions for states in ^{34}Cl having both $l=0$ and $l=2$ transfer; the full curves are linear combinations of the DWBA predictions for $l=0$ and $l=2$ as described in the text.

Table 2. Pick-up spectroscopic strengths for the states in ^{34}Cl[a].

E_x[b] (MeV)	$J^\pi; T$[b]	l	$100C^2S$[c]	$100C^2S$[d]	Theory[e] E_x(MeV)	$J^\pi; T$	$100C^2S$
0.0	$0^+;1$	2	; 41;	; 43 ± 7;	0.0	$0_1^+;1$	; 30;
0.146	$3^+;0$	2	; 118;	; 140 ± 30;	0.448	$3_1^+;0$	; 109; 2
0.461	$1^+;0$	0, 2	11; 21;	9 ± 3; 27 ± 5;	0.324	$1_1^+;0$	9; 28; 7
0.666	$1^+;0$	0, 2	6; 22;	9 ± 6; 31 ± 8;	1.069	$1_2^+;0$	13; 4; 0
1.230	$2^+;0$	0, 2	23; 9;	36 ± 14; 7 ± 2;	1.416	$2_1^+;0$	32; 0; 6
1.887	$2^+;0$	0, 2	4; 12;	11 ± 5; 14 ± 4;	2.108	$2_2^+;0$	1; 6; 3
	$\Sigma C^2S(2s_{1/2}; T=0)=0.44$						0.55
	$\Sigma C^2S(1d_{3/2}; T=0)=1.82$						1.47
	$\Sigma C^2S(1d_{3/2}; T=1)=0.41$						0.30

[a] In the columns labelled $100C^2S$, the spectroscopic strengths are given in the notation $100C^2S(s_{1/2})$; $100C^2S(d_{3/2})$; $100C^2S(d_{5/2})$.
[b] Endt and Van der Leun (1978). Energies measured in the present experiment are indicated in figure 1(*a*).
[c] Present work.
[d] Endt (1977). For a complete listing of spectroscopic strengths from all the previous experiments, see Endt and Van der Leun (1978).
[e] Wildenthal *et al* (1971); also Wildenthal and Chung (private communication).

admixtures for the two possible l values are determined by minimising the value of χ^2 (see, for example, Fortune *et al* 1969).

4. Results

4.1. States in ^{34}Cl

The angular distributions measured for the transitions to the states of ^{34}Cl are shown in figures 3 and 4 together with the DWBA fits and l values transferred. The experimental results for ^{34}Cl are summarised in table 2 together with the values evaluated by Endt (1977) from other experiments and the results of recent sd-shell-model calculations by Wildenthal *et al* (1971; also Wildenthal and Chung, private communication).

The transitions to the ground state (0^+; 1) and the first excited state (3^+; 0) at 0.15 MeV have dominant $l=2$ transfer. The angular momentum selection rule requires $l=2$ (and $j=\frac{3}{2}$) for the ground state and allows no $l=0$ admixture for the 0.15 MeV state. The C^2S values for all $l=2$ transitions are obtained by considering neutron pick-up from the $d_{3/2}$ sub-shell. The summed spectroscopic strength $\Sigma\, C^2S\,(1d_{3/2};\, T=0)$ is 1.82 and is close to the theoretically predicted value of 1.47.

4.2. States in ^{36}Cl

Out of ten transitions studied in the ^{37}Cl(d, t)^{36}Cl reaction, four transitions exhibit dominant $l=2$ transfer. The angular distributions are shown in figures 5 and 6. The

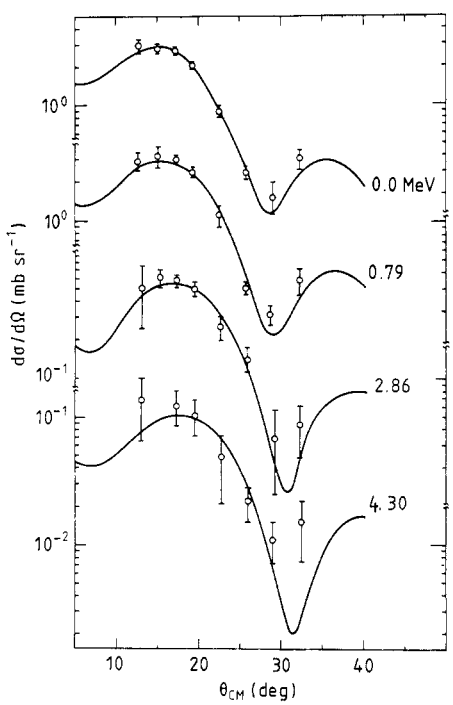

Figure 5. Angular distributions for states populated in the ^{37}Cl(d, t)^{36}Cl reaction with $l=2$; the full curves are the DWBA predictions.

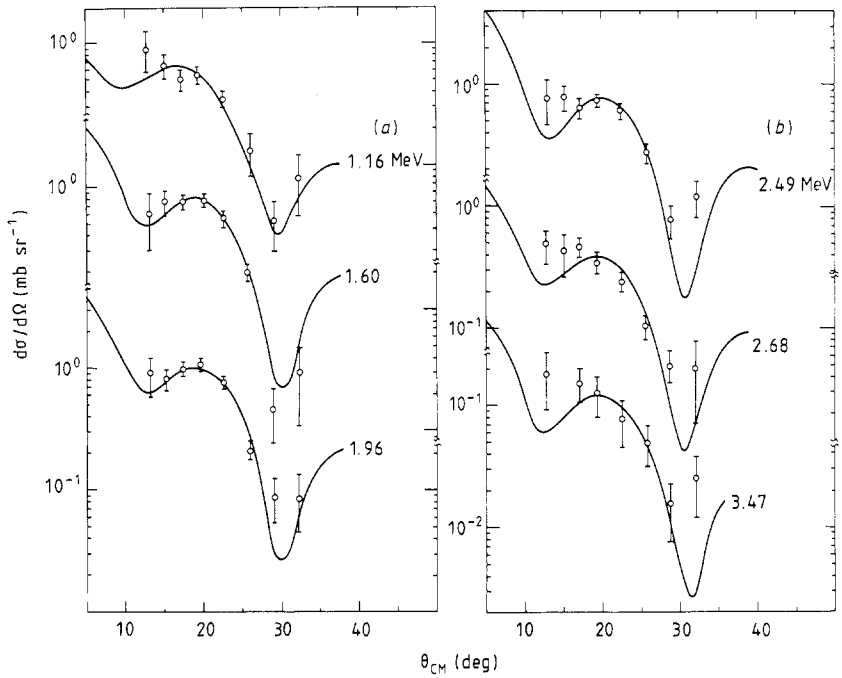

Figure 6. Angular distributions for the states in ^{36}Cl having both $l=0$ and $l=2$ transfer; the full curves are linear combinations of the DWBA predictions for $l=0$ and $l=2$ as described in the text.

GS (2^+; 1) is predominantly populated by $l=2$, even though the angular momentum selection rule allows an admixture of $l=0$. The spectroscopic strengths measured for the states in ^{36}Cl are given in table 3. The previous experimental results of Rice *et al* (1975), of Berg and Quin (1976), the values evaluated by Endt (1977) and the sd-shell-model prediction of Wildenthal *et al* (1971; also Wildenthal and Chung, private communication) are also tabulated for comparison. In general there is good agreement for the spectroscopic strengths. In the case of the states at 1.60 and 1.96 MeV, the C^2S values obtained by us differ from those of others. This may be due to the procedure adopted to obtain admixtures of two l values and the spectroscopic strengths depend sensitively on the exact shapes assumed for the DWBA curves (Fortune *et al* 1969). The $\Sigma\, C^2S\,(1d_{3/2}; T=1)$ is 4.21 while a value of 3.24 is predicted theoretically.

5. Discussion and conclusion

The absolute values of the neutron pick-up spectroscopic strengths extracted from the present experiment are generally in good agreement with the previous experimental results. However, small differences in the values displayed in tables 2 and 3 may be expected to arise from differences in the optical-model parameters and from finite-range and nonlocality corrections.

The sd-shell-model calculations of Wildenthal *et al* (1971; also Wildenthal and Chung, private communication) have particularly succeeded in explaining the neutron pick-up spectroscopic strengths for the low-lying positive-parity states of ^{34}Cl and ^{36}Cl. However,

Table 3. Pick-up spectroscopic strengths for the states in ^{36}Cl[a].

E_x[b] (MeV)	$J^\pi; T$[b]	l	$100C^2S$[c]	$100C^2S$[d]	$100C^2S$[e]	$100C^2S$[f]	Theory[g] E_x(MeV)	Theory[g] $J^\pi; T$	Theory[g] $100C^2S$
0.0	$2^+; 1$	2	; 90;	; 110;	; 121;	; 95 ± 17;	0.0	$2_1^+; 1$	2; 101; 2
0.788	$3^+; 1$	2	; 130;	; 166;	; 141;	; 150 ± 20;	0.928	$3_1^+; 1$	; 159;
1.165	$1^+; 1$	0, 2	1; 28;	5; 36;	5; 36;	9 ± 3; 34 ± 5;	1.101	$1_1^+; 1$	3; 25; 3
1.601	$1^+; 1$	0, 2	8; 28;	16; 11;	19; 8; 17; ; 11	20 ± 3; 15 ± 8;	1.640	$1_2^+; 1$	27; ;
1.959	$2^+; 1$	0, 2	10; 43;	23; 24;	20; 25; 20; ; 20	38 ± 8; 21 ± 5;	1.767	$2_2^+; 1$	30; 1; 23
2.492	$2^+; 1$	0, 2	13; 25;	17; 19;			2.397	$2_3^+; 1$	13; 2; 3
2.675	$1^+; 1$	0, 2	6; 28;	7; 31;		6 ± 2; 32 ± 4;	2.793	$1_3^+; 1$	2; 34; 3
2.864	$(2, 3)^+; 1$	2	; 42;	; 45;			2.424	$3_2^+; 1$	; 1; 70
3.469	$(1, 2)^+; 1$	0, 2	2; 7;	5; 7;			3.361	$1_4^+; 1$	9; 1;
4.300	$0^+; 2$	2	; 14;	; 29;			4.340	$0^+; 2$	; 23;
	$\Sigma C^2S(2s_{1/2}; T=1)=0.40$								0.85
	$\Sigma C^2S(1d_{3/2}; T=1)=4.21$								3.24
	$\Sigma C^2S(1d_{3/2}; T=2)=0.14$								0.23

[a] In the columns labelled $100C^2S$, the spectroscopic strengths are given in the notation $100C^2S(s_{1/2})$; $100C^2S(d_{3/2})$; $100C^2S(d_{5/2})$.
[b] Endt and Van der Leun (1978). Energies measured in the present experiment are indicated in figure 1(*b*).
[c] Present work.
[d] Rice *et al* (1975). The spectroscopic factors have been normalised to yield $C^2S = 1.10$ for the ground-state transition.
[e] Berg and Quin (1976).
[f] Endt (1977). For a complete listing of spectroscopic strengths from previous experiments, see Endt and Van der Leun (1978).
[g] Wildenthal *et al* (1971); also Wildenthal and Chung (private communication).

this model predicts the $(1^+; 0)$ state in ^{34}Cl to be at a lower energy than the $(3_1^+; 0)$ state (see table 2), in contradiction to the experimental results. By extending the shell-model space and by adding a tensor force to the modified surface delta interaction, Evers and Stocker (1970) obtain the correct ordering of the levels. It is also interesting to note that a vibrational coupling model (Singh *et al* 1972) can account for the correct sequence of the low-lying states in ^{34}Cl. The pick-up spectroscopic strengths, however, are not yet available.

The level sequence of ^{36}Cl below an excitation energy of 2.68 MeV is fairly well reproduced by the sd-shell-model calculation (Wildenthal *et al* 1971, see table 3) and also by the $2s_{1/2}-1d_{3/2}-1f_{7/2}-2p_{3/2}$ shell-model calculation (Hasper 1979). The latter calculation also predicts a few negative-parity states below 3 MeV. Some of the negative-parity states in ^{36}Cl were observed by Rice *et al* (1979) via the (p, d) reaction. These states are, however, weak and are not resolved in our (d, t) experiment.

Acknowledgments

The work at Argonne National Laboratory has been performed under the auspices of the US Atomic Energy Commission. We are extremely grateful to Dr M Raja Rao for his constant help during the analysis of the data. Our thanks are due to Dr C R Ramaswamy for useful discussions. One of the authors (CMB) is grateful to the Council of Scientific and Industrial Research, New Delhi, for the award of a Senior Research Fellowship. The help of Mrs Pushpalatha C Bhat at various stages of this work is acknowledged. One of the authors (NGP) wishes to thank Dr W Oelert for many useful discussions.

References

Bassel R H 1966 *Phys. Rev.* **149** 791
Becchetti F D Jr and Greenlees G W 1971 *Polarization Phenomena in Nuclear Reactions* ed H H Barschall and W Haeberli (Madison: The University of Wisconsin Press) p 682
Berg G P A and Quin P A 1976 *Nucl. Phys.* A **274** 141
Daehnick W W, Childs J D and Vrcelj Z 1980 *Phys. Rev.* C **21** 2253
Endt P M 1977 *Atomic Data and Nuclear Data Tables* **19** 52
Endt P M and Van der Leun C 1978 *Nucl. Phys.* A **310** 1
Evers D and Stocker W 1970 *Phys. Lett.* **33B** 559
Fortune H T, Puttaswamy N G and Yntema J L 1969 *Phys. Rev.* **185** 1546
Grard F 1965 *Nucl. Instrum. Methods* **34** 242
Halbert M L 1977 *Nuclear Data Sheets* **22** 59
Hardekopf R A, Haglund R F Jr, Ohlsen G G, Thompson W J and Veeser L R 1980 *Phys. Rev.* C **21** 906
Hasper H 1979 *Phys. Rev.* C **19** 1482
Ionnides A A, Nagarajan M A and Shyam R 1980 *Preprint*
Kunz P D 1969 *University of Colorado Report* (unpublished)
Puttaswamy N G 1973 *Nucl. Phys. Solid St. Phys. (India)* A **16** 87
Puttaswamy N G and Yntema J L 1967 *Bull. Am. Phys. Soc.* **12** 1123
Rice J A, Wildenthal B H and Preedom B M 1975 *Nucl. Phys.* A **239** 189
Singh B P, Castel B, Johnstone I P and Stewart K W C 1972 *Phys. Rev.* C **5** 1613
Wildenthal B H, Halbert E C, McGrory J B and Kuo T T S 1971 *Phys. Rev.* C **4** 1266

Nuclear Physics **A394** (1983) 109–117
© North-Holland Publishing Company

STUDY OF THE ^{39,41}K(d, ^{3}He)^{38,40}Ar REACTIONS AT 22.8 MeV

C. M. BHAT, M. RAJA RAO and N. G. PUTTASWAMY

Department of Physics, Bangalore University, Bangalore 560001, India

and

J. L. YNTEMA

Argonne National Laboratory, Argonne, Illinois 60439, USA

Received 10 August 1982
(Revised 20 September 1982)

Abstract: The ^{39,41}K(d, ^{3}He)^{38,40}Ar reactions have been investigated at $E_d = 22.8$ MeV to study the low-lying positive-parity levels in ^{38}Ar and ^{40}Ar. The transitions to fourteen levels in the residual nuclei have been analysed with distorted wave Born approximation calculations. The spectroscopic strengths for proton pickup to the levels in ^{40}Ar are reported here for the first time. The experimental results are compared with recent shell-model calculations.

E | NUCLEAR REACTION ^{39,41}K(d, ^{3}He), $E = 22.8$ MeV; measured $\sigma(E(^3\text{He}), \theta)$, ^{38,40}Ar deduced levels, C^2S. DWBA analysis.

1. Introduction

Nuclei around ^{40}Ca have been the subject of numerous experimental and theoretical investigations. From the simplest shell-model point of view, the low-lying positive-parity levels of ^{38}Ar can be characterized by two proton holes in the $1d_{\frac{3}{2}}$ shell. Calculations involving the complete sd shell-model space by Wildenthal *et al.* [1,2]) and a core-excitation model by Gray *et al.* [3]) predict the proton pickup spectroscopic factors for the levels in ^{38}Ar. The ^{39}K(d, ^{3}He)^{38}Ar reaction has been studied earlier by Gray *et al.*. [3]) at $E_d = 28.9$ MeV and by Wildenthal and Newman [4]) at $E_d = 34.5$ MeV. For ^{40}Ar the situation is more complicated because of the presence of two extra neutrons in the $1f_{\frac{7}{2}}$ shell. Gloeckner *et al.* [5]) have performed a shell-model calculation in the $\pi(1d_{\frac{3}{2}})\nu(1f_{\frac{7}{2}}, 2p_{\frac{3}{2}})$ model space and have compared the theoretical spectroscopic factors with the results of our preliminary analysis of the ^{41}K(d, ^{3}He) reaction [6]).

In this paper, a detailed analysis of the ^{39,41}K(d, ^{3}He)^{38,40}Ar reactions at $E_d = 22.8$ MeV are presented and the proton pickup spectroscopic factors for the levels in ^{38}Ar and ^{40}Ar are reported; the results on ^{40}Ar are presented here for the first time.

2. Experimental procedure

The experiment was performed with the 22.8 MeV deuteron beam from the Argonne National Laboratory cyclotron. The out-going ^{3}He particles were detected by a $dE/dX - E$ counter telescope. The detailed experimental set-up and procedure have been discussed by Fortune *et al.*[7]). The energy resolution obtained with the counter telescope is about 140 keV (FWHM).

The target thickness was obtained from a measurement of the deuteron elastic scattering by K from 45° to 65°. The experimental angular distributions were normalized to the angular distribution calculated from the optical-model parameters listed in table 1 and yielded target thicknesses of 130 μg/cm^2 for ^{39}K and 160 μg/cm^2 for ^{41}K.

TABLE 1

Optical-model parameters used in the DWBA analysis[a])

	V_R (MeV)	r_0 (fm)	a_0 (fm)	W_S (MeV)	$4W_D$ (MeV)	r_I (fm)	a_I (fm)	V_{LS} (MeV)	r_{LS} (fm)	a_{LS} (fm)	r_C (fm)	β_{NL} (fm)
^{39}K + d[b])	87.5	1.17	0.748	0.6	48.4	1.325	0.727	6.7	1.07	0.66	1.3	0.54
^{38}Ar + ^{3}He[c])	150.8	1.20	0.720	36.9		1.40	0.880	2.5	1.2	0.72	1.3	0.2
^{41}K + d[b])	87.4	1.17	0.745	0.6	48.4	1.325	0.757	6.7	1.07	0.66	1.3	0.54
^{40}Ar + ^{3}He[c])	153.3	1.20	0.720	39.3		1.40	0.880	2.5	1.2	0.72	1.3	0.2
p	[d])	1.2	0.65					$\lambda = 25$			1.25	

[a]) The notation used here is the same as in Daehnick *et al.*[11]).

[b]) Ref.[11]). The potential set L has been used. A value of $2V_{LS}$ is used in DWUCK.

[c]) Ref.[12]). The value of V_R and W_S are given for the ground-state transition and are varied according to the expressions $V_R = 151.9 - 0.17E + 50\alpha$ and $W_S = 41.7 - 0.33E + 44\alpha$, where $\alpha = (N-Z)/A$ and E is the ^{3}He laboratory energy. A value of $4V_{LS}$ is used in DWUCK.

[d]) The bound proton well-depth is adjusted to give a binding energy of $(5.494 - Q)$ MeV.

Typical excitation spectra taken at 21° are shown in fig. 1. The energy calibration of the spectra from the ^{39}K(d, ^{3}He)^{38}Ar reaction was made by means of the 0.0, 2.167 and 4.564 MeV [ref.[8])] levels of ^{38}Ar. For the ^{41}K(d, ^{3}He)^{40}Ar reaction the energy calibration was made from the 0.0, 2.127, 3.303 and 4.114 MeV levels of ^{34}S [refs.[8, 9])] which were obtained from the ^{35}Cl(d, ^{3}He)^{34}S reaction run under the same experimental conditions. The excitation energies determined in the present study have been indicated in fig. 1 and the estimated accuracy is ± 30 keV for $E_x \leqslant 6$ MeV.

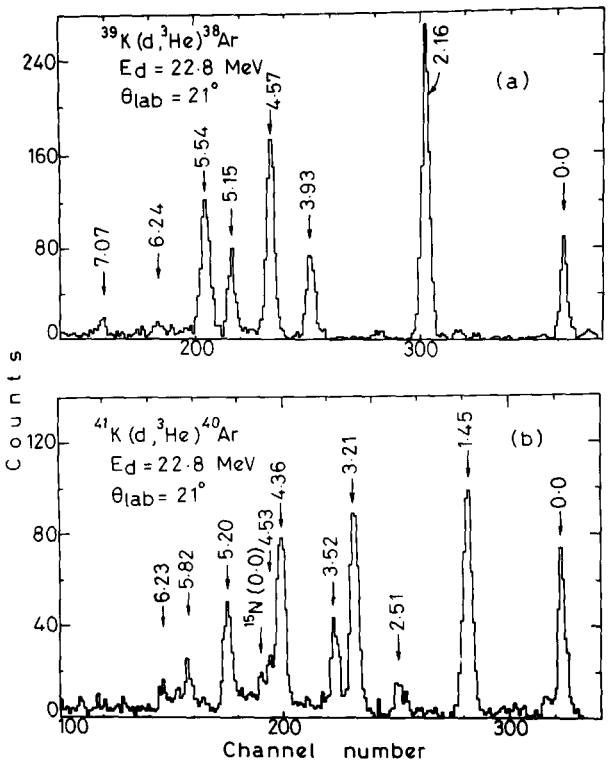

Fig. 1. Spectrum of ^{3}He particles at $\theta_{lab} = 21°$ (a) from the $^{39}K(d, {}^3He)^{38}Ar$ reaction and (b) from the $^{41}K(d, {}^3He)^{40}Ar$ reaction at $E_d = 22.8$ MeV. The excitation energies (in MeV) determined in the present experiment are indicated above the peaks.

3. DWBA analysis

The DWBA analysis was made with the code DWUCK [10]) for the extraction of spectroscopic information for the levels in the residual nuclei. The deuteron optical-model parameters of Daehnick *et al.* [11]) and the ^{3}He particle parameters of Becchetti and Greenlees [12]) were used in all DWBA calculations. The optical-model parameters have been listed in table 1. Some alternative sets of optical-model parameters for deuterons from the collections of Perey and Perey [13]) and the mass-dependent ^{3}He parameters of Trost *et al.* [14]) were also tried in combination with the parameters given in table 1 for a few transitions. The spectroscopic strengths determined with these different sets of parameters were found to lie within about 20% from those obtained from the first set. The DWBA calculations in all these cases employed corrections for finite range and nonlocality in the local energy approximation. A finite-range correction parameter of 0.77 fm has been used. The nonlocality corrections were used only for the deuteron and ^{3}He channels and the values of the parameters have been listed in table 1.

The proton pick-up spectroscopic strengths C^2S_{lj} have been calculated using the relation

$$\sigma_{\exp}(\theta) = N \sum_{l,j} C^2S_{lj}\sigma^{lj}_{\mathrm{DW}}(\theta),$$

where l and j are respectively the orbital and total angular momenta transferred in the reaction, $\sigma^{lj}_{\mathrm{DW}}$ is the DWBA cross section and $\sigma_{\exp}$ is the experimental cross section. A normalization constant $N = 2.95$ of Bassel[15]) for the (d, ^{3}He) reaction has been used in the present analysis. Recent calculations by Ioannides *et al.*[16]) give a value of $D_0 = -153.73$ MeV fm$^{\frac{3}{2}}$ for the (d, ^{3}He) reaction and hence $N = 2{,}363$; the use of this value of N would enhance the C^2S values by a factor of about 1.2. However, σ_{DW} would increase by a factor of 1.25 if a nonlocality correction $\beta = 0.85$ fm is also included in the proton bound state. Thus, if one uses $N = 2.363$ and σ_{DW} with nonlocality corrections for bound protons, one would get nearly the same values of C^2S as those quoted in tables 2 and 3.

The angular distribution of ^{3}He particles for low-lying proton-hole states in ^{38}Ar and ^{40}Ar excited in the (d, ^{3}He) reaction have characteristic $l = 0$ or 2, or admixtures $l = 0$ and 2 shapes. When both l-values are possible, the relative $l = 0$ and 2 strengths have been adjusted to get good visual fits.

4. Results and discussions

4.1. LEVELS IN ^{38}Ar

The angular distributions for the transitions to the levels in ^{38}Ar with their DWBA fits are shown in fig. 2. The experimental results deduced from the ^{39}K(d, ^{3}He)^{38}Ar reaction have been summarized in table 2. The previous experimental results[3,4]) along with two different model calculations[1,3]) have also been tabulated for comparison.

The $1d_{\frac{3}{2}}$ proton pickup strength is exhausted by the three levels below 4 MeV excitation. The 4.57, 5.16 and 5.56 MeV levels are excited predominantly by $l = 0$ transfer even though the angular momentum selection rule permits both $l = 0$ and 2 transfer. The 6.24 MeV level excited weakly in the present experiment is expected to have $l = 3$ and $C^2S \leqslant 0.08$ from Gray *et al.*[3]). For the transition to the 7.13 MeV level in ^{38}Ar, a proton pickup from the $1d_{\frac{5}{2}}$ shell is assumed.

It can be seen that there is, in general, good agreement between the spectroscopic strengths deduced from the present experiment compared to the previous experimental results[3,4]). Small differences in the values of the spectroscopic strengths deduced by various studies may be expected to arise from the differences in the optical-model parameters and the bound-state parameters.

The full sd shell-model calculation[1]) correctly predicts the pickup strength for the first two levels in ^{38}Ar which are expected to be the two components of $1d_{\frac{3}{2}}$ proton configuration. On the other hand this model does not explain the $l = 0$ strength distributions among the next four levels. This fragmentation can perhaps be accounted

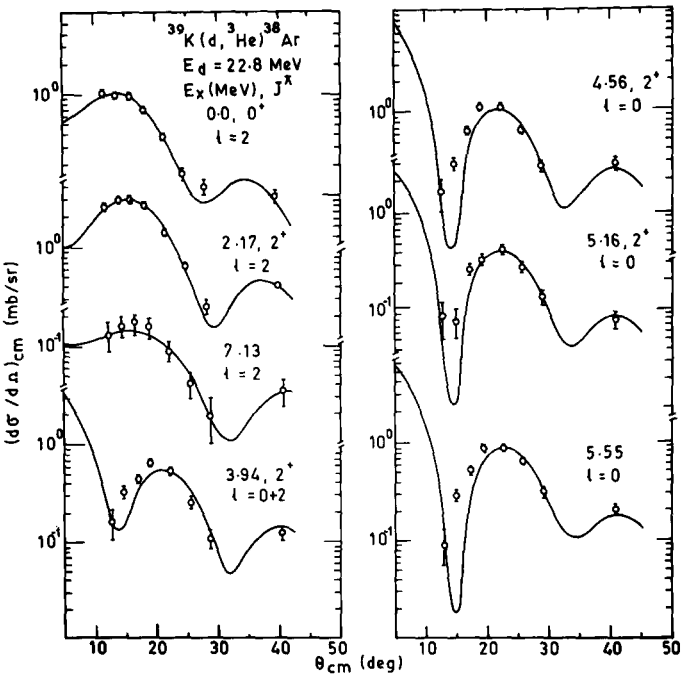

Fig. 2. Angular distribution for the levels in ^{38}Ar populated in the ^{39}K(d, ^{3}He)^{38}Ar reaction at $E_d = 22.8$ MeV. The curves are the results of DWBA fits.

for either by considering core excitation or by extending the shell-model space. It can be seen from the table 2 that the spectroscopic strengths predicted by a core-excitation-model calculation of Gray *et al.* [3]) agree with the experimental results for the levels below 4.57 MeV excitation.

The summed spectroscopic strengths indicated in table 2 are in good agreement with each other. The value of $\sum C^2S(2s_{\frac{1}{2}}) = 2.37$ is slightly higher than the value of 2.0 and this may be due to the fact that the experimental spectroscopic strengths have been deduced by normalizing at the second maximum of the DWBA curves.

4.2. LEVELS IN ^{40}Ar

The angular distributions for the transitions to the levels in ^{40}Ar observed in the ^{41}K(d, ^{3}He)^{40}Ar reaction are shown in fig. 3. The l-values and the spectroscopic strengths have been given in table 3. The results of the $\pi(1d_{\frac{3}{2}})\nu(1f_{\frac{7}{2}}, 2p_{\frac{3}{2}})$ model calculation of Gloeckner *et al.* [5]) for sets A and B are also listed for comparison.

The ground state (0^+), the 1.46 MeV (2^+) and the 3.52 MeV levels are populated dominantly by $l = 2$ transfer. The predicted [5]) $1d_{\frac{3}{2}}$ proton pickup strength for the ground state and for the 1.46 MeV level are in agreement with the measured values.

TABLE 2

Proton pickup spectroscopic strengths for the levels in ^{38}Ar [a])

E_x [b]) (MeV)	J^{π} [b])	Present study				Theory				
		l	$100C^2S$	$100C^2S$ [c])	$100C^2S$ [d])	E_x [e]) (MeV) (s-d space)	J^{π} [e])	$100C^2S$ [e])	E_x [e])	$100C^2S$ [e])
0.0	0^+	2	; 44;	; 53;	; 49;	0.00^+	0^+	; 45;	0.0	; 39;
2.168	2^+	2	;241;	5;250;	;250;	2.025	2^+	;246;	2.07	9;200;
3.937	2^+	0,2	26; 17;	16; 17;	26; 13;	4.145	2^+	117; ;	4.33	22; 32;
4.565	2^+	0	81; ;	49; ;	62; ;				4.79	80; 9;
5.157	2^+	0	37; ;	23; ;	33; ;				6.39	4; 6;
5.552	$(1,2)^+$	0	93; ;	63; ;	78; ;	5.078	1^+	75; ;	6.65	75; ;
7.13	$(1-4)^+$	2	; ;50	; ;40	; ;44	7.786	4^+	; ;221	7.97	; ;220
						8.604	2^+	; ;120		
						10.760	2^+	7; 3; 4		
$\sum C^2S(2s_{1/2})$	=		2.37	1.56	2.00			1.99		1.90
$\sum C^2S(1d_{3/2})$	=		3.02	3.20	3.02			2.94		2.86
$\sum C^2S(1d_{5/2})$	=		0.50	0.40	0.44			3.45		2.20

[a]) In the columns labelled $100C^2S$, the spectroscopic strengths are given in the notation $100C^2S(2s_{\frac{1}{2}})$; $100C^2S(1d_{\frac{3}{2}})$; $100C^2S(1d_{\frac{5}{2}})$.

[b]) Ref. [8]). Energies measured in the present experiment are indicated in fig. 1(a).

[c]) Ref. [3]).

[d]) Ref. [4]). The values of C^2S are normalized to give $\sum C^2S(2s_{\frac{1}{2}}) = 2.00$.

[e]) Ref. [1]).

The levels at 2.52 MeV (2^+) and 3.21 MeV (2^+) exhibit an admixture of $l = 0$ and 2. However, the model prediction of the $C^2S(1d_{\frac{3}{2}})$ value [5]) for the 2.52 MeV level is larger than the experimental value by an order of magnitude. The 4.36 and the 5.17 MeV levels have been populated dominantly by $l = 0$ transfer and hence the assignment 1^+ or 2^+ is suggested for both these levels. The levels at 4.53, 5.82 and 6.23 MeV are weakly excited in the present experiment and hence the angular distributions for these levels could not be compared with DWBA calculations.

The sum rule values for the spectroscopic strengths (see table 3) indicate that substantial strengths lie at higher excitation energies in ^{40}Ar.

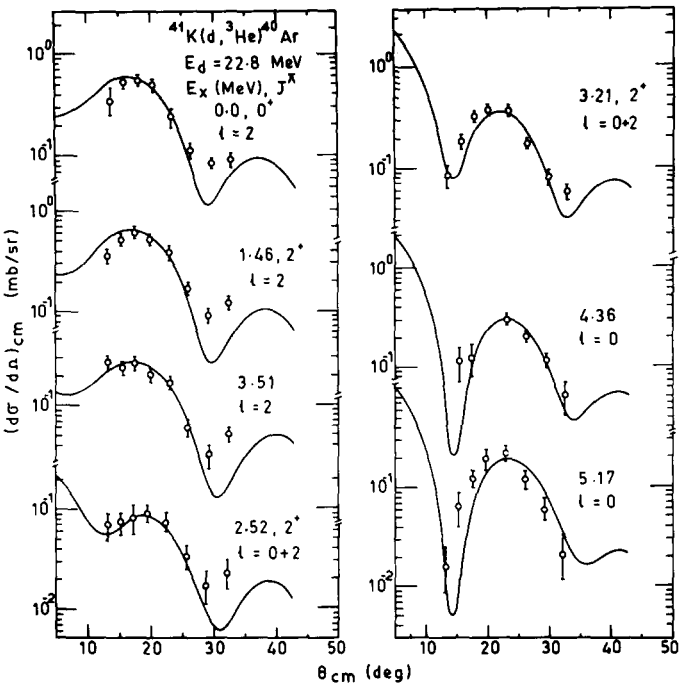

Fig. 3. Angular distribution for the levels in ^{40}Ar populated in the ^{41}K(d,^{3}He)^{40}Ar reaction at E_d = 22.8 MeV. The curves are the results of DWBA fits.

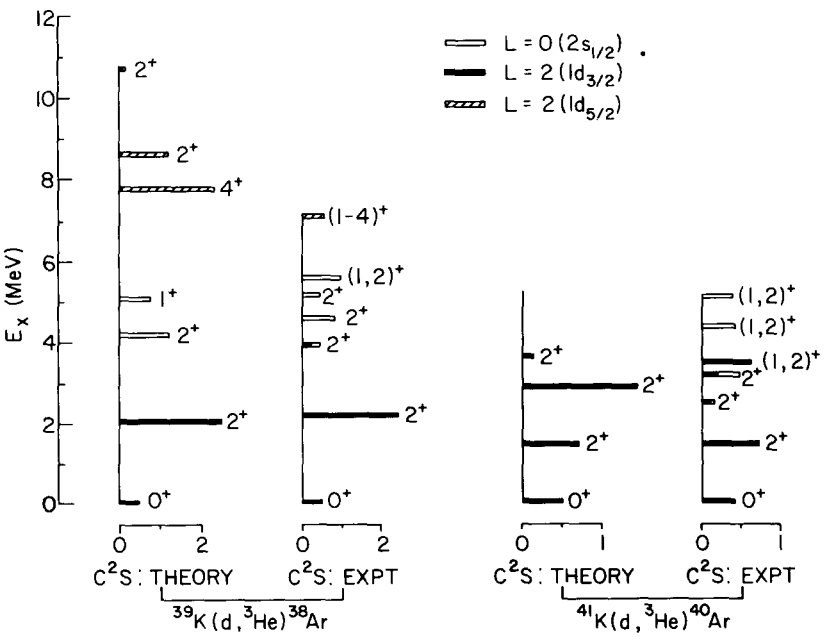

Fig. 4. Comparison of shell-model and experimental spectroscopic strengths for transitions to the states in ^{38}Ar and ^{40}Ar. The theoretical spectroscopic strengths for ^{38}Ar are from ref. [1]) and for ^{40}Ar from ref. [5]).

TABLE 3

Proton pickup spectroscopic strengths for the levels in ^{40}Ar [a])

		Present study		Theory [c])				
E_x [b]) (MeV)	J^{π} [b])	l	$100C^2S$	J^{π}	Set A		Set B	
					E_x (MeV)	$100C^2S$	E_x (MeV) (f-p-d space)	$100C^2S$
0.0	0^+	2	;43;	0^+	0.0	; 50;	0.0	; 50;
1.461	2^+	2	;72;	2^+	1.44	; 71;	1.42	; 69;
2.524	2^+	0,2	2;11;	2^+	2.91	;142;	2.89	;149;
3.208	2^+	0,2	28;18 [d]);	2^+	3.68	; 9;	3.65	; 6;
3.511	$(1,2^+)$	2	;66;					
4.358	$(1,2^+)$	0	39; ;					
5.166	$(1,2)^+$	0	35; ;					
	$\sum C^2S(2s_{1/2})$	=	1.04			—		—
	$\sum C^2S(1d_{3/2})$	=	2.10			2.72		2.74

[a]) See footnote of table 2.

[b]) Ref. [8]). Energies measured in the present experiment are indicated in fig. 1(b).

[c]) Ref. [5]). For the definition of set A and set B see ref. [5]).

[d]) The strength of the d-wave contribution has an error of $\pm 30\%$.

5. Conclusions

The experimental and theoretical spectroscopic strengths for the positive-parity levels in ^{38}Ar and ^{40}Ar are summarized in fig. 4. In the case of ^{38}Ar, there is good agreement for the $1d_{\frac{3}{2}}$ pickup between the experimental values and the prediction from the full sd shell-model calculation. However, the strength for the $2s_{\frac{1}{2}}$ pickup is not correctly predicted. This deficiency is overcome in the core-excitation model [3]). The recent shell-model calculation by Hasper [17]) in the $2s_{\frac{1}{2}}$-$1d_{\frac{3}{2}}$-$1f_{\frac{7}{2}}$-$2p_{\frac{3}{2}}$ space predicts more 0^+ and 2^+ levels around an excitation energy of 4 MeV compared to those from the full sd shell-model calculation and hence shows that the spectrum of core-excited states (obtained by promoting pairs of particles to the $1f_{\frac{7}{2}}$ orbit) as assumed by Gray *et al.* [3]) is essentially correct. Unfortunately, the proton pickup spectroscopic factors for the calculation of Hasper [17]) are not yet available. In the case of ^{40}Ar,

we note that the splitting of the $1d_{\frac{3}{2}}$ strength is not well accounted for by the $\pi(1d_{\frac{3}{2}})\nu(1f_{\frac{7}{2}}, 2p_{\frac{3}{2}})$ model calculation [5]). Further, inclusion of the $2s_{\frac{1}{2}}$ excitations would be necessary to account for the $l = 0$ pickup strength. Hence, a shell-model calculation in the space used by Hasper [17]) is desirable for the nuclei ^{40}Ar and ^{41}K.

The work at Argonne National Laboratory was performed under the auspices of the US Department of Energy under Contract W-31-109-ENG-38. The authors are grateful to Drs. A. Amusa and R. D. Lawson for providing us with the spectroscopic factors for the ^{41}K(d, ^{3}He)^{40}Ar reaction. We are thankful to Dr. H. T. Fortune for his help during the experiment and to Dr. K. S. Puttaswamy for his help in the preliminary analysis of the data. One of the authors (CMB) is grateful to the Council of Scientific and Industrial Research, New Delhi for the award of a senior research fellowship.

References

1) B. H. Wildenthal and W. Chung, private communication
2) B. H. Wildenthal, E. C. Halbert, J. C. McGrory and T. T. S. Kuo, Phys. Rev. **C4** (1971) 1266
3) W. S. Gray, P. T. Ellis, T. Wei, R. M. Polichar and J. Jänecke, Nucl. Phys. **A140** (1970) 494
4) B. H. Wildenthal and E. Newman, Nucl. Phys. **A118** (1968) 347
5) D. H. Gloeckner, R. D. Lawson and F. J. D. Serduke, Phys. Rev. **C7** (1973) 1913
6) N. G. Puttaswamy and J. L. Yntema, Bull. Am. Phys. Soc. **13** (1968) 87;
N. G. Puttaswamy, Nucl. Phys. and Solid Stat. Phys. (India) **16A** (1973) 87
7) H. T. Fortune, N. G. Puttaswamy and J. L. Yntema, Phys. Rev. **185** (1969) 1546
8) P. M. Endt and C. van der Leun, Nucl. Phys. **A310** (1978) 1
9) N. G. Puttaswamy and J. L. Yntema, Phys. Rev. **177** (1969) 1624
10) P. D. Kunz, code DWUCK, University of Colorado Report (1969), unpublished
11) W. W. Daehnick, J. D. Childs and Z. Vrcelj, Phys. Rev. **C21** (1980) 2253
12) F. D. Becchetti, Jr., and G. W. Greenlees, Polarization phenomena in nuclear reactions, ed. H. H. Barschall and W. Haeberli (University of Wisconsin Press, Madison, 1971) p. 682
13) C. M. Perey and F. G. Perey, Atom. Nucl. Data Tables **17** (1976) 1
14) H.-J. Trost, A. Schwarz, U. Feindt, F. H. Heimlich, S. Heinzel, J. Hintze, F. Körber, R. Lekebusch, P. Lezoch, G. Möck, W. Paul, E. Roic, M. Wolff, J. Worzeck and U. Strohbusch, Nucl. Phys. **A337** (1980) 377
15) R. H. Bassel, Phys. Rev. **149** (1966) 791
16) A. A. Ioannides, M. A. Nagarajan and R. Shyam, Nucl. Phys. **A363** (1981) 150
17) H. Hasper, Phys. Rev. **C19** (1979) 1482

Levels in ^{38}K from the ^{40}Ca(d,α) reaction at 22.8 MeV

C. M. Bhat
Department of Physics, Bangalore University, Bangalore, India

N. G. Puttaswamy,* H. T. Fortune,† and J. L. Yntema
Argonne National Laboratory, Argonne, Illinois 60439
(Received 11 January 1983)

Twenty levels in ^{38}K up to an excitation energy of 10.26 MeV have been identified in a study of the ^{40}Ca$(d,\alpha)^{38}$K reaction at an incident deuteron energy of 22.8 MeV. Differential cross sections were measured at forty-four angles in an angular range $11° \leq \theta \leq 165°$. Distorted-wave Born approximation analysis has been performed for eight transitions using two-nucleon spectroscopic amplitudes derived from a full *sd* shell-model calculation. For other levels, distorted-wave Born approximation calculations were performed assuming simple two-nucleon configurations. The 7.32-MeV level is found to be populated by $L=0+2$ transfer and hence has $J^\pi=1^+$. A newly identified level at 9.88 MeV is found to be excited by $L=2$ transfer and hence has $J^\pi=1^+$, 2^+, or 3^+.

[NUCLEAR REACTIONS ^{40}Ca$(d,\alpha)^{38}$K, $E_d=22.8$ MeV, measured E_α and $\sigma(\theta,E_\alpha)$, DWBA analysis, deduced levels, L transfer.]

I. INTRODUCTION

There has been a great deal of interest in the (d,α) reaction, especially on even-even nuclei[1–7] because of its highly selective nature in populating the levels in the residual nuclei.[8,9] Some states which are weakly populated in single-nucleon transfer reactions can be very strongly excited in this reaction. The angular distributions are characteristic of the transferred orbital angular momenta and can be reproduced with distorted-wave Born approximation (DWBA) calculations. The (d,α) reaction has therefore become an important tool in the elucidation of nuclear structure.

In a simple shell-model picture for the low-lying positive-parity levels of ^{38}K, the $(1d_{3/2}{}^{-1})_p(1d_{3/2}{}^{-1})_n$ configuration is expected to be the dominant one. Pickup reactions, such as (d,α) and $(p,{}^3\text{He})$ on ^{40}Ca, are expected to populate levels with such configurations and ought to give direct information on proton-neutron hole states in ^{38}K. Higher levels are necessarily excited by pickup of nucleons from deeper subshells. Spectroscopic amplitudes derived from a full *sd*-shell—model calculation[10,11] can be used in a DWBA prediction of the cross section and the results can then be compared with experiments. Excitation of some odd-parity levels of ^{38}K can also be expected because the ground state of ^{40}Ca is known to contain *fp*-shell admixtures.[12,13]

The levels of ^{38}K have been investigated previously by single as well as multinucleon transfer reactions.[12] Abou-Zeid *et al.*[14] and Sens and de Meijer[15] have studied the low-lying levels via the $(p,{}^3\text{He})$ reaction at $E_p=42.5$ MeV and 30 MeV, respectively. Frascaria *et al.*[14] have investigated the ^{40}Ca(d,α) reaction at $E_d=80$ MeV with emphasis on excitation of the $(1f_{7/2}{}^{-1})_p(1f_{7/2}{}^{-1})_n$, $J^\pi=7^+$ configuration in ^{38}K. Recently, a study of the dependence of vector analyzing power (VAP) on the orbital angular momentum L and on the total angular momentum J transferred in the reaction has been made for the ground state and for the 0.46-MeV level of ^{38}K via the ^{40}Ca$(\vec{d},\alpha)$ reaction at $E_d=16.5$ MeV,[16] and the data have been analyzed assuming a proton-neutron cluster pickup. A study of the levels at 0.0, 0.46, and 1.69 MeV has been made by Merzet *et al.*[17] at $E_d=23$ MeV with a view to understanding the mechanism of $(\vec{d},\alpha)$ reactions. No levels beyond an excitation energy of 7.35 MeV have been reported in any of the above experiments.

In the present investigation of the ^{40}Ca$(d,\alpha)^{38}$K reaction at $E_d=22.8$ MeV, the levels up to an excitation energy of 10.26 MeV in ^{38}K have been studied. The angular distributions have been measured over a wide angular range. DWBA analyses have been performed for ten out of twenty transitions observed; orbital angular moment L transferred and J^π values are deduced.

 ©1983 The American Physical Society

TABLE I. Optical-model potential parameters used in the analysis of $^{40}Ca(d,\alpha)^{38}K$ reaction at 22.8 MeV.

Channel	V_R (MeV)	r_0 (fm)	a_0 (fm)	W_S (MeV)	$4W_D$ (MeV)	r_I (fm)	a_I (fm)	$2V_{LS}$ (MeV)	r_{LS} (fm)	a_{LS} (fm)	r_C (fm)	β_{NL} (fm)
d	87.7	1.17	0.748	0.7	48.4	1.325	0.729	13.4	1.07	0.66	1.3	0.54
α_1	183.7	1.4	0.564	26.6		1.4	0.564				1.4	0.2
α_2	215.8	1.111	0.785	22.6		1.111	0.785				1.34	0.2
p,n[a]		1.18	0.68					$\lambda=25$			1.25	0.85

[a]The proton and neutron Woods-Saxon well depths are adjusted to reproduce the proper separation energy.

II. EXPERIMENTAL PROCEDURE

The experiment was carried out with a 22.8-MeV deuteron beam from the Argonne National Laboratory cyclotron. The ^{40}Ca target was prepared by evaporating the enriched isotope onto a thin carbon film. The target was always kept in vacuum in order to avoid oxidation. The outgoing α particles were simultaneously detected using a set of four dE/dX-E counter telescopes which were separated by 7.5° from each other. An energy resolution (FWHM) of about 135 keV was obtained. The spectra were recorded at 44 angles in an angular range from 11° to 165°. Other details of the experimental setup and procedure have been discussed previously.[18]

The target thickness was determined to be 60 ± 15 $\mu g/cm^2$ by comparing the experimental deuteron elastic-scattering cross section around the maximum at $\theta=55°$ with that obtained by using optical-model potential parameters for deuterons listed in Table I.

The spectra were analyzed with a peak-fitting computer program MALIK.[19] A typical α-particle spectrum at a laboratory angle of 45° is shown in Fig. 1. A consistent energy calibration has been obtained using the levels of ^{38}K at 0.0, 0.459, 1.698, 3.431, and 3.978 MeV,[12] and the levels of ^{10}B at 0.0, 0.718, and 2.155 MeV.[20] The excitation energies of the ^{38}K levels determined in the present experiment are indicated in Fig. 1 and are also listed in Table II. The accuracy of the excitation energies is expected to be ±30 keV for the levels below 4 MeV excitation and about ±50 keV for levels above 4 MeV.

The angular distributions of α particles corresponding to various transitions have been determined and are displayed in Figs. 4—7. The error bars, where shown, contain statistical errors and errors due to background subtraction. The integrated cross sections for some of the levels have been determined using

$$\sigma_{\text{int}}=2\pi\int_0^{\pi}\left[\frac{d\sigma}{d\Omega}\right]_{\text{expt}}\sin\theta\,d\theta$$

and are listed in Table II. The $(d\sigma/d\Omega)_{\text{expt}}$ is the measured differential cross section in the center of mass system, and θ is the center of mass angle.

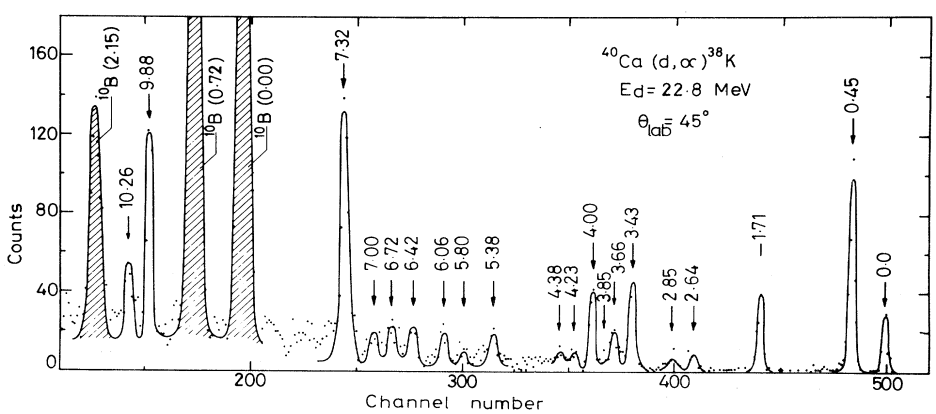

FIG. 1. The spectrum of α particles from the $^{40}Ca(d,\alpha)^{38}K$ reaction at $E_d=22.8$ MeV and $\theta_{lab}=45°$. The excitation energy (in MeV) shown on the peaks has been determined from the present experiment. Transitions from the $^{12}C(d,\alpha)^{10}B$ reaction are shown by hatched peaks.

TABLE II. Comparison of the excitation energies of the levels in ^{38}K.

Adopted energy levels[a]		^{40}Ca(d,α)^{38}K Present study		Ref. 4[b]
E_x (MeV)	J^π	E_x[c] (MeV)	σ_{int} (mb)	E_x (MeV)
0.0	3^+	0.0	0.99	0.0
0.459	1^+	0.45	1.46	0.45
1.698	1^+	1.71	0.74	1.70
2.649	$(2,4)^-$	2.64	0.14	2.63
2.870	2^-	2.85	0.26	2.85
3.431	2^+	3.43	1.06	3.42
3.668	3^+	3.66	0.37	3.60
3.857	1^+	3.85		
3.978	1^+	4.00	0.52	3.97
		4.23		4.28
		4.38		
		5.38		5.28
		5.80		
		6.06		
		6.42		6.35
		6.72		6.60
		7.00		6.90
		7.32	5.51	7.35
		9.88	3.16	
		10.26		

[a]Reference 12.
[b]E_x values are taken from Fig. 4 of Ref. 4.
[c]The errors in E_x are estimated to be ±30 keV for the levels below 4 MeV and about ±50 keV for higher levels.

III. ANALYSIS

A. Optical-model parameters

Previous studies of (d,α) reactions[2,4,21] indicated that the shapes of the DWBA angular distributions are not very sensitive to the choice of the deuteron optical-model (OM) parameters, while they are quite sensitive to the choice of α-particle parameters. Therefore, we have compared the DWBA angular distributions calculated using different sets of α-particle OM parameters with the experimental angular distributions for the 0.0-MeV (3^+) and 3.43-MeV (2^+) transitions. In particular the 3.43-MeV level can be expected to be populated by pure $L=2$ transfer.

The deuteron OM parameters are taken from the global fits (potential set L) of Daehnick *et al.*[22] For α particles, two different sets from the compilation of Perey and Perey[23] have been tried. The OM parameter sets are listed in Table I. The set α_1 is the average parameter set used by Bock *et al.*[24] to fit elastic scattering of 19.47-MeV α particles on nuclei near ^{40}Ca. The set α_2 is derived from an analysis of elastic scattering of 27-MeV particles on ^{39}K. The fits corresponding to these α-particle OM parameters are shown in Fig. 2. (The shell-model spectroscopic amplitudes for the DWBA calculations are taken from Table III.) The set d-α_1 seems to give better fits at forward angles and hence the DWBA analyses for all other transitions have been performed using this set.

B. Form factors

The two-nucleon form factors were calculated from a microscopic model using the method of Bayman and Kallio.[25] The single-particle wave functions of the transferred proton and neutron were generated in a real potential of Woods-Saxon shape with the values of $r_0=1.18$ fm and $a_0=0.68$ fm for the radius and diffuseness parameters, respectively. These bound-state parameters have been derived from an extrapolation to zero energy of the parameters obtained in a proton elastic scattering experiment.[26] For comparison, the set $r_0=1.25$ fm and $a_0=0.65$ fm commonly used for the calculation of form factors has also been tried for a few transitions. The shapes of the DWBA curves are very similar and σ_{DW} for the latter case is about 1.3 times

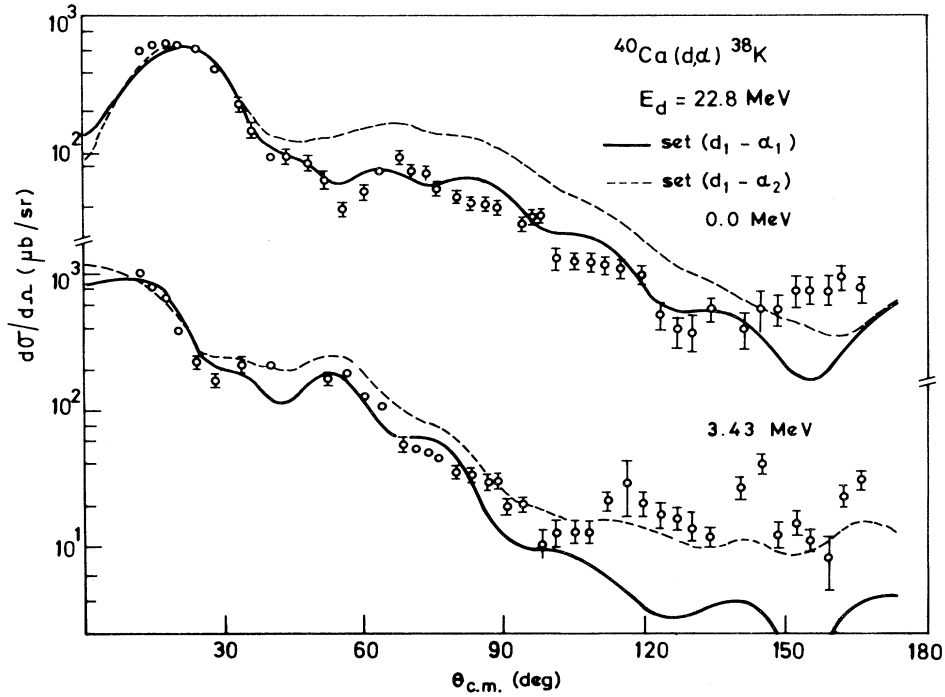

FIG. 2. Comparison of the experimental angular distributions with the DWBA curves obtained using different sets of the optical model parameters listed in Table I.

that for the former case. The nucleon binding energy has been taken to be $S_d/2$, where S_d is the deuteron separation energy of levels under consideration; a relative s state has been assumed for the transferred pair of nucleons.

Mixed configurations in the *sd*-shell—model space[11] have been used in the calculation of form factors for most of the levels. The two-nucleon spectroscopic amplitudes used in the analyses are listed in Table III. For negative-parity levels, pure two-particle configurations from an *sdf*-shell—model space have been tried.

C. DWBA cross sections

The DWBA analyses have been made using the code DWUCK (Ref. 27) by including a finite-range correction of 0.4 fm and nonlocality correction given in Table I. The contribution from different L transfers for a transition is determined by the shell-model spectroscopic amplitudes (listed in Table III).

TABLE III. Two-nucleon spectroscopic amplitudes for the ^{40}Ca$(d,\alpha)^{38}$K reaction and the results of the DWBA analysis. The DWBA angular distributions for these transitions are shown in Figs. 4 and 5.

E_x			Two-nucleon spectroscopic amplitudes[a]						
(MeV)	L	$J^{\pi a}$	$(D5,D5)$	$(D5,S1)$	$(D5,D3)$	$(S1,S1)$	$(S1,D3)$	$(D3,D3)$	N^b
0.0	2,4	3_1^+	−0.0193	0.0421	−0.5684			2.5836	1.00
0.45	0,2	1_1^+	0.1137		−0.9324	0.4773	−1.2344	0.6052	1.17
1.71	0,2	1_2^+	−0.3501		0.7336	−0.3344	0.0160	1.4924	1.26
3.43	2	2_1^+		0.6228	0.9889		1.9064		0.53
3.66	2,4	3_2^+	−0.7077	−1.7597	−1.7964			0.4186	0.14
4.00	0,2	1_3^+	−0.1855		0.7270	−0.8470	−1.1771	−0.5781	0.61
7.32	0,2	1_4^+	0.1930		−0.9477	−1.3935	0.2908	0.1957	15.8
9.88	2,4	3_3^+	0.0861	−1.9293	−1.7726			−0.3579	7.00

[a]Reference 11. The notation $(D5,D5)$ implies a $(1d_{5/2}{}^{-1})(1d_{5/2}{}^{-1})_n$ configuration.

[b]Normalized relative to the ground state value of $N=0.30\times10^4$.

TABLE IV. Two-nucleon configurations assumed for odd-parity levels in ^{38}K and the results of the DWBA analysis. The resulting DWBA angular distributions are shown in Fig. 6.

E_x (MeV)	L	Assumed J^π	Two-nucleon configurations[a]	N[b]
2.64	1,3	2^-	($D3,F7$)	1.06
2.85	1,3	2^-	($D3,F7$)	2.44

[a]The notation ($D3,F7$) implies a $(1d_{3/2}{}^{-1})_p(1f_{7/2}{}^{-1})_n$ configuration.
[b]Normalized relative to the ground state value of $N=2.08\times10^4$.

For odd J-even parity transitions, the contributions for two different L transfers have been added together incoherently and the summed curves are represented by solid lines in Figs. 4 and 5. Each of them has been independently normalized for each state according to

$$\left[\frac{d\sigma}{d\Omega}\right]_{\text{expt}}=\frac{N}{2J+1}\left[\frac{d\sigma}{d\Omega}\right]_{\text{DW}}.$$

The resulting normalization factors N have also been listed in Table III. In the case of negative-parity levels the values of N are listed in Table IV.

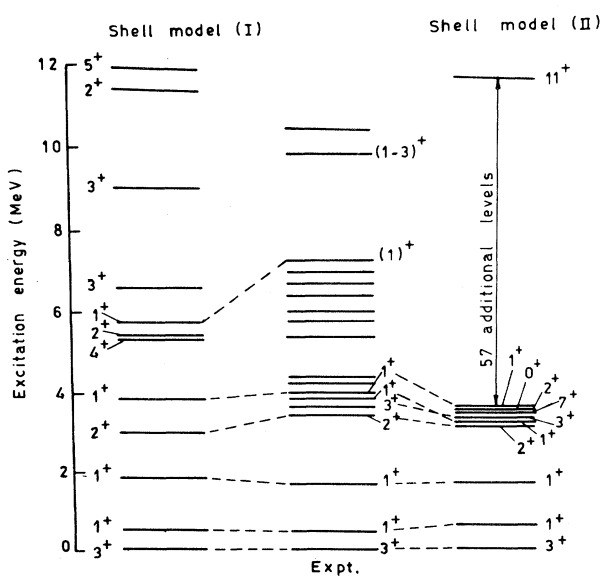

FIG. 3. The positive-parity levels in ^{38}K excited in the ^{40}Ca(d,α) reaction at $E_d=22.8$ MeV and a comparison with shell-model calculations. Shell model (I) refers to the full sd-shell—model calculation (Ref. 11) and shell model (II) refers to the $sdfp$-model calculation (Ref. 28).

IV. RESULTS AND DISCUSSION

A. Excitation energies

The excitation energies of the levels in ^{38}K deduced from the present experiment are compared in Table II with those adopted by Endt and van der Leun,[12] and with the results of the 80-MeV study of the ^{40}Ca(d,α) reaction by Frascaria *et al.*[4] A one-to-one correspondence of our results with the various levels of ^{38}K could be made only for levels up to an excitation energy of 4 MeV. Our results compare well with those obtained by Frascaria *et al.*[4] except for the 5.28-MeV level ($J^\pi=7^+$), which is weakly excited in our experiment.

The excitation energies of positive-parity levels of ^{38}K deduced here are shown in Fig. 3 along with the theoretical predictions of $1d_{5/2}$-$2s_{1/2}$-$1d_{3/2}$-shell—model[11] and $2s_{1/2}$-$1d_{3/2}$-$1f_{7/2}$-$2p_{3/2}$-shell—model[28] calculations.

B. Even-parity levels

The experimental angular distributions to eight even-parity transitions studied in the present ^{40}Ca(d,α)^{38}K reaction are shown in Figs. 4 and 5. The DWBA curves calculated using the spectroscopic amplitudes of Wildenthal and Chung[11] are also shown in the figures. The ground state and the 3.66-MeV level show dominant $L=4$ and 2 transfers, respectively. Previous studies by Frascaria *et al.*[4] and VAP measurements in the ($\vec{d},\alpha$) experiment[16] had strongly suggested the ground-state angular distribution to be $L=4$. The level at 3.43 MeV is found to show a characteristic $L=2$ shape; a pure $L=J=2$ is expected on the basis of the selection rules for this level.

The newly identified level at 9.88 MeV was excited with a total cross section of 3.16 mb, which is three times that for the ground-state transition (see, e.g., Table II). The DWBA calculation was made initially with all possible pure two-nucleon configurations in the sdf-shell—model space. This suggests a dominant $L=2$ shape for the experimental angular distribution for the 9.88-MeV level. Hence $J^\pi=1^+$, 2^+, or 3^+ is expected. A DWBA calculation was performed with mixed configurations corresponding to the theoretically predicted 3_3^+ level at 9.06 MeV and the spectroscopic amplitudes listed in Table III. The predicted shape fits the experimental data quite well (see Fig. 4) and hence the 9.88-MeV level is most likely to have the assignment 3^+, $T=0$.

The levels at 0.45, 1.71, and 4.00 MeV are known[12] to have $J^\pi=1^+$. Therefore an $L=0+2$ transfer is expected. The experimental angular dis-

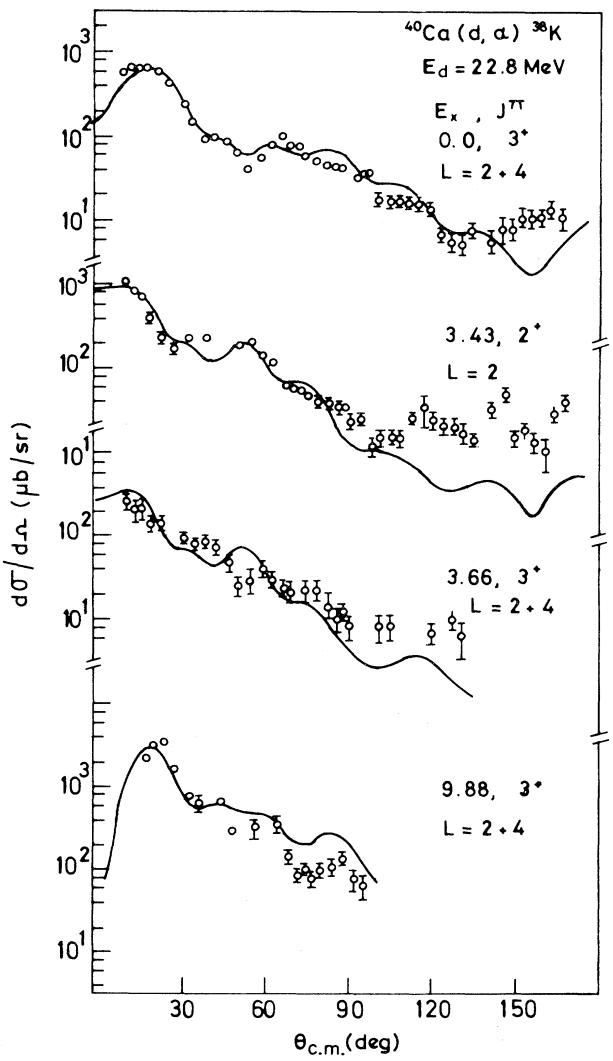

FIG. 4. Angular distributions for the levels excited in the ^{40}Ca(d,α) reaction at $E_d=22.8$ MeV. The curves are the results of the DWBA analysis. The two-nucleon spectroscopic amplitudes of Wildenthal and Chung used here are listed in Table III.

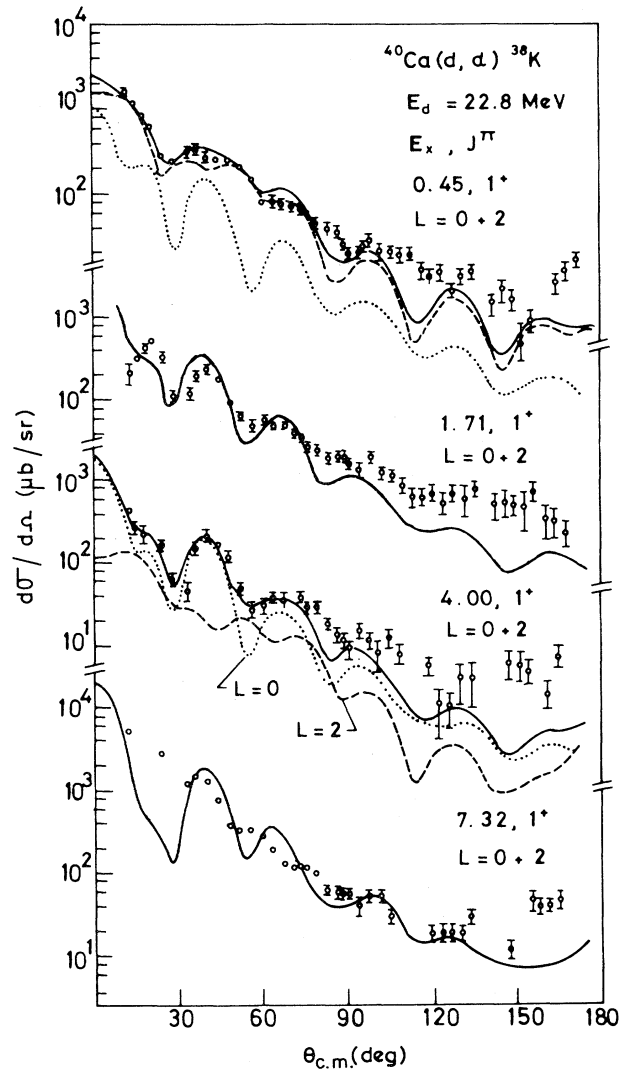

FIG. 5. Angular distributions for the 1^+ levels in ^{38}K. The curves are the DWBA fits for the $L=0+2$ transfer.

tributions and the curves calculated using *sd*-shell—model wave functions[11] are shown in Fig. 5. The shapes of the experimental angular distributions for all these transitions indicate dominance by a single L transfer. The partial contributions due to $L=0$ and 2 in the case of the 0.45- and 4.00-MeV levels are indicated in Fig. 5 along with their incoherent sums. It can be seen that the 0.45-MeV level has largely an $L=2$ shape, which supports the VAP measurements by Ludwig *et al.*[16] The 1.71- and 4.00-MeV levels show dominant $L=0$ shapes.

In the 80-MeV study of ^{40}Ca(d,α) by Frascaria *et al.*,[4] a level at 7.35 MeV excitation was observed; no spectroscopic information was, however, deduced. In the present study, the level at 7.32 MeV was excited very strongly. The integrated cross section for the transition to this level is about five times that for the ground-state transition (see Table II). DWBA calculations were made initially with all possible pure two-nucleon configurations in the *sdf*-shell—model space; the DWBA angular distributions obtained by assuming $(2s_{1/2})_p(2s_{1/2})_n$ pickup, and $J^\pi=1^+$ and $L=0$ have been found to fit the experimental angular distribution fairly well. Calculations have therefore been made assuming the two-nucleon spectroscopic amplitudes (see Table III) for a predicted level at 5.75 MeV (1_4^+). The results of the DWBA analysis are shown in Fig. 5. The 7.32-

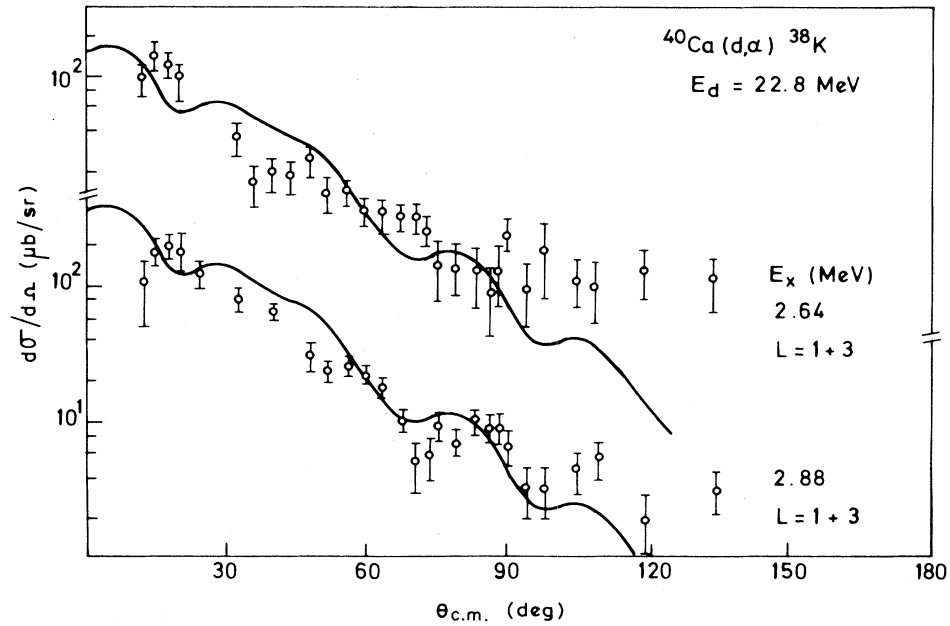

FIG. 6. Angular distributions for the odd-parity levels excited in the ^{40}Ca(d,α) reaction at $E_d=22.8$ MeV. The curves are the results of the DWBA analysis using the configurations indicated in Table IV.

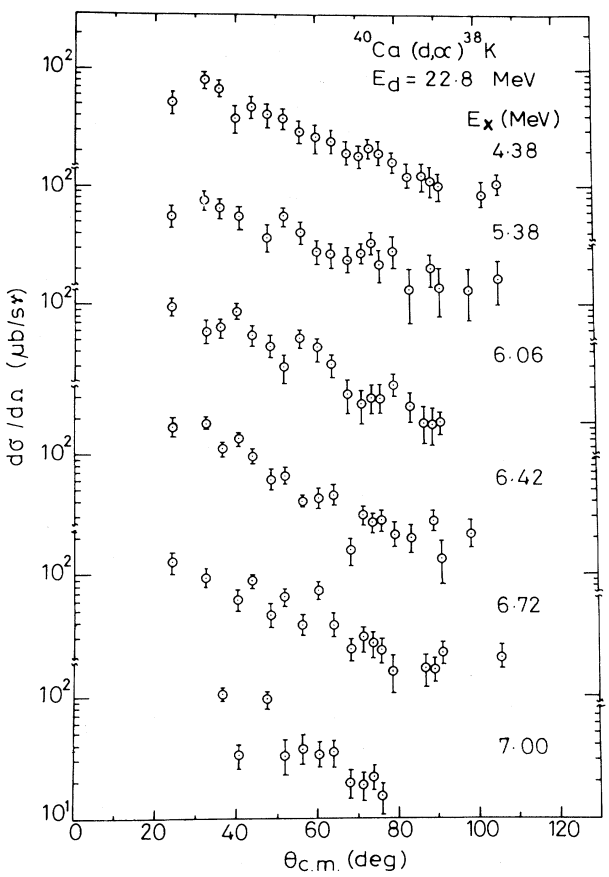

FIG. 7. Angular distributions for the levels in ^{38}K for which L-value assignments could not be made.

MeV level is therefore most likely to have a value $J^\pi=1^+$. The large value of N and the large difference in energies, however, make it likely that the 7.32-MeV level is to be identified with a higher theoretical 1^+ state.

C. Odd-parity levels

Two levels in ^{38}K, one at 2.64 MeV and another at 2.85 MeV are weakly excited in the present (d,α) experiment. From a study of the ^{39}K(d,t)^{38}K reaction, Fortune *et al.*[18] found that the 2.64-MeV level has an $l=1$ angular distribution, while a high resolution study of the ^{39}K(p,d)^{38}K reaction by Wildenthal *et al.*,[29] suggests an $l=3$ pickup for the same level. However, the parity of the level is determined to be negative and the value $J^\pi=(2,4)^-$ is adopted for this level by Endt and van der Leun.[12] It may be that (p,d) favors somewhat higher l transfers than does (d,t). If the transfer results are correct, then $J^\pi=4^-$ is not allowed.

In the present experiment angular distribution patterns for the 2.64- and 2.85-MeV transitions (as shown in Fig. 6) are similar. A good DWBA fit is obtained with $L=1+3$ and $J^\pi=2^-$ transfers for both the transitions. The assumed two-nucleon configurations for these levels are given in Table IV. According to the *sdfp*-shell—model calculation[28] the lowest odd-parity level having a significant *fp*-shell configuration is at 2.52 MeV excitation and has $J^\pi=4^-$. We expect that the 2.64-MeV level is probably a 2^- state. Our spin assignment for the 2.85-

MeV level, however, is $J^{\pi}=2^{-}$, in agreement with previous studies.[12]

D. Other levels

The experimental angular distributions for a few other weak levels in ^{38}K are displayed in Fig. 7 and they do not exhibit distinctive patterns. Therefore, not much spectroscopic information could be obtained for them. There is a clear indication for the presence of a level in ^{38}K at 10.26-MeV excitation energy. The present data, however, do not enable us to extract an angular distribution for this level.

V. CONCLUSIONS

The excitation energies of various levels in ^{38}K obtained in the present study are in good agreement with the previous results.[4,12]

In spite of the ambiguities in the detailed DWBA predictions for the (d,α) reactions,[6,30,31] additional spectroscopic information on ^{38}K has been obtained via the ^{40}Ca(d,α) reaction. The shapes of the angular distributions for most positive-parity levels below the 9.88-MeV excitation are rather well predicted by DWBA calculations performed using the two-nucleon spectroscopic amplitudes from the full *sd*-shell—model calculation.[11] Tentative J^{π} assignments made here are consistent with the previous assignments.

Our analysis indicates that the 7.32-MeV level has a large $(2s_{1/2}{}^{-1})_p(2s_{1/2}{}^{-1})_n$ component and hence has $J^{\pi}=1^{+}$. Two new levels, one at 9.88 MeV and another at 10.26 MeV have been identified. The 9.88-MeV level exhibits a characteristic $L=2+4$ transfer and probably corresponds to the predicted 3_3^{+} level at 9.06 MeV.

The energies in ^{38}K deduced from a recent shell-model calculation[28] in the $2s_{1/2}$-$1d_{3/2}$-$1f_{7/2}$-$2p_{3/2}$—model space compare well with those obtained in the present work up to an excitation energy of 3.5 MeV. Since the spectroscopic amplitudes are not available from this *sdfp* calculation, it has not been possible to compare our experimental angular distributions with the theoretical predictions.

Values of the normalization constant N obtained for the levels in ^{38}K from the (d,α) reaction are quoted in the last columns of Tables III and IV. Large variations in the values of N have been found. Similar variations in the relative values of N have been observed in the study of the ^{58,60}Ni(d,α) reaction by Nann *et al.*[32]; these variations are attributed to the type of residual interaction used in evaluating the shell-model wave functions. In the present case the variation in the normalization constant (e.g., normalization constants calculated relative to the ground state) for the levels below the 4.00-MeV excitation is rather small. The variations in the values of the normalization constant could perhaps be further reduced with improvements in the shell-model calculations. The *sd*-shell—model calculation[11] assumes that ^{40}Ca is a good closed shell nucleus. Several experiments[12] have established that a small amount of 2p-2h and 4p-4h admixtures have to be included in the ground state of ^{40}Ca. Therefore, it is strongly felt that an elaborate *sdfp*-shell—model calculation of two-nucleon spectroscopic amplitudes for the levels in ^{38}K is highly desirable. Unfortunately the two-nucleon spectroscopic amplitudes for the levels in ^{38}K are not available from the *sdfp*-shell—model calculation of Hasper.[28]

ACKNOWLEDGMENTS

The work at Argonne National Laboratory was supported by the U.S. Department of Energy under Contract No. W-31-109-Eng-38. One of us (N.G.P.) wishes to thank Dr. W. Oelert for many useful discussions. The help of Dr. M. Raja Rao, Dr. C. R. Ramaswamy, and Mrs. Pushpaltha C. Bhat at various states of this work is acknowledged. One of the authors (C.M.B.) is grateful to the Council of Scientific and Industrial Research, New Delhi, India for the award of a senior research fellowship.

*Permanent address: Department of Physics, Bangalore University, Bangalore, India.

†Permanent address: University of Pennsylvania, Philadelphia, PA 19104.

[1]M. B. Lewis and W. W. Daehnick, Phys. Rev. C 1, 1577 (1970).

[2]N. Frascaria, J. P. Didelez, N. S. Chant, and C. C. Chang, Phys. Rev. C 16, 603 (1977).

[3]Y. S. Park and W. W. Daehnick, Phys. Rev. C 4, 778 (1971).

[4]N. Frascaria, J. P. Didelez, J. P. Garron, E. Gerlic, and J. C. Roynette, Phys. Rev. C 10, 1422 (1974).

[5]A. van der Woude and R. J. de Meijer, Nucl. Phys. A258, 199 (1976).

[6]R. M. DelVecchio and W. W. Daehnick, Phys. Rev. C 6, 2095 (1972).

[7]W. W. Daehnick, J. H. Orloff, T. Canada, and T. S. Bhatia, Phys. Rev. C 10, 136 (1974).

[8]N. K. Glendenning, Phys. Rev. 137, B102 (1965); At. Data Nucl. Data Tables 16, 1 (1975).

[9]I. S. Towner and J. C. Hardy, Adv. Phys. 18, 401 (1969).
[10]B. H. Wildenthal, E. C. Halbert, J. B. McGrory, and T. T. S. Kuo, Phys. Rev. C 4, 1266 (1971).
[11]B. H. Wildenthal and W. Chung (private communication).
[12]P. M. Endt and C. van der Leun, Nucl. Phys. A310, 1 (1978).
[13]W. J. Gerace and A. M. Green, Nucl. Phys. A93, 110 (1967).
[14]O. Abou-Zeid, L. Ph. Roesch, and W. R. Falk, Phys. Rev. C 20, 1198 (1979).
[15]J. C. Sens and R. J. de Meijer, Kernfysisch Versneller Instituut Report, 1979 (unpublished), p. 15.
[16]E. J. Ludwig, T. B. Clegg, W. W. Jacobs, and S. A. Tonsfeldt, Phys. Rev. Lett. 40, 441 (1978).
[17]F. Merz, H. Clement, R. Frick, G. Grow, N. Seichert, and P. Schiemenz, (private communication).
[18]H. T. Fortune, N. G. Puttaswamy, and J. L. Yntema, Phys. Rev. 185, 1546 (1969).
[19]F. Grard, Nucl. Instrum. Methods 34, 242 (1965).
[20]F. Ajzenberg-Selove and T. Lauritsen, Nucl. Phys. A227, 1 (1974).
[21]M. Pual, A. Marinov, J. Burde, Ch. Drory, J. Lichtenstadt, S. Mordechai, and E. Navon, Nucl. Phys. A289, 94 (1977).
[22]W. W. Daehnick, J. D. Childs, and Z. Vrcelj, Phys. Rev. C 21, 2253 (1980).
[23]C. M. Perey and F. M. Perey, At. Data Nucl. Data Tables 17, 1 (1976).
[24]R. Bock, P. David, H. H. Duhm, H. Hafele, U. Lynen, and R. Stock, Nucl. Phys. A92, 539 (1967).
[25]B. F. Bayman and A. Kallio, Phys. Rev. 156, 1121 (1967).
[26]A. Nadasen, P. Schwandt, P. P. Singh, W. W. Jacobs, A. D. Bacher, P. T. Debevec, M. D. Kaitchuck, and J. T. Meek, Phys. Rev. C 23, 1023 (1981).
[27]P. D. Kunz, University of Colorado report, 1969 (unpublished).
[28]H. Hasper, Phys. Rev. C 19, 1482 (1979).
[29]B. H. Wildenthal, J. A. Rice, and B. M. Preedom, Phys. Rev. C 10, 1184 (1974).
[30]J. R. Comfort, H. T. Fortune, G. C. Morrison, and J. V. Maher, Phys. Rev. C 10, 2399 (1974).
[31]S. Mordechai, M. E. Cobern, G. E. Moore, and H. T. Fortune, Nucl. Phys. A289, 36 (1977).
[32]H. Nann, A. D. Bacher, W. W. Jacobs, W. P. Jones, and E. J. Stephenson, Phys. Rev. C 24, 1984 (1981).